Aus dem Lehrstuhl für Molekularbiologie
(im Biomedizinischen Centrum München, BMC)
der
Ludwig-Maximilians-Universität München
Vorstand: Prof. Dr. Peter Burkhard Becker

In Vivo Reconstitution of Heterochromatin

Dissertation
zum Erwerb des Doktorgrades der Medizin
an der Medizinischen Fakultät der
Ludwig-Maximilians-Universität zu München

vorgelegt von
Sebastian Sommer
aus Düren
2019

Mit Genehmigung der Medizinischen Fakultät
der Universität München

Berichterstatter: PD Dr. Philipp Korber

Mitberichterstatter: PD Dr. Alois Schepers

Prof. Dr. André Werner Brändli

Mitbetreuung durch den
promovierten Mitarbeiter: Prof. Dr. Axel Imhof

Dekan: Prof. Dr. med. dent. Reinhard Hickel

Tag der mündlichen Prüfung: 02.05.2019

Eidesstattliche Versicherung

Sommer, Sebastian

Name, Vorname

Ich erkläre hiermit an Eides statt,
dass ich die vorliegende Dissertation mit dem Thema

„*In Vivo* Reconstitution of Heterochromatin“

selbständig verfasst, mich außer der angegebenen keiner weiteren Hilfsmittel bedient und alle Erkenntnisse, die aus dem Schrifttum ganz oder annähernd übernommen sind, als solche kenntlich gemacht und nach ihrer Herkunft unter Bezeichnung der Fundstelle einzeln nachgewiesen habe.

Ich erkläre des Weiteren, dass die hier vorgelegte Dissertation nicht in gleicher oder in ähnlicher Form bei einer anderen Stelle zur Erlangung eines akademischen Grades eingereicht wurde.

München, 03.09.2018	Sebastian Sommer
Ort, Datum	Unterschrift Doktorand

Für meine Eltern Ruth und Fritz

Teile dieser Arbeit wurden veröffentlicht in:

Ansari SA, Paul E, Sommer S, Lieleg C, He Q, Daly AZ, Rode KA, Barber WT, Ellis LC, LaPorta E, Orzechowski AM, Taylor E, Reeb T, Wong J, Korber P, Morse RH. (2014). Mediator, TATA-binding protein, and RNA polymerase II contribute to low histone occupancy at active gene promoters in yeast. *J Biol Chem, 289*(21), 14981-14995.

Table of contents

I. Summary

Our body consists of about 200 different cell types, each one of them specialized in its own way. Groups of cells form similarly specialized organs. Despite this heterogeneity of cells in our body, all cells contain largely the same DNA, and cell diversity is achieved through the differential regulation of gene expression in each cell. Chromatin plays an important role, not just in DNA packaging, but also in gene regulation. In the 1930s scientists already distinguished two types of chromatin in the interphase nuclei of many eukaryotic cells: a highly condensed form, called heterochromatin, and a less condensed form, called euchromatin. Euchromatin is associated with transcriptionally active genes, whereas heterochromatin contains mainly repressed genes. Although many factors are already identified responsible for this highly condensed chromatin, it is still unclear which factors are sufficient for gene repression.

Methylation of histone H3 at lysine 9 (H3K9) and binding of Heterochromatin Protein 1a (HP1a) at this modification mark are strongly associated with heterochromatin and well conserved from the unicellular fission yeast *S. pombe* to humans.

Using a synthetic biology approach, we asked to what extent heterochromatin features can be reconstituted with just the combination of methylated H3K9 and HP1. We tested the reconstitution of heterochromatin *in vivo* by expressing the *Drosophila melanogaster* H3K9 methyltransferase dSu(var)3-9 and HP1a into the budding yeast *S. cerevisiae*, which serves as an in this regard neutral cellular background as this yeast lacks H3K9me and HP1 and posseses only rudimentary heterochromatin.

We followed two approaches. First, we targeted the methyltransferase via sequence specific DNA-binding domains to the well-studied *PHO* genes and analysed chromatin changes at these loci. Second, we looked at genome-wide expression changes after introduction of HP1a and / or the methyltransferase. As readout we employed a wide variety of methods, i.e., mass spectrometry, chromatin immunoprecipitation (ChIP), DNAseI indirect-endlabeling, gene product activity assays, and microarray transcriptome analysis.

To our knowledge, we were the first to successfully introduce H3K9me as a novel histone modification in budding yeast. To our surprise, *S. cerevisiae* viability and global gene expression was not much affected. Nonetheless, targeting of dSu(var)3-9 to the *PHO* genes repressed these. The repressive effect was independent of H3K9 methylation and probably mediated by a highly conserved direct interaction between dSu(var)3-9 and the histone deacetylase (HDAC) Rpd3. Coexpression with HP1a led to synergistic repression at the *PHO* genes and an altered chromatin structure, again independent of H3K9 methylation.

Very surprisingly, non-targeted HP1a alone already led to significant reduction of gene expression at the *PHO* and *HIS3* genes. Throughout our studies the HP1a chromoshadow domain was essential for the repressive effects and for interacting with dSu(var)3-9.

Transcriptome analyses revealed that HP1a and / or dSu(var)3-9 were not global transcriptional repressors.

In summary, our synthetic biology approach is feasible to study heterochromatin mechanisms in a “neutral background” system. This way, we found that the methylation of H3K9 as such had hardly any effect on gene expression or heterochromatin formation. Instead, we identified a highly conserved role of this methyltransferase in recruiting a histone deacetylase and found HP1a effects that were dependent on its chromoshadow domain but independent on binding methylated H3K9.

II. Zusammenfassung

Unser Körper besteht aus ca. 200 verschieden Zellen, jede Zelle für sich ist hochspezialisiert. Die menschlichen Organe setzen sich aus riesigen Zellverbänden zusammen. Trotz dieser unglaublichen Vielfalt im menschlichen Köper besitzen alle Zellen das gleiche Genom. Diese Zelldifferenzierung wird letztendlich durch differentielle Genregulation erreicht. Chromatin ist nicht nur für eine kompakte Verpackung der DNA verantwortlich, sondern spielt auch eine maßgebende Rolle in der Genregulation. Bereits in den 1930 er Jahren des vergangenen Jahrhunderts wurde zwischen zwei Chromatinarten bei Interphase Zellkernen unterschieden, Heterochromatin als eine stark kondensierte Chromatinstruktur mit vorwiegend reprimierten Genen und Euchromatin als eher lose und zugängliche Chromatinstruktur mit aktiv transkribierten Genen. Obwohl in den letzten 30 Jahren viele Proteine, die für das Heterochromatin verantwortlich sind, identifiziert worden sind, ist es immer noch unklar, welches Minimum an Faktoren ausreichend ist. Die Methlyierung von Histon H3 am Lysin 9 (H3K9me) und das Binden vom Heterochromatin Protein 1a (HP1a) an diese Histonmodifikation sind zwei wiederkehrende Merkmale von Heterochromatin, und sind evolutiv von der Spalthefe (*S. pombe*) bis zum Menschen konserviert.

In dieser Arbeit wollten wir nun mit Hilfe eines synthetisch-biologischen Ansatzes untersuchen, ob diese beiden Faktoren, ausreichen um heterochromatische Chromatinstrukturen zu etablieren. Hierzu haben wir die H3K9 Methyltransferase dSu(var)3-9 und HP1a der Taufliege (*Drosophila melanogaster*) in die Bäckerhefe (*S. cerevisiae*) eingebracht, die diese beiden Faktoren natürlicherweise nicht und nur rudimentäres Heterochromatin besitzt.

Zum einen brachten wir dSu(var)3-9 mittels einer entsprechenden DNA-Bindungsdomäne gezielt an die gut untersuchten *PHO* Gene. Zum anderen untersuchten wir die genomweiten Veränderungen durch HP1a und/oder dSu(var)3-9. Methodisch untersuchten wir die Effekte mittels Massenspektrometrie, Chromatinimmunopräzipitation, DNaseI-indirekter Endmarkierung, Aktivitätsassays und Genexpressionsanalysen.

Nach unserem besten Wissen konnten wir zum ersten Mal diese Histonmodifizierung neu in *S. cerevisae* einführen. Zu unserer Verwunderung hatte dies keinen Einfluss auf die Lebensfähigkeit von *S. cerevisiae*. Das Fusionkonstrukt mit einer Pho4-DNA-Bindungsdomäne konnte die Expression der *PHO* Gene reduzieren, wahrscheinlich mittels Rekrutierung der Histondeacetylase (HDAC) Rpd3. Die Genrepression war unabhängig von der H3K9 Methylierung. Eine Koexpression von HP1a zeigte einen Synergismus und veränderte die Chromatinstruktur des *PHO5* Promoters.

HP1a allein reprimierte überraschenderweise bereits die *PHO* und *HIS3* Gene. In allen Experimenten erwies sich die *chromoshadow* Domäne von HP1a als essentiell für dessen Funktion. Unsere genomweiten Expressionsanalysen zeigten, dass weder HP1a noch dSu(var)3-9 generelle Repressoren sind.

Zusammenfassend lässt sich sagen, dass sich mit Hilfe der synthetischen Biologie heterochromatische Mechanismen in einem „neutralen Hintergund“ gut untersuchen lassen. So konnten wir zeigen, dass H3K9me für sich nahezu keinen Effekt auf die Genexpression oder auf die Ausbildung von Heterochromatin hatte. Stattdessen identifizierten wir eine hochkonservierte Funktion einer HDAC-Rekrutierung durch eine Methyltransferase und zeigten, dass HP1a-Effekte von der *chromoshadow* Domäne abhängen und unabhängig von einer Bindung an H3K9me sein können.

1 Introduction

1.1 Chromatin

If one tried arranging the human DNA strands of the 46 chromosomes of one cell in one line, it would amount to a length of roughly 2 meters. How is this fitted into a nucleus, which has a diameter of only 6 µm on average? This can be compared to packing a fine thread of 40 km length into a tennis ball (Alberts, *et al* 2007). Making it even more complicated, the folding of the DNA polymer is counteracted/encumbered by the negatively charged DNA backbone, which creates electrostatic repulsion between adjacent DNA regions and stiffens the DNA (Jiang and Pugh 2009, Maeshima, *et al* 2014).

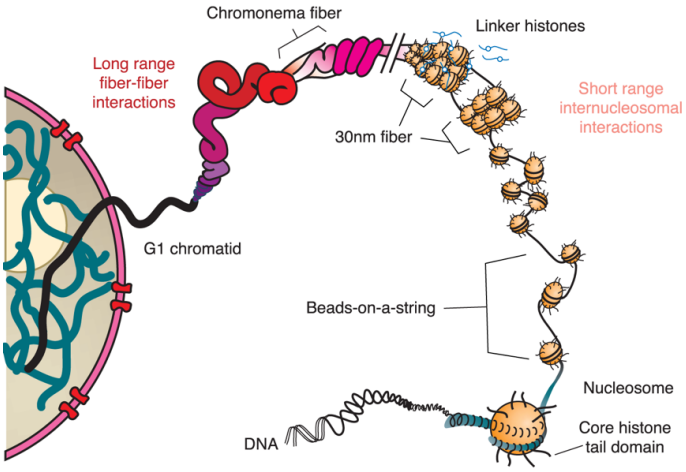

Fig. 1. Scheme of the stepwise packaging of DNA. In a first step, DNA is wrapped around histone octamers to form nucleosomes. Nucleosomes line up as nucleosomal arrays, also referred to as beads-on-a-string. Nucleosomes interact with each other and / or linker histones creating the 30 nm fiber. The 30 nm fiber is again compacted creating higher chromosomal structures. From Horn, P. J., & Peterson, C. L. (2002). Molecular biology. Chromatin higher order folding - wrapping up transcription. *Science, 297*(5588), 1824-1827. Reprinted with the permission of AAAS.

Chromatin manages to pack DNA into a compact structure. It consists of nuclear DNA, proteins, especially histones, and RNA. Besides facilitating the packing of DNA, chromatin plays also a major role in gene regulation, genome replication, genome maintenance and many more genomic processes.

The first step of compaction is achieved by the nucleosome, leading to a six-fold compaction (Olins and Olins 2003).

Each nucleosome consists of a nucleosome core particle with 147 base pairs (bp) of DNA wrapped around a histone octamer and a linker region of DNA, which may be associated with the histone H1. The linker length between the nucleosome core particles varies among different species, tissues and even within a single cell genome (Szerlong and Hansen 2011). For example, the linker in the baker`s yeast *Saccharomyces cerevisiae* (*S. cerevisiae*) is 18 bp (Jiang and Pugh 2009), in *Schizosaccharomyces pombe* (*S. pombe*) 7 bp (Lantermann, *et al* 2010), in *Drosophila melanogaster* 28 bp (Mavrich, *et al* 2008), or in humans 38 bp (Jiang and Pugh 2009). Nucleosomes are aligned

into nucleosomal arrays, which corresponds to the so called 10 nm chromatin fiber or is often referred to as “beads-on-a-string” (Kornberg and Klug 1981, Olins and Olins 2003). Such chromatin fibers are successively folded into higher order structures (Fig. 1) as discussed in the next sections.

1.1.1 The nucleosome core particle

147 bp of DNA wrapped around a positively charged histone octamer consisting of two copies each of the four highly conserved histones H2A, H2B, H3 and H4 make up the nucleosome core particle. Each of the core histones shares the central histone-fold domain made out of three α-helices (α1- α3) connected by two loops (L1-L2). The histone-fold domain mediates the formation of heterodimers (H3-H4 and H2A-H2B). Two H3-H4 heterodimers form a tetramer through a single H3´-H3 interaction (Kornberg 1974, Kornberg and Lorch 1999, Luger*, et al* 1997). During nucleosome assembly *in vitro* as well as *in vivo* the H3-H4 tetramer binds to DNA first followed by incoporation of the two H2A-H2B dimers. The dimers interact with the tetramer via H2B and H4 (Akey and Luger 2003, Eickbush and Moudrianakis 1978, Luger*, et al* 1997, MacAlpine and Almouzni 2013, Polo and Almouzni 2006). The DNA is wrapped 1.65 times in a left handed superhelix around the histone octamer (Luger*, et al* 1997). DNA binding to each H2A-H2B dimer is accomplished by two L1-L2 binding sites located at both ends of the dimer and one central α1α1 binding site, which is formed by the two N-terminal α1 helices of each histone fold domain. This way 12 of the 14 minor grooves of DNA are bound by the histone fold motive, covering 121 bp of DNA. The remaining 26 bp are bound by an α-helical histone fold extension of H3 (H3αN) at the entry and exit site of the nucleosome (Luger*, et al* 1997, Luger and Richmond 1998a).

The N-terminal histone tail, which extends out of the disc-shaped nucleosome core particle through narrow channels formed by the minor grooves of the DNA (Luger and Richmond 1998b), is subject to various posttranslational modifications, which play a role in chromatin structure, replication, DNA repair and transcription (Bannister and Kouzarides 2011).

1.1.2 H1 and the higher orders of chromatin structure

Upon addition of histone H1, nucleosomes are in closer contact to each other forming a higher order structure (Finch and Klug 1976, Thoma and Koller 1977). Unlike the other histones, H1 is less conserved and not essential, for example, in *S. cerevisiae* (Patterton*, et al* 1998), but essential in mammals (Fan*, et al* 2003, Fan*, et al* 2001, Harshman*, et al* 2013).

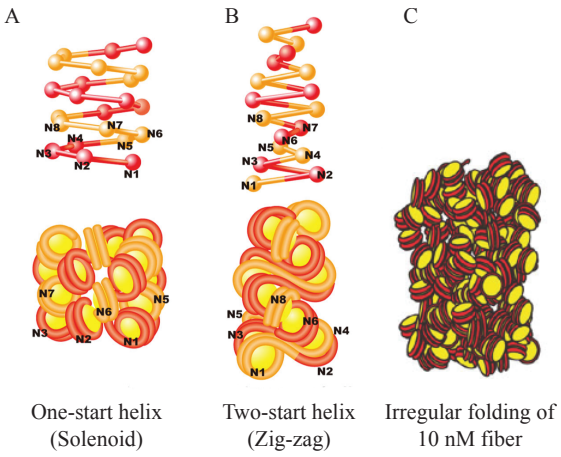

Fig. 2 Three suggested models for the next chromatin folding level beyond the 10 nm fiber. (A) Solenoid model in which consecutive nucleosomes are aligned next to each other. (B) Zig-Zag model in which one nucleosome is bound to the next but one nucleosome. (C) Irregularly folded nucleosome fibers. Reprinted with the permission of Springer (Maeshima, *et al* 2014).

The linker histone H1 protects additional 20 bp of DNA and binds to the nucleosomal dyad and linker DNA entering and existing the nucleosome (Allan, *et al* 1980, Noll and Kornberg 1977, Syed, *et al* 2010, Zhou, *et al* 1998). In 1976 a 30 nm fiber was already suggested, consisting of nucleosomes and histone H1, and formed at high salt conditions (Finch and Klug 1976). A solenoid model was proposed, consisting of a one start-helix, in which nucleosomes are lined up after each other. Based on electron microscopy data Woodcock and colleagues preferred a second model, the Zig-zag model. Here a nucleosome binds to the next but one nucleosome, e.g., nucleosome number one interacts with nucleosome number three (Fig. 2) (Maeshima, *et al* 2010, Woodcock, *et al* 1984). A recent cryo-EM structure showed an H1 dependent two-start Zig-Zag conformation of a left handed tetranucleosome (Song, *et al* 2014). Although the 30 nm fiber was extensively studied during the past 30 years (for reviews see (Robinson and Rhodes 2006, Tremethick 2007)), the *in vivo* relevance has been questioned lately (Fussner, *et al* 2011, Hansen 2012, Maeshima, *et al* 2010, Maeshima, *et al* 2014). A rather dynamic irregular folding of the 10 nm fiber was suggested, which still allows accessibility to the DNA (Maeshima, *et al* 2014). Using ChromEMT, a technique combining electon microscopy tomography (EMT) with a DNA enhancing labeling method (ChromEM), an irregular folding of the chromatin fiber was recently visualized, with fiber diameters ranging from 5-24 nm (Ou, *et al* 2017)

Chromatin architectural proteins are another key factor for secondary or tertiary chromatin structure. These include for example one of the three isoforms of Heterochromatin Protein 1 (HP1a), Methyl-CpG binding protein 2 (MeCP2) or the Polycomb Group proteins (Horn and Peterson 2002, McBryant, *et al* 2006).

One of the first observations of different chromatin compaction states was made by Emil Heitz (Heitz 1928). In experiments with mosses he could distinguish by light microscopy two different states of chromatin. Regions, which decondense after mitosis, he termed euchromatin, those that stayed condensed after mitosis he named heterochromatin. Later it was shown

that euchromatin is gene rich and associated with active gene transcription, whereas heterochromatin contains only a few genes and is more condensed.

1.1.3 Regulation of chromatin structure

Nucleosomes do not just pack DNA, they also play an important role in gene regulation. In vitro studies in the 1980s showed that nucleosomes at a promoter inhibit the initiation of transcription by RNA polymerase (Knezetic and Luse 1986, Lorch*, et al* 1987). The Grunstein lab showed another example for the repressive nature of nucleosomes. Depleting H4 *in vivo* activated promoters (Han and Grunstein 1988, Han*, et al* 1988). Especially yeast studies of the *PHO* and *GAL1-10* genes showed that repressed promoters were covered with well-positioned nucleosomes, hindering transcription factors to access their binding sites (Rando and Winston 2012).

Despite the repressive nature of nucleosomes and the various compaction levels, which are still not well understood, chromatin is a highly dynamic structure and accessibility to the DNA is essential and regulated for a functioning cell.

This DNA accessibility within chromatin is modified via the interplay of six general mechanisms:

DNA methylation, histone variants, histone modifications, chromatin remodeling by ATP hydrolysis, non-coding RNAs and nuclear organization.

1.1.3.1 DNA methylation

DNA methylation in human cells occurs at CpG dinucleotides of which 60-80% are methylated in differentiated cells. Its repressive effect is mediated by methyl-CpG-binding domain proteins (MBDs), which recruit histone deacetylases, HP1, chromatin remodelers, and other chromatin proteins. DNA methylation has especially an important role in long-term silencing of transposable elements and X-chromosome inactivation (reviewed in (Bird 2002, Bird and Wolffe 1999, Guy*, et al* 2011, Jones 2012, Smith and Meissner 2013)). At transcription start sites, especially of housekeeping genes, so called CpG islands are found. Those CpG islands are very CpG rich, but generally lack DNA methylation. In cancer cells, hypermethylation of these regions inactivates genes like *MLH1*, *APC*, *BRCA1* and others (Jones and Baylin 2002). In contrast to such locus-specific hypermethylation, cancer cells show global hypomethylation, which mainly pertains to satellite DNA and contributes to genome instability via hyperrecombination (Eden*, et al* 2003, Gaudet*, et al* 2003). DNA methylation is found in mammals, and plants, but is missing in *S. cerevisiae*, the model organism of this study (Capuano*, et al* 2014).

1.1.3.2 Histone variants

Besides the four canoncial core histones, which are expressed during DNA replication, variants of the histones H2A, H2B and H3 were discovered. These variants are usually constitutively expressed and were linked to DNA repair (H2A.X), gene activation (H3.3), gene silencing (macroH2A), or chromosome segregation (CENP-A). For H3.3 and H2A.Z roles both in gene activation and in gene repression and chromosome segregation were described (for reviews see (Buschbeck and Hake 2017, Maze*, et al* 2014, Talbert and Henikoff 2010, Zink and Hake 2016)).

1.1.3.3 Chromatin remodeling

ATP-dependent chromatin remodeling enzymes are responsible for modulating the packing of chromatin and changing DNA accessibility by nucleosome sliding, nucleosome eviction/assembly, localized unwrapping or by altering the nucleosome composition via exchanging histone variants (reviewed in (Clapier and Cairns 2009, Narlikar*, et al* 2013)).

1.1.3.4 Non-coding RNAs

Non-coding RNAs influence chromatin in many ways. The most prominent example is the dosage compensation complex in flies and mammals. In mammals the X-inactive specific transcript (*XIST*) initiates the formation of a repressive heterochromatin state by recruiting chromatin modifying enzymes to the inactive X-chromosome. Other forms of regulation include transcriptional control in *cis* or *trans* by recruiting transcriptional regulators (reviewed in (Fatica and Bozzoni 2014, Mercer*, et al* 2009)).

1.1.3.5 Nuclear organization

Even the nucleus organization itself can influence the expression of genes. It has been proposed that movement of chromatin to a different location within the nucleus influences gene expression. For some genes it has been shown that movement to the periphery correlates with gene repression and movement to the interior with gene activation (reviewed in (Lanctot*, et al* 2007)).

1.2 Histone modifications and the histone code

Especially the histone tails are subject to various posttranslational modifications. So far mainly acetylation at lysine, methylation at lysine and arginine, phosphorylation at serine and threonine, ubiquitylation, ADP ribosylation and sumoylation of lysine, deimination of arginine or isomerization of proline residues were described (Table 1) (Kouzarides 2007). Due to recent advances in mass spectrometry even more modifications were identified, e.g., crotonylation,

Histone	Residue	Modification	Modification enzymes
H2A	K5	Ac	Esa1, Rpd3
	K8	Ac	Esa1, Hat1, Rpd3
	S122	P	
	T126	P	
	K126	Sumo	
	S129	P	Mec1, Tel1, Pph3
H2AZ	K3	Ac	Esa1
	K8	Ac	Esa1
	K10	Ac	Esa1
	K14	Ac	Esa1
H2B	K6/K7	Sumo	
	S10	P	Ste20
	K11	Ac	Esa1, Rpd3
	K16	Ac	Gcn5, Esa1, Rpd3, Hda1
	K123	Ub	Rad6, Ubp8
H3	R2	Me	
	K4	Me, Ac	Set1, Jhd2, Rtt109, Gcn5
	K9	Ac	Gcn5, Rpd3, Hos2, Hda1
	S10	P	Snf1
	K14	Ac	Gcn5, Rpd3, Hos2, Hda1
	K18	Ac	Gcn5, Rpd3, Hos2, Hda1
	K23	Ac	Gcn5, Rpd3, Hos2, Hda1
	K36	Me	Set2, Rph1, Jhd1
	K42	Me	
	K56	Ac	Rtt109, Hst3, Hst4
	K79	Me	Dot1
H4	S1	P	CK2
	R3	Me	
	K5	Ac	Esa1, Rpd3, Hos2
	K8	Ac	Esa1, Rpd3, Hos2
	K12	Ac	Esa1, Rpd3, Hos2
	K16	Ac	Esa1, Sas2, Sir2, Hos2, Hst1
	K20	Ac	Esa1, Sas2, Sir2, Hos2, Hst1
	K31	Me	

Table 1 Histone modifications in *S. cerevisiae*. Adapted from (Rando and Winston 2012).

N-formylation, or hydroxylation of lysine residues (Arnaudo and Garcia 2013, Tan*, et al* 2011).

The histone modifications mainly exert their effects as proteins and protein complexes specifically bind to certain histone modifications and mediate changes in chromatin structure.

A "histone code" was suggested by David Allis and colleagues (Jenuwein and Allis 2001, Strahl and Allis 2000). They proposed that a histone modification attracts chromatin-binding proteins with respect to the surrounding chromatin modifications on the same histone tails and / or the tails of the other histones. Depending on the different combinations of histone modifications and the associated chromatin binding proteins the readout of a gene or the chromatin landscape might be completely different. While such mechanisms are well supported, the "code" metaphor is highly debated due to insufficient analogy to the "genetic code", and mostly abandoned (Nightingale*, et al* 2006, Turner 2014).

1.2.1 Histone acetylation

Histone acetyltransferases (HATs) use acetyl-CoA as cofactor to transfer an acetyl group to the ε-aminogroup of a lysine residue. Examples for HATs in yeast are Gcn5, Esa1 or Rtt109. All of them can acetylate multiple histone residues. Early on, histone acetylation was suggested to be tightly connected to active gene expression (Allfrey*, et al* 1964). Acetylated histones are bound by special domains, the bromodomain and PHD finger, which are found in various chromatin associated proteins (Bannister and Kouzarides 2011), for example, in several transcription factors or chromatin remodeling complexes (Hassan*, et al* 2002, Jacobson*, et al* 2000, Kurdistani and Grunstein 2003). ATP-dependent remodeling enzymes, like SWI/SNF

and RSC in yeast, contain bromodomains and bind preferentially to acetylated histones. Via nucleosome remodeling they mediate higher DNA-accessibility to the transcriptional machinery and thus transcription is enhanced (Bannister and Kouzarides 2011). Acetylation sites are partially redundant, as shown for the H3 and H4 tail (Martin, *et al* 2004, Megee, *et al* 1990, Zhang, *et al* 1998). Dion et. al could show, that for the H4 tail it is rather the sum of acetylation at K5, K8 and K12 which influence gene expression and not a certain lysine residue (Dion, *et al* 2005).

Of all histone acetylation sites, H4K16 acetylation has the most pronounced effect on its own. H4K16ac alone precludes 30 nm fiber formation *in vitro* (Robinson, *et al* 2008, Shogren-Knaak, *et al* 2006). In line with this are different expression profiles of H4K16R compared to K5R, K8R or K12R mutants (Dion, *et al* 2005).

Mutations mimicking acetylation of various histone core lysine residues in yeast showed enhanced expression of ribosomal DNA (Hyland, *et al* 2005). Also, modifications of the globular histone domains may affect nucleosome stability. For example, it was shown with single molecule FRET experiments that acetylation of H3K56 at the entry/exit point of DNA leads to a higher dissociation rate of the DNA from the histones (Jack and Hake 2014, Neumann, *et al* 2009, Tropberger and Schneider 2013). H3K122 is located at the lateral surface of the nucleosome where the histone DNA interaction is the strongest. Acetylation of this single site is sufficient for transcriptional activation, probably due to the disruption of histone-DNA binding (Tropberger and Schneider 2013).

Besides gene activation, histone acetylation was also linked to DNA repair and replication (Kurdistani and Grunstein 2003).

Histone deacetylases (HDACs) are the counterpart to HATs as they remove acetyl groups from lysine residues. Thus, they play an important role in gene repression. With Rpd3, Hos1, Hos2, Hos3 and Hda1 there are five related HDACs in yeast and a not related NAD^+-dependent HDAC Sir2 (Kurdistani and Grunstein 2003) .

Rpd3 and Hda1 show little overlap at most promoters and Hos1 and Hos3 are found at the ribosomal DNA loci (Robyr, *et al* 2002).

Whereas the large Rpd3 complex (Rpd3L) is primarily recruited to promoters via specific transcription factors. The small Rpd3 complex (Rpd3S) and Hos2 are recruited to actively transcribed gene bodies (Reynolds, *et al* 2013, Wang, *et al* 2002). Deacetylation in the gene body during transcription is thought to be needed to reestablish the chromatin state after the RNA polymerase passed through and to prevent cryptic transcription initiation (Kurdistani and Grunstein 2003).

S. cerevisiae only possesses rudimentary heterochromatin, e.g., at the silent mating type loci and subtelomeric regions. These are silenced by the Sir Complex. Here the NAD^+-dependent HDAC Sir2 in concert with the structural proteins Sir3 and Sir4 are recruited by DNA binding proteins and create a repressed chromatin structure. Heterochromatin formation starts at nucleation sites. In case of the silent mating loci, HML and HMR are flanked by short DNA silencer elements, which are bound by Rap1, Abf1 and the ORC complex. At the telomere, telomerase maintains a short TG-rich repeat sequence, which provides binding sites for Rap1. Silencers themselves recruit either Sir4 or Sir3, which then form the Sir2-3-4 (SIR) complex. Sir2 deacetylates H4K16ac and increases the affinity of the SIR complex for chromatin. Sir4 and Sir3 can be seen as structural proteins with various interactions between each other, nucleosomes, and linker DNA. Spreading is linked to Sir2 deacetylating neighboring nucleosomes. The spreading mechanism is stopped by boundaries, which are enriched in H3K16 acetylated nucleosomes and thus are commonly associated with the histone acetlytransferase Sas2. They are either active transcription sites or have a high transcriptional potential. At HMR a tRNA gene functions as boundary. In subtelomeric regions general transcription factors (Reb1, Tbf1) lead to hyperacetylation of histones and serve as boundary elements (reviewed in (Grunstein and Gasser 2013)).

1.2.2 Histone phosphorylation

Transcriptional regulation, apoptosis, cell cycle progression, DNA repair and chromosome condensation were all linked to phosphorylation of threonine or serine residues of histones. The negative charge of the phosphate group weakens DNA-histone interactions and increases DNA accessibility as shown for H3T118phos (North*, et al* 2011). Phosphorylation also plays an important role in chromosome condensation (Fischle*, et al* 2005, Hendzel*, et al* 1997).
In case of DNA damage one of the first events to occur in *S. cerevisae* is phosphorylation of H2AS129. This modification is found several kbp up- and downstream of the DNA break and serves as mark for the recruitment of acetyltransferases, remodelers, and DNA repair enzymes (Rossetto*, et al* 2012).

1.2.3 Histone methylation

Subject to methylation are lysine and arginine residues within the histones. Lysine residues can be mono-, di- or trimethylated, and arginine residues may be symmetrically or asymmetrically mono- or dimethylated. As this work will be focused on lysine methylation and also most of the research was conducted on lysine methylation, the focus of this introduction is

kept on lysine methylation. The methylation of arginine can be either activating or repressive (Di Lorenzo and Bedford 2011).

It took until the beginning of this century to finally discover the first histone methyltransferase (HMT) SUV39H1 (Rea, *et al* 2000). Jenuwein and colleagues identified the SET domain being responsible for the HMT activity. Subsequently, many more HMTs with SET domains were described. So far only DOT1b methylating H3K79 in a nonprocessive manner was found not to contain a SET domain (Frederiks, *et al* 2008, van Leeuwen, *et al* 2002).

Another four years later the first lysine demethylase (KDM), LSD1/KDM1A, was discovered (Shi, *et al* 2004, Shi, *et al* 2003). LSD1/KDM1a possesses a FAD-dependent amine oxidase that demethylates H3K4me3. With JmjC domain containing proteins a second class of KDM was described, utilizing a radical attack catalytic mechanism with α-ketoglutarate, molecular oxygen and Fe(II) as cofactors (Black, *et al* 2012, Tsukada, *et al* 2006).

The role of histone methylation is also very diverse among the single methylation sites. Fig. 3 shows the methylation sites of H3 and their enrichment relative to chromosome and gene regions. In general, methylation marks either correlate with active or repressive chromatin.

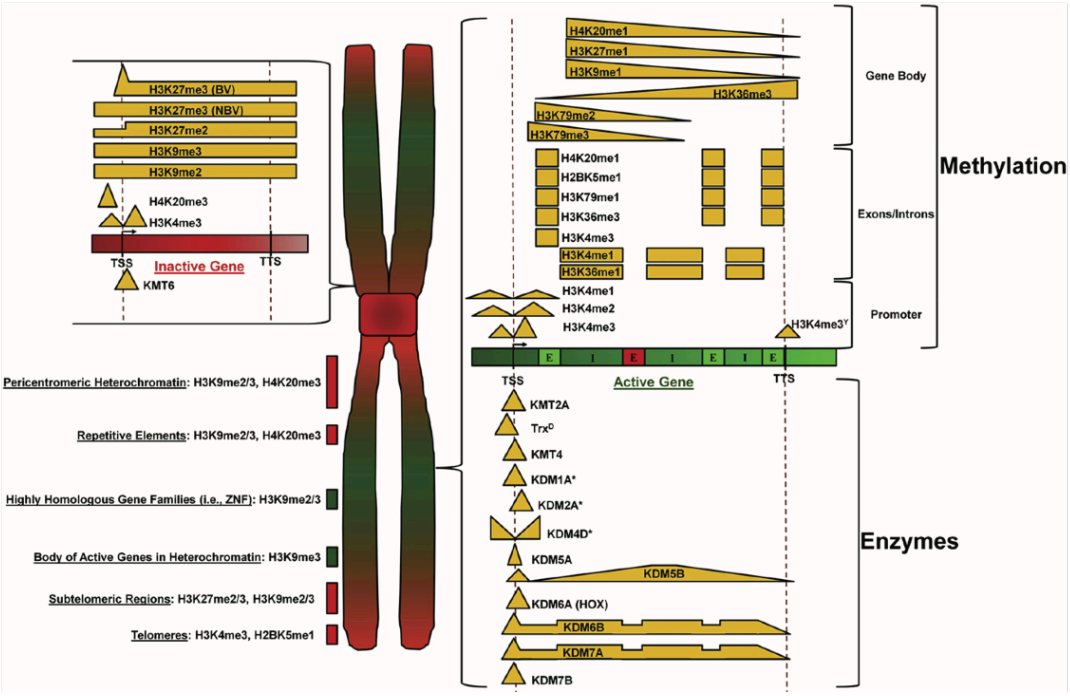

Fig. 3 Correlation of specific methylation marks with their chromosomal location or with their gene location depending on the activity state of the genes. Green represents active genes, red repressed genes. E stands for exons with green marked exons being transcribed, while red marked exons are not transcribed. I depicts introns. Data derived from various meta-anlyses that included data from both the TSS and TTS. * indicates when this was not the case. Specific characteristics of species are denoted with Y (*S. cerevisiae*) or D (*Drosophila melanogaster*). Reprinted from (Black, *et al* 2012) with the permission by Elsevier.

1.2.3.1 Histone methylation as an active mark for transcription

H3K4me, K3K36me and H3K79me were all linked to active transcription. Historically H3K4me3 is tought to be a hallmark for active transcription. Set1/COMPASS is the only H3K4 HMT in yeast. It is only active in the complex and associates with the initiation form of the RNA polymerase II phosphorylated at Ser-5 in the C- terminal domain (Shilatifard 2012, Wood*, et al* 2007). This leads to a high trimethylation level at the transcriptional start site (TSS) that decreases over the gene body. But the view as an active transcription mark has been challenged recently. Those conclusions have mostly been drawn from genome-wide studies of steady states, but Single gene studies along with stress responses in yeast point to a repressive function of H3K4 methylation (Carvin and Kladde 2004, Pinskaya*, et al* 2009, Wang*, et al* 2011, Weiner*, et al* 2012).

H3K4 monomethylation is a well-established marker for enhancers (Ernst*, et al* 2011), but it was also recently shown to play a role in certain repressed promoter-subsets, which are inducible (Cheng*, et al* 2014).

Set2 methylates H3K36 while binding to the Ser-2 phosphorylated form of the elongating RNA polymerase II. This results in increased H3K36 methylation along the transcribed gene toward the 3' end (Li*, et al* 2003, Schaft*, et al* 2003, Strahl*, et al* 2002). The chromodomain of Eaf3, a part of the Rpd3 HDAC complex, interacts with the H3K36 methylated histones. Rpd3 is recruited to actively transcribed genes, deacetylates histones of the transcribed gene and prevents cryptic transcription (Carrozza*, et al* 2005, Joshi and Struhl 2005).

The H3K79 methylation mark is set by the enzyme Dot1. Its similarity to class I SAM-dependent methyltransferases is unique among the HMTs (Min*, et al* 2003, Sawada*, et al* 2004). As for now, a H3K79me-demethlyase has not been identified. H3K79me also highly correlates with gene transcription and was shown to be associated with elongating RNA polymerase II (Krogan*, et al* 2003, Steger*, et al* 2008). H3K79me interferes with spreading of heterochromatin in yeast as it weakens binding of Sir3 to the nucleosome. As yeast mostly contains actively transcribed genes, this might explain the high occurrence of H3K79me (at about 90% of H3 histones). Besides its role in gene transcription, it was also shown that H3K79me is important in DNA repair and cell cycle regulation (for review see (Nguyen and Zhang 2011).

1.2.3.2 Repressive histone methylation marks

H3K9me and H4K20me are highly conserved repressive marks from the fission yeast *S. pombe* to humans, while H3K27me is only found in higher eukaryotes (Maison and Almouzni

2004, Simon and Kingston 2009). *S. cerevisiae*, the model organism of this work, lacks repressive histone methylation marks (Millar and Grunstein 2006).

1.3 Euchromatin and heterochromatin – the first try to distinguish different chromatin states

Heitz already discriminated in the early 1930s two different states of chromatin by light microscopy (Heitz 1928). As chromatin research has advanced since then, this basic distinction between active chromatin, called euchromatin and repressed chromatin, termed heterochromatin is still in use but debated regarding the corresponding molecular structures. The lightly stained euchromatin is gene rich, more loosely packed, replicated earlier, and contains hyperacetylated histones and activating histone methylation marks.

Heterochromatin on the other hand is more condensed, rather gene poor, and rich in repetitive sequences. Here histone tails are hypoacetlyated and show H3K9 methylation. Heterochromatic regions are replicated late in S phase (Elgin and Grewal 2003) and are enriched for DNA methylation.

With the advent of genome-wide mapping of histone modifications and chromatin binding proteins, van Steensel and colleagues defined five different states of chromatin using 53 broadly selected chromatin proteins in *Drosophila* (Filion*, et al* 2010), two states of euchromatic regions, and three repressive states. One repressive state is directly associated with the polycomb silencing pathway and its H3K27me mark, the second with HP1, SU(VAR)3-9, and HP1 interacting proteins LHR and HP6. This repressive state also correltated well with H3K9me2 enrichment. While the third, although covering close to 50% of the genome, is enriched for inactive genes, but the associated proteins are not the classical repressive proteins.

Park and colleagues went further and defined even nine different chromatin states (Kharchenko*, et al* 2011) in *Drosophila melanogaster*. They further distinguished the H3K9me enriched chromatin state into two states: the classical pericentric heterochromatin and a facultative heterochromatin found in euchromatic regions with lower H3K9me2 levels.

1.4 Position-effect variegation – an old model to study a new topic

More than 80 years ago, Muller treated fruitflys, *Drosophila melanogaster*, with X-rays and created the In(l)w^{m4} strain with a phenotype where the characteristic red pigmentation of the eye was patchy, i.e., also showed patches of white facets (Muller 1930). In wild type *Drosophila*, the *white* gene lies in a euchromatic region and is responsible for the red eye color. Upon radiation chromosomal breaks were induced, placing the *white* gene in the vicinity of

pericentric heterochromatin (Tartof, *et al* 1984). Spreading of heterochromatin silences the nearby *white* gene, creating the observed phenotype. The red/white patches are explained by variegated relaxation of silencing during differentiation (Lu, *et al* 1996). This model has turned out to be a great asset to study and screen for factors involved in the formation of heterochromatin. Using chemical mutagens in screens, around 150 genes were identified to have an influence on position effect variegation. Products of "Suppressor of varigation" (Su(var)) genes promote heterochromatin formation, while "Enhancer of variegation" (E(var)) genes counteract heterochromatin formation. Indeed, of these 150 genes, dSu(var)3-9 was identified to encode the H3K9 methyltransferase, Su(var)2-5 the Heterochromatin Protein 1(HP1a), and Su(var)3-7 a zinc finger protein. All of these play a crucial role in heterochromatin formation (Elgin and Reuter 2013).

1.4.1 Domains of *Drosophila* dSu(var) 3-9

For dSu(var)3-9 three functionally important domains were identified so far. The SET domain, the chromodomain and the N-terminus. The SET domain is responsible for the site-specific methylation of H3K9, which was first shown for the human homolog SUV39H1 (Rea, *et al* 2000) and later for dSu(var)3-9 (Czermin, *et al* 2001). The SET domain consists of eight β-strands and two short α-helices, creating a knot like structure as its active site (Jacobs, *et al* 2002). S-Adenosyl methionine serves as the methyl donor. N-terminal to the SET domain is a preSET domain necessary for the structural stability of the SET domain (Rea, *et al* 2000, Wilson, *et al* 2002). The postSET domain C-terminal to the SET domain contributes to the catalytic activity (Min, *et al* 2002, Wilson, *et al* 2002, Zhang, *et al* 2002).

The chromodomain binds to methylated H3K9, with higher affinity for the trimethlyated state. The chromodomain of the *S. pombe* homolog Clr4 is important for heterochromatin spreading (Al-Sady, *et al* 2013, Zhang, *et al* 2008).

The role of the N-Terminus appears very diverse. The first 81 amino acids are shared with the exon of the eukaryotic transcription factor 2 followed by a rather unstructured region (Schotta, *et al* 2002). The latter interacts with a domain of HP1 and Su(var)3-7 (Eskeland, *et al* 2007, Schotta, *et al* 2002). Besides these various interactions it is also important for the methyltransferase activity and homodimerization (Eskeland, *et al* 2004, Qian and Zhou 2006, Trievel, *et al* 2002).

1.4.2 HP1

1.4.2.1 Structure of HP1

HP1 consists of two well conserved globular domains connected by a flexible hinge. One of the globular domains is the chromodomain (CD), which binds highly selectively to methylated H3K9. Structural analysis revealed that the chromodomain forms a hydrophobic cage that recognizes the methylated lysine residue, while an extended groove establishes additional interactions with the histone tail. This makes the sequence specificity of the chromodomain possible (Bannister*, et al* 2001, Jacobs*, et al* 2001, Nielsen*, et al* 2002). The chromodomain of paraloge HP1a is also associated with transcripts of active genes. In conjunction with heterogeneous nuclear ribonucleoproteins (hnRNPs) HP1a might be important for packaging and stability of RNA (Piacentini*, et al* 2009).

On the C-Terminal side of HP1, the chromoshadow domain (CSD) recognizes PxVxL pentapeptidemotifs and serves as hub for various interaction partners of HP1, such as HP2, Su(var)3-9, or the globular domain of H3 (Lavigne*, et al* 2009, Lomberk*, et al* 2006b). But it is also necessary for homodimerization of HP1 (Brasher*, et al* 2000, Cowieson*, et al* 2000).

The hinge region is much less conserved among the HP1 variants within and between species and thus its function among the various homologs and paralogs may vary (Wallrath and Elgin 1995). It contains several sites for posttranslational modifications, like methylation, acetylation, phosphorylation or SUMOylation (LeRoy*, et al* 2009, Maison*, et al* 2011). Nucleic acids have also been reported to bind to the hinge region (Muchardt*, et al* 2002).

1.4.2.2 HP1 is a multipurpose protein with at first sight contradictory properties

Although HP1 was one of the first proteins identified to play a pivotal role in heterochromatin (Eissenberg*, et al* 1990, James and Elgin 1986) it is also a multifunctional factor. Indeed, HP1 was also implicated to be important for many more nuclear processes, as for example transcriptional activation, elongation, DNA repair, RNA splicing, or telomere maintenance (Canzio*, et al* 2014, Kwon and Workman 2011). How is this functional diversity with seemingly contradictory functions achieved?

First, this is accomplished by different paralogs. *Drosophila* and metazoans have three main HP1 isoforms: HP1a, HP1b and HP1c (HP1α, HP1β and HP1γ in humans). HP1a is the classical heterochromatin associated protein. HP1c is primarily found in euchromatic regions, while HP1b is found in both types of regions (Smothers and Henikoff 2001).

Further, some genes within heterochromatin regions are dependent on this otherwise repressive chromatin environment to be properly expressed. Translocation of such genes to euchromatic regions led to their variegated expression (Wakimoto and Hearn 1990). HP1a is also

found in euchromatic genes, preferentially at the gene body, where it is involved in transcription elongation. The exact mechanism of how HP1 can repress or activate gene expression remains elusive, but different interaction partners play certainly an important role (de Wit, *et al* 2007, Eissenberg and Elgin 2014, Kwon and Workman 2011, Piacentini, *et al* 2003).
HP1a protects telomeres by capping their ends. This is done independently of H3K9me as HP1a binds via its hinge region to telomere sequences. Still, silencing of telomere sequences is also maintained by H3K9me and HP1a (Fanti, *et al* 1998, Perrini, *et al* 2004).
Whether HP1 has a negative or positive effect on DNA repair is still debated. The function of HP1 in a possible repair mechanism remains obscure, but with only CSD needed for recruitment it seems to be independent of H3K9me (Ayoub, *et al* 2008, Ball and Yokomori 2009, Dinant and Luijsterburg 2009, Luijsterburg, *et al* 2009).

1.4.3 Heterochromatin formation through H3K9me and HP1a recruitment

1.4.3.1 Initiation of heterochromatin formation

The targeting of hetrochromatin is so far best understood in *S. pombe*. Proteins involved in the RNA interference system in *S. pombe* are necessary for centromeric silencing and heterochromatin assembly (Allshire and Madhani 2018, Volpe, *et al* 2002). Centromere repeats are transcribed by polymerase II, an RNA dependent RNA polymerase complex transcribes the single stranded RNA into dsRNA. Dicer cuts the dsRNA into a 22-nucleotide long siRNA. Ago1, a subunit of the "RNA induced initiation of transcription silencing" complex (RITS), binds the siRNA and is responsible for targeting the RITS complex to the loci where the respective siRNA sequence originated. For sufficient targeting, Chp1, another subunit of the RITS complex, contains a chromodomain, which has a high affinity for methylated H3K9 and is important for the initiation of heterochromatin (Hall, *et al* 2002, Schalch, *et al* 2009, Verdel, *et al* 2004). The RITS complex itself contributes to heterochromatin formation by interacting with a complex containing the Su(var)3-9 homolog Clr4 (reviewed in (Holoch and Moazed 2015, Volpe and Martienssen 2011)).
In *Drosophila*, another class of small RNAs fulfills a similar role in silencing transposable elements. The PIWI protein binds piRNAs and targets in a complex with Aubergine and Ago3 the heterochromatin machinery to transposons (Haynes, *et al* 2006, Huang, *et al* 2013, Le Thomas, *et al* 2013, Pal-Bhadra, *et al* 2004, Sienski, *et al* 2012). The integral part of RNA in human pericentric heterochromatin showed a simple RNaseA treatment experiment. Cells digested with RNaseA lost their typical pericentric staining of HP1α and H3K9me. Adding purified RNA to cells could rescue it (Maison, *et al* 2002).

Besides this RNA-based targeting mechanism there were also proteins identified, like D1 or SU(VAR)3-7 in *Drosophila* or Pax3 and Pax9 in mouse, that recruit heterochromatin factors by binding to specific satellite repeats (Aulner, *et al* 2002, Blattes, *et al* 2006, Bulut-Karslioglu, *et al* 2012, Cleard and Spierer 2001).

1.4.3.2 HP1 deposition in chromatin

Although the chromodomain has high specificity for H3K9me, the respective affinity is rather low and not sufficient for binding of HP1a to chromatin (Eskeland, *et al* 2007, Jacobs, *et al* 2001, Nielsen, *et al* 2002). The CSD and hinge region are essential for chromatin binding, and, surprisingly, the H3 tail is dispensable (Cowieson, *et al* 2000, Dawson, *et al* 2009, Lavigne, *et al* 2009, Meehan, *et al* 2003, Richart, *et al* 2012, Zhao, *et al* 2000). So far various models were suggested how the different HP1a domains interact with each other, bind to nucleosomes and also enable a spreading mechanism for heterochromatin. Fig. 4 shows two possible models. The model shown in Fig. 4B resulted from *in vitro* studies with Swi6, the *S. pombe* HP1 homolog. Using sedimentation velocity analytical ultracentrifugation, Canzio et. al showed that two Swi6 dimers bind to a mononucleosome (Canzio, *et al* 2011). In their model, not only the chromoshadow domains interact with each other, but also the chromodomains self-associate. They also proposed that the neighboring chromodomains help align Swi6 to recognize the H3K9 methylation mark. As of now the CD-CD association was described only in *S. pombe*, while *in vitro* studies of human HP1β could only show that the chromodomains bind to the methylated H3 peptide, but did not interact with another chromodomain (Munari, *et al* 2012) (Fig. 4A). As a mechanism for efficient spreading of the H3K9 methylation mark, it was proposed that the chromodomain of Clr4 has a higher affinity to H3K9me3 than Swi6. At heterochromatic initiation sites H3K9me2 is predominant and covered by Swi6, at the borders H3K9me3 states are found. The chromodomain of Clr4 binds here and methylates the neighboring nucleosome (Fig. 5)(Al-Sady, *et al* 2013).

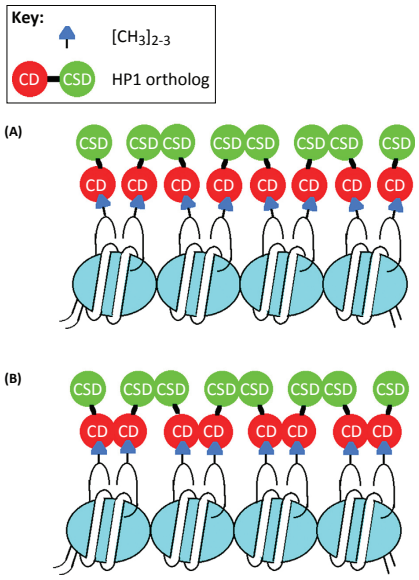

Fig. 4 Nucleosomal array with proposed HP1a binding to H3K9 methylated nucleosomes. (A) Model in which the homodimerization of CSD is sufficient for regular nucleosome positioning and silencing (Azzaz, *et al* 2014). (B) Model with homodimerization of both the CD and CSD (Canzio, *et al* 2011). Reprinted from (Eissenberg and Elgin 2014), with the permission of Elsevier.

Recently a new mechanism of phase separation was described (Larson, *et al* 2017, Strom, *et al* 2017). Interaction of HP1a molecules lead to the formation of droplets, they fuse to larger liquid like droplets. The surface of the droplets acts as a barrier for molecules.

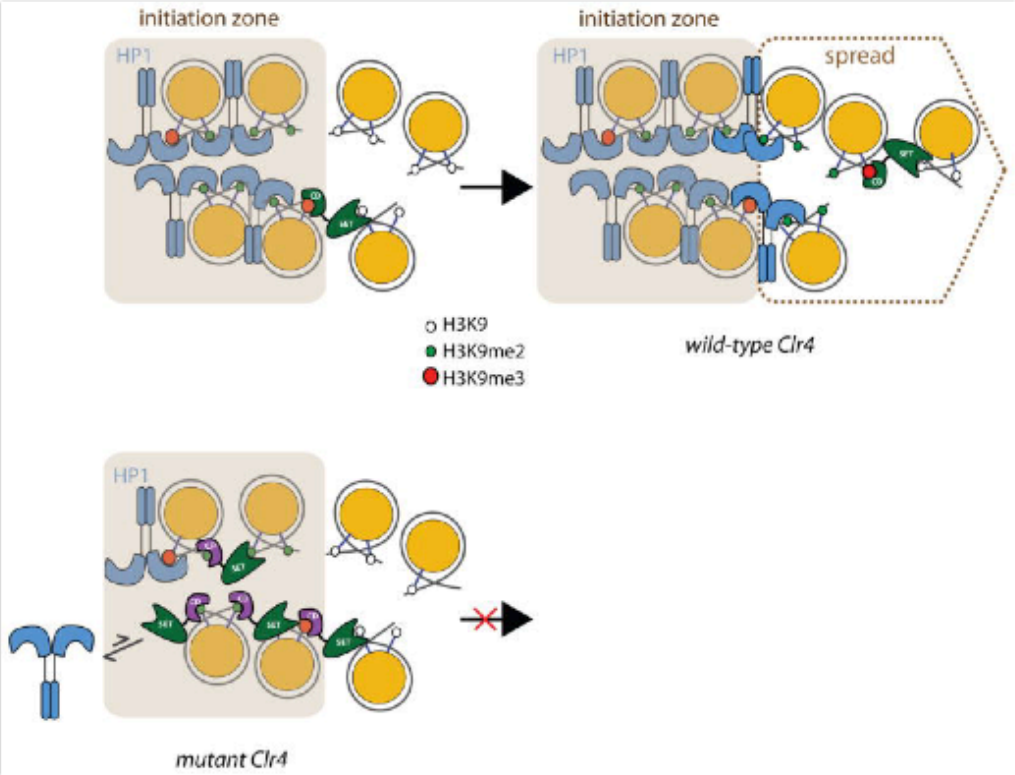

Fig. 5 Model of heterochromatin spreading in *S. pombe*. Clr4 sets H3K9 me2 or me3 marks in the initiation zone after direct recruitment. Swi6 binds with its chromodomain methylated histones in the initiation zone and homodimerizes with other HP1 molecules. At the edge of the initiation zone, Clr4 methylates more histones, creating a large pool of H3K9me2 and to a lesser extent H3K9me3. The spreading mechanism is established by a different affinity of the chromodomains. The chromodomain of Clr4 has a higer affinity for H3K9me3 and thus is not competing with HP1 at the already H3K9me2 domains. This spreading mechanism does not work if the chromodomain of Clr4 is swapped with the chromodomain of Chp1 (Chp1CD^{F61A}). With the swapped chromodomain, Clr4 has now a higher affinity for H3K9me2, creating a competition with HP1. In turn the spreading mechanism fails. Reprinted from (Al-Sady, *et al* 2013) with the permission of Elsevier**.**

1.5 Histone crosstalk and posttranslational HP1a modifications modify heterochromatin

Not only the extensive repertoire of possible posttranslational modifications makes it difficult to decipher a putative "histone code", but a single histone modification may also influence neighboring modifications (Kouzarides 2007).

One of the first described so-called histone crosstalks, was the H3K9/H3S10 methyl-phospho-switch. H3S10 is phosphorylated by the kinase Aurora A during mitosis. The new phosphorylation at the site next to the H3K9me site ejects HP1a from chromatin (Fischle, *et al* 2005). H3S10 phosphorylation also enhances the ability of Gcn5 to recognize its acetylation site

(Clements, *et al* 2003). In *S. pombe,* the RITS complex binds via Chp1 to H3K9me histones during S-phase and recruits Clr4 for methylation of newly deposited nucleosomes. In transition to the G2-phase H3K4 acetylation decreases the affinity of Chp1 to H3K9me, making the H3K9 methylation mark accessible for Swi6/Chp2 (Xhemalce and Kouzarides 2010).
Serine residues of HP1a are also subject to posttranslational phosphorylation and are necessary for heterochromatin assembly (Nishibuchi and Nakayama 2014, Zhao and Eissenberg 1999, Zhao, *et al* 2001). Phosphorylation of the N-terminal tail of HP1a seems to increase the binding affinity of HP1a to H3K9me (Hiragami-Hamada, *et al* 2011). Again, as for the posttranslational histone modifications, phosphorylation at different sites of HP1 results in different readouts, e.g., human HP1γ phosphorylation at serine 83 leads to an interaction with Ku70 and results in transcription elongation (Lomberk, *et al* 2006a). Phosphorylation within the chromodomain of HP1β impairs its binding to H3K9me (Ayoub, *et al* 2008). Sumolyation of the hinge region targets HP1α to pericentric domains (Maison, *et al* 2011).

1.6 Mechanism of silencing by heterochromatin

Until now, the transcriptional repression mechanism of heterochromatin remains poorly understood. Historically, heterochromatin was viewed as a rigid inaccessible chromatin fiber. But FRAP experiments with GFP-tagged human HP1 paralogs showed, surpisingly, a very high turnover rate of HP1 (Cheutin, *et al* 2003, Festenstein, *et al* 2003), suggesting a very dynamic structure. One of the possible ways might be the positioning of the nucleosomes.
Nucleosomes at active genes are well organized with a nucleosome depleted region upstream of the transcriptional start site flanked by two well positioned nucleosomes. The nucleosome depleted regions contain the TATA box, transcription factor binding sites and the site for the assembly of the transcription machinery (Jiang and Pugh 2009). Heterochromatin consists of more regularly spaced nucleosomes and harbors fewer nucleosome free regions or hypersensitive sites. This is also true for genes and transgenes placed ectopically in heterochromatin. There they lose their typical nucleosome positioning, especially the NFR (Sun, *et al* 2001). For example, a loss of TFIIB, GAGA factor and RNA polymerase II was observed when heat shock genes were placed in heterochromatin (Cryderman, *et al* 1999). With the recruitment of HDACs, the histone turnover is slowed down, enforcing the repressive nature of histones (Aygun, *et al* 2013). In *S. pombe* a different mechanism was recently proposed. Swi6 dissociates from heterochromatin upon binding RNA transcripts. Swi6 passes the RNA on to Cid14, which degrades the RNA. This proposed mechanism also leads to transcriptional repression but still allows transcription of heterochromatic regions (Keller, *et al* 2012).

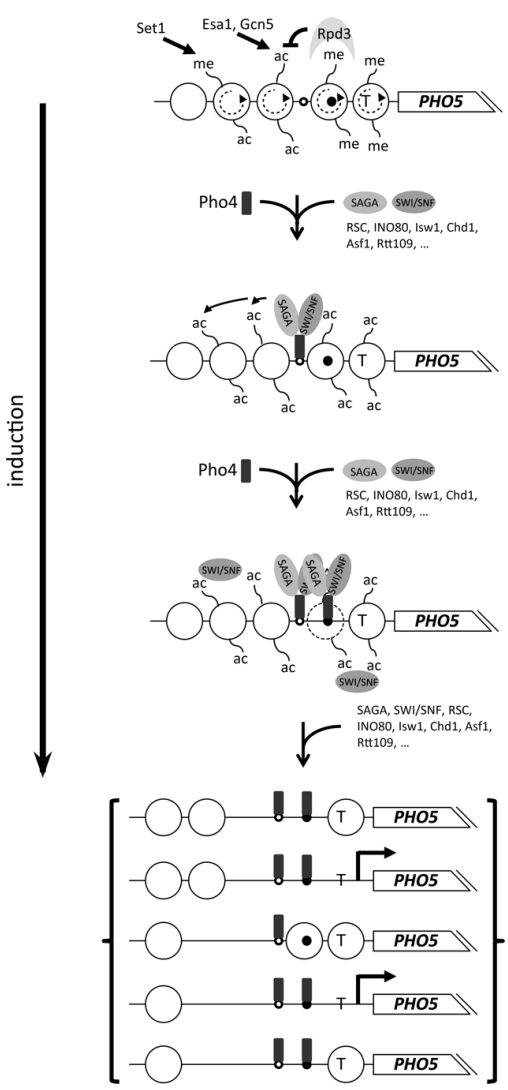

Fig. 6 Model of *PHO5* activation. On the top the repressed state of the *PHO5* promoter is shown with 5 well-positioned nucleosomes. Methylation of H3K4 by Set1 recruits histone deacetlyase Rpd3. Rpd3 keeps histone acetylation levels low and thus the histone turnover (shown by stippled arrows). Upon phosphate starvation, Pho4 (rounded rectangle) binds UASp1 (open small circle). Pho4 recruits the SAGA complex (containing Gcn5) and SWI/SNF. Histones are hyperacetylated and the -2 nucleosome (stippled circle in third panel) is remodeled by SWI/SNF and / or additional remodelers. This makes the UASp2 site available for binding of Pho4. Continued recruitment of cofactors by Pho4 leads to further remodeling and disassembly of the nucleosomes. Different possible states of remodeled *PHO5* promoter chromatin in the induced state are shown in the bracket. Reprinted from (Korber and Barbaric 2014) with the permission of Oxford University press.

1.7 The *PHO* promoters – prime examples for the interplay of chromatin modifying enzymes in gene regulation

The dissection of the mechanism underlying the induction of *PHO5* yielded great inside in chromatin biology during the past 30 years.

Upon extracellular and especially intracellular phosphate starvation *PHO* regulon genes are induced, among them *PHO5*, coding for an acid phosphatase, *PHO8*, an alkaline phosphatase and *PHO84*, an inorganic phosphate transporter (Korber and Barbaric 2014). The promoters of *PHO5*, *PHO8* and *PHO84* in the repressed state have well positioned nucleosomes, covering the TSS (transcription start sites) and in case of *PHO5* and *PHO84* also some upstream activating sequences of the *PHO* regulon (UASp) (Almer and Horz 1986, Almer*, et al* 1986, Barbarić*, et al* 1992, Wippo*, et al* 2009). In phosphate rich cells, the principal transcription activator Pho4 is phosphorylated by the cyclin/cyclin dependent kinase pair Pho80/85. This directly impairs the interaction with the transcription co-factor Pho2, exports Pho4 to the cytoplasm and hinders the translocation into the nucleus. During phosphate starvation, Pho81 inhibits the Pho80/Pho85 complex, Pho4 is no longer phosphorylated and is translocated into the nucleus (reviewed in (Korber and Barbaric 2014)). At the *PHO5* promoter, Pho4 binds to the UASp sites in conjunction with the homeobox-type transcription cofactor Pho2. This leads to recruitment of the SAGA complex, which hyperacetylates histones (Fig. 6) (Reinke and Hörz 2003). Remodelers are tethered via bromodomains to the acetylated histones but are also directly recruited by the acti-

vation domain of Pho4. Chromatin remodeling leads to eviction of histones thereby creating an extensive hypersensitive site (Boeger, *et al* 2003, Boeger, *et al* 2004, Korber, *et al* 2004). Interestingly, it was shown at *PHO5* that the hyperacetylation by Gcn5 does not affect the final transcription levels of *PHO5* but is rather responsible for rapid induction kinetics of *PHO5* (Barbaric, *et al* 2001a, Gregory, *et al* 1998). Despite their common transcription factor Pho4, other *PHO* promoters have different cofactor requirements for promoter opening (Gregory, *et al* 1999b, Musladin, *et al* 2014, Wippo, *et al* 2009). While at *PHO5* five remodelers (RSC, SWI/SNF, INO80, ISWI and CHD1) participate in a redundant way, *PHO8* promoter remodeling mainly depends on SWI/SNF with some participation of INO80. At the *PHO84* promoter the so-called upstream nucleosome is essentially dependent on SWI/SNF for remodeling. This argues that the local chromatin structure rather than the transactivator determines cofactor requirements for promoter chromatin opening.

1.8 Aim of this study

The H3K9 methylation mark and HP1a binding are clearly necessary for heterochromatin formation from *S. pombe*, to *Drosophila melanogaster*, mouse and humans. We ask here to which extent these two factors are sufficient to create a repressive chromatin state.

In a synthetic biology approach, we expressed the *Drosophila* H3K9 methyltransferase dSu(var)3-9 and HP1a in *S. cerevisiae*, which lacks H3K9me and HP1 and only possess rudimentary heterochromatic regions silenced by the SIR proteins. This heterologous system gives us the excellent opportunity to study the effect of H3K9me and HP1a in a mechanistically "neutral" background *in vivo*.

dSu(var)3-9 was fused to the Pho4 DNA binding domain (DBD), allowing a targeted approach at the well-studied *PHO* promoters. With the powerful yeast genetics, we studied effects of HP1a and dSu(var)3-9 containing mutants on *PHO* promoter chromatin and induction, also in different yeast backgrounds regarding chromatin cofactor gene mutations. In addition to the targeted approach we also examined genome-wide effects upon introduction of H3K9me and HP1a in yeast.

2 Materials and Methods

2.1 Materials

2.1.1 Chemicals

Name	Supplier
3-amino-1,2,4-triazole	Sigma-Aldrich
4-nitrophenyl-β-D-galactopyranoside	Fluka
5-fluoroorotic acid	Toronto Research Chemicals Inc
acetic acid	Sigma-Aldrich
acidic phenol	Roth
agarose	Seakem ME Biozym
amino acids	Sigma-Aldrich /Merck
ampicillin	Roth
bacto agar	Becton Dickinson
bacto peptone	Becton Dickinson
bacto yeast extract	Becton Dickinson
bacto yeast nitrogen base	Becton Dickinson
bromphenol blue	Merck
bsa	Sigma-Aldrich
chloroform	VWR
Novex, colloidal blue staining kit	Invitrogen
complete® protease inhibitors	Roche
diamide	Sigma-Aldrich
dNTP mix	NEB
EDTA	Sigma-Aldrich
EGTA	Sigma-Aldrich
ethanol	Sigma-Aldrich
ethidiumbromide	Roth
ficoll	Sigma-Aldrich
formaldehyde	Sigma-Aldrich
g418 sulfate	Calbiochem, VWR
galactose	Sigma-Aldrich
gel loading dye (6x)	NEB
glucose	Sigma-Aldrich
glycogen	Roche
HEPES	Roth
Igepal CA-630 (NP-40)	Sigma-Aldrich
isoamylalcohol	Merck
methanol	Sigma-Aldrich
4-nitrophenyl phosphate disodium salt hexahydrate	Sigma-Aldrich

PEG 4000	Roth
phenol	Roth
PMSF	Sigma-Aldrich
raffinose	Sigma-Aldrich
RNAlater	Ambion
SDS	Serva
sorbitol	Serva
sulfuric Acid	Sigma-Aldrich
ß-Mercaptoethanol	Sigma-Aldrich
trichloroacetic acid	Sigma-Aldrich
Tris	national diagnostics
triton X-100	Sigma-Aldrich
tween 20	Sigma-Aldrich
ECL Western blotting detection reagents	GE Healthcare
Yeast Nitrogen Base without AA and without phosphate	Formedium
γ-P^{32}-ATP	Hartmann Diagnostics

All other chemicals not mentioned above were obtained from Merck (analytical grade).

2.1.2 Enzymes

Name	Supplier
Cla I	Roche
DNase I (RNase-free)	Roche
Pfu turbo polymerase	Agilent
Phusion polymerase	Finnzymes/NEB
Proteinase K	Roche
RNase	Roche
Taq Polymerase	NEB
TaqMan Universal PCR Master Mix	Applied Biosystems
Trypsin	Promega
Zymolyase	MP Biomedicals

All other enzymes not mentioned above and especially restriction enzymes were purchased from NEB.

2.1.3 Antibodies

Name	Supplier	Application	Dilution / Volume
α-FLAG (mouse)	Sigma-Aldrich	Western Blot	1:1000
α-H3 (1791) (rabbit)	Abcam	ChIP, Western Blot	2 µl / 1:1000
α-H3K9me2 (1220) (mouse)	Abcam	ChIP	10 µl
α-FLAG M1 affinity gel	Sigma-Aldrich	ChIP	12 µl
ECL secondary antibodies	VWR	Western blot	1:10 000

2.1.4 Others

Name	Supplier
100 bp Ladder	NEB
2-Log Ladder	NEB
Agilent DNA 1000	Agilent
Agilent RNA 6000 nano	Agilent
Agilent RNA 6000 pico	Agilent
Bürker counting chamber	Marienfeld
Bioruptor TPX tubes 15 ml	Diagenode
Freeze 'N' squeeze DNA Gel Extraction Spin Columns	Biorad
Carbon top tips	Glygen
GeneChip Hybridization, Wash and Stain Kit	Affymetrix
GeneChip 3'IVT Express Kit	Affymetrix
GeneChip Yeast Genome 2.0 Array	Affymetrix
Glass beads 0,5mm dia	Roth
MaXtract™ High Density	Qiagen
MicroAmp Optical 96-Well Reaction Plate	Applied Biosystems
Nitrocellulose Blotting Membrane	GE Healthcare
Nylon Tranfer Membrane, Biodyne B 0.45 µm	Pall Corporation
Prime-It II Random Primer Labeling Kit	Agilent
Protein G Sepharose 5 Fast Flow	Agilent
Protein Marker IV	Peqlab
QIAquick Gel Purification Kit	Qiagen
QIAquick PCR Purification Kit	Qiagen
Quiagen Plasmid Kits (Mini, Midis, Maxis)	Qiagen
RNeasy Mini Kit	Qiagen
Super RX Fuji medical X-Ray	Fuji
SpikeTides – Peptide Librarys (see supp. table 5.4)	JPT Peptide Technologies GmBH
XCell SureLock Mini-Cell	Invitrogen
XCell SureLock Mini-Cell Blot Module	Invitrogen

2.2 Standard protocols for working with DNA

Standard protocols and buffers, that are not mentioned here were done according to (Sambrook*, et al* 1989). This includes especially agarose gel electrophoresis, SDS-PAGE gel electrophoresis, cloning and standard buffers. For standard applications, DNA was measured with a Nanodrop system (Thermo Scientific). Quiagen kits were used for plasmid preparations.

2.2.1 Plasmids

All Plasmids were verified by sequencing (MWG-Biotech AG).

Plasmid	vector-backbone	Primer	REs for cloning	comments	Source
bluescript sk-					Korber group
cleu					Korber group
dSu(var)3-9	pEG202	5'-GCT AGC GGG CCT CAG GGG ATG GCC ACG GCT GAA GCC-'3 5'-AAG CTT GGA GTT GAT TGT ATG CTT GGT ATA GCT TG-'3		lexA-DBD was cut out of vector (lexA-DBD/dSu(var)3-9 (pEG202) using the given primers	this study
dSu(var)3-9	pRS406	5'-GCT AGC GGG CCT CAG GGG ATG GCC ACG GCT GAA GCC-'3 5'-AAG CTT GGA GTT GAT TGT ATG CTT GGT ATA GCT TG-'3		lexA-DBD was cut out of vector (lexA-DBD/dSu(var)3-9 (pRS406) using the given primers	this study
FLAG-HP1a	pEG202		NcoI / XhoI	FLAG-HP1a orig-inaly in HP1a pPac FLAG	this study
HP1a pPac FLAG	pPac FLAG				Jochen Abel, Imhof group
lexA-DBD/dSu(var)3-9	pEG202				kind gift of Gunter Reuter, Halle
lexA-DBD/Su(var)3-9	pRS406	5'-GGC AGA CCA GAG CTC TGG GAA ATG ATG GTA AAT GAA ATA G-'3 5'-GGC AGA CCA GAG CTC TGG CGA TCC GTG TGG AAG AAC GAT TAC-'3	SacI	ADHpromoter LexA-DBD/dSu(var)3-9 and ADH termina-tor were amplified with given primers (template: lexA-DBD/dSu(var)3-9 pEG202)	this study
p416-GAL1-lacZ					Korber group
pCB84a_1					Korber group
pEG202 empty	pEG202	5'-GAA TTC CCG GGG ATC CGT CGA CCA TGG CGG		lexA-DBD/dSu(var)3-9	this study

		CCG CTC GA-'3 5'-AAG CTT GGA GTT GAT TGT ATG CTT GGT ATA GCT TG-'3		was cut out of vector using given primers	
Pho4-DBD/dSu(var)3-9	pRS406	5'-TCA GTA CGG CCC TCA GGC GTG CTC ACG TTC TGC TGT A-'3 5'-TCA GTA CGG CCC TCA GGC GTG CTC ACG TTC TGC TGT A-'	NHE I / BSU 36 I	PHO4-DBD fragment (template pP4-12 SP4 SP6 mutated) was blunt-end in bluescript sk-, PHO4-DBD was cut out with Nco I / Xho I, then inserted in dSu(var)3-9 (pRS406)	this study
pP4-12neu					Korber group
pP8apain					Korber group
pPZ Ura Var33		5'-CTA GAT AA GCT T C TGA GAG TGC AC CAT ACC AC-'3 5'-CTA GAT AA GCT T T TAG TTT TGC TGG CCG CAT C-'3	Hind III	Leu marker was cut out by Hind III, ura marker was inserted	this study
pPZleuV33					this lab
pUG6					Kind gift of Ramón Ramos Barrales, Barcelona/ Munich

2.2.2 Chemically competent *E. coli*

A logarithmic *E. coli* culture, grown in 100 ml LB medium to an OD_{600} of 0.5 (Spectrophotometer, Pharmacia Biotech, Ultrospec 2000), were centrifuged (15 min, 6000 x g, 4°C, Heraeus Kendro Cryofuge 6000i), resuspended in 30 ml ice cold TFBI buffer (30 mM KOAc, 100 mM KCl, 50 nM $MnCl_2$, 15% (v/v) glycerol, pH 5.8 adjusted with acetic acid; sterile filtered with 0.2 µm filter, stored at 4°C), and incubated for 30 min on ice. Cells were centrifuged again (5 min, 1000 x g, 4°C, Eppendorf 5810R), resuspended in 4 ml ice cold TFBII buffer (0 mM MOPS/NaOH, pH 7.0 75 mM $CaCl_2$, 10 mM KCl, 15% (v/v) glycerol, sterile filtered: 0.2 µm filter, stored at 4°C), and incubated for 10 min on ice. Aliquots of 200 µl were shock frozen in liquid nitrogen and stored at -80°C.

2.2.3 Transformation of chemically competent *E. coli*

DNA was added to 50 µl or 100 µl of chemically competent cells (XL1 Blue, DH5α). The cells were incubated on ice for 30 min and heat shocked for 45 sec at 42°C. Afterwards 900 µl

of LB medium were added and cells were incubated for 30 min at 37°C. Then cells were plated on LB plates with the respective antibiotics. Plates were placed o/n at 37°C. Colony-forming units (CFU) were picked the next day and streaked out for single colonies.

2.2.4 Special cloning techniques

2.2.4.1 Site directed mutagenesis

The lexA binding sites at the *PHO* promoters and other point mutations were created using the Quickchange II Site-Directed Mutagenesis Kit with alterations made to the protocol. Primers were designed using the recommendations of the manual provided or using the Primer Design Program provided by Agilent. For multiple site directed changes more than one primer pair was necessary. All primers are listed in 2.4.2.2.

PCR reaction:

10x *Pfu* buffer	2 µl
dNTPs	200 µM
each Primer	0.2 µM
Pfu Turbo Hotstart Polymerase (2,5 U/µl)	0,5 µl
Plasmid	50-60 ng

fill up to 20 µl with water

PCR cycle:

95°C	30 sec	
95°C	30 sec	x 17
55°C	1 min	
68°C	10.5 min	
4°C	∞	

After the PCR, methylated template was digested by the addition of 1 µl *Dpn I (20000 units/ml),* incubated for 1 h at 37°C, and the DNA was transformed into chemically competent *e. coli* cells.

2.2.4.2 Primers for site directed mutagenesis

Plasmids	Primer (5'-3')
cleu_neu1 (correction of reading frame, insertion at bp580)	5'-GTG ACC AAT TCA ACA TCA CCT TGC AGA CTG TCA GTG AAG-3' 5'-CTT CAC TGA CAG TCT GCA AGG TGA TGT TGA ATT GGT CAC-3'
cleu_lexA_BS (insertion of lexA_BS)	5'-AAA CGA AGG TAA AAG GTT CAT AGC GCT TTT TCT TTG TCT GCT ACT GTA TAT ATA TAT TAA ATT AGC ACG TTT TCG CAT AGA ACG CAA CTG-3' 5'-CAG TTG CGT TCT ATG CGA AAA CGT GCT AAT TTA ATA TAT ATA TAC AGT AGC AGA CAA AGA AAA AGC GCT ATG AAC CTT TT A CCT TCG TTT-3' 5'-GTT CTA TGC GAA AAC GTG CTA ATA CTG TAT ATA TAT ACA

	GTA GCA GAC AAA GAA AAA GCG CTA TGA ACC-3’ 5’-GGT TCA TAG CGC TTT TTC TTT GTC TGC TAC TGT ATA TAT ATA CAG TAT TAG CAC GTT TTC GCA TAG AAC-3’
pP8apain_lexA_BS (insertion of lexA_BS)	5’-AGA AGA AGG CGT AGC AGA TAA GAA GTA CTG TAT ATA TAT ACA GTA CGG GTA AAG GCA AGG AAG A-3’ 5’-TCT TCC TTG CCT TTA CCC GTA CTG TAT ATA TAT ACA GTA CT T CTT ATC TGC TAC GCC TTC TTC T-3’
pCB84a_l_lexA_BS	5’-AAG AAA CTA ATT TAT CAG CTA CTG TAT TAT CAA CCG TTA TTA CCA AAT TA-3’ 5’-TAA TTT GGT AAT AAC GGT TGA TAA TAC AGT AGC TGA TAA ATT AGT TTC TT-3’ 5’-CTA ATT TAT CAG CTA CTG TAT ATA TAA CCG TTA TTA CCA A-3’ 5’-TTG GTA ATA ACG GTT ATA TAT ACA GTA GCT GAT AAA TTA G-3’ 5’-TTT ATC AGC TAC TGT ATA TAT ATA CAG TAT TAC CAA ATT A-3’ 5’-TAA TTT GGT AAT ACT GTA TAT ATA TAC AGT AGC TGA TAA A-3’ 5’-GGC AGA CCA GAG CTC TGG GAA ATG ATG GTA AAT GAA ATA G-3’ 5’-GGC AGA CCA GAG CTC TGG CGA TCC GTG TGG AAG AAC GAT TAC-3’ 5’-AGG GAA TTC ACA TGA CGA AAC TAA TCG CTC C-3’ 5’-GGA GCG CCT CGA GTC AGT TTA AAG GTG TAC TCT G-3’ 5’-GGA GCG CCT CGA GAG AAG AGA ACT TTC TTT GGC-3’ 5’-TCA GTA CGG CAC CGG TAT GGG CCG TAC AAC TTC TG-3’ 5’-TCA GTA CGG CCC TCA GGC GTG CTC ACG TTC TGC TGT A-3’ 5’-ACC GGT GGG CCT CAG GGG ATG GCC ACG GCT GAA GCC-3’ 5’-TTT ATC AGC TAC TGT ATA TAT ATA CGT TAT TAC CAA ATT A-3’ 5’-TAA TTT GGT AAT AAC GTA TAT ATA TAC AGT AGC TGA TAA A-3’ 5’-TTT ATC AGC TAC TGT ATA TAT ATA CAG TAT TAC CAA ATT A-3’ 5’-TAA TTT GGT AAT ACT GTA TAT ATA TAC AGT AGC TGA TAA A-3’
lexA-DBD/dSu(var)3-9 set_mut (pEG202) Pho4-DBD/dSu(var)3-9 set_mut (pRS06) dSu(var)3-9 set_mut (pRS06)	5’-ACT ATG GCA ACA TCT CGC ACT TTA TCA ATA AGT CTT GCG ATC CTA AT-3’ 5’-ATT AGG ATC GCA AGA CTT ATT GAT AAA GTG CGA GAT GTT GCC ATA GT-3’
FLAG-HP1a V26M (pEG202)	5’-GGA GGA GGA GTA CGC CAT GGA AAA GAT CAT CGA-3’ 5’-TCG ATG ATC TTT TCC ATG GCG TAC TCC TCC TCC-3’
FLAG-HP1a I152F (pEG202)	5’-TGG AGG CCG AAA AGT TCT TGG GTG CCT CC-3’ 5’-GGA GGC ACC CAA GAA CTT TTC GGC CTC CA-3’
PHO4_SP4S152A_1 PHO4_SP4S152A_2 (for continous nuclear import)	5’-AGG TCC TCT TTG GAA TTC ACG GAG CCC CGT ATT TGA-3’ 5’-TCA AAT ACG GGG CTC CGT GAA TTC CAA AGA GGA CCT-3’
PHO4_SP6P223A_1 PHO4_SP6P223A_2 (for continous nuclear import)	5’-GTA GCA AGT GAG TCT GCT GTA ATC GCG CCG C-3’ 5’-GCG GCG CGA TTA CAG CAG ACT CAC TTG CTA C-3’

2.2.4.3 Gibson cloning

Gibson cloning was performed as previously described (Gibson, *et al* 2010, Gibson, *et al* 2009). This cloning technique was performed to insert FLAG-HP1a into the promoter Library (see below). Vector was Dpn I digested after PCR.

Gibson Assembly 5x Buffer:

Tris/HCL pH 7.5	450 mM
PEG 8000	25 mM
$MgCl_2$	50 mM
DTT	50 mM
dNTPs	1 mM
NAD^+	5 mM

1.33x final reagent mix

5x Buffer	1.33 µl
T5 exonuclease	0.005 U/µl
Phusion Polymerase	0.033 U/µl
Taq Ligase	5.333 U/µl

15 µl aliquot was added to a 5 µl mix of plasmid/insert (1:2 molar ratio). 150 ng of vector was used. Molar ratio was calculated using the In-Fusion Molar Ratio Calculator: (http://bioinfo.clontech.com/infusion/molarRatio.do ("In-Fusion® Molar Ratio Calculator,"). Reaction was incubated for 60 min at 50°C. 2 µl of the reaction were transformed into *E. coli* cells.

2.2.4.3.1 Plasmids and primers used for Gibson cloning

Gibson cloning was done for expressing HP1a in a promoter library published by (Blazeck, *et al* 2012). Plasmids and Primers are listed below. YFP was cut out by PCR.

2.2.4.3.1.1 Plasmids: galactose inducible promoter library

Tube number	Plasmid name
284	Gal4pBS2 Pleum
285	Gal4pBS1 Pleum
286	Gal4pBS12 Pleum
287	Gal4pBS24 Pleum
288	UASgal CU2 Pcyc
289	Gal4pBS4 Pleum
290	Gal4pBS3 Pleum
291	UASgal CU1 Pcyc
292	Gal4pBS13 Pleum
293	UAS gal Pcyc
294	UAS gal A9 Pcyc

295	Gal4pBS34 Pleum
296	Gal4pBS134 Pleum
297	UASgal
298	Pgal
299	UASgal Pgal

Kind Gift of (Blazeck, *et al* 2012).

2.2.4.3.1.2 Primers

Primer name	Primer Sequence	specific for
Express_lib_for	5'-ATCGATACCGTCGACCTCGA-'3	
Express_lib_rev	5'-TTTTCTAGATAGAATGGTATATCCT-'3	for plasmids #284-297
Express_lib_ UASgal1_pgal1_rev	5'-TTTTCTAGATAGAATGGTATATCCT-'3	for plasmids #298-299
HP1a_libr_int_for	5'-TTTCAAGGATATACCATTCTATCTAGAAAAATG-GACTACAAGGACGACGA-'3	for plasmids #284-297
HP1a_libr_int_rev	5'-ATTACATGACTCGAGGTCGACGGTATCGATT-TAATCTTCATTATCAGAGTACCAGGAT-'3	
HP1a_UASgal1_pgal1_for	5'-GTCAGGAGAAAAACCCCGGATTCTAGAAAAAT-GGACTACAAGGACGACGA-'3	for plasmids #298-299

2.2.5 DNA purification and precipitation

2.2.5.1 Ethanol precipitation

2.6 volumes of ethanol were added to the sample, mixed by flicking and incubated on ice for 10 min. Then centrifuged in a tabletop centrifuge at top speed for 30 min at 4°C. Supernatant was discarded, pellet washed with 70% ethanol and centrifuged at RT for 2.5 min. Pellet was dried at RT and resuspended in TE or respective buffer.

2.2.5.2 Phenol extraction

Sodium perchlorate ($NaClO_4$) was added to a final concentration of 1 M. One volume of phenol was added and thoroughly vortexed. The same volume of isoamyl alcohol/chloroform (4%/96%) (IAC) was added, vortexed, and then centrifuged in a tabletop centrifuge at maximum speed at RT for 5 min. Aqueous upper phase was transferred to a new tube, one volume of IAC was added, and sample was again vortexed and centrifuged. Upper phase was transferred to a new tube and was further processed.

2.3 Working with *S. cerevisiae*

2.3.1 *S. cerevisiae* strains

yeast strain	genotype	source
CY337	*MAT**a** ura3-52 lys2-801 ade2-101 leu2-Δ1 his3-Δ200*	C. Peterson
CY339	CY337 *pho5*::*URA3*	(Wippo, *et al* 2009)
CY339 *pho5::ura3*	CY339 *pho5::ura3* (mutated *ura3* allele after passage over 5-FOA plates)	this work
YS18	*MATα*, *his*3-11 *his*3-15 *leu*2-3 *leu*2-112 can^R *ura3*Δ5	(Sengstag and Hinnen 1987)
BY4741		(Brachmann, *et al* 1998) via EUROSCARF
BY4742	*MATα his3Δ1 leu2Δ0 lys2Δ0 ura3Δ0*	Kind gift of Randy Morse
LPY7091		(Lo, *et al* 2005); kind gift of Shelly Berger via Slobodan Barbaric
LPY7091 *pho5::ura*	LPY7091 *pho5::ura*	this work
CY339 *rph1::KanMX4*	CY339 *rph1::KanMX4*	this work
CY339 *rph1::KanMX4*	CY339 *rph1::KanMX4*	this work
Y04315	BY4741; *Mat a his3D1 leu2Δ0 met15D0 ura3D0 pho8::kanMX4*	EUROSCARF
Y06165	BY4741; *MAT a his3Δ1 leu2Δ0 met15Δ0 ura3Δ0 YER169w::kanMX4 (rph1Δ)*	EUROSCARF
CY337 *hos1::KanMx6*	CY337 *hos1::KanMx6*	this work
CY337 *hos2::KanMx6*	CY337 *hos2::KanMx6*	this work
CY337 *hos3::KanMx6*	CY337 *hos3::KanMx6*	this work
CY337 *hda1::KanMx6*	CY337 *hda1::KanMx6*	this work
CY337 *rpd3::KanMx6*	CY337 *rpd3::KanMx6*	this work
gal11Δmed3Δ	*MATα pgd1Δ::kanMX4 gal11Δ::kanMX4 his3Δ1 leu2Δ0 lys2Δ0 met15Δ0 ura3Δ0*	Kind gift of Randy Morse
RMY521 (*SRB4* WT)	*MATa his3Δ1 leu2Δ0 met15Δ0 ura3Δ0 srb4Δ::KanMx SRB5-13MCY::HIS3 (S.K.) RY2844 (CEN LEU2 SRB4)*	Kind gift of Randy Morse
RMY522 (*srb4 ts*)	*MATa his3Δ1 leu2Δ0 met15Δ0 ura3Δ0 srb4Δ::KanMx SRB5-13MCY::HIS3 (S.K.) RY2844 (CEN LEU2 srb4-138)*	Kind gift of Randy Morse
Z579 (WT)	*Mat a, his3Δ200, leu2-3,122, ura3-52, srb4Δ2::HIS3 [pCT181/RY2882 (SRB4 LEU2 CEN)]*	Kind gift of Randy Morse
Z111 (*rpb1-1ts*))	*Mat alpha, ura3-52, his3Δ200, leu2-3,122, rpb1-1, ade2*	Kind gift of Randy Morse

A complete list of generated strains for this work can be found in the Supplementary.

2.3.2 HDAC disruptions

Primer	Sequence	Source
HOS1 ko5	5'ATGTCGAAATTGGTCATATCAACGTCAATATT TCAGTCTCGCATAGGCCACTAGTGGATCTG'3	kind gift of Ramón Ramos Barrales
HOS1 ko3	5'TTACAGTTCGTAAAACTTCATAAGTTCGACCA TATCTCTACAGCTGAAGCTTCGTACGC'3	
HOS2 ko5	5'ATGTCTGGAACATTTAGTTATGATGTGAAAAC AAAGGAGAGCATAGGCCACTAGTGGATCTG'3	
HOS2 ko3	5'CTATGAAAAGGCAATCAATCCACTGTTTTCTT TTTCCATTCAGCTGAAGCTTCGTACGC'3	
HOS3 ko5	5'ATGTCTTCCAAGCATTCAGATCCATTGGAGAG ATTTTATAGCATAGGCCACTAGTGGATCTG'3	
HOS3 ko3	5'TCACCATCTTCCACCACTTCTTGTTGTATGTTT TCTTGAACAGCTGAAGCTTCGTACGC'3	
HDA1 ko5	5'ATGGATTCTGTAATGGTTAAGAAAGAAGTAC TGGAAAATCGCATAGGCCACTAGTGGATCTG'3	
HDA1 ko3	5'TCATTCTTCATCACTCCATTCTTCAAACGAAT CCAGTATACAGCTGAAGCTTCGTACGC'3	
RPD3 ko5	5'AAGCAACACCTTTTGATCCGATCACGGTCAA GCCAAGCGAGCATAGGCCACTAGTGGATCTG'3	
RPD3 ko3	5'ATTGTCATGCTCAACATGTAGGTCCCTCGCAT ATTGCGAACAGCTGAAGCTTCGTACGC'3	

Disruptions were done as previously described (Barrales*, et al* 2012, Lorenz*, et al* 1995). PCR was performed with above-mentioned primers, as template served the pUG6 vector.

2.3.3 *S. cerevisae* growth conditions and media

Yeast strains were grown, if not stated otherwise, at 30°C in their respective medium, either YPDA or YNB selection medium for strains carrying plasmids. For phosphate starvation, yeast was grown logarithmically in YPDA or YNB medium, washed and then resuspended in YNB without phosphate (Formedium). Galactose induction was done as previously described in (Barbaric*, et al* 2001a).

2.3.3.1 Diamide induction

Cells were grown to log-phase at 30°C while shaking, then treated for 15 min with 1.5 mM Diamide. At 13 min, cells were collected in pre-warmed (30°) Eppendorf R5810 centrifuge at 4000 rpm for two minutes. Cells were immediately resuspended in 500 µl RNAlater (Ambion, AM7020) and snap frozen in liquid nitrogen.

2.3.3.2 Yeast extract peptone dextrose adenine (YPDA)

1% (w/v) yeast extract, 2% (w/v) peptone, 2% (w/v) glucose, 100 mg/l adenine, 1 g/l KH_2PO_4

2.3.3.3 Yeast nitrogen base (YNB)

6.7 g/l YNB w/o amino acids, 1.6 g drop-out mix, 2% (w/v) glucose
add according to auxotrophy: 84 mg/l histidine, 84 mg/l uracil, 84 mg/l tryptophan, 164 mg/l leucine
drop-out mix: 3 g adenine, 2 g L-alanine, 0.2 g p-aminobenzoic acid, 2g L-arginine, 2 g L-asparagine, 2 g L-aspartic acid, 2 g L-cysteine, 2 g glutamic acid, 2 glutamine, 2 g glycine, 2 g isoleucine, 2 g myo-inositol, 2 g L-lysine, 2 g L-methionine, 2 g L-phenylalanine, 2 g L-proline, 2g L-serine, 2 g L-threonine, 2 g L-tyrosine, L-valine

2.3.3.4 Yeast nitrogen base without phosphate

5.9 g/l YNB w/o amino acids w/o phosphate (Formedium), 1.6 g drop-out mix, 0.55 g KCl 2% (w/v) glucose
add according to auxotrophy: 84 mg/l histidine, 84 mg/l uracil, 84 mg/l tryptophan, 164 mg/l leucine.

2.3.4 Yeast transformation

OD was measured using the Zeiss PMQII photometer.

Yeast were grown logarithmically o/n to 2-4 OD_{600}/ml. Cells were centrifuged (5 min, 4000 rpm, 20°C, Eppendorf R5810) and washed once with sterile TE (pH 7.5). Cell pellet was re-suspended in TE to a final concentration of OD_{600}/ml of 50. The same volume of sterile lithium acetate (0.2 M lithium acetate) was added. Suspension was incubated in a shaker at 30 °C and 180 rpm. 100 µl of the cells were added to either 1 µg of plasmid DNA or 10 µg of fragment DNA. DNA was usually in 20 µl of buffer. Yeast-DNA mix was incubated at 30°C in an incubator for 30 min. The same volume (120 µl) of 70% polyethylene glycol (PEG) was added to the cell suspension, vortexed, and incubated again at 30°C not agitating for 1 hour. Cells were heat shocked at 42°C for 5 min, washed once in sterile H_2O. Pellet was resuspended in 100 µl sterile H_2O and plated on pre-warmed (30°C) YNB plates selective for the corresponding marker. In case of the KanMX marker, cells were grown in 5 ml YPDA at 30°C o/n not shaking and then plated on kanamycin containing plates (final concentration 200 µg/ml G418). Genome integrations were controlled by PCR. Because transformations are inherently mutagenic, 3 clones picked of each transformation.

2.3.5 Glycerol stocks

Of each yeast transformation 3 CFUs were picked and streaked out on a new plate to get single colonies. For glycerol stocks one colony of each of the 3 CFUs were picked, plated as a patch on a new plate and the inoculation loop was also put in 10 ml of the respective medium. Cells were grown to stationary phase o/n. The next day, cells were collected by centrifugation (5 min, 4000 rpm, RT, Eppendorf R5810), resuspended in 0.8 ml of the respective medium or YPDA and transferred to a screw cap tube containing 1 ml sterile 87% glycerol. After thorough vortexing cells were stored at -80°C.

2.3.6 Yeast colony PCR

With a 1 µl inoculation loop a small amount of yeast was picked from a streaked out yeast patch and resuspended in 10 µl zymolyase solution (2.5 mg/ml zymolyase, 1.2 M sorbitol, 0.1 M NaH_2PO_4 (pH7,4)). Cell suspension was incubated at 37°C for 5 min. Subsequently 2 µl were used as template for the PCR reaction (Ling*, et al* 1995).

PCR reaction:

1x PCR Buffer
200 µM dNTPS
1 µM each primer
0.5 µl *Taq* DNA Polymerase
2 µl template
add to 50 µl with ddH_2O

PCR cycle:

94°C	2 min	
94°C	30 sec	x 30
55°C	1 min	
72°C	2 min	
72°C	7 min	
4°C	∞	

2.3.7 DNA preparation from yeast

DNA preparation from yeast 10 ml culuture of stationary yeast were centrifuged at 4000 rpm for 5 min at RT (Eppendorf R5810) and washed with autoclaved water once. Pellet was resuspened in 250 µl Buffer (0.9 M Sorbitol, 50 mM NaH2PO, 140 mM β-mercaptoethanol (14.3 M)), transferred in an Eppendorf tube, 10 µl of Zymolyase 100T solution (20 mg/ml) was added and the cells were incubated at 37°C for 40 min. Optionally one can also check the lysis grade of the cells, by measuring the OD before and after the incubation with Zymolyase.

Then 10 µl (Proteinase K 20 mg/ml in 10 mM Tris-HCl, pH 8.0), 60 µl 2 M EDTA and 44 µl 20% SDS was added, mixed by inverting and the reaction was incubated for 30 min. $NaClO_4$ was added to a final concentration of 1 M (70-80 µl 5 M $NaClO_4$). 400 µl of phenol was added to the sample, vortexed at maximum speed, 400 µl isoamyl alcohol-chloroform mix (IAC) was added, vortexed again and centrifuged at maximum speed in a tabletop centrifuge (Hettich Microliter) at RT. The aqueous phase was transferred to a new tube. 400 µl of IAC was once again added, sample vortexed thoroughly, and centrifuged again. Aqueous phase was transferred in a new tube. Subsequently an ethanol precipitation was done. The pellet was resuspended in 250 µl TE. DNA/RNA mixture was digested with RNase A (10 mg/ml) for one hour at 37°C. Ehtanol precipitation was repeated and the resulting pellet was resuspended in 100 µl TE.

2.3.8 Western blot

2.3.8.1 Rapid and reliable protein extraction from yeast.

Protocol as described in (Kushnirov 2000). In short, 2.5 OD_{600} of cells were collected from liquid culture or scraped of a plate with an inoculation loop. Cells were resuspended in 100 µl distilled H_2O. 100 µl 0.2 M NaOH was added and cell suspension was incubated for 5 min at RT. Cells were centrifuged for 5 min at top speed in a tabletop centrifuge. Pellet was resuspended in 50 µl 2x PAGE sample buffer (120 mM Tris/HCl (pH 6.8), 10% glycerol, 4% SDS, 5% β -mercaptoethanol, 0.004% bromophenol blue) and boiled at 98°C for 5 min. Sample was pelleted again and supernatant transferred to a new tube. For SDS-PAGE gel 6 µl of the supernatant was used.

2.3.8.2 SDS-PAGE gel and Western blot

Proteins were separated by SDS-PAGE gel (12.5%). Gel was blotted using a wet chamber (Invitrogen). Gel, 3 mm blotting paper (Whatman) and Amersham Hybond P PVDF blotting membrane (GE healthcare) were soaked in transfer buffer (1.4 g Tris, 7.2 g glycine ad 0.4 l; 0.1 M methanol; 2% SDS). Blotting chamber was assembled according to manufacture's instructions. Blotting was performed for 3 h at a constant electric current of 300 mA.

Membrane was blocked with 5%-milk powder solution in TBS-T (5 mM Tris, 15 mM NaCl, 0.01% Tween-20, pH 7.5 adjusted with HCl) for 1 h shaking at 4°C. Primary antibody was added to a fresh 5%-milk powder TBS-T solution. Blot was incubated overnight on a rotator at 4°C. The next day blot was washed three times with TBS-T for 10 min. Suitable secondary antibody in TBS-T was added and blot was incubated for at least 1 hour on a rotator at room

temperature. Blot was washed again three times. Secondary antibody was detected with ECL Western blotting detection reagents and Super RX Fuji medical X-Ray films.

2.3.9 Growth curve

Cells were grown to a stationary OD overnight and on the next day diluted to an OD of 0.1 with 30°C fresh medium, OD was measured again and cells were shaken in an Infors shakers for 2 h. Regular measurement of OD was done after two hours and then every one to two hours for 10-14 h. It is important to always have the right dilution in order to be in the optimal measurement range of the photometer. For example, at the beginning of measurement, no dilution is necessary and after 12 h a 1:10 dilution might be necessary. Using the equation for exponential growth, doubling time of the yeast was calculated:

$$y(t) = A \cdot e^{\lambda \cdot t}$$
$$y(t2) \stackrel{\text{def}}{=} 2 \cdot y(t1)$$
$$(t2 - t1) = \Delta t = \frac{\ln(2)}{\lambda}$$

2.4 Chromatin analysis

2.4.1 Preparation of yeast nuclei

Nuclei were prepared as previously decribed in (Almer and Hörz 1986, Gregory, *et al* 1999a, Gregory and Hörz 1999). One liter of yeast culture was grown in a Fernbach flask to an OD_{600} of 2-4. Cells were collected by centrifugation (4000 rpm, 4°C, 15 min, Heraeus Kendro Cryofuge 6000i) and washed once with 50 ml ice cold water. After discarding the water, the yeast pellet was weighed. The pellet was resuspened in twice the volume of the pellet of preincubation solution (0.7 M β-Mercaptoethanol) and incubated in a shaking water bath at 30°C for 30 min. Subsequently, cells were centrifuged at 4000 rpm for 5 min (4°C, Eppendorf R5810). The pellet was washed with 1 M sorbitol and resuspended in 5 ml sorbitol-β-mercaptoethanol per gram wet-weight (1 M sorbitol, 5 mM β-mercaptoethanol). In order to check the efficiency of the cell lysis, the OD_{600} of a 1:100 dilution of the cells was measured before and after incubation with Zymolyase. 100 µl of a fresh prepared 2% Zymolyase suspension (20 mg / 1 ml H_2O) was added per gram wet-weight. The cells were then incubated again in a shaking water bath at 30°C for 30 min. OD_{600} was measured again and should be at least 60% of the initial OD_{600}. The spheroplasts were then washed with 1 M sorbitol. The final lysis step was done in a hypotonic Ficoll buffer (180 mg/ml Ficoll, 20 mM KH_2PO_4, 1 mM $MgCl_2$, 0.25 mM EGTA, 0.25 mM EDTA, pH of the solution adjusted to 6.8 with KOH). 7 ml Ficoll buff-

er per gram wet-weight were used to resuspend the spheroplasts. Aliquots were prepared ranging from 0.5 – 1 g wet weight of the initial cell pellet. The aliquots were then centrifuged at 15 000 rpm for 30 min at 4°C in a Sorvall centrifuge using an SM24 rotor. Supernatant was discarded and nuclei frozen for 10 min in a -70°C ethanol dry ice mixture and afterwards stored at -80°C.

2.4.2 DNase I digestion of yeast nuclei

Protocol was prepared as previously described (Almer*, et al* 1986, Reinke and Horz 2004). One gram of nuclei was resuspended in 6 ml cold DNase I buffer (15 mM Tris/HCl pH 7.5, 75 mM NaCl, 3 mM $MgCl_2$, 0.05 mM $CaCl_2$, 1 mM 2-mercaptoethanol), centrifuged at 4000 rpm for 8 min at 4°C (Eppendorf R5810), resuspended in 1.8 ml DNase I buffer, and divided into 6 aliquots. Nuclei were digested with different concentrations of DNase I (usually final concentration was 0.5/1/2/4/8 units/ml) for 20 min at 37°C and reactions was stopped with 28.5 µl of a SDS/EDTA/Tris premix (7,5 µl 20% SDS, 6 µl 0.2 M EDTA 8.0, 15µl 1 M Tris/HCl pH 8.8). Proteins were digested by adding 1/10 vol. of Prot K (20 mg/ml) and incubated for 30 min at 37°C. DNA was isolated by phenol/chloroform-isoamyl alcohol extraction and afterwards ethanol precipitation. Pellet was resuspended in 250 µl TE and 10 µl RNase (10mg/ml) was added for 1 h at 37°C. Again, DNA was precipitated by ethanol precipitation and resolved in 100 µl TE. Digestion degree was controlled by agarosegel. Optimal digestion degree still has some undigested DNA in the lane and the smear is in the upper half of the lane.

Secondary cleavage was performed with 40 units of restriction enzyme and 50 µl of DNA in a total volume of 150 µl for 2 h at 37°C. DNA was ethanol precipitated and resolved in 10 µl TE.

Enzymes for secondary cleavage:

PHO5 locus: ApaI

PHO8 locus: Bgl II

PHO84 locus: Ssp I

2.4.3 Restriction enzyme digestion of yeast nuclei

Protocol was prepared as previously described in (Gregory*, et al* 1999a).

0.5 g of nuclei was washed with 3 ml STEEM (0.15 mM spermine, 0.5 mM spermidine, 10 mM Tris 7.4, 0.2 mM EDTA pH 8, 0.2 mM EGTA pH 8.3, 10 mM $MgCl_2$, 5 mM 2-mercaptoethanol, 50 mM NaCl), centrifuged at 4000 rpm for 8 min at 4°C (Eppendorf

R5810), resuspended in 2 ml STEEM and aliquotized to 0.2 ml per tube. For each restriction enzyme two concentration were used that are at most 4-fold different (see table below). Reaction was carried out for 45 min (1 h for Hpa I) and stopped with 19 µl of the SDS/EDTA/Tris premix (5 µl 20% SDS, 4 µl 0.2 M EDTA 8.0, 10µl 1 M Tris/HCl pH 8.8). Followed by digestion with 1/10 vol of Prot K (20 mg/ml) and incubated for 30 min at 37°C. DNA was isolated by phenol/chloroform-isoamyl alcohol extraction and afterwards ethanol precipitation. Pellet was resuspended in 200 µl TE and 8 µl RNase (10mg/ml) was added for 1h at 37°C. Again, DNA was precipitated by ethanol precipitation and resuspended in 70 µl TE.
Secondary cleavage was performed with 40 units of restriction enzyme and 35 µl of DNA in a total volume of 200 µl for 2 h at 37°C. DNA was ethanol precipitated and resolved in 10 µl TE.

First cleavage:
PHO5 locus: Cla I (low concentration: 60 units, high concentration 240 units)
PHO8 locus: Hpa I (low concentration: 75 units, high concentration 150 units)
PHO84 locus: Hha I (low concentration: 60 units, high concentration 240 units)

Enzymes for secondary cleavage:
PHO5 locus: Hae III
PHO8 locus: EcoR V
PHO84 locus: HIND III

2.4.4 Southern blotting

DNA was separated on a 1.2% (restriction enzymes) or 1.5% (DNase I) agarose gel in 1 x TAE buffer (40 mM Tris acetate, 1mM EDTA pH8) (restriction enzymes) or 1x Loehing buffer (40 mM Tris acetate, 20 mM NaOAc, 1 mM EDTA pH8, 0.2% (v/v) acetic acid) (DNase I). 0.5 µl of sheared salmon DNA (2.5 mg/ml) and 5 µl 6 x loading dye was added to the DNase samples. The DNase samples were also run in a custom vertical chamber with a build in cooling system, this allows a smoother surface, which makes the blotting more efficient.
Nylon Transfer membrane (Biodyne B 0.45µm, Pall corporation) was soaked for 10 min in double distilled (dd) H_2O and then in 20xSSC (3M NaCl, 0.3 M Tri-NaCitrate dihydrate) for at least 10 min. Meanwhile the agarose gel was shaken in denaturation buffer (0.5 M NaOH, 1.5 M NaCl) for 20 min.

Blotting was done as original described in (Southern 1975). Two thick whatman paper were placed on a glas plate, which each end being placed in 20x SSC, on top of them the gel was placed, then the nylon membrane and two thick whatman papers soaked in 20x SSC. Putting dry tissue stacks on top of them created the capillary forces. After o/n blotting, membrane was baked for 2 h at 80°C, washed in 3x SSC for 30 min at 68°C and 3x SSC / 1 x Denhardt (0.5% SDS, 1mM EDTA, 0,02% BSA, 0,02% PVP40, 0,02% ficoll) for 2 h at 68°C.
Membrane was prehybridized in 2x SSC and 1x Denhardt with denatured salmon sperm DNA for 1 h or longer at 68°C in hybridization oven.
Preparation of Probe was done with the Prime-It II Random Primer Labeling Kit according to the manufacturer's instructions.

Input DNA for labeling reaction was generated using genomic or plasmid DNA and the following primers:

Locus	Primer
PHO5	5'-GTCTTCAGCGTCAACTTTAG-3' 5'-GCCAATGTGCAGTAGTAACT-3'
PHO8	5'-GACGGATCTCGAAGAGATCA-3' 5'-CCTGCCATCTGTAATCAACA-3'
PHO84	5'-CCTTGAGAACTTCAGTTGAC-3' 5'-GAGTGAAGGCCATCAAAATC-3'

2.5 Histon Analysis by Mass spectrometry

2.5.1 Histone preparation

Nuclei, as previously described, were prepared out of one liter of yeast cultures grown logarithmically to an OD of 2-4 OD/ml. Nuclei were resuspended with an inoculation loop and vortexed at medium speed in 7 ml of Buffer A (10 mM Tris-HCl, pH 8 / 75 mM NaCl/ 0.5% NP-40/ 1 mM PMSF), incubated for 15 min on ice and followed by a centrifugation step in an Eppendorf 5810R (4°C, 4000rpm, 5min). This was repeated two times. Afterwards the pellet was resuspended in 7 ml of Buffer B (10 mM Tris-HCl, pH 8 / 400mM NaCl / 0.5% NP-40 / 1mM PMSF), incubated for 10min on ice and centrifuged as above. This step was repeated one more time. Histones were acid extracted by resuspending the pellet in 5 ml of ice cold 0.4 N H_2SO_4. Suspension was incubated for 30 min on ice and pelleted using a Sorvall centrifuge with a SM24 rotor at 12 500 rpm (16 000 g), at 4°C for 15min. Supernatant was transferred in a new tube. For precipitation of the histones 100% TCA was added to a final concentration of 20%, followed by an incubation step for at least 1 h on ice with occasional inversion. Histones were pelleted again using the SM24 rotor (12 500 rpm, 15 min, 4°C). The pellet was washed

twice with ice-cold acetone without resuspending the pellet. Histone pellet was dried on ice afterwards and stored at -20°C or resuspended in 500 µl H_2O and stored at -20°C. Protocol was adapted from (Davie*, et al* 1981, Edmondson*, et al* 1996).

2.5.2 Preparations for Mass spectrometry

Mass spectrometry was performed as previously described in (Alabert*, et al* 2015). Histones were separated on a 17.5% SDS-PAGE gel. Gel was stained using Colloidal Blue Staining Kit (Invitrogen) according to manufacture's instructions. Corresponding H3 gel bands were cut out.

2.5.3 Destain, Acylation and Trypsin Digestion

Gel pieces were cut into pieces and resuspended in chromatography water, shaking for 5 min at 37°C or room temperature. Gel pieces were spinned down, supernatant removed and washed once with 200 µl 10 mM ammonium bicarbonate shaking for 5 min at 37°C. Followed by an incubation step of 60 min with 50% acetonitrile/50 mM ammonium bicarbonate. If gel pieces were still blue, the two previous steps were repeated.

For acetylation, gel pieces were incubated in 1 µl propionic anhydride and 10 µl 0.1 M ammonium bicarbonate. Five minutes later another 39 µl 0.1 M ammonium bicarbonate was added to the reaction, pH was checked with pH paper (should be between 7-8) and incubated for 30 min at RT. Afterwards pieces were wash 3 times with 0.1 M ammonium bicarbonate for 10 min shaking at 37°C, once with water for 10 min, and once with 50% acetonitrile.

Dehydration of gels was performed by adding 50 µl of acetonitrile after supernatant was removed. The acetonitrile was incubated for 5 min on ice. This step was repeated for another time.

Supernatant was removed again. For in gel digestion 12,5 µl of a trypsin master mix (10 µl 50 mM Ammoniumbicarbonat,1 µl trypsin (0,2 µg/µl) and 1,5 µl Spike tides (200 femtomol/µl)) were added to each well and incubated at 37°C over night. Spike tides are heavily labeled peptides that make the identification of histone peptides afterwards easier.

After digestion the peptides were now in solution and desalted using Carbon Top tips (Glygen). First the tips were washed three times with 100% ACN and equilibrated three times with 0,1% Trifluoroacetic acid. In between each step, columns were centrifuged at 1000 rpm in a tabletop centrifuge. Before the loading of the peptide solution, the columns were dried using a tabletop centrifuge at a higher speed without destroying the fragile columns.

Peptide solution was acified with TFA to a final concentration of .1% and then loaded on the column, centrifuged at around 1000 rpm in a table top centrifuge and reloaded one more time.

Collums were washed five times with 0.1% TFA. Peptides were eluted with 70% ACN / 0.1% TFA. Flow through was reloaded two more times. Eluate was speedvaced to dryness (Maxi-Vac Alpha, ScanVac/Labogene). Peptides were resuspendend in 7 µl 0.1% TFA.

2.5.4 Analyzing probes using LC-MS/MS

Resuspended peptides were injected in an Ultimate 3000 high-performance liquid chromotography using a gradient from 5% to 60% ACN in 0.1% formic acid over 40 min at 300 nl/min on a 75 µm ID x 10-cm ReproSil-Pur C1-AQ analytical column (2,4-µm) (Dr. Maisch GmBH). Outflow was directly electrosprayed in the LTQ Orbitrap XL mass spectrometer (Thermo Fisher Scientific), which operated in the data-dependent mode to automatically switch between full-scan mass spectrometry and tandem mass spectrometry acquisition. Survey full-scan spectra (m/z 250/2000) were attained with a resolution R=60,000 at m/z 400. Three lock mass ions from ambient air (m/z = 371.10123, 445.12002, and 519.13882) were used for internal calibration.

The six most intense peptide ions with charge states between 2 and 5 were sequentially isolated (window = 2.0 m/z) to a target value of 10,000 and fragmented in the linear ion trap by collision-induced dissociation (CID). Fragment ion spectra were recorded in the linear trap of the instrument. A dynamic exclusion time of 180 sec was applied. Typical mass spectrometric conditions were spray voltage 1.4 kV, no sheath and auxiliary gas flow, heated capillary temperature 200°C, and normalized collision energy 35% for CID in the linear ion trap. An activation Q = 0.25 and activation time of 30 msec were used. Data analysis was performed with XCalibur Qual browser software (Thermo Fisher Scientific) by using doubly and triply charged peptide masses for extracted ion chromatograms (XICs). XICs were checked manually, and values were exported to Excel for further calculations. (Alabert*, et al* 2015)

2.6 Chromatin Immunoprecipitation

The following protocol derived from (Aparicio*, et al* 2005, Fan*, et al* 2008, Mayer*, et al* 2010).

Yeast were grown logarithmically over at least 1 day. A 50 ml or 200 ml culture was grown overnight to a final OD of 1/ml (about 2 x 10^7 cells per ml). For crosslinking of the cells 37% formaldehyde was added to a final concentration of 1% formaldehyde (1,35 / 5,4 ml). Cells were incubated shaking slowly at RT. For quenching of the formaldehyde 5 ml / 25 ml of 3 M glycine was added and incubated shaking slowly for 5 min to a max. of 10 min at RT. Cells were harvested by centrifugation (5min, 4000 rpm, 4°C). Pellet was carefully resuspended by

gentle shaking with 20 ml / 100 ml of ice cold TBS (100 mM Tris-Cl pH 7.5, 150 mM NaCl). Afterwards pellet was resuspended in ice cold FA-Lysis buffer (50 mM HEPES pH 7.5 (adjust with KOH), 150 mM NaCl, 1 mM EDTA, 1% Triton X-100, 0,1% sodium deoxycholate, 0,1% SDS) and transferred to a 50 ml falcon and centrifuged again. The final pellet was resuspended in 1ml or 1,5 ml ice-cold lysis buffer, transferred to a 2 ml tube centrifuged again (5min, 3000 rpm, 4°C, tabletop centrifuge). Supernatant was discarded. To make the lysis more efficient the pellet was flash frozen in liquid nitrogen.

For the cell lysis, pellet was resuspended in 250 µl freshly prepared FA-Lysis buffer with protease inhibitors (Roche complete) per 50 OD and aliquotized into 50 OD cell batches in flat bottom tubes. 350µl glass beads were added to each sample and vortexed at full speed for 3 min followed by a 2 min incubation on ice in a cold room. This was repeated 12 times. For cell lysis efficiency, the OD_{600} (1:100 dilution) can be measured before and after the bead beating.

To collect the lysed cells, tubes were punctured with a hot 25-G needle and placed in a 15 ml Biorupter disposable conical tube. In our case the upper part of a 5 ml syringe served as a tube holder, because the diameter of the 15 ml tube was to big for a 2 ml tube.

Volume was adjusted to 1.2 ml with FA-lysis buffer with protease inhibitors and tubes were placed with screwed sonicator needles in the precooled water bath of the biorupter (4.5°C).

Biorupter ran on high intensity 35 cycles with 30 sec on/off. Sample was transferred to a low binding tube, centrifuged (10 min, 13 000 rpm, 4°C) and supernatant of each biological sample was pooled again. Chromatin concentration was measured using the Nanodrop and resulted in concentrations of around 1300 ng/µl. 670µl of the chromatin solution (whole cell extract) was pre-cleared with 25 µl ProtG beads for 2 h at 4°C on a rotator. Size of sheared DNA was controlled by agarose gel. For Input DNA, 30 µl of WCE was frozen away. For each immunoprecipitation 670 µl of WCE was incubated with the appropriate antibody overnight on a rotator at 4°C.

The next day ProtG beads were blocked with 10% BSA and 0.5 µg in FA-Lysis buffer for 1-2 h. 25 µl of blocked beads were added to each sample and incubated for 4 h at 4°C. Beads were pelleted and washed twice with 1 ml FA lysis buffer (high salt, 0.5 M NaCl), twice with ChIP wash buffer (10 mM Tris-Cl 8.0, 250 mM LiCl, 0.5% NP-40, 0,5% sodium deoxycholate; 1 mM EDTA) and once with TE 8.0 on a tumble board each time for 5 min. Beads were eluted with 100 µl of ChIP elution buffer (50 mM Tris-Cl, 10 mM EDTA, 1% SDS, pH 7.5) shaking at 65°C for 15min. Supernatant was transferred to new tube (screw-top) and elution was repeated.

Volume of Input DNA was adjusted to the IP-DNA volume and samples were reverse cross-linked at 65°C o/n. Samples were digested with RNaseA (final concentration 0.5 mg/ml) for 30 min at 37°C. ProtK (1 mg/ml) in TE 8.0 and 10 µg of glycogen were added to the samples and incubated for 2 h at 37°C. DNA was extracted with Phenol. For better phase separation and precise recovery of DNA high density MaXtract (Quiagen) columns were used. 400 µl of Phenol and 400 µl of IAC were added to sample, vortex for 3 min at max. speed and centrifuged for 15 min at 14.000 rpm at RT. Aqueous phase was transferred to new tube and 400 µl of IAC added to sample, mixed by inverting and centrifuged again. DNA was precipitated by standard Ethanol precipitation with the exception that LITE 8.0 (5 M LiCl, 50 mM Tris-CL pH 8) was used instead of NaCl. Pellet was resuspended and further purified using the Quiagen PCR purification kit. DNA was eluted with 100 µl EB (1/10 TE 8.0).

2.6.1.1 Taqman PCR

Quantification of IP-DNA was done using the ABI PRISM 7000 Sequence Detection System. For each sample 3 technical replicates were pipetted.

PCR reaction:

1.25 µl	Probe (5µM)
4.75 µl	forward and reverse primer (10 µM each)
6.5 µl	DNA (1:3 dilution for IP-DNA, 1:10 dilution for Input DNA)
12.5 µl	2x TaqMan Universal PCR Mastermix
25 µl	total volume

PCR cycle

50°C	2 min	
95°C	10 min	
95°C	15 sec	x 45
60°C	1 min	

2.6.1.2 Analysis of Taqman RT-PCR

Analysis of RT-PCR was done with the provided software to the ABI PRISM 7000 Sequence Detection System. For each amplicon standard curves of serial dilutions (1:5, 1:50, 1:500, 1:5000, 1:50 000) of input DNA was obtained. The logarithm of each dilution was plotted against its corresponding cycle threshold value (Ct-value). With three replicates for each dilution a standard curve was fitted. The relative amount of the immunoprecipitated DNA was derived from the slope and intercept on y-axis of the standard curve.

We further normalized the IP-DNA amount to the Input DNA prepped at the same time (% Input). For histone modifications we normalized the % IP of H3K9me2 to the H3 %IP.

2.6.1.3 Amplicons used for ChIP

Amplicon	Forward Primer (5'-3')	Reverse Primer (5'-3')	Taqman probe (5'-3')	Source
PHO5 farup	GATCAAACGGTTCATTAGACAATAGGT	TGAGTGGATATTAATCGATGGAACTC	CAGCCCGATATTTGCGCACGATG	Tim Luckenbach (LMU)
PHO5 UASp2	GAATAGGCAATCTCTAAATGAATCGA	GAAAACAGGGACCAGAATCATAAATT	ACCTTGGCACTCACACGTGGGACT AGC	Tim Luckenbach (LMU)
PHO5 5'ORF	TTATTCAATTTTAGCCGCTTCTTTG	CAATCTTGTCGACATCGGCTAGT	CCAATGCAGGTACCATTCCCTTAGGCA	Tim Luckenbach (LMU)
PHO5 cod	TGCAGACTGTCAGTGAAGCTGAA	CCCAAGCAGGACATGAGTTACA	CGCTGGTGCCAACACTTTGAGTGC	Tim Luckenbach (LMU)
PHO8 UAS	TGCGCCTATTGTTGCTAGCA	AGT CGG CAA AAG GGT CAT CTA C	ATCGCTGCACGTGGCCCGA	Tim Luckenbach (LMU)
PHO84	GAAAAACACCCGTTCCTCTCACT	CCCACGTGCTGGAAATAACAC	CCCGATGCCAATTTAATAGTTCCACGTG	Tim Luckenbach (LMU)
PHO84 cod	TACTGCCGTCGAATCTCTTG	CCATTGACCAAAATGTCTGC	TCATCCTCCAAAGGCTTCGTTCA	This study
ACT1 (Actin coding region)	TGGATTCCGGTGATGGTGTT	TCAAAATGGCGTGAGGTAGAGA	CTCACGTCGTTCCAATTTACGCTGGTTT	Tim Luckenbach (LMU)
TEL (Telomere)	TCCGAACGCTATTCCAGAAAGT	CCATAATGCCTCCTATATTTAGCCTTT	TCCAGCCGCTTGTTAACTCTCCGACA	Tim Luckenbach (LMU)
ATF2 (Alcohol O-acetyltransferase; promoter)	CGCCACAATCTCAGGCTACAT	GAAACTCGTTGAATTCGTTTACTCATT	AACTCTGTAGGCCACCGATAAATATTGCGG	Tim Luckenbach (LMU)
TRP1 (Phosphoribosylanthranilate isomerase; coding region)	TGTTTTGGCTCTGGTCAATGATT	TGGTATTCTTGCCACGACTCATC	CGGCATTGATATCGTCCAACTGCATG	Tim Luckenbach (LMU)

2.7 mRNA expression analysis

2.7.1 RNA extraction

To avoid contamination with RNase, RNase free filter tips (Gilson) and tubes (Sarstedt) were used and all buffers were prepared with DEPC water.

Yeast was grown logarithmically overnight to an OD_{600} of around 0.4-0.6 (Zeiss PMQII photometer). Cells corresponding to 15-20 OD_{600} units (for $-P_i$ conditions around 30 OD_{600}) were centrifuged (Eppendorf 5810R, 2 min, 4000 rpm, 30°C) and either resuspended in 500 µl RNAlater (Ambion, AM7020) and immediately snap frozen in liquid N_2, or resuspended in 400 µl TES (10 mM Tris-HCl, pH 7.5, 5 mM EDTA, 1% SDS). In the latter case, 400 µl acidic phenol (pH 4.3; Roth A980.2) was added, vortexed for 1 min and incubated at 65 °C for 1 h. During the incubation step, samples were vortexed every 10 min for 1 min using an Eppendorf shaker. Afterwards samples were centrifuged (Eppendorf 5810R, 5 min, 14 000 rpm, 4°C) and the upper phase transferred to a new tube. 400 µl of chloroform was added. Samples were vortexed and centrifuged (as above). The upper phase was transferred into a new tube and precipitated with 2 M LiCL and 1 ml of ice cold 100% ethanol and washed with 70% Ethanol. Pellet was air dried and resuspended in either 80 or 160 µl nuclease free water (Qiagen RNeasy kit) depending on the size of the pellet (or how well the pellet becomes resuspended in water).

80 µl of sample were incubated at RT for 15 min with 10 units of DNase I (Roche, same as for DNaseI blots) to remove DNA contamination and the RNA was purified using the RNeasy Mini kit (Quiagen). RNA was eluted with 50 µl nuclease free water.

Quality of RNA was determined with the Agilent Bioanalyzer.

2.7.2 cDNA synthesis

cDNA was prepared using the Protoscript First Strand cDNA Synthesis Kit (NEB) with random Primer mix and according to manufacturers protocol. 1 µg of total RNA was used per reaction.

2.7.3 Quantification of mRNA levels

PCR reaction:

1.25 µl	Taqman probe (stock conc. 5 µM) (MWG)
4.75 µl	forward and reverse primer (stock conc. 10 µM each)
0.75 µl	cDNA (1 µg RNA)
5.75 µl	H_2O
12.5 µl	2x TaqMan Universal PCR Mastermix (Applied Biosystems, Part no. 4304437)
25 µl	total volume

PCR cycle:

50°C	2 min	
95°C	10 min	
95°C	15 sec	x 45
60°C	1 min	

Primers/probes used for Quantification (same as described in ChIP-Protocol):
ACT1, *PHO5* cod, *PHO8* cod, *PHO84* cod

Quantification of the mRNA levels was done in three technical replicates each using the ABI PRISM 7000 Sequence Detection System.

2.7.4 Comperative Transcriptome Analysis with the use of S. pombe spike-in

Protocol was adopted from (Sun*, et al* 2012).

2.7.4.1 S. pombe RNA preparation

S. pombe cells were logarithmically grown at 30 °C in 1 l (YES medium) to an OD_{600} (Zeiss PMQII of 1, harvested (Eppendorf 5804R, 4000 rpm, 3 min, 30 °C), resuspended in 1 ml RNAlater (Ambion, AM7020) per 50 ml culture and put on ice. Cells were pooled and five replicates of 1:100 dilutions in H_2O were counted using a Bürker counting chamber under the M205 FA Leica microscope. For each dilution replicate, cells in 20 small squares were counted. The cell concentration was calculated by the mean of all five dilutions replicates. Aliquots corresponding to 1 x 10^8 cells were stored at -80 °C.

2.7.4.2 S. cerevisiae preparation

S. cerevisiae cells were logarithmically grown in 100 ml (YNB) to an OD_{600} of 1. 2x 40 ml of culture were collected by centrifugation at 4000 rpm for 3 min at 30 °C (Eppendorf 5804R), resuspended in 0.5 ml RNAlater per 40 ml culture and pooled. A 50 µl aliquot was put on ice for counting, the rest snap frozen in liquid N_2. Cells were counted as for *S. pombe* above using three 1:100 dilution replicates.

2.7.4.3 RNA preparation

One aliquot of *S. pombe* (1x10^8 cells) was mixed with 3x10^8 *S. cerevisiae* cells. RNA preparation was done as previously described.

2.7.4.4 Transcriptome analysis with Affymetrix microarrays

Beforehand RNA was analyzed using the Agilent Bioanalyzer, RNA with a better RNA Integration number then 7.0 was used for microarrays.

Transcriptome analysis was done using the Gene Chip 3'IVT Express Kit from Affymetrix

according to the supplier's manual with the following alterations: 300 ng of total RNA was used as starting material. Preparation of the Poly-A RNA Controls was adapted to the RNA amount (First dilution 1:20; second 1:50; third 1:50; fourth 3:7). 3'IVT reaction was carried out for 16 h.

RNA after 3'IVT reaction was either cleaned up with the supplied beads or Agilent RNA Clean XP beads.

Hybridization, staining and washing of microarrays (Gene Yeast Genome 2.0 Array) was again done according to manufacture's instructions (GeneChip Hybridization, Wash & Stain Kit, Affymetrix). Microarrays were scanned using the GeneChip 3000 7G scanner (Affymetrix) and GCOS (Affymetrix) software.

2.7.4.5 Bioinformatics

Bioinformatics were done by Tobias Straub. Microarray analyis was performed using R/Bioconductor. Expression values were extracted using GCRMA (library 'simpleaffy'). Subsequently, we removed probe sets that did not get MAS5 "present" calls in any condition and exhibited zero variance across all samples. Many-to-one probe set to gene relationships were resolved by retaining the one probe set with the highest inter-array variance.

Differentially expressed genes were identified by fitting a linear model and deriving a moderated t-statistics (library 'limma'). Genes with an adjusted p-value < 0.05 were called differentially expressed.

Assessment of global expression changes using S. pombe spike-in RNA was performed exactly as described in (Sun*, et al* 2012).

2.8 Enzymatic assays

2.8.1 Acid phosphatase assay

Acid phosphatase assay was measures as described in (Musladin*, et al* 2014).

Cells were grown either in phosphate containing or phosphate free medium. For phosphate induction cells were grown logarithmically to an OD_{600} (Zeiss PMQII) of around 0.5-1. Cells corresponding to 3.5 OD_{600} units were transferred into a new tube, centrifuged (Eppendorf 5810R, 5 min, 4000 rpm, 30 °C), washed once with 30 °C warm water (millipore autoclaved), resuspended in 10 ml of prewarmed phosphate free medium and further incubated overnight. For induction kinetics a larger culture volume was used (30 ml should be fine, 50 ml is on the safe side).

Cells corresponding to 2 OD_{600} units (for induced cells, but 4 OD_{600} units for $+P_i$ or early timepoints of induction when only low levels of phosphatase activity are expected) were

washed with 5 ml of 0.1 M sodium acetate (NaAc) buffer (pH 3.6, RT) and resuspended in 2 ml of the same buffer. OD_{600} of cells was measured. Cells corresponding to 0.15-0.3 OD_{600} for induced or 0.6-0.8 OD_{600} for not induced cells were collected in a final volume of 1 ml NaAc buffer.

A 20 mM solution of 4-nitrophenyl phosphate disodium salt hexahydrate in 0.1 M NaAC pH 3.6 was prepared freshly (NPP solution). NPP solution and samples were prewarmed to 30 °C in a water bath shaker for 10 min. Reaction was started by adding 1 ml of NPP solution to the 1 ml sample while shaking in the water bath at 30 °C and stopped after exactly 10 min with NaOH to a final concentration of 0.2 M NaOH. Cells were centrifuged (Eppendorf 5810R 5 min, 4000 rpm, RT), and the supernatant transferred to a cuvette. A_{410} was measured (Zeiss PMQII) against the blank (20 mM NPP solution in 0.1 M NaAC pH 3.6 and 0.2 M NaOH). Acid phosphatse activity was calculated using the following formula:

$$\frac{mOd410}{\left(\frac{OD600}{ml} \times Vol\ in\ ml \times Zeit\ in\ min\right)}$$

2.8.2 Alkaline phosphatase assay

Alkaline phosphatase assay was measured as described in (Münsterkötter*, et al* 2000).

Cells were grown as described under 2.8.1. 3 OD_{600} for induced cells (5 OD_{600} for $+P_i$) were washed in alkaline phosphatse buffer (50 mM Tris-HCl pH 8.8, 5 mM $MgSO_4$) and resuspended in 2 ml of alkaline phosphatase buffer. OD_{600} was measured (1:2,5 dilution) and 800 µl were transferred to a new tube. Cell lysis was done by adding 50 µl 0.1% SDS and 20 µl chloroform to the 800 µl od cells. Cells were vortexed and incubated at 30°C for 5 min shaking in a water bath. The reaction was started by adding 100 mM NPP in 200 µl phosphate buffer. Reaction was incubated for 5 min at 30°C and stopped with 500 µl 1 M NaOH. Cell debris was removed by centrifugation. Supernatant was transferred to a cuvette and A_{410} was measured against the blank using a Zeiss PMQII photometer.

Alkaline phosphatase activity was calculated using the same formula as mentioned under 2.8.1.

2.8.3 β-galactosidase assay

Assay was performed as previously described in (Guarente 1983, Musladin*, et al* 2014, Straka and Horz 1991). In short, 4 OD_{600} for induced cells (10 OD_{600} for not induced cells) were centrifuged and resuspended in 2 ml lac-Z buffer (60 mM Na_2HPO_4 x 2 H_2O, 40 mM NaH_2PO_4 x H_2O, 10mM KCl, 50 mM $MgSO_4$ x 7 H_2O, pH 7). For OD_{600} measurement 200µl were tak-

en (1:10 dilution). 1.6 ml was transferred to a new tube and cells were lysed by adding 100 µl 0.1% SDS and 50 µl chloroform and vortexing. Cells were shaking in a water bath for 5min at 30°C. Reaction was started with the addition of 400 µl 2-nitrophenyl β-D-galactopyranoside (ONPG) (24mg in 6ml H_2O). As soon as probe turned yellow, reaction was stopped by transferring 1 ml of the probe to a new tube with prefilled 500 µl 1 M Na_2CO_3 and time was taken. Cell debris was removed by centrifugation. Blank was prepared by adding 1 ml 1 M Na_2CO_3 to a sample before the ONPG was added. Supernatant was transferred to a cuvette and A_{410} was measured against the blank using a Zeiss PMQII photometer.
β-galactosidase activity was calculated with the following formula:

$$\frac{mOd420x1000}{\left(\frac{OD600}{ml} \times Vol\ in\ ml\ (0{,}8ml) \times Zeit\ in\ min\right)}$$

2.9 Spotting assay

Yeast were grown o/n to stationary phase. Cells corresponding to 5 OD_{600} units (Zeiss PMQ II) were transferred to a new tube and topped off to 1 ml with sterile ddH_2O. Six 1:10 serial dilutions were made with sterile ddH_2O. 10 µl of dilutions 10 exp-1 to exp-6 were spotted onto respective plate. 20 mM, 40 mM, 60 mM or 80 mM 3-amino triazole (Sigma, A8056, powder was directly added to the medium) was added to the freshly autoclaved, cooled down (hand-warm) Medium.

3 Results

3.1 Introducing H3K9me as a new methylation in mark in *S. cerevisiae*

3.1.1 dSu(var)3-9 constructs for expression in yeast

Heterochromatin in *Drosophila melanogaster*, and especially the methyltransferase dSu(var)3-9, has been extensively studied in our lab. Therefore, we chose this H3K9 methyltransferase for our studies in *S. cerevisiae*. As mentioned in the introduction, we used two approaches to investigate the effect of dSu(var)3-9 and Fig. 7 shows the respective constructs created for this work. In the non-targeted approach dSu(var)3-9 was either expressed under control of the constitutively active *ADH1* promoter from a single gene copy integrated in a chromosome via a pRS406 vector or overexpressed driven by the same promoter but using an episomal multicopy plasmid (pEG202). Analogous plasmids were used for the targeted approach. Here, we used either the lexA-DBD, taken from a yeast two hybrid system, or the Pho4-DBD of the Pho4 transcription factor.

For the Pho4-DBD, the previously described truncated Pho4 (Δ12-152) with the DBD and the Pho2 binding site was chosen (Svaren, *et al* 1994). For constitutive translocation into the nucleus, even under repressive conditions, *PHO4* was mutated at the SP4 (P152A) and SP6 (P223A) phosphorylation sites (Komeili 1999).

The catalytically inactive dSu(var)3-9 point mutant (H561K) was used as negative control for all constructs (Eskeland, *et al* 2004).

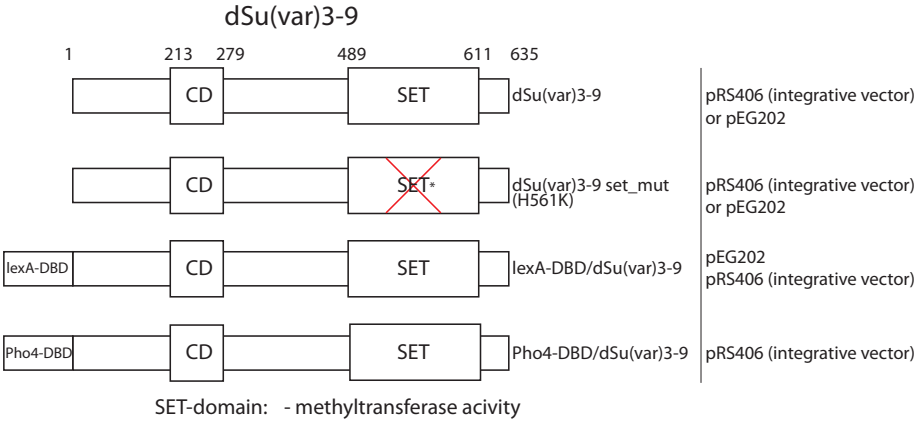

Fig. 7 Scheme of the different dSu(var)3-9 constructs used in this work. Chromodomain (CD), SET domain (SET). Numbers indicate amino acid positions.

3.1.2 dSu(var)3-9 methylates H3K9 in *S. cerevisiae*

We assessed the activity of heterologously expressed dSu(var)3-9 in yeast by liquid chromatography coupled mass spectrometry (LC-MS/MS). This is a highly sensitive method for detecting posttranslational modifications and also allows for a relative quantification of peptide modifications of interest. For purification of histones we combined our well-established nuclei preparation with an acid histone extraction (Davie, et al 1981, Edmondson, et al 1996). Histone analysis was done as described (Alabert, et al 2015). Fig. 8 shows the posttranslational modifications of the H3 peptide (amino acids 9-17) comparing four different strains carrying the dSu(var)3-9 constructs. dSu(var)3-9 inserted in the genome and driven by the ADH1 promoter mono-methylates H3K9, but to a very low level. This changed dramatically if dSu(var)3-9 was overexpressed and coupled to a DBD. The lexA-DBD/dSu(var)3-9 construct showed high mono- and dimethylation levels, while the percentage of H3K9me3 mark was lower with about 2.5%. This increase in methylation efficiency may have been due to the further overexpression or due to the additional DBD that may allow unspecific targeting to DNA. A DBD alone was already sufficient to raise H3K9 methylation levels as seen with the integrated Pho4-DBD/dSu(var)3-9 construct. As expected, the SET domain mutant of lexA-DBD/dSu(var)3-9 showed no methylation activity at all. Interestingly, acetylation levels stayed rather constant across all strains, while the increase in methylation levels was mainly at the expense of the unmodified H3K9 peptides levels.

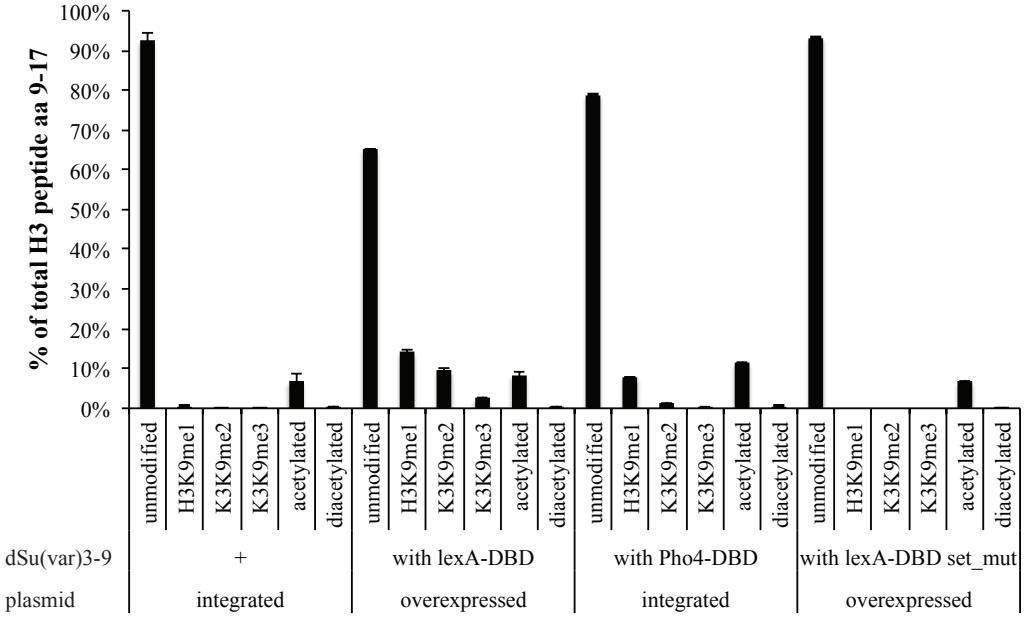

Fig. 8 Posttanslational modification of the H3 aa 9-17 peptide. LC MS/MS was performed of trypsin digested H3. PTMs were compared relative to each other. Integrated dSu(var)3-9 (pRS406 vector) with or without DBD was expressed in CY337 strain. The CY337 dSu(var)3-9 strain carried an additional empty pEG202 vector. LexA-DBD/dSu(var)3-9 (pEG202 vector) was expressed in CY339 with the additional plasmid carrying *PHO5* with insertion of lexA binding site (cleu_lexA_BS). Cells were grown logarithmically in YNB medium. Samples for mass spectromety were prepared at the same time and run in one mass spectrometry run. Error bars indicate SEM of 3 biological replicates.

3.1.3 Effect of the histone modifying enzymes Snf1 and Rph1 on H3K9 methylation levels

Although H3K9me does not occur naturally in *S. cerevisiae*, we wondered if histone modifying enzymes of yeast could have an effect on H3K9 methylation levels (Fig. 9A). The first candidate was Snf1, a kinase subunit of the AMP-activated protein kinase complex. Among its multiple targets is H3S10 (Lo*, et al* 2001). Phosphorylation of H3S10 hinders methylation of H3K9 (Duan*, et al* 2008, Rea*, et al* 2000). The second enzyme of interest was Rph1, which demethylates specifically H3K36me3 via its JmjC domain (Klose*, et al* 2007, Kwon and Ahn 2011). Because of the structural similarity of the human HDM3/JMJD2, known to demethylate both H3K9me3 and H3K36me3, Klose et. al. could show that H3K9me3 was also demethylated by Rph1 *in vitro*. To investigate the possible effects of those enzymes, we created respective deletion strains and overexpressed lexA-DBD/dSu(var)3-9. H3K9 methylation levels were again monitored using LC-MS/MS. Comparing the *rph1Δ* and the double deletion *rph1Δ snf1Δ* to the wt background, we did not observe significant changes in the H3K9 methylation levels (Fig. 9B).

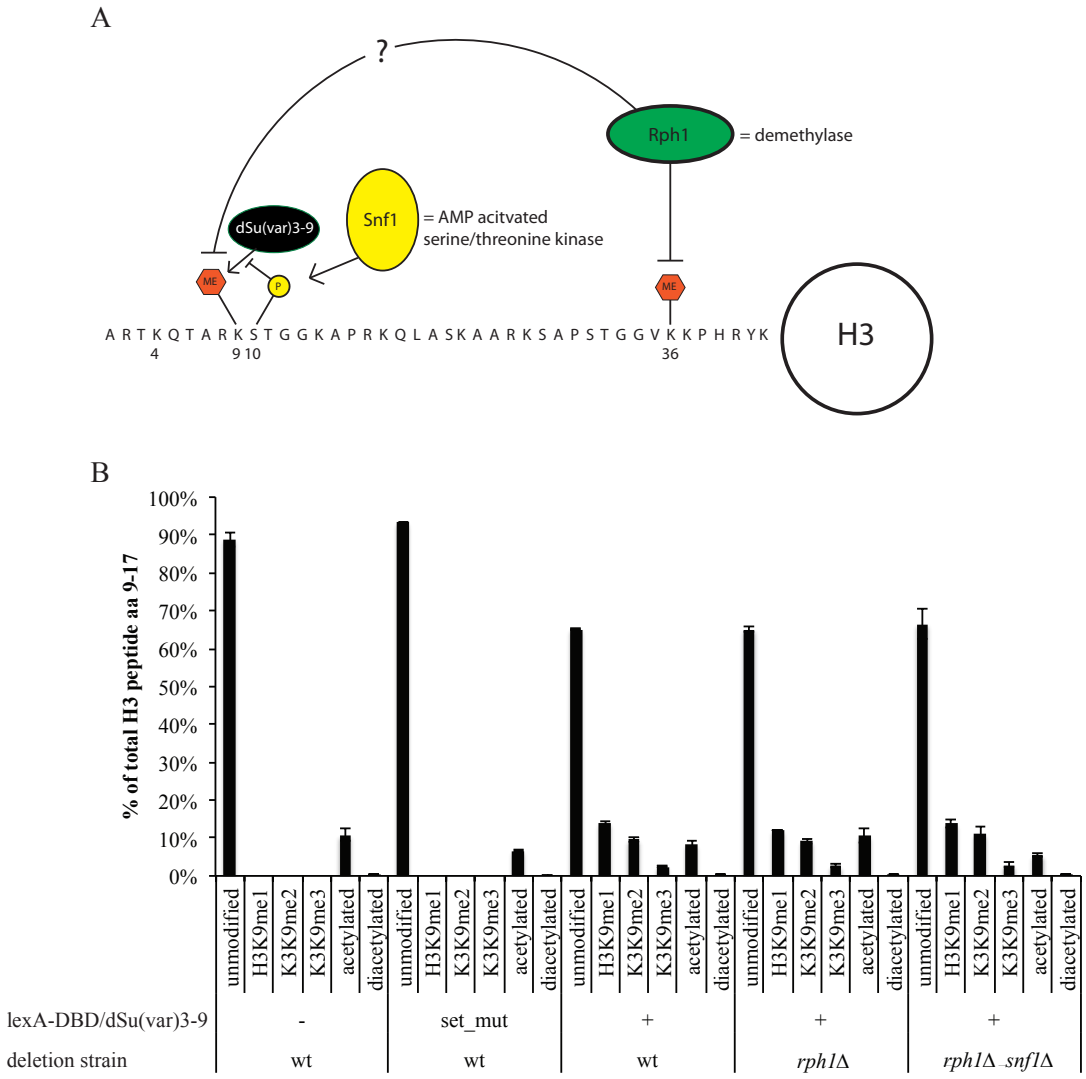

Fig. 9 Rph1 and Snf1 and their influence on H3K9me. (A) Scheme showing the possible influence of Rph1 and Snf1 on H3K9me levels. Not filled circle represents globular domain of H3 from which the N-terminal tail amino acid sequence with respective numbering emanates. Red hexagons symbolize methylation, while the yellow circle stands for phosphorylation. Rph1 (green oval) is a known H3K36 demethylase and was also shown to demethylate H3K9 (Klose, *et al* 2007). SNF1 (yellow oval) phosphorylates H3S10, which hinders methylation of H3K9 by dSu(var)3-9 (black oval). (B) Relative PTM levels of the H3 aa9-17 peptide. Wt and *rph1Δ* had the CY339 as a strain background. The double deletion was derived from LPY7091. All strains carried the additional cleu_lexA_BS plasmid. Cells were grown logarithmically in YNB medium. Samples for mass spectrometry were prepared in parallel and run in one mass spectrometry run. Data of the wt strains with lexA-DBD/dSu(var)3-9 constructs were already shown in Fig. 8. Error bars indicate SEM of 3 biological replicates.

3.1.4 H3K9 methylation by dSu(var)3-9 is increased by HP1a depending on its CD and CSD

After the successful H3K9me introduction in *S. cerevisiae* we also introduced HP1a. The H3K9me2/me3 mark set by dSu(var)3-9 is recognized by the chromodomain of HP1a (Bannister, *et al* 2001, Jacobs, *et al* 2001, Nakayama, *et al* 2001). Additionally, dSu(var)3-9

interacts via its N-terminus with the chromoshadow domain of HP1a (Schotta, *et al* 2002). These two interactions may provide a possible mechanism for spreading of heterochromatin.

To dissect the different functions of the HP1a domains we introduced a chromo domain (CD) point mutation, which abolishes HP1a binding to methylated H3K9 (Jacobs, *et al* 2001, Lachner, *et al* 2001, Nielsen, *et al* 2002, Platero, *et al* 1995), and a point mutation (I152F) in the chromoshadow domain (CSD), which corresponds to the previously described I126F mutation in human HP1α (Lavigne, *et al* 2009). Mutation of the CSD disrupts, among others, the interaction of HP1a and H3. Flag-tagged versions of HP1a were overexpressed using the high copy number plasmid pEG202. Equal expression levels of the HP1a mutants were confirmed by western blotting with H3 as loading control (Fig. 10).

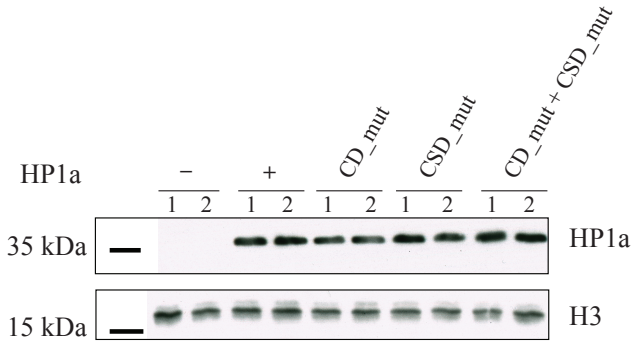

Fig. 10. Expression of HP1a mutants. Western blot of whole cell extracts (CY337). αFlag antibody recognizes FLAG-tagged HP1a variants. Detection of histone H3 by αH3 antibody was used as loading control. Cells were grown overnight to stationary phase. 10 OD_{600} cells were used for protein extraction. Two biological replicates of each yeast strain are shown. Not the same strains as in Fig. 11.

To see a potential effect of HP1a and HP1a mutants on H3K9 methylation levels, we overexpressed the HP1a constructs alongside the integrated dSu(var)3-9 construct and performed mass spectrometry.

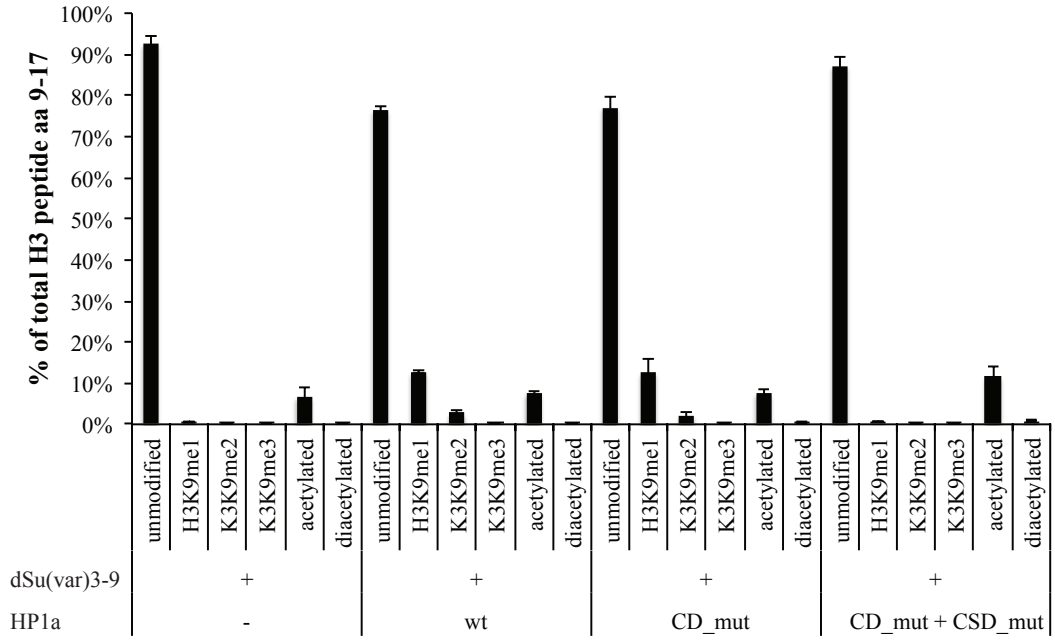

Fig. 11 Methylation of H3K9 is enhanced in the presence of HP1a. Relative PTM levels of the H3 aa9-17 peptide. CY337 strains with dSu(var)3-9 genomically integrated. HP1a or its mutants were overexpressed with the pEG202 vector. The CY337 dSu(var)3-9 strain without HP1a carried an empty pEG202 vector, data of this strain were already diplayed in Fig.8. Cells were grown logarithmically in YNB medium. Samples for mass spectromety were prepared at the same time and processed in one mass spectrometry run. Error bars indicate SEM of 3 biological replicates.

Interestingly, in the presence of HP1a we saw a great increase in H3K9me1 levels and also a significant raise of H3K9me2 levels (Fig. 11). This effect was independent of the chromodomain but abolished upon simultaneous deletion of the CD and CSD. This suggests that the activity of dSu(var)3-9 on chromatin is enhanced by HP1a and that this mainly depends on the HP1a chromoshadow domain.

3.1.5 Local H3K9me2 enrichment at the targeted promoters

In our targeted approach with lexA-DBD/dSu(var)3-9, a consensus sequence of the lexA binding site (Lewis*, et al* 1994) was introduced to the *PHO5*, *PHO8* and *PHO84* promoters by site directed mutagenesis. In case of the *PHO5* promoter, a *pho5* deletion strain was transformed with a plasmid containing either the wild type *PHO5* promoter (cleu_neu1) or the *PHO5* promoter with a lexA binding site (cleu_lexA_BS) (Fig. 12A). LexA-DBD/dSu(var)3-9 was overexpressed. Chromatin immunoprecipitation (ChIP) allows mapping of protein-DNA interactions. Proteins and DNA are crosslinked and the DNA sheared to fragment sizes of around 200 bp. The protein of interest is immunoprecipitated with a specific antibody, in this case an anti-H3K9me2 antibody, and cross-linked DNA is purified and analyzed using real-time PCR. Given the targeting of the methyltransferase via the lexA-DBD to the *PHO5*

promoter, it was unexpected that we did not see an enrichment of methylated H3K9 compared to the telomeric control locus (*TEL;*Fig. 12C), while we did see enrichment relative to the *PHO8* control locus. We perfomed the ChIP in the wt and the *rph1Δ snf1Δ* background. This might be due to the fortuitous lexA binding site close to the telomere amplicon which was found by a consensus data search on yeastgenome.org (WU-BLAST2 search) for conserved lexA binding sites in yeast (Fig. 12B). Thus, targeting lexA-DBD/Su(var)3-9 to the *PHO5* promoter works. In the *rph1Δ snf1Δ* background we also didn't observe a higher enrichment of H3K9me2 compared to the wt.

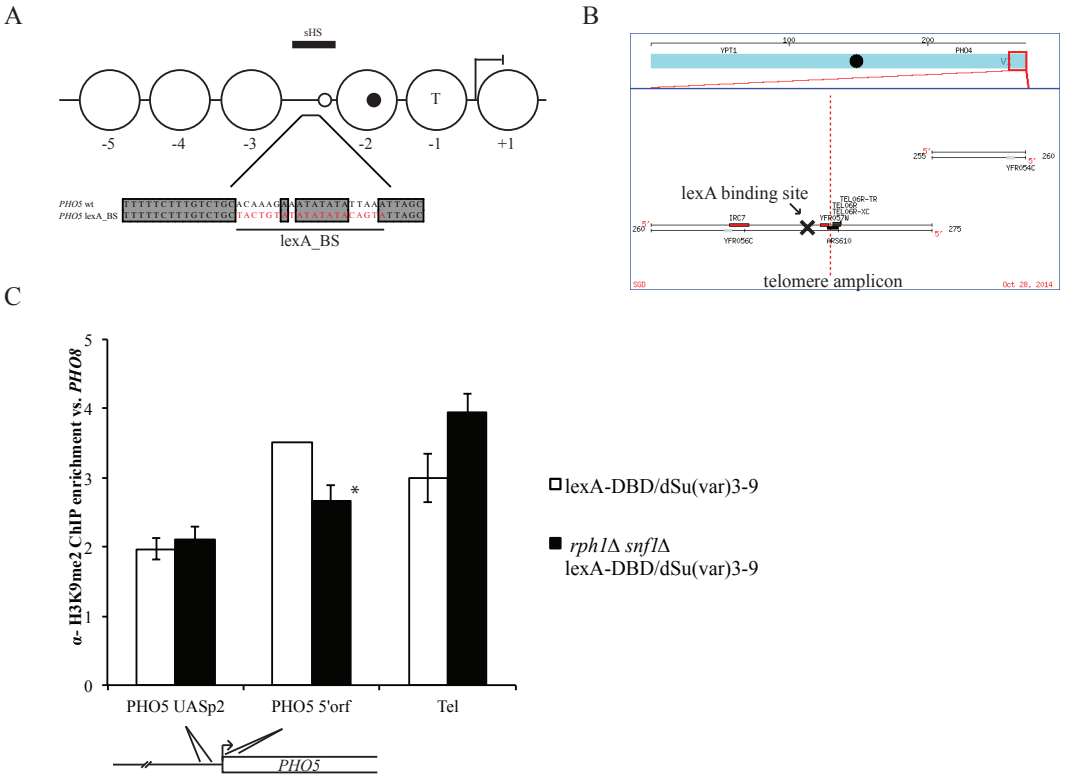

Fig. 12 (A) Scheme of the *PHO5* promoter in the repressed state with the lexA binding site. The large circles represent positioned nucleosomes, numbers indicate the position of the nucleosome relative to the ATG. The small filled circle shows the high affinity Pho4 binding sites, the small-unfilled circle stands for a low affinity Pho4 binding site. Horizontal bar indicates the short DNase I-hypersensitivity site (sHS). T stands for TATA-Box, ATG is represented by the blunted arrow. Below the promoter structure the wild type sequence of *PHO5* is compared with the mutated *PHO5* lexA_BS sequence. Consensus lexA binding site as reported (Lewis, *et al* 1994) is marked red and underlined**. (B) Location of the lexA consensus sequence using the webtool (WU-BLAST2 search) on yeastgenome.org.** X shows the binding site, the dotted line the position of the RT-PCR amplicon. **(C) H3K9me2 ChIP showing the H3K9me2 enrichment at the *PHO5* UASp2, the *PHO5* 5'orf and the TEL amplicons relative to the control locus *PHO8*.** Below is the *PHO5* promoter scheme showing the approximate regions of the amplicons used for RT-PCR. Open rectangle represents the *PHO5* open reading frame. LexA-DBD/dSu(var)3-9 was expressed either in CY339 background or in the double mutant *rph1Δ snf1Δ* (LPY7091 strain), all strains carry the plasmid with the modified lexA binding site at the *PHO5* promoter (cleu_mut4_neu1, one strain (CY339 lexA-DBD/dSuvar)3-9 cleu_mut4) carriers the original cleu_mut4, which has a missense mutation in the orf, which is not relevant in this experiment). Error bars indicate SEM of 3 biological replicates, asterisk indicates 2 biological replicates.

3.1.6 Targeting Pho4-DBD/dSu(var)3-9 to the *PHO* promoters leads to increased H3K9me at *PHO5* and *PHO84* and HP1a enrichment

We performed the analogous and extended ChIP experiment with our Pho4-DBD/dSu(var)3-9 construct. Local enrichment of H3K9me2 was additionally normalized against H3 occupancy to account for overall differences in nucleosome density. For Pho4-DBD/dSu(var)3-9 alone, we see a clear enrichment of H3K9me2 at *PHO5* and *PHO84* UASp sites, i.e., where targeting of the methylase was expected, compared to the control loci up- and downstream of the *PHO5* promoter and at the *ACT1*, *ATF2* and *TRP1* loci (Fig. 13A, Fig. S 1). Surprisingly, there was hardly any enrichment at the *PHO8* UASp amplicon.

As coexpression of HP1a increased global H3K9 methylation levels (Fig. 11), we also included coexpression of HP1a in the locus-specific ChIP experiments. Indeed, overall yield of methylated histones were again increased compared to expressing only Pho4-DBD/dSu(var)3-9 as measured by % input (Fig. S 2). After normalization to H3 levels, we observed at least an additional increased of H3K9me2 level at the *PHO5* promoter and also a consistent enrichment over the coding region of *PHO84*. On the other side, such an increase was not detected at the *PHO84* and *PHO8* UAS. H3K9me2 levels stayed similar over all control loci when HP1a was added.

HP1a alone, not targeted, was not enriched at the studied promoters nor at the other examined loci (Fig. 13C, D). With the addition of Pho4-DBD/dSu(var)3-9 we have a strong enrichment of HP1a over the targeted *PHO5* UASp site (Fig. 13C, Fig. S 1). Enrichment was persistent over the downstream amplicon *PHO5* 5'orf, maybe because this amplicon is very close to the UASp site. A spreading across the gene body could not be observed at *PHO5*. The SET mutant of Pho4-DBDdSu(var)3-9 was not sufficient to enrich HP1a at *PHO5*. Conversely, at the *PHO8* and *PHO84* loci, HP1a was enriched in the Pho4-DBDdSu(var)3-9 strain as well as in the SET mutant (Fig. 13D). At the *PHO84* locus we also observed considerably more enrichment of HP1a than at the other two targeted loci. This could be due to the increased number of Pho4 binding sites at the *PHO84* promoter.

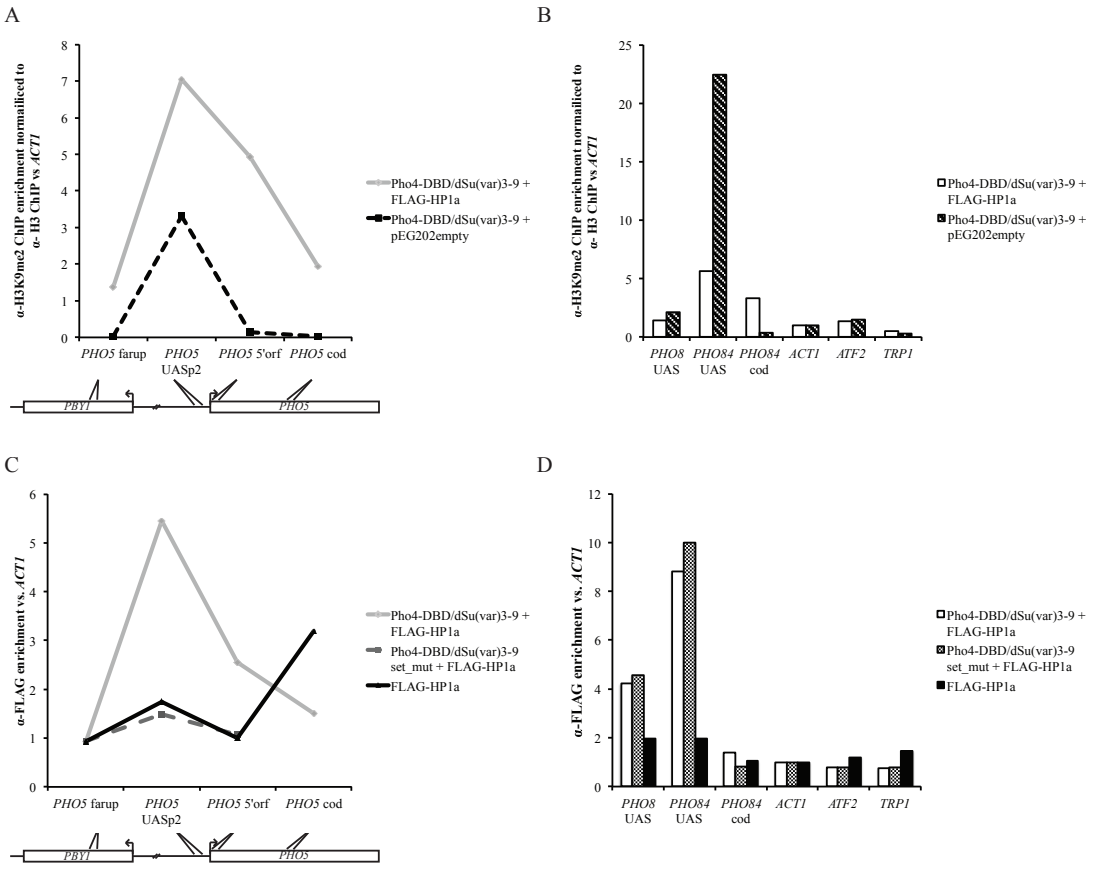

Fig. 13. H3K9me2 and HP1a enrichment at targeted and control loci. (A) H3K9me2 enrichment at different sites of the *PHO5* locus in strains (CY337) expressing Pho4-DBD/dSu(var)3-9 with or without HP1a (FLAG-tagged). The H3K9me2 % input was normalized to the H3 % input of the sample and then to that at the *ACT1* control locus. Shown below the graph is a schematic of the *PHO5* locus to show, where the amplicons used in this study are approximately located. The rectangles represent the open reading frame of the *PHO5* and *PBY1* gene, respectively. The pointed arrows stand for the ATG. The open shafts show the location of the amplicons. (B) H3K9me2 enrichment at *PHO8*, *PHO84* and control loci. *PHO8* UAS, *PHO*84 and the control amplicon *ATF2* are located in the promoter region. While *PHO84* cod and the control loci *ACT1* and *TRP1* all lie within the coding region of their gene. Experimental setup and normalization is the same as in (A). (C) HP1a enrichment at the *PHO5* locus using anti-FLAG beads in strains (CY337) with FLAG-tagged HP1a with Pho4-DBD/dSu(var)3-9 variants or without. FLAG % input was normalized to *ACT1*. Below the graph is the same scheme as in (A). (D) FLAG-ChIP at the *PHO8*, *PHO84*, and control loci as used in (B). Experimental setup and normalization is the same as in (C).
Legends in the graphs show the strains used for this study. See supplement Fig. S 2 for raw data. See supplement Fig. S 1 for the other biological replicate.

3.1.7 Methylation levels have no impact on yeast viability

After we demonstrated the successful introduction of the new histone modification H3K9me into *S. cerevisiae* with more than 25% H3K9 methylated histones in some strains (Fig. 11), it was clear that yeast survives this newly introduced modification. Nonetheless, we wished to assess if yeast was compromised nonetheless by comparing growth rates. We compared the growth rates of yeasts, with different strain backgrounds, that carry dSu(var)3-9 constructs

(Table 2A). There were no major differences in doubling time comparing the empty vector with dSu(var)3-9 or the SET mutant. This showed that H3K9me in yeast had hardly any impact regarding the viability and doubling times under standard conditions.

The lexA-DBD/dSu(var)3-9 constructs, which displayed the highest H3K9 methylation levels as detected by LC-MS/MS (Fig. 9) somewhat slowed down the doubling times (Table 2B), but this was methylation independent, as the SET mutant had about the same doubling time as the active methyltransferase. H3K9 methylation had no effect, but the slight increase in doubling time may be attributed to global effects from overexpressing a chromatin binding protein.

As H3K9 methylation levels caused by the integrated dSu(var)3-9 gene were further increased in the presence of HP1a (Fig. 11), we also tested these respective strains (Table 2C). Doubling times only slightly increased upon the addition of dSu(var)3-9 or HP1a.

Overall, H3K9 methylation, even the highest levels that we introduced, did not substantially affect yeast growth rates.

A

Background	dSu(var)3-9 (overexpression plasmid)	Doubling time in h
BY4741	+	1.7 ± 0.12
BY4741	set_mut	1.6 ± 0.09
CY337	+	1.7 ± 0.07
CY337	set_mut	1.6 ± 0.01
YS18	empty vector	1.7 ± 0.02
YS18	+	1.8 ± 0.06
YS18	set_mut	1.8 ± 0.12

B

Background	lexA-DBD/dSu(var)3-9	Doubling time in h
CY339	empty vector	1.8 ± 0.01
CY339	+	2.1 ± 0.06
CY339	set_mut	2.0 ± 0.04

C

Background	dSu(var)3-9	HP1a	Doubling time in h
YS18	empty vector	empty vector	1.7 ± 0.02
YS18	empty vector	+	1.8 ± 0.01
YS18	+	empty vector	1.8 ± 0.07
YS18	+	+	1.9 ± 0.1

Table 2 Doubling times of *S. cerevisiae* upon expression of dSu(var)3-9 and / or HP1a. Strains given in the table were grown logarithmically. Doubling times were calculated using the equation of the exponential trendline.

3.2 Effects of H3K9me or dSu(var)3-9 on gene expression

3.2.1 Untargeted dSu(var)3-9 alone has no effect on gene expression of *PHO5* and *HIS3*

Despite no obvious growth defect, we wondered if the heterologous H3K9 methylation mark alone could already have an effect on gene expression, as H3K9 acetylation is associated with gene activation and may be impaired by H3K9 methylation.

We turned again to the *PHO* promoters as well-characterized models for a role of chromatin in gene regulation. The gene product of *PHO5*, the acid phosphatase Pho5, is exported into the periplasm and can easily be measured by a an acid phosphatase activity assay with whole cells (Haguenauer-Tsapis*, et al* 1986). We used this assay to measure changes in *PHO5* gene expression after introducing H3K9me and / or HP1a.

We measured the acid phosphatase activity comparing wild type yeast to the not targeted dSu(var)3-9 under inducing conditions (Fig. 14). Here we did not see an effect of dSu(var)3-9 on the expression level of *PHO5*.

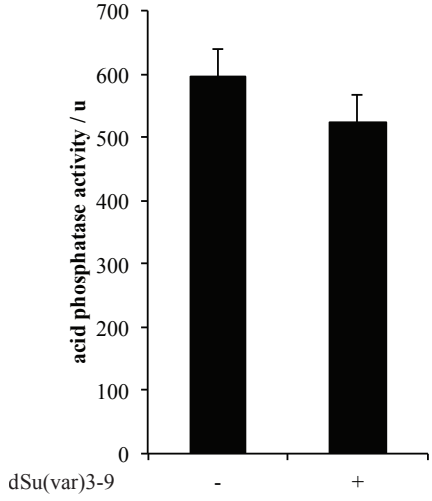

Fig. 14. Not targeted dSu(var)3-9 has no effect on *PHO5* expression. *PHO5* activity of overnight-induced cells was measured by acid phosphatase activity. CY337, with or without dSu(var)3-9 genomically integrated (pRS406), was grown logarithmically in phosphate rich medium. Cells were induced by washing and resuspending them in phosphate-free medium. Both strains carried an additional empty pEG202 vector. Error bars indicate SEM (from left to right n=9, n=6).

Another fast method to see effects of gene expression is the spotting assay on 3-amino-1,2,4-aminotriazole (3-AT) containing and histidine lacking plates. 3-AT is a competitive inhibitor of the imidazole-glycerol-phosphate dehydratase encoded by *HIS3* and catalyzes the 6th step in histidinie biosynthesis (Hilton*, et al 1965,* Struhl and Davis *1977*). *HIS3* expression is necessary for yeast growth without exogenous histidine, and higher expression levels of *HIS3* are needed when simultaneously exposed to 3-AT. If expression of d(Su(var)3-9 impaired *HIS3* expression, reduced growth in the presence of 3-AT would be expected. However, this was

not the case (Fig. 15), arguing for no effect of the low levels of untargeted H3K9 methylation on *HIS3* expression.

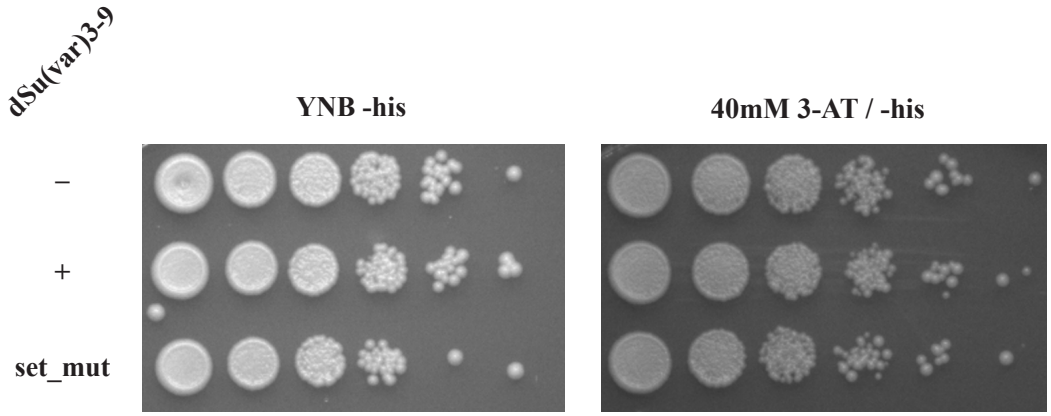

Fig. 15. No repression at the *HIS3* locus by dSu(var)3-9. Yeast was grown overnight to stationary phase, diluted to an OD600 of 5 and serial dilutions (10^{-1} - 10^{-6}) were plated on YNB –his ± 40 mM 3-AT at 30°C for 2 days. Wt (YS18) carried a pRS406empty vector. dSu(var)3-9 is expressed by an pRS406 integration vector. All strains bearing the empty *HIS3* vector pEG202. One representative biological replicate of at least 2 replicates are shown here, see supplementary (Fig. S 4) for further replicates. Same data as shown in Fig. 27.

3.2.2 Targeting dSu(var)3-9 with lexA shows a repressive effect on *PHO5* expression

In a next step, we turned to our targeted approach. Again, *PHO5* was induced by phosphate starvation overnight. Although the global methylation level of the lexA-DBD/dSu(var)3-9 construct was much higher compared to the not targeted dSu(var)3-9, we still saw no repressive effect of lexA-DBD/dSu(var)3-9 in combination with the wild type *PHO5* promoter, i.e. without locus-specific targeting, albeit possibly unspecific DNA targeting (Fig. 16B). Upon using the mutated *PHO5* promoter variant with the introduced lexA binding site, we realized that this site overlaps with and compromised the Pho2 binding site at the *PHO5* promoter (Fig. 16A). As Pho2 is important for *PHO5* induction (Fascher et al., 1990), just the introduction of the lexA binding site already led to a 3-fold reduction of acid phosphatase activity. Adding lexA-DBD/dSu(var)3-9, a further small decrease in the expression level was seen. However, this decrease was methylation independent as the SET domain mutant of dSu(var)3-9 showed the same small decrease (Fig. 16B).

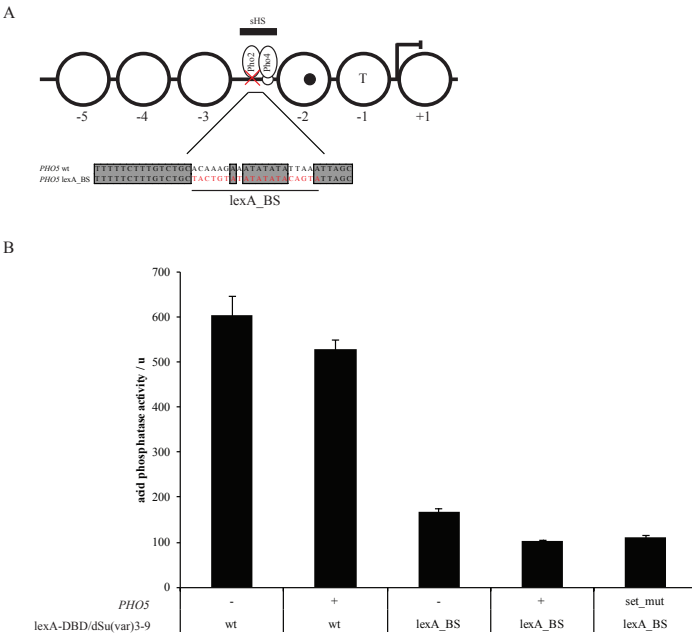

Fig. 16. Recruitment of lexA-DBD/dSu(var)3-9 leads to a minor repression of *PHO5* independent of H3K9 methylation. (A) Scheme of the *PHO5* promoter in the repressed state with the lexA binding site. The large circles represent positioned nucleosomes; numbers indicate the position of the nucleosome relative to the ATG. The small filled circle shows the high affinity Pho4 binding sites, the small unfilled circle stands for a low affinity Pho4 binding site. Horizontal bar indicates the short DNase I-hypersensitivity site (sHS). The ellipses represent the transcription factors with the red cross symbolizing the Pho2 binding site compromised by insertion of the lexA_BS. T stands for TATA-Box, ATG is represented by the blunted arrow. Below the promoter structure the wild type sequence of *PHO5* is compared against the mutated *PHO5* lexA_BS. Consensus lexA binding site as reported (Lewis*, et al* 1994) is marked red and underlined.
(B) *PHO5* overnight induction in phosphate-free medium measured by acid phosphatase activity. A chromosomal *pho5* strain (CY339) was used with the reporter plasmid being either wild typ *PHO5* (cleu_neu1) or *PHO5* with the lexA_BS (cleu_mut4_neu1). The lexA-DBD/dSu(var)3-9 constructs were expressed on the high copy plasmid (pEG202) with either a functioning or a nonfunctioning SET domain (set_mut). Error bars show the SEM of three biological replicates.

With the same experimental setup, we looked at the *rph1Δ* and *snf1Δ rph1Δ* deletions strains. In the *rph1Δ* strain we saw largely the same effect of dSu(var)3-9 as in the wild type background (Fig. 17). In contrast, there was a stronger relative repression by lexA-DBD/dSu(var)3-9 in the double mutant. Here, the impaired *PHO5* promoter with a lexA binding site had a higher phosphatase activity of around 300 units that decreased to almost one third upon the addition of lexA-DBD/Su(var)3-9. However, this repression was still methylation independent (Fig. 17).

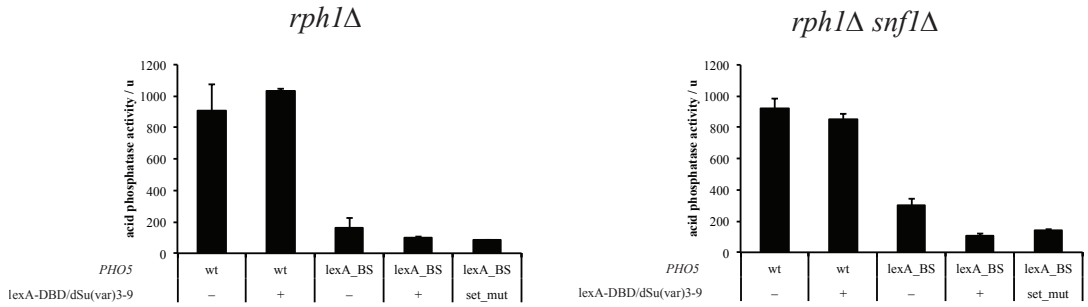

Fig. 17 No further repression of *PHO5* in a *rph1*Δ or *rph1*Δ *snf1*Δ knockout strain. Acid phosphatse activity after overnight induction in phosphate-free medium. *rph1*Δ (CY339) or *rph1*Δ *snf1*Δ (LPY7091

rph1::KANMX4) carried the same reporter and lexA-DBD/dSu(var)3-9 plasmids as previously described in Fig. 2. Error bars show SEM of 3 biological replicates in the right chart or 6 biological replicates in the left graph.

Overall, the compromised Pho2 binding site had the strongest effect on *PHO5* activation. Even though we saw a further reduction with a targeted dSu(var)3-9, this rather small effect could be explained by binding competition of the lexA construct with Pho2. To test this binding competition, another control with just the lexA-DBD would be necessary but was not investigated so far. Nonetheless, already now we can conclude from this series of experiments that H3K9 methylation alone has not much influence on the induction level of *PHO5*.

3.2.3 No effect of lexA-DBD/dSu(var)3-9 on *PHO8* and *PHO84* induction

We also introduced a lexA binding site at the other two *PHO* promoters. In case of the *PHO8* promoter we introduced the lexA site further upstream of the ATG (Fig. 18A) compared to our *PHO5* construct and here the lexA site should not interfere with other sites required for *PHO8* induction. *PHO8* encodes an alkaline phosphatase, which can also be readily measured by an enzymatic assay. Consistent with our previous results, targeting dSu(var)3-9 via the lexA-DBD to *PHO8* didn't reduce the alkaline phosphatase activity.

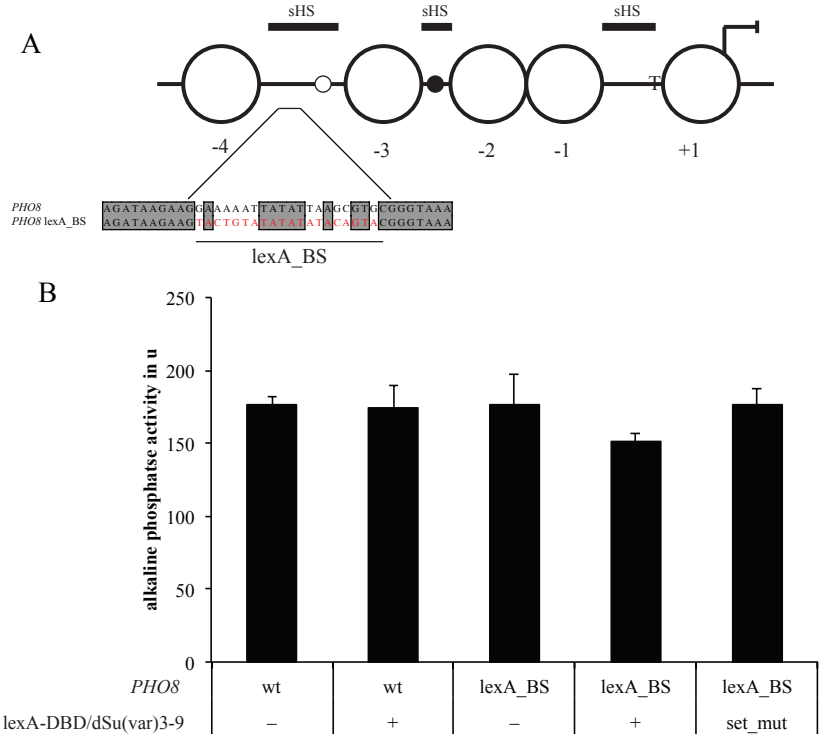

Fig. 18. lexA-DBD/dSu(var)3-9 constructs show no repression of *PHO8*. (A) Scheme of the repressed *PHO8* promoter region with the site of the integrated lexA_BS. Design is analogous to Fig.16. (B) *PHO8* overnight induction by phosphate starvation measured by alkaline phosphatase activity. A chromosomal *pho8* strain (Y04315) was used with the reporter plasmid carrying either the wild type *PHO8* promoter (pP8apain) or a *PHO8* promoter variant with a lexA_BS (pP8apain_lexA_BS). The lexA-DBD/dSu(var)3-9 constructs were

expressed on a high copy plasmid (pEG202) with either a functioning or a non-functioning SET domain (set_mut). Error bars show the SEM of three biological replicates.

A similar result was seen at the last promoter, *PHO84*. As *PHO84* codes for a P_i-Transporter we used pCB84a_l as a reporter plasmid (Wippo*, et al* 2009). This plasmid has the *PHO84* promoter coupled to the *PHO5* coding region. Thereby the expression can easily be measured by acid phosphatase activity. The lexA binding site was inserted close to the nucleosome upstream of the short hypersensitive site (Fig. 19A). Initial steady state results of overnight-induced cells showed the same effect as with *PHO8*. For *PHO5* it has been shown that hyperacetylation of histones by the histone acetyltransferase Gcn5 plays a role at the very beginning of induction. In a previous study it was shown that in *gcn5* deletion strains the *PHO5* overnight induction was the same as in the wild type, but the *gcn5* strain showed a delayed induction kinetic (Barbaric*, et al* 2001a, Barbaric*, et al* 2001b, Gregory*, et al* 1998), i.e., looking at induction kinetics is a more sensitive assay for effects on *PHO* promoter chromatin remodeling. To test if dSu(var)3-9 and with it, H3K9 methylation, had a kinectic effect on *PHO84* induction, yeasts were washed with water and resuspended in phosphate-free medium. Timepoints of measurements can be seen in Fig. 19B. Here we saw that the targeted lexA-DBD/dSu(var)3-9 constructs had hardly any effect on the kinetics of induction. Also, the endpoint of induction was hardly altered when compared to the non-targeted wt promoter. Even though the latter showed statisicially significantly higher values, this increase was probably not biologically relevant as in this extremely high range of phosphatase activity the biological resolution of this system is compromised (Philipp Korber, personal communication).

A

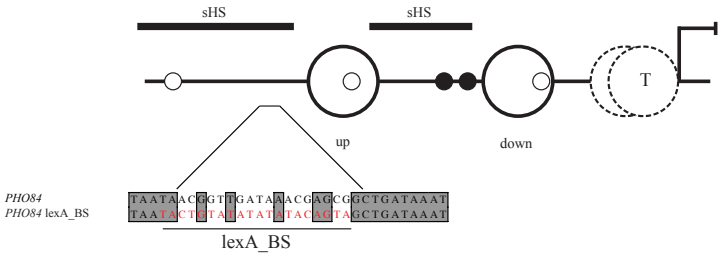

B

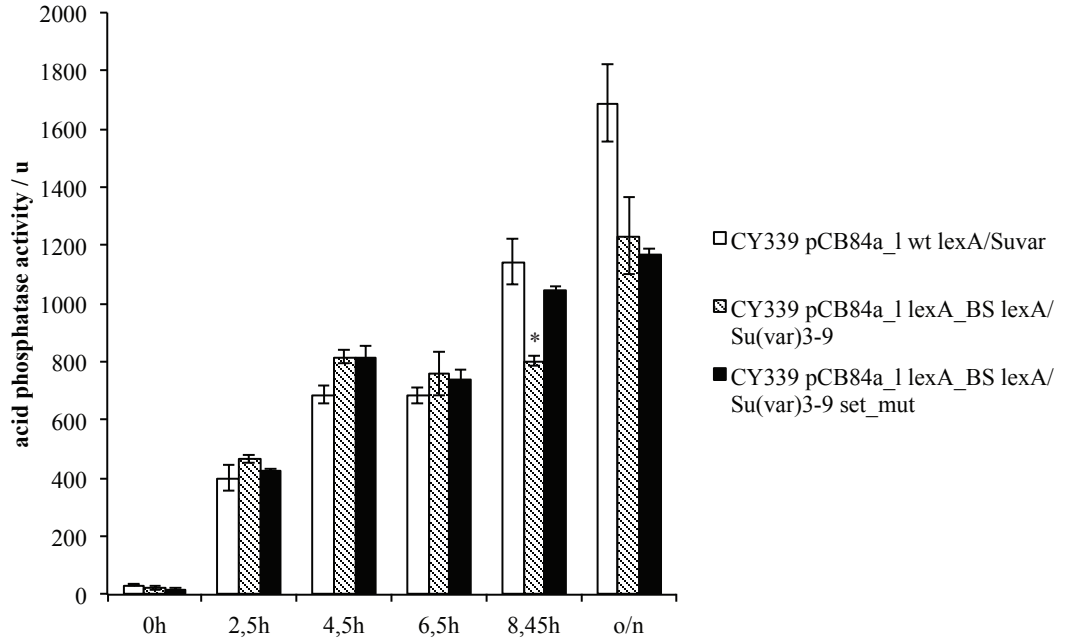

Fig. 19. lexA-DBD/dSu(var)3-9 constructs have no effect on *PHO84* induction kinetics. (A) *PHO84* promoter structure of the repressed state with the introduction site of the lexA_BS. Design is as in Fig. 16 with the exception of the dotted circles representing an ambiguously positioned nucleosome (Wippo*, et al* 2009). Nucleosomes are named after their position relative to the right sHS. (B) *PHO84* induction kinetics upon phosphate starvation measured by acid phosphatase activity. Reporter plasmid carried the *PHO84* promoter region (either wt *PHO84* (pCB84a_l) or *PHO84* with lexA_BS (pCB84a_l_lexA_BS)) with the reporter gene being *PHO5* in a CY339 *pho5::ura3* strain. The lexA-DBD/dSu(var)3-9 construct was genomically integrated with a pRS406 vector. All strains carried an empty pEG202 vector. Error bars show the SEM of two (*, outlier was not considerated valid) or three biological replicates.

3.2.4 Targeting of dSu(var)3-9 via Pho4-DBD represses *PHO5* and *PHO84* independently of methylation status

The approach of targeting dSu(var)3-9 with the lexA-DBD either crippled the *PHO5* promoter or did not have an effect on the *PHO8* and *PHO84* promoters. Instead, we tried targeting dSu(var)3-9 with the Pho4-DBD to the *PHO* promoters. Pho4-DBD was N-terminally tagged, C-terminally tagged dSu(var)3-9/Pho4-DBD was not expressed as confirmed by western blot (data not shown). As the Pho4-DBD/dSu(var)3-9 construct may negatively dominate by competing with the Pho4 activator, we used just Pho4-DBD alone as a control to distinguish between the solely competitive effect and an additional effect of dSu(var)3-9. In Fig. 20A *PHO5* induction levels monitored by acid phosphatase activity are shown. The competitive effect of the Pho4-DBD amounted to a roughly 2-fold reduction in activity. Interestingly, expressing Pho4-DBD/dSu(var)3-9 led to a reduction of about 6-fold compared to the wt. This effect was again methylation independent as seen earlier with the lexA construct at *PHO5* (Fig. 20, Fig. 16).

As a complementary method, we also monitored mRNA levels by quantitative RT-PCR (Fig. 20B). This approach also allows to directly compare induction of all three *PHO* promoters from the same cell culture. As reference value for a fully repressed promoter we also analyzed the wt mRNA under repressed conditions in phosphate-containing medium (see right bar Fig. 20B). The results confirmed our results obtained with the acid phosphatase assay. Shown in Fig. 20 is the fold change of expression in log2 scale. A more negative bar indicates a stronger repression of the *PHO5* promoter. The dSu(var)3-9 constructs again showed a stronger effect than the Pho4-DBD alone, in a methylation independent way.

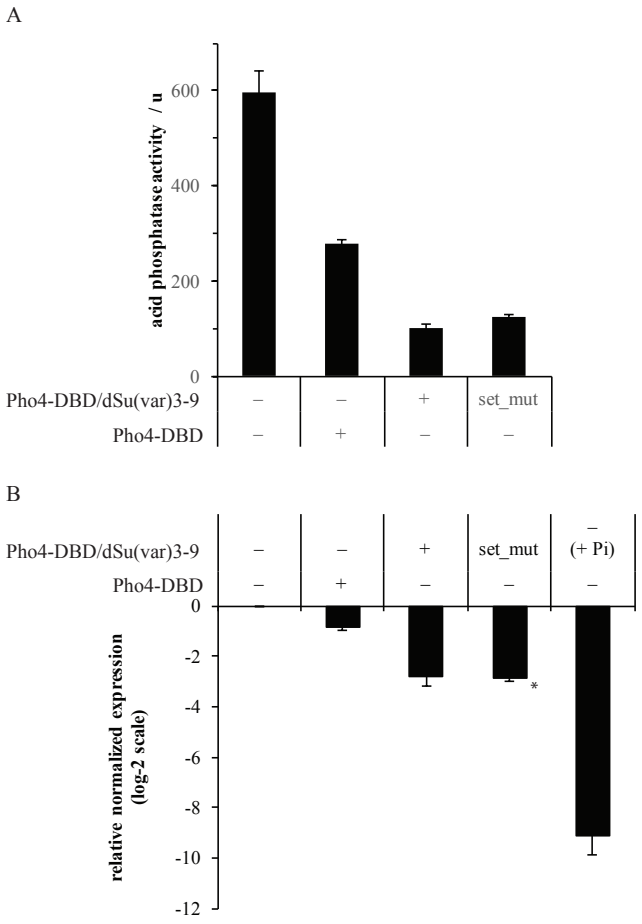

Fig. 20. *PHO5* expression analysis with Pho4-DBD/dSu(var)3-9 and Pho4-DBD constructs. (A) Overnight acid phosphatase activity in a CY337 background. Strains with none or integrated pRS406 vector carrying Pho4-DBD/dSu(var)3-9 or Pho4-DBD. All strains had an empty pEG202 vector. Error bars SEM of at least 3 biological replicates. (B) qRT-PCR of overnight phosphate starved cells. Same strains as in (A) were used. Change of gene expression is shown on a log2 scale compared to the induced wt. mRNA of each run were normalized to a housekeeping gene (*ACT1*) and then put in relation to the induced wt of the same run. Same dataset as shown in Fig. 30. Pho5 cod and Act were used as amolicons. Error bars indicated SEM of 2 (*) or 3 in-dependent prepared biological samples.

At *PHO8* the additional effect of dSu(var)3-9 relative to the Pho4-DBD alone was not as pronounced as at *PHO5*, but at *PHO84* it was similar (Fig. 21). Even though the repressive effect of our target protein was not as pronounced as at *PHO5*. Having just two biological replicates of the SET mutant resulted in large error bars and the results have to be seen as preliminary. Here, further validation would be necessary with more replicates to see if the SET mutant had effects as at *PHO5*.

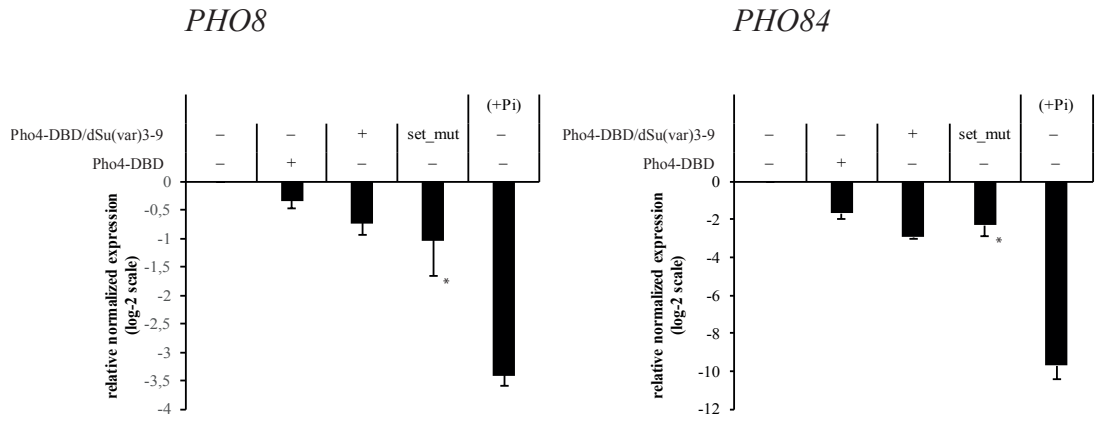

Fig. 21. *PHO8* and *PHO84* mRNA levels measured by qPCR. Same strains and gowth conditions as previously described (Fig. 20). As in Fig. 20 cells were grown in phosphate-free medium o/n. mRNA of the samples were normalized to a housekeeping gene (*ACT1*) and then put in relation to induced wt, which was prepared at the same time. Same dataset as shown in Fig. 31. Pho8 cod, Pho 84 cod, and Act1 were used as amplicons. Error bars indicated SEM of 2(*) or 3 independently prepared biological samples.

3.2.5 *PHO5* repression by Pho4-DBD and the additional dSu(var)3-9 effect depends on Rpd3

It was shown in our lab that dSu(var)3-9 interacts with the histone deacetylase (HDAC) HDAC1 in *Drosophila* (Czermin*, et al* 2001). To look for potential interactions of dSu(var)3-9 with HDACs in yeast, we created deletion strains of the five described HDACs in yeast (Lorenz*, et al* 1995). The influence of the Pho4-DBD/dSu(var)3-9 in the different deletion backgrounds was again examined using the acid phosphatase assay as a quick and reliable method. In the *hos1Δ*, *hos2Δ*, *hos3Δ* and *hda1Δ* mutants, the repression of *PHO5* with Pho4-DBD/dSu(var)3-9 was still seen (Fig. 22). Interestingly, the expression level was restored to almost wt level in the *rpd3Δ* Pho4-DBD/dSu(var)3-9 strain. At the same time, the competition effect of Pho4-DBD was nearly annihilated. This was to us a quite surprising result maybe implicating that dSu(var)3-9 recruits Rpd3 in a heterologous system. Even more surprisingly, Pho4-DBD requires Rpd3 for it repressional effect. We would have expected that the competition effect would persist even in the absence of a HDAC. But this also might be a special case for the *PHO5* promoter since it is a known target of Rpd3 (Vogelauer*, et al* 2000). Further experiments have to follow to verify this result, e.g., ChIP of Rpd3 at the *PHO5* promoter in dependence of Pho4-DBD or with the lexA-DBD/dSu(var)3-9 construct.

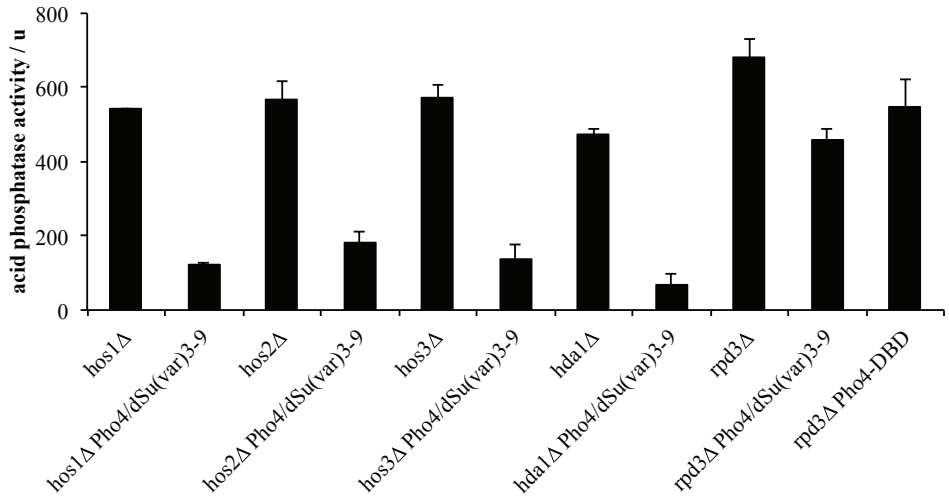

Fig. 22. Expression of *PHO5* is restored in *rpd3Δ* mutant. Acid phosphatase activity of over night induced cells. HDACs were deleted in CY337. Pho4-DBD/dSu(var)3-9 and Pho4-DBD were genomically integrated via a pRS406 vector. Error bars indicated SEM. N left to right 3, 3, 5, 5, 6, 6, 3, 3, 12, 12, 3.

3.3 Effects of HP1a on gene expression

3.3.1 HP1a alone leads to a decrease of the expression levels at the *PHO* and *HIS3* genes

The influence of HP1a on *PHO5* expression was analyzed using acid phosphatase activity and qPCR. Fig. 23 shows a twofold reduction of acid phosphatase activity in the presence of HP1a compared to the wt. The CD mutant led to the same reduction in the activity. Interestingly, the CSD mutant had full activity as the wt. This was in agreement with the qPCR results (Fig. 23B). Here we observed the same result on mRNA level for *PHO5*. A similar picture was observed at *PHO8* and *PHO84*. HP1a always showed a repression, which was about twofold, while the CSD mutant restored wt levels. At *PHO84,* the CSD mutants still showed a decreased expression level, which was slightly higher than the level in the presence of wt HP1a.

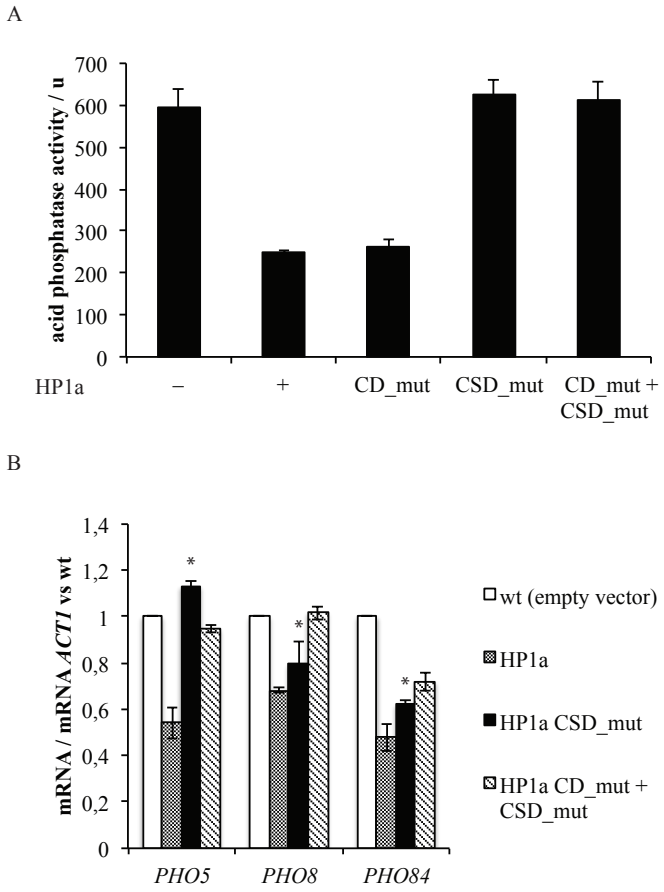

Fig. 23. Repression of *PHO* genes by HP1a. (A) Acid phosphatase assay of CY337 strains carrying either an empty vector (pEG202) or FLAG-tagged HP1a variants. CD_mut describes a point mutation in the chromo domain and csd_mut the point mutation in the chromo shadow domain of HP1a. The assay was carried out as previously described for **Fig. 14**. Error bars represent SEM of at least 3 biological replicates. (B) qRT-PCR analysis of *PHO* gene mRNAs. Same yeast strains as in (A) were used for this experiment. Cells were grown overnight in phosphate-depleted medium, then harvested and RNA was immediately extracted with acid phenol. mRNA levels were normalized to a control locus (*ACT1*) and then to the wild type (CY337 pEG202 empty). Pho5 cod, Pho8 cod, Pho 84 cod, and Act1 were used as amplicons. Error bars indicate SEM of 2(*) or 3 independent biological replicates.

To check if also *HIS3* might be repressed by HP1a, we also did the 3-AT spotting assay with the different HP1a variants (Fig. 24).

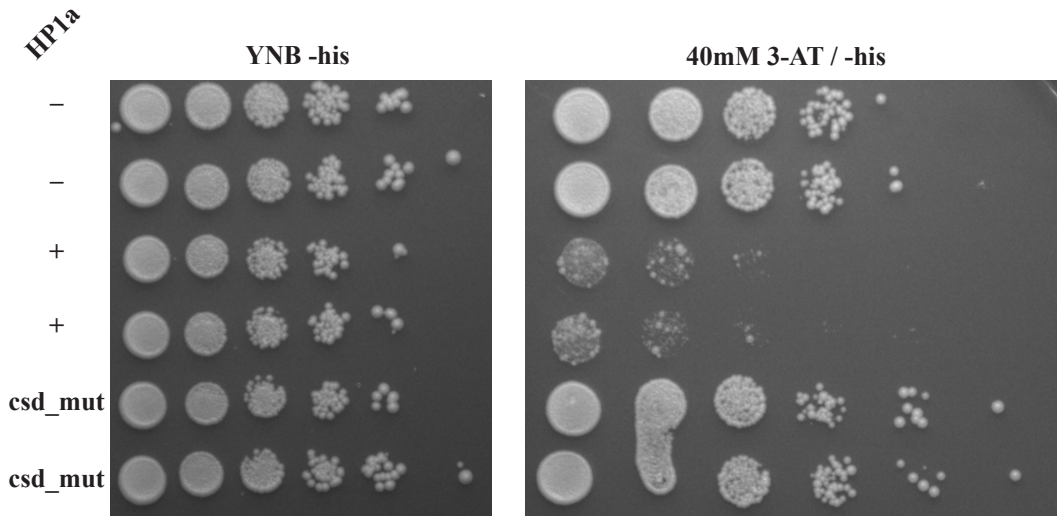

Fig. 24. HP1a strains show slow growth in the presence of 3 –AT. YS18 pRS406empty bearing either an empty expression vector (pEG202 empty) or one of the three FLAG-tagged HP1a variants on the pEG202 vector was grown overnight to stationary phase, diluted to an OD600 of 5 and serial dilutions (10^{-1} - 10^{-6}) were plated on YNB –his +/- 40 mM 3-AT at 30°C for 2 days. Two biological replicates of at least two are shown.

Yeast expressing the different HP1a variants did not show a growth defect when plated on standard YNB-his medium. In the presence of 40 mM 3-AT the HP1a containing strains showed a strong phenotype compared to the wt. Again, the CSD mutant was not able to suppress *HIS3* expression, which is in concordance with our data at the *PHO* loci.

3.3.2 Repression of HP1a is dosage dependent

In the course of unraveling the mechanism behind the position variegation effect, early on it was shown that the effect possibly depended on the dosage (Locke*, et al* 1988). To titrate the level of HP1a we used a galactose-inducible promoter library encompassing a 50-fold dynamic expression range (Blazeck*, et al* 2012). The different strains were induced in galactose-containing medium before plating on 3-AT –his plates or control plates (Fig. 25, Fig. S 5). Only the strain with the promoter driving strongest HP1 expression (UASgal Pgal) showed a reduced viability on 3-AT (second last one) compared to the control. The effect is rather minor compared to the one in Fig. 24. The positive control with HP1a expression from pEG202 did also not show the same effect as in Fig. 24. It has been reported that the activity of *ADH1*, which drives transcription of HP1a inserted in the pEG202 vector, drops by 50% in presence of carbon sources raffinose and galactose, used in this experiment (Pagano 1996). A definitive Western blot to proof the expressional differences has not been done yet. Until then this experiment is still somewhat preliminary with regard to the effect of HP1a on *HIS3* expression.

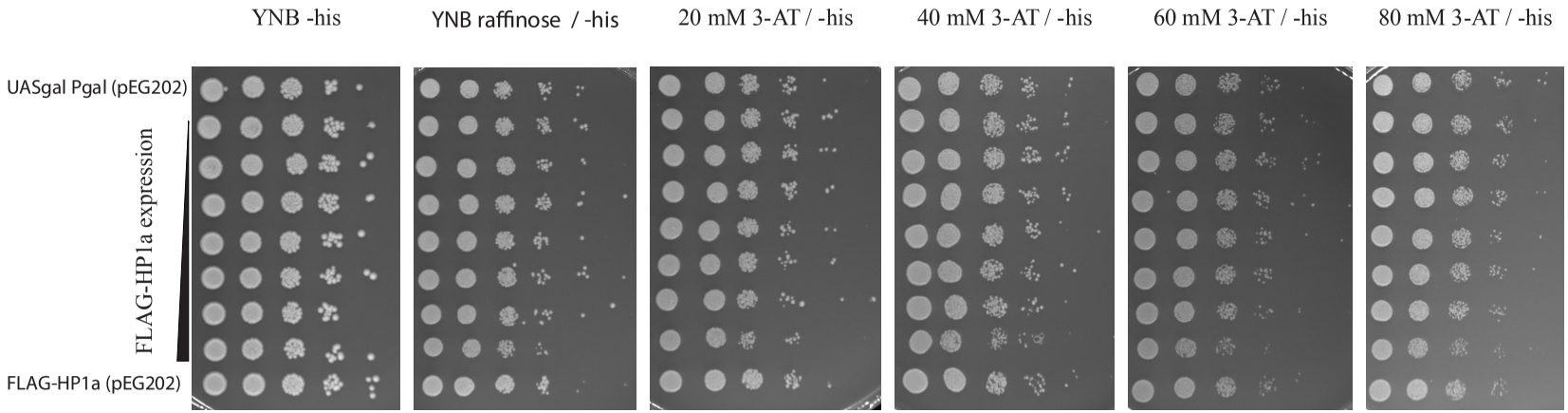

Fig. 25 Dosage dependent silencing by HP1a. HP1a was integrated in a plasmid library with different promoter strength (Blazeck, *et al* 2012). All plasmids were transformed into YS18 with the empty pEG202 vector (carrying *HIS3* gene necessary for this assay). On top, the negative control with an empty UASgal Pgal vector, then from top to bottom HP1a inserted in plasmids with rising promoter strength HP1a: Gal4pBS2 Pleum, UASgal CU2 Pcyc, Gal4pBS13 Pleum, Gal4pBS134 Pleum, UASgal, Pgal, UASgal Pgal. At the bottom the standard HP1a (pEG202) in YS18 pRS406empty is spotted on the plates. Yeast were grown in raffinose containing medium, induced with the addtion of galactose over night, then spotted either on standard YNB glucose medium, or YNB raffinose, or YNB medium with raffinose, galactose and the above indicated 3-AT concentration.

3.3.3 HP1a increases expression from the *GAL* promoter

We used a *GAL1* promoter fused to the lacZ gene. The bacterial gene lacZ encodes a β-galactosidase. This allowed us to measure the induction of *GAL1* with a β-galactosidase assay. Cells were grown in raffinose-containing medium and *GAL1* was induced by the addition of galactose to the medium. Here we measured two time points, one after 6 h and o/n (Fig. 26). In contrast to our previous results that pointed to a general repressive effect of HP1a, here we observed a stronger induction of *GAL1* in the presence of HP1a at the 6-h time point. After o/n induction the wild type caught up with the HP1a strain. The observed effect might also be influenced by the lower expression of HP1a in the presence of galactose as described in the previous paragraph.

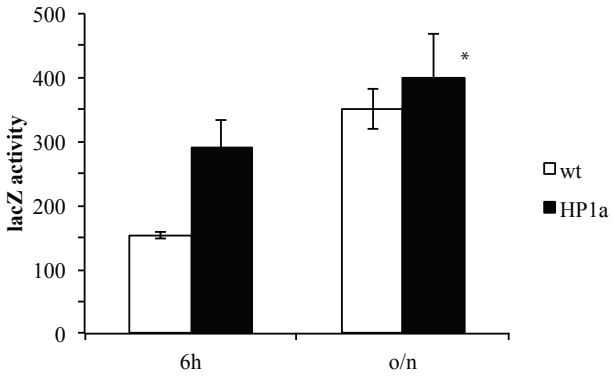

Fig. 26. Increased expression of *GAL1* by HP1a. β-galactosidase activity of GAL1-lacZ fusion constructs (p416-GAL1-lacZ) in CY337 harboring pEG202 empty or pEG202 HP1a. Induction by adding galactose to raffinose medium for 6 h or o/n. The p416-GAL1-laZ plasmid is driven by a GAL1 promoter and expresses lacZ. Activation was measured by β-galactosidase activity. Error bars indicate SEM of 3 or 2 biological replicates (*, outlier was not considerated valid).

3.4 Combined Effects of dSu(var)3-9 and HP1a on gene expression

3.4.1 Expression of dSu(var)3-9 and HP1a together show no stronger effect than expression of HP1a alone regarding *HIS3* expression

In the previous section, we showed a repressive effect of dSu(var)3-9, when targeted either by Pho4-DBD or lexA-DBD to the *PHO5* promoter, and also at *PHO8* and *PHO84,* but only if targeted by Pho4-DBD. HP1a led to a roughly twofold expression decrease at all three *PHO* promoters and a repressive effect for *HIS3*. In the next step, we expressed both factors in yeast, as this may reconstitute the basic cofactor set for heterochromatin formation.

Since HP1a showed such a strong effect in the 3-AT plating assay, we also wanted to investigate in this assay the effect of HP1a coexpressed with dSu(var)3-9.

In Fig. 15 we already showed that dSu(var)3-9 alone had no effect on *HIS3* expression. Displayed in Fig. 27 is the complete set of the samples of the experiment belonging to Fig. 15. The addition of HP1a, either as wt or CD mutant, resulted in a diminished growth of the yeast. But comparing Fig. 27 with Fig. 24 the effect was not stronger in the strain expressing both HP1a and dSu(var)3-9. The activity of dSu(var)3-9 did not further influence the expression levels, as the SET mutant itself showed the same effect as wt dSu(var)3-9. The repressional effect of the HP1a CD mutant was also the same.

In agreement with our previous results, the HP1a CD/CSD double mutant lacked the HP1a phenotype. It appears from this experiment that the not targeted dSu(var)3-9 and HP1a together do not have a stronger effect on gene expression compared to HP1a alone.

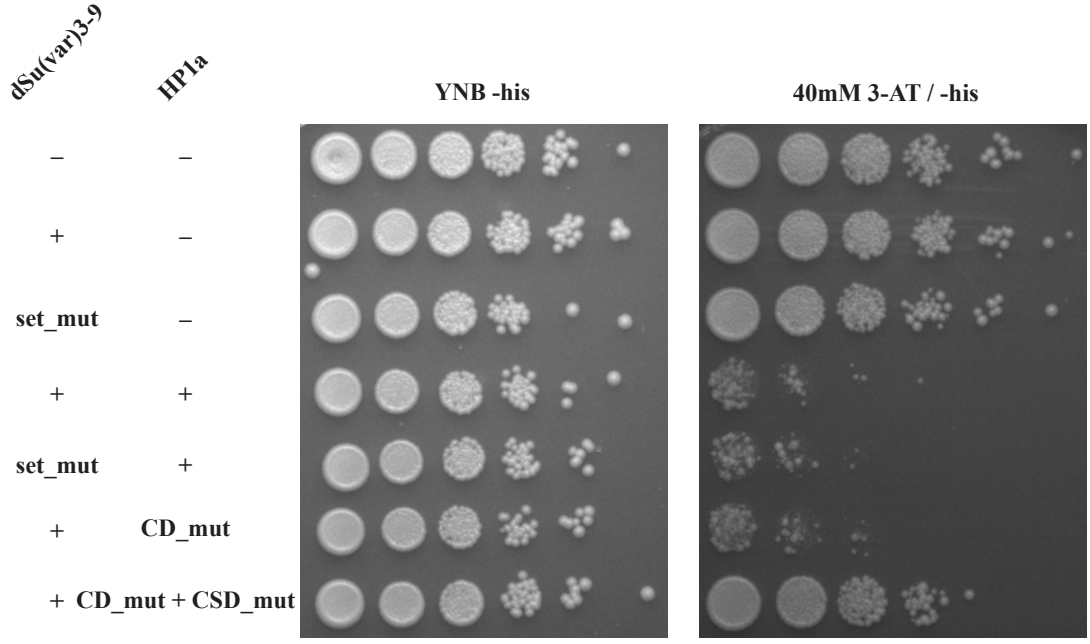

Fig. 27. The diminished growth on 3-AT plates due to HP1a is not stronger in combination with dSu(var)3-9. Same experiment as described in Fig. 15. dSu(var)3-9 was expressed from an pRS406 integration vector, while the FLAG-tagged HP1a variants were expressed from a pEG202 vector in an YS18 strain. The yeast strain in the first row carries also the two vectors, but without an insert. One representative biological replicate of at least 2 replicates is shown here (partially same data as in Fig. 15), see supplementary material for further replicates (Fig. S 4).

3.4.2 Synergistic repression of PHO5 by lexA/dSu(var)3-9 and HP1a

With the lexA-DBD/Su(var)3-9 construct we have a targeted approach with the inserted lexA-BS at the *PHO5* promoter and a not-targeted approach, when combined with the wt *PHO5* promoter. Looking at the non-targeted approach first, HP1a alone reduced the acid phosphatase activity about twofold (Fig. 28). LexA-DBD/Su(var)3-9 did not show an effect at the wt *PHO5* promoter (Fig. 16, Fig. 28). Supporting our previous data shown in Fig. 16, expressing both proteins together with a wt *PHO5* background resulted in the same expressional change

as seen with HP1a alone. So, in a not targeted approach we did not see a synergism between HP1a and lexA-DBD/Su(var)3-9. In contrast, targeting lexA-DBD/Su(var)3-9 via the inserted lexA_BS at the *PHO5* promoter and coexpressing HP1a resulted in an even stronger repression of *PHO5*, pointing to a synergistic effect (Fig. 28). Investigating the effect of the methylation of H3K9 and HP1a, we included the SET mutant. Although there is a minimal increase in the phosphatase activity, we would still conclude that methylation once again has no major role in this synergistic effect.

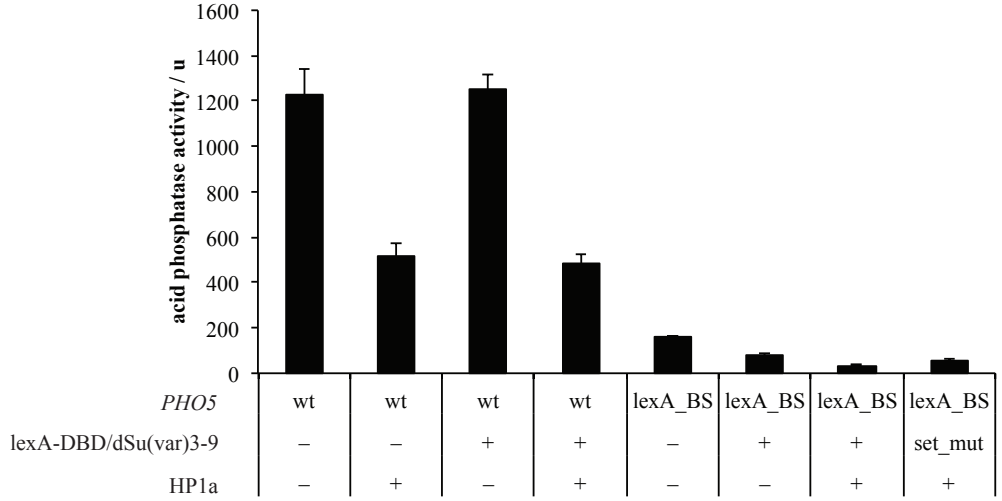

Fig. 28. Repression of *PHO5* in a *rph1Δ* background with dSu(var)3-9 and HP1a. Acid phosphatase activity after o/n induction. CY339 *pho5::ura3 rph1::KANMX4* with or without lexA-DBD/dSu(var)3-9 genomically integrated (pRS406) carrying additionally either an empty expression vector (pEG202) or a FLAG-tagged HP1a. *PHO5* was on a reporter plasmid either as wt or with a lexA-BS (see Fig. 3). The strain carrying only the lexA_BS did not carry an empty vector or HP1a as the rest did. Error bars indicated SEM. N left to right 4, 4, 3, 9, 3, 3, 9, 9.

3.4.3 HP1a slows down induction of *PHO84* independently of lexA targeted dSu(var)3-9

In Fig. 23 we already demonstrated on the level of mRNA that HP1a alone reduced the expression of *PHO84*, while a lexA targeted dSu(var)3-9 at *PHO84* did not show a repressional effect neither at steady state nor during induction (Fig. 19). Within the same experiment we also coexpressed HP1a to investigate a potential synergistic mechanism of HP1a and lexA-DBD/dSuvar(3-9). Here we could reproduce the repressional effect of HP1a that we already showed with reduced levels of mRNA. In contrast, on the level of phosphatase activity assay only the kinetics, but not final levels of *PHO84* induction were reduced in all strains carrying HP1a (Fig. 29). This might be due to higher stability of the acid phosphatase compared to mRNA, i.e., acid phosphatase accumulates over time.

We did not observe any synergistic effect between HP1a and the targeted dSu(var)3-9, as all HP1a strains showed a reduced activity of the acid phosphatase independent of coexpression of a targeted, non-targeted or SET mutant lexA-DBD/dSu(var)3-9 (Fig. 29).

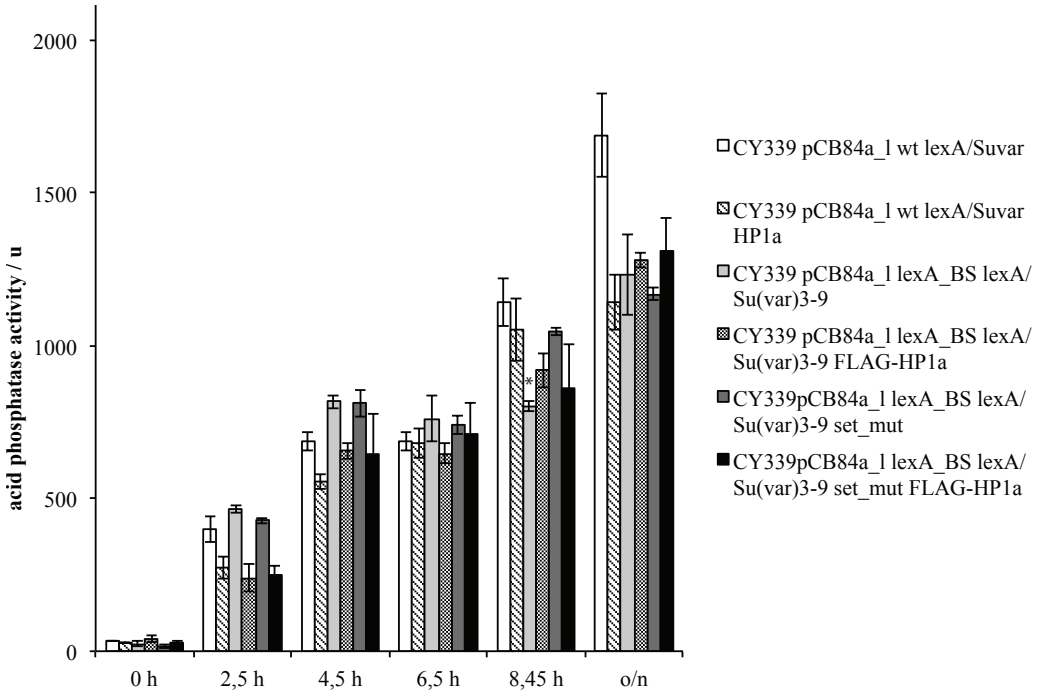

Fig. 29 HP1a delays *PHO84* induction, but independently of dSu(var)3-9. *PHO84* induction kinetics upon phosphate starvation measured by acid phosphatase activity. Reporter plasmid carried the *PHO84* promoter region (either wt *PHO84* (pCB84a_l) or *PHO84* with lexA_BS (pCB84a_l_lexA_BS)) with the reporter gene being *PHO5* in a CY339 *pho5::ura3* strain. The lexA-DBD/dSu(var)3-9 construct was genomically integrated with a pRS406 vector. Strains carried either an empty vector (pEG202) or HP1a (same vector). Parts of dataset were already shown in Fig. 19. Error bars show the SEM of two (*, outlier was not considerd valid) or three biological replicates.

3.4.4 Synergistic repression of *PHO* genes by Pho4-DBD/dSu(var)3-9 and HP1a

Targeting dSu(var)3-9 with the Pho4-DBD showed a repressional effect not only at *PHO5*, but also at *PHO84* and to some degree at *PHO8* (Fig. 20, Fig. 21). Fig. 30 presents the previous data of Pho4/dSu(var) with the additional data for coexpressing HP1a and its mutants in the various strains. Fig. 30A shows the acid phosphatase activity in the various strains. The strongest effect was seen with dSu(var)3-9 and HP1a or its CD mutant. The activity was almost as low as in wt yeast grown in repressive phosphate-containing medium (data not shown, personal communication Philipp Korber). This confirms our previous data regarding that binding of the CD to H3K9me2 is not necessary for the repression of a gene. The SET mutant of dSu(var)3-9 with HP1a or the CD mutant did show a slightly but significantly higher expression level. However, we would not base very firm conclusions on this result. Especially as the strain with dSu(var)3-9 and the CD mutant of HP1a behaved similar to the strain

with the SET mutant and wt HP1a., i.e., in the former strain the ability of HP1a to bind methylated H3K9 is compromised, and in the latter case the SET mutant cannot set the methylation mark.

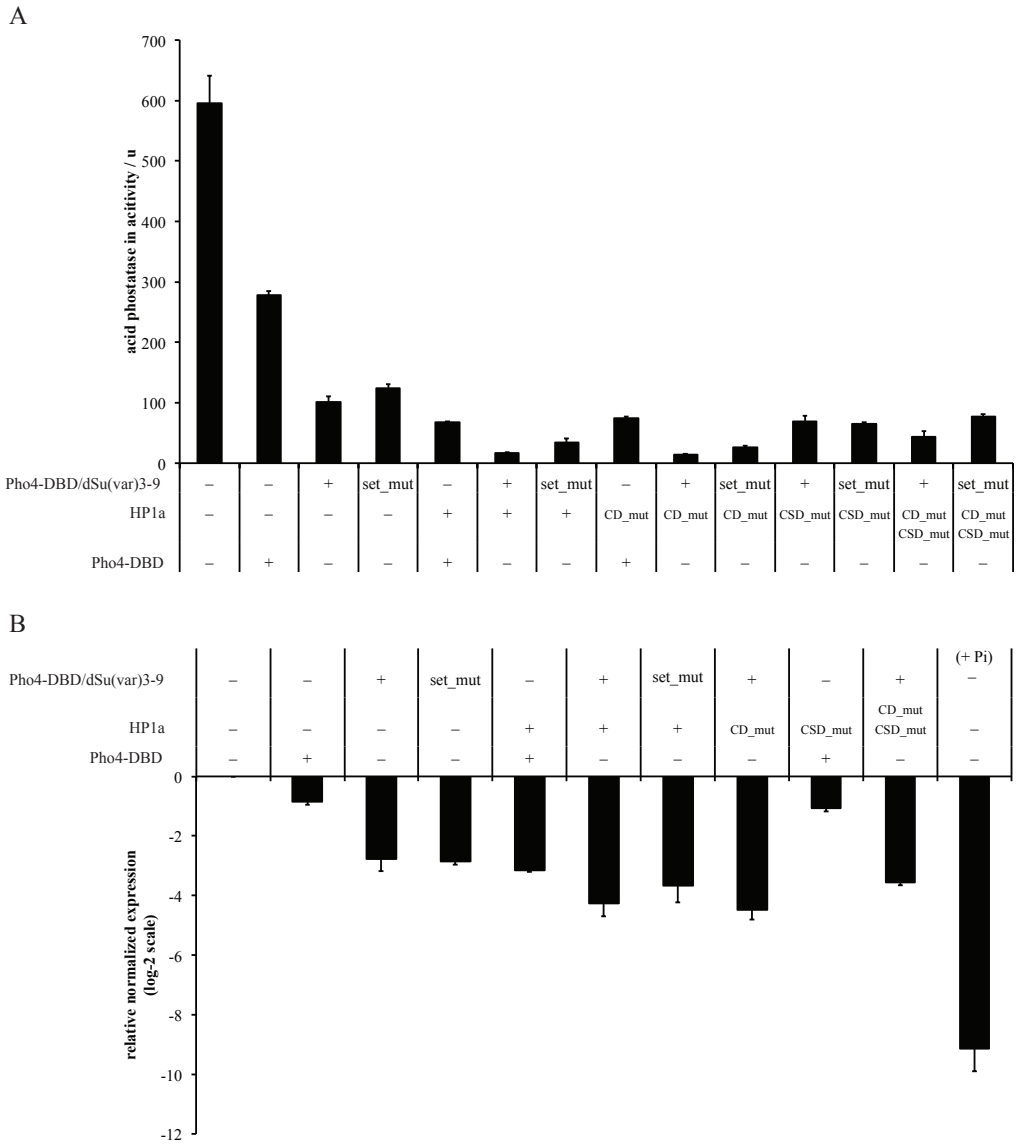

Fig. 30 *PHO5* expression analysis with Pho4-DBD/dSu(var)3-9, Pho4-DBD and HP1a constructs. (A) Overnight acid phosphatase activity in a CY337 background. Strains with none or integrated pRS406 vector carrying Pho4-DBD/dSu(var)3-9 or Pho4-DBD. FLAG-tagged HP1a variants were expressed on a pEG202 vector. Strains not carrying HP1a variants had an empty pEG202 vector. Error bars indicate SEM. Numbers (n) of biological replicates from left to right: 9, 6, 6, 9, 6, 9, 9, 6, 6, 9, 3, 3, 3, 3 (B) qRT-PCR of overnight phosphate starved cells. Same strains as in (A) were used. Change of gene expression is shown on a log2 scale. mRNA level of each run was normalized to a housekeeping gene (*ACT1*) and then put in relation to the induced wt of the same run. Parts of dataset were already shown in Fig. 20. Error bars indicate SEM. N left to right: 3, 3, 3, 2, 2, 3, 3, 3, 2, 2, 3.

Compared to the control with coexpression of Pho4-DBD and HP1a, the dSu(var)3-9 variants coexpressed with HP1a or the CD mutant all showed a more pronounced decrease in the acid phosphatase activity. In contrast to that, the CSD domain again played an important role in the ability of HP1a to repress *PHO5*. The CSD mutant coexpressed with Pho4-DBD/dSu(var)3-9 led to an expression level of *PHO5* that was not as much repressed as with the full length HP1a coexpressed with Pho4-DBD/dSu(var)3-9, but still more repressed than the activity level of expressing dSu(var)3-9 alone. So, the CSD was important for achieving the synergistic repression by HP1a together with dSu(var)3-9, but even without this domain HP1a could still exert its repressive effect as the activity level was similar to that of HP1a cexpressed with Pho4DBD. The HP1a CD/CSD double mutant showed similar results as the CSD mutant alone.

To confirm our data, we also looked at mRNA levels. Yeast cells were induced overnight in phosphate-depleted medium. A wt grown in phosphate containing YNB served as control for the repressed state of the *PHO* genes.

The results for *PHO5* are given in Fig. 30B. The left part was already presented in Fig. 20B and showed the repressive effect of Pho4-DBD/dSu(var)3-9. The greatest expressional reduction of *PHO5* is seen, as expected from previous results, in strains carrying HP1a or the CD mutant together with Pho4-DBD/Suvar)3-9. It could have been assumed from the acid phosphatase activity measurements, that the repressive effect would be comparable to the not induced wt. But here we clearly see that the wt in a repressive state had by far the lowest expression of *PHO5*. Consistent with our acid phosphatase assay we see an increase of the expression in a HP1a CD/CSD double mutant coexpressed with Pho4-DBD/dSu(var)3-9.

At *PHO8* (Fig. 31) we see a similar result as at *PHO5*. Since *PHO8* is rather a weak promoter (Barbarić*, et al* 1992), the expression level changes are not as strong as at *PHO5*. Coexpression of HP1a led again to a stronger repression of *PHO8*, regardless of the SET domain activity or the functional status of the CD. The HP1a CD/CSD double mutant did not lead to a decreased expression of *PHO8* compared to the sole expression of Pho4-DBD/dSu(var)3-9.

To our surprise, the Pho4DBD with HP1a had the biggest impact on gene expression here. Taking into consideration that we just have 2 biological replicates for this strain, this has to be viewed as preliminary data.

In line with our results obtained by the acid phosphatase activity and mRNA levels of *PHO5* and *PHO8*, the expression data of *PHO84* showed the same synergistic effect of Pho4-DBD/dSu(var)3-9 and HP1a (Fig. 31). Pho4DBD coexpressed with HP1a resulted in the same repressional effect as Pho4-DBD/dSu(var)3-9 alone. HP1a or the CD mutant together with

Pho4-DBD/dSu(var)3-9 repressed *PHO84* almost four-fold compared with Pho4-DBD/dSu(var)3-9 alone showing the synergistic effect of both factors. The SET mutant with HP1a showed, as previously at *PHO5,* a slight increase of the expression level when compared to the Pho4-DBD/dSu(var)3-9 HP1a strain. Nevertheless, we would still not interpret too much into this slight increase. Expression levels in the CSD mutant Pho4-DBD strain did not change compared to just the Pho4-DBD strain. In contrast to that the HP1a CD/CSD double mutant with Pho4-DBD/dSu(var)3-9 still led to a small decrease in the mRNA levels, pointing to a possible residual interaction of dSu(var)3-9 and HP1a.

In general, we saw the strongest repression of our *PHO* promoters when expressing Pho4-DBD/dSu(var)3-9 with HP1a, although we did not reach the level of the repressed wt reference state. The expressional changes were independent of H3K9me or the CD, but did mostly depende on the CSD.

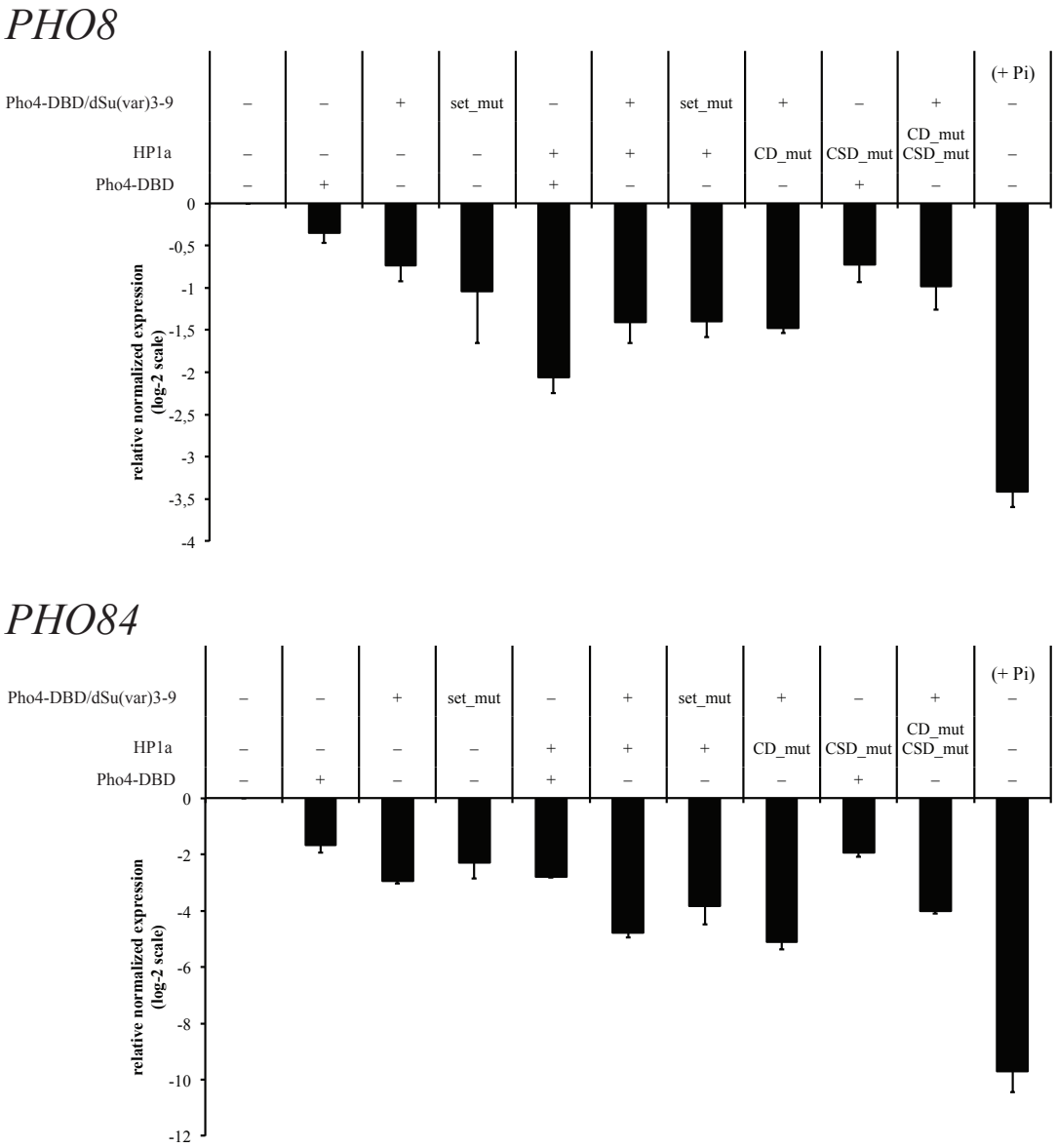

Fig. 31 *PHO8* and *PHO84* mRNA levels in strains carrying Pho4-DBD or Pho4-DBD/dSu(var)3-9 and HP1a variants. Same strains were used as previously described (Fig. 30). As in Fig. 30 cells were grown in phosphate-free medium o/n. mRNA of the samples were normalized to a housekeeping gene (*ACT1*) and then put in relation to induced wt, which was prepared at the same time. Parts of dataset were already shown in Fig. 21. Error bars indicated SEM. N left to right: 3, 3, 3, 2, 2, 3, 3, 3, 2, 2, 3.

3.5 Chromatin remodeling was reduced by Su(var)3-9 and HP1a

In the past section we showed that dSu(var)3-9 and HP1a had the strongest repressive effect on our *PHO* genes. As already mentioned in the introduction, the nucleosomes of the *PHO* promoters are remodeled into an extensive hypersensitive site upon induction. In order to see structural changes of chromatin at these promoters we performed limited DNase I digestion and digestion with specific restriction enzymes combined with indirect end-labeling.

Limited DNase I digestion and digestion with restriction enzymes allows the mapping of nucleosome positioning at the locus of interest. Canonical nucleosomes protect the DNA from being cut by DNase I or restriction enzymes, while naked DNA or DNA in regions where nucleosomes are remodeled is highly susceptible for DNase I and restriction enzymes.
But quantitating the accessibilities with DNase I has been difficult. In this case, the digestion with restriction enzymes allows measuring the absolute accessibility of a certain DNA region (Almer*, et al* 1986, Gregory*, et al* 1999a, Reinke and Horz 2004).
We compared HP1a, Pho4-DBD/dSu(var)3-9 as well as HP1a plus Pho4-DBD/dSu(var)3-9 expressing strains under inducing conditions to the wt (induced and not induced). The wt grown in phosphate-containing medium showed 4 well-positioned nucleosomes at the *PHO5* promoter. Upon induction in phosphate-free medium, the nucleosomes were remodeled leading to an extensive hypersensitive site (Fig. 32). The accessibility of the -2 nucleosome was measured by ClaI digestion. The closed promoter in the wt had an accessibility of 9% compared to 48% of the induced wt. The induced strains carrying HP1a or Pho4-DBD/dSu(var)3-9 alone showed the same DNase I pattern compared to the induced wt. The ClaI accessibility was also not affected. Expression of HP1a and Pho4-DBD/dSu(var)3-9 together showed an altered chromatin remodeling at *PHO5*, the region protected by the -3 nucleosome was wider than at the induced wt promoter. The accessibility was also reduced to 29%.
Pho4-DBD/dSu(var)3-9 or HP1a alone did not affect chromatin remodeling much neither at the *PHO8* nor the *PHO84* promoter (Fig. 33A, B). Chromatin opening was only slightly affected at *PHO8* measured by HpaI accessibility in both strains (66% wt vs. 55% with HP1a vs 50% with Pho4-DBD/Su(var)3-9). *PHO84* promoter opening was even completely unaffected by HP1a (Fig. 33B) (75% wt vs. 73% with HP1a vs. 66% with Pho4-DBD/dSu(var)3-9).
Although the DNase I pattern of the Pho4/Su(var)3-9 HP1a strain was rather unchanged compared to the induced wt, HpaI accessibility at the *PHO8* promoter was markedly reduced in the Pho4-DBD/dSu(var)3-9 Hp1a strain to 30%.
At the *PHO84* promoter the binding of Pho4-DBD/dSu(var)3-9 protected the DNA from being cleaved by DNase I, resulting in a protected site at the short hypersensitive site (Fig. 33B). Even tough both Pho4-DBD/dSu(var)3-9 strains showed a similar DNase I pattern, the promoter opening was only affected in the strain coexpressing HP1a, showing a reduced HhaI accessibility of 31% compared to 66% (Pho4-DBD/dSu(var)3-9) or 76% (wt).
The disjunction between the effect on expression by HP1a and Pho4-DBD/dSu(var)3-9 and the unchanged chromatin opening might point towards a posttranscriptional repressive effect.

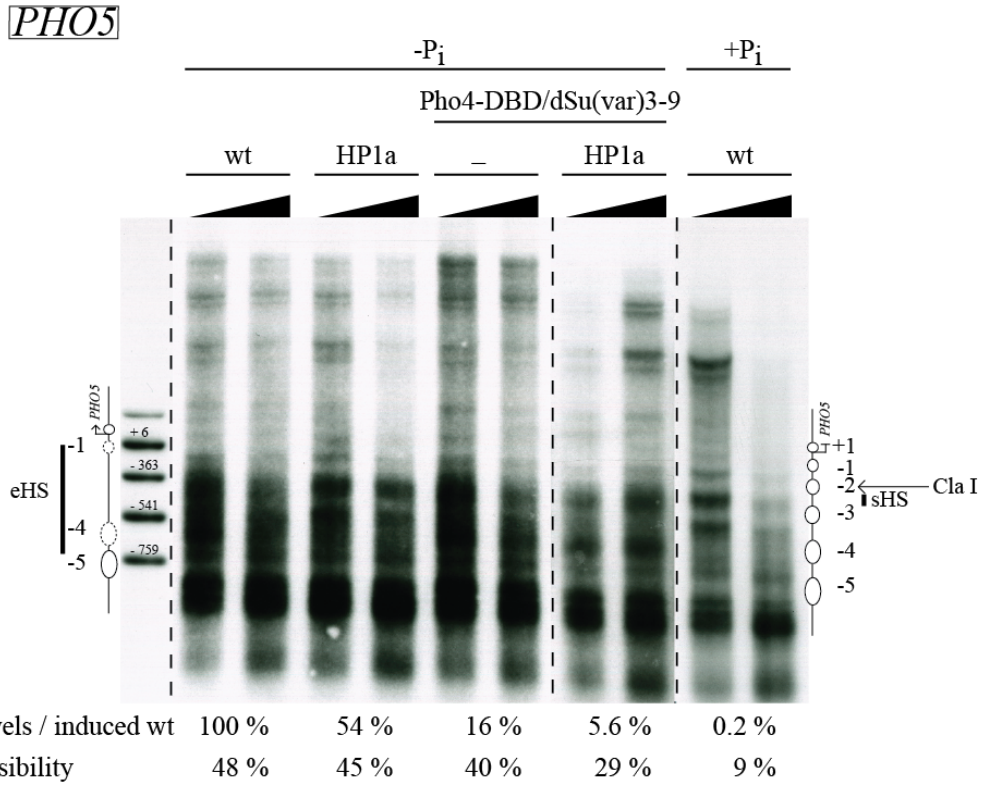

Fig. 32 Chromatin remodeling at the *PHO5* promoter was affected by expression of Pho4-DBD/dSu(var)3-9 together with HP1a. DNase I indirect end-labeling and ClaI accessibility at the *PHO5* locus in CY337 strains in phosphate-containing or phosphate-free medium as indicated above the upper bar (+P_i/ -P_i). Other horizontal bars indicate the respective strains: wt (pEG202 empty vector), HP1a and Pho4-DBD/dSu(var)3-9 with HP1a or without (pEG202 empty vector). Black triangles show increase of DNase I concentration. On both sites of the blot a *PHO5* promoter scheme is shown. The repressed state is shown on the right, the induced state on the left. The numbered circles indicate the positioned nucleosome relative to the ATG (broken arrow), dotted circles represent not totally remodeled nucleosomes upon induction. sHS shows the short hypersensitve site, eHS the extended hypersensitive site of the remodeled open promoter. Marker fragments were prepared by double digestion of a pUC19 plasmid carrying the *PHO5* locus with ApaI and one of the following enzymes: DraI, ClaI, BamHI, FokI (from top to bottom; highest band: artefact band). Numbers at each marker band show the respective position relative to the ATG. All samples ran on the same gel, but the blot was put together with the best exposure of each sample using Adobe Illustrator CS5. In this case the marker was rearranged to the left side and the 2 samples on the right side were cut from blots with longer exposure times. Files were merged to one blot with Adobe Illustrator. Below the DNase I blots the percentage of the mRNA levels relative to the induced wt (see **Fig. 30**) and total ClaI accessibility are given.

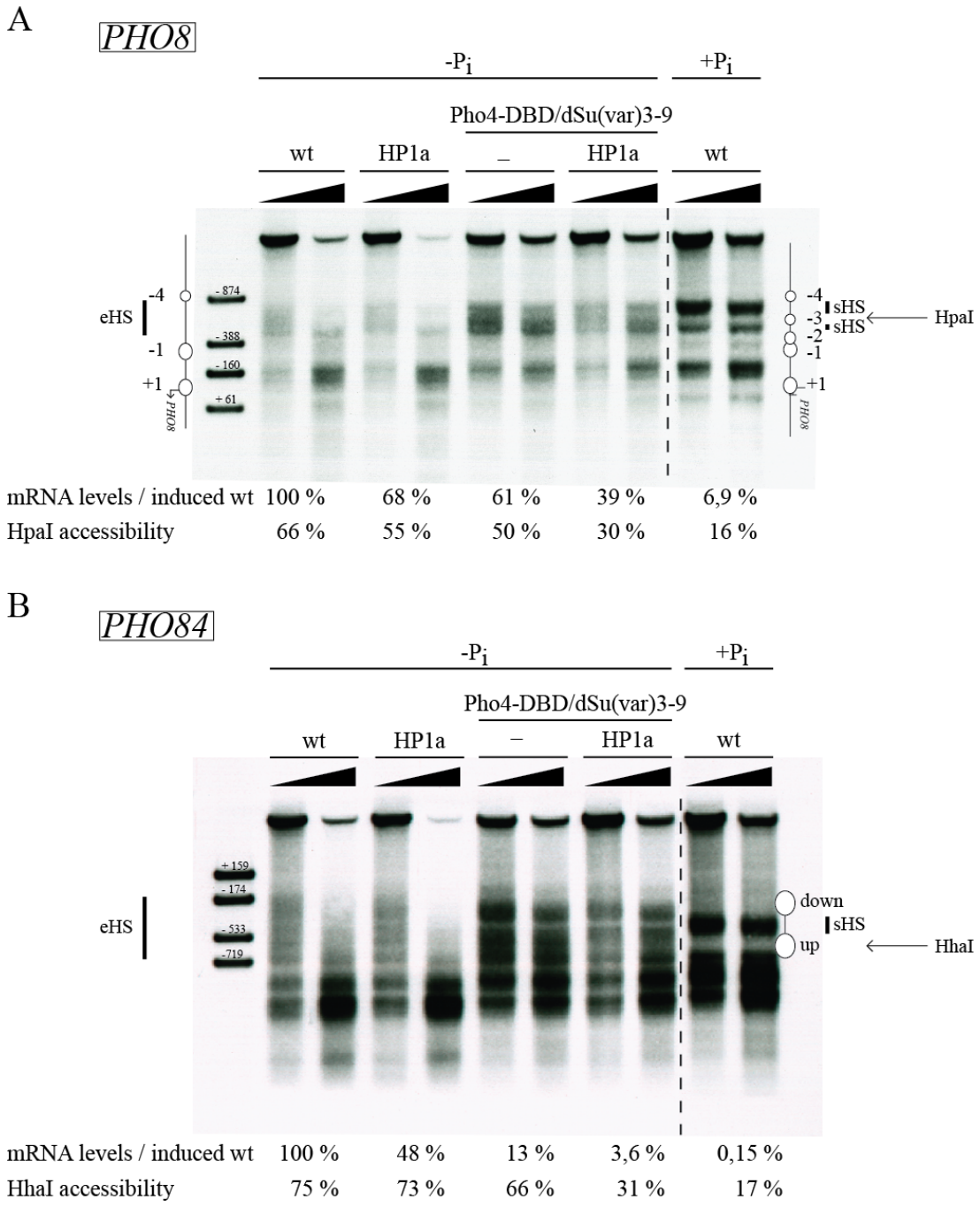

Fig. 33 Remodeling of *PHO8* and *PHO84* promoter in the presence of HP1a and / or Pho4-DBD/dSu(var)3-9. (A) DNase I indirect-end-labeling at the *PHO8* promoter. Description and scheme as in Fig. 19. Marker was a double digested with BglII and SacI, HindIII, NdeI or EcoRV (from top to bottom). Blot image was not modified further. Below the DNase I blots the percentage of the mRNA levels relative to the induced wt (see **Fig. 31**) and the HpaI accessibility are given. (B) Same blot as in (A), but stripped and re-hybridized with PHO84-specific probe. Marker was a double digested with SspI and ClaI, Age I, ApaI or BsrBI (from top to bottom). In the left scheme, "up" and "down" stands for nucleomes positioned relative upstream or downstream of the sHS. Blot was modified with Adobe Illustrator, i.e., the wt under $+P_i$ condition is shown with a shorter exposure time. Below the DNase I blots the percentage of the mRNA levels relative to the induced wt (see **Fig. 31**) and the HhaI accessibility are given.

3.6 Genome-wide effects of dSu(var)3-9 and HP1a expression

With the repressive effect of HP1a alone and the synergistic effect of the targeted dSu(var)3-9, we also looked for genome-wide effects of expressing HP1a and / or dSu(var)3-9. Deletion strains of genes encoding chromatin modifying proteins, grown in steady state, usually do not show very pronounced genome-wide changes in gene expression relative to the wild type. Rather, the important role of chromatin regulators becomes more apparent during dynamic processes like gene activation, which has been pioneered in single locus studies (Barbaric*, et al* 2001b, Gregory*, et al* 1998, Korber*, et al* 2006)). In contrast to single locus studies, Weiner et. al. did a comprehensive study of hundreds of chromatin-associated gene mutants in steady state versus upon stress by the oxidative stress inducer diamide (Weiner*, et al* 2012). Diamide stress has been shown to have a rapid effect on the transcriptome, inducing 602 genes more than 2-fold and repressing 593 genes. We thought such acute stress induction could allow us to detect a possible repressive effect, to compare our strains to this extensive previous work and search for possible similarities.

We compared the wild type strain to either a strain expressing HP1a or HP1a and Su(var)3-9. Shown in Fig. 34 is the change of gene expression upon the stress induction with diamide compared to the wt. Expression of dSu(var)3-9 and / or HP1a led to 4 distinct sets of expression changes. In the largest set (#1; 77 genes) dSu(var)3-9 and / or HP1a led to relatively higher gene expression upon stress induction compared to the wt (Fig. 34). In the second set (#2, 16 genes), expression of HP1a led to lower gene expression as in the wt, but in presence of HP1a and dSu(var)3-9 expression was enhanced. The third set (#3, 25 genes) consisted of what we have observed at our single loci, here both HP1 and HP1a together with dSu(var)3-9 repress genes. The fourth set (#4, 7 genes) behaves as the second one, just in an opposite way, i.e., HP1a and dSu(var)3-9 repressed genes, which were induced in the wt and the HP1a-expressing strains. This analysis only allows us to see relative changes.

With view of our notion that HP1a had a general repressive effect, we wondered if HP1a, dSu(var)3-9, or both are global transcriptional repressors. This would still be consistent with the relative upregulation of some genes, which we saw in our transcriptome analysis, but would be undetectable in our analyses so far. To measure changes in absolute mRNA levels, we did again a transcriptome analysis, but this time we spiked-in *S. pombe* RNA as an external reference (Sun*, et al* 2012). The microarrays we used contained probes for both yeast *S. cerevisiae* and *S. pombe,* making this spike-in normalized comparison of absolute expression levels possible.

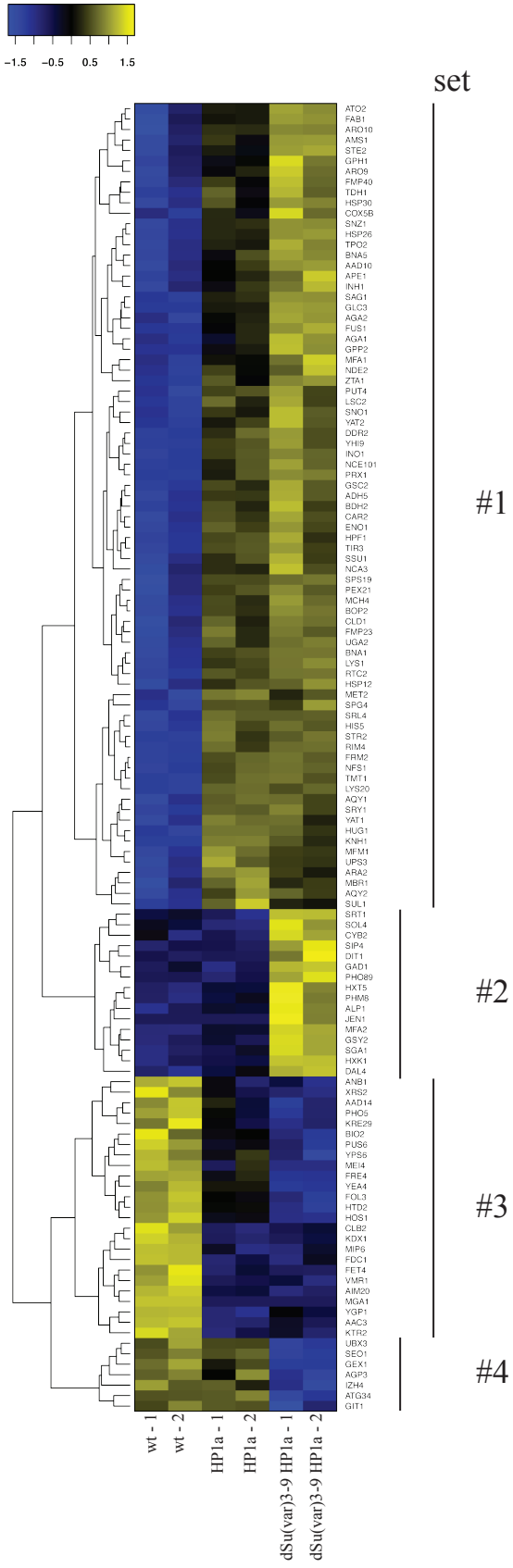

Fig. 34 mRNA expression changes upon stress. Cells were treated 15 min with diamide for stress induction. Data were normalized to wt before stress exposure. YS18 carried either an empty pRS406 vector ("wt") or dSu(var)3-9 on pRS406 and either an empty pEG202 vector or HP1a was expressed from pEG202. Two biological replicates (no. 1 and 2) were prepared and hybridized the same day.

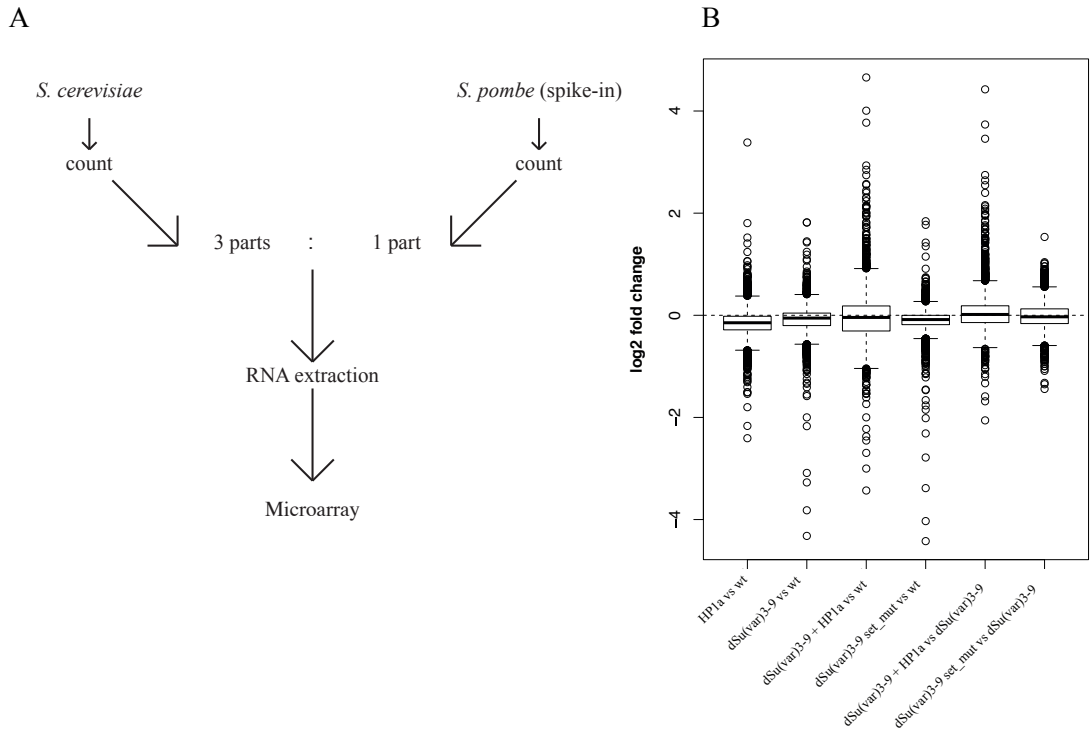

Fig. 35 No absolute gene expression changes oberserved using an *S. pombe* spike-in. (A) Experimental set up: *S. cerevisiae* and *S. pombe* cells were grown logarithmically, resuspended in RNAlater (Ambion) and counted using a counting chamber. RNA was isolated out of 3 parts (cell number) of *S. cerevisiae* and 1 part *S. pombe* and hybridized to the microarray. (B) Y axis presents the log2 fold change of the pair-wise comparison between the strains stated on the x axis. YS18 strains carried either an empty pEG202 empty vector or HP1a expressed from pEG202. dSu(var)3-9 or the respective SET mutant was integrated via a pRS406 vector. Two biological replicates were prepared and hybridized the same day.

Yeast cell were collected, counted, and mixed in relation 3:1. The cell mixture was further processed, RNA isolated and the RNA hybridized to a microarray.

Comparing the mutant strains to the wt and eachother, we did not see on average expression level changes (Fig. 35).

3.7 Excursus

3.7.1 The involvement of the mediator in histone remodeling and eviction

As a side project we collaborated with the group of Randy Morse (published in (Ansari*, et al* 2014)). He observed at the *CHA1* promoter an uncoupling of chromatin remodeling and histone eviction in mediator mutants. Consisting of 25-30 subunits with a structural head, middle, tail and a DK8/kinase module, the mediator has a vital role in the regulation of polymerase II transcribed genes. Via its subunits various interactions are made with histones, activa-

tors, co-activators, general transcription factor and polymerase II subunits (Ansari and Morse 2013).

We investigated the observed uncoupling of chromatin remodeling and histone eviction at the *PHO5* promoter. We chose a *PHO5* variant, in which the Pho4 binding sites are replaced by Gal4 binding sites making it a galactose-inducible promoter driving a lacZ gene where induction is replication independent (Barbaric 2000 EMBO J.). This was important as inactivation of mediator subunits would strongly affect growth rate and thereby physiological *PHO* induction. Upon addition of galactose the wt strain was quickly induced, while the mutant severely lagged behind as measured via lacZ activity (Fig. 36A). Restriction enzyme accessibility to ClaI and thus chromatin remodeling at the *PHO5* promoter was unchanged between both strains (Fig. 36B, performed by Corinna Lieleg). Histone eviction was very strong in the wt upon induction as measured by ChIP and was similar in the med3Δ med15Δ mutant (Fig. 36C). This shows that the uncoupling of nucleosome remodeling and histone eviction in a meditor mutant as seen at the CHA1 promoter is not universal but promoter-specific probably due to different promoter chromatin environments.

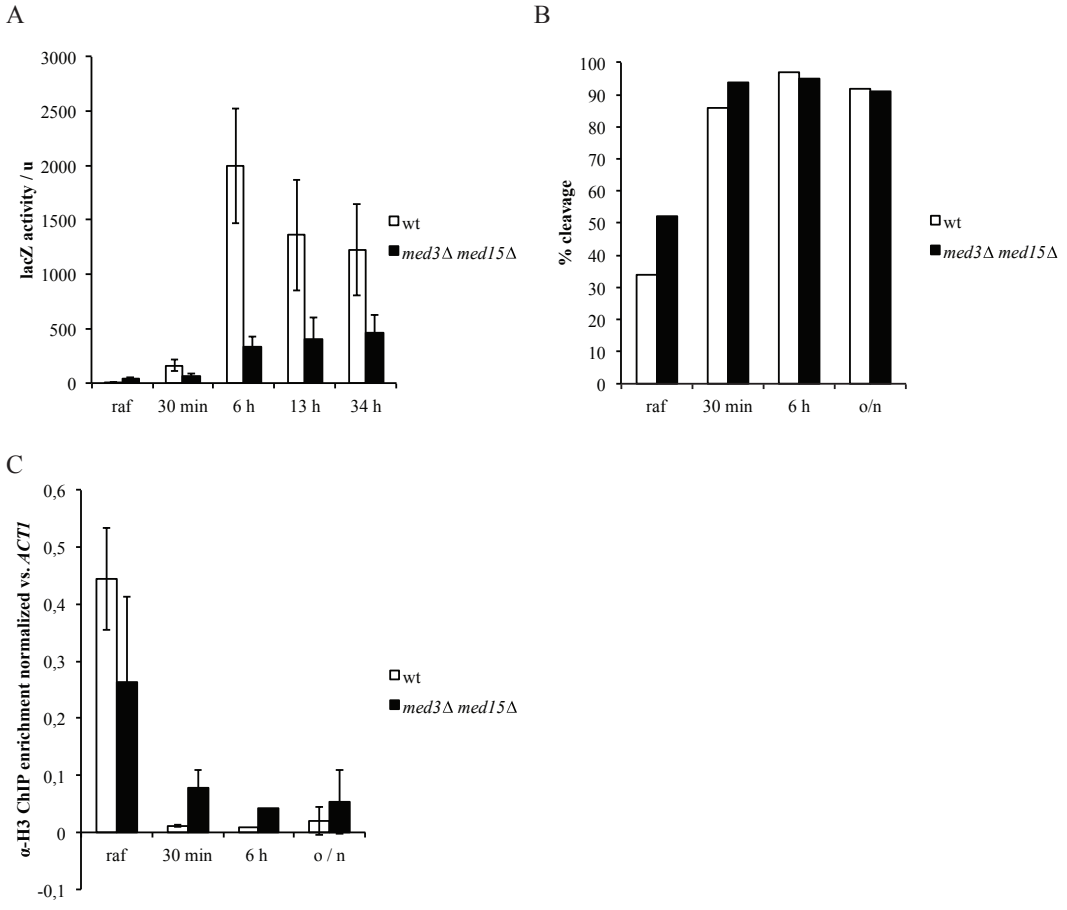

Fig. 36 Nucleosome remodellling or eviction are not dependent on mediator. (A) β-Galactosidase activity measured by LacZ assay for wt (BY4742) or *med3Δ med15Δ* (LS3) containing the p$P_{pho5V33}$-lacZ plasmid. Yeast were grown in raffinose containing medium and induced with the addition of galactose. Error bars show standard deviation of 3 biological replicates. (B) Cla I accessibility at the *PHO5* promoter of the same strains as in (A) with the same induction. (C) Histone occupancy measured by ChIP using above mentioned strains, growth and induction conditions.

4 Discussion

Methylation of histone H3 at lysine 9 (H3K9) and colocalization of heterochromatin protein 1 (HP1) are strongly associated with heterochromatin and well conserved from the unicellular yeast *S. pombe* to humans. In the past 20 years, great advances have been made in chromatin biology. Despite the well characterized domains of HP1a and dSu(var)3-9, the understanding of how these factors mediate the repressive effect of heterochromatin is still not well understood.

Here we used a synthetic biology approach to investigate if H3K9 methylation and HP1a are sufficient for heterochromatin reconstitution in *S. cerevisiae* where these factors do not belong to the endogenous chromatin structure.

4.1 Genome-wide studies

4.1.1 Methylation of histone H3 at lysine 9 by dSu(var)3-9 is enhanced by auxiliary factors

To our knowledge, we were the first to successfully introduce H3K9me as a novel histone modification in *S. cerevisiae*. Using mass spectrometry, we showed that all our constructs were active but to various degrees. Maybe to our biggest surprise *S. cerevisiae* viability and even the transcriptome were unchanged in the presence of H3K9me, even at high global levels, compared to wt yeast or to expression of a SET-domain mutant of dSu(var)3-9 (Table 2, Fig. 8, Fig.35).

The dSu(var)3-9 fusion constructs containing one of the two tested DBDs all showed high global monomethylation levels of 14% (lexA-DBD/dSu(var)3-9) and 7.7% (Pho4-DBD/dSu(var)3-9) and to a small degree di-/ trimethylation of histone H3 (Fig. 8). Overexpression of the lexA-DBD/dSu(var)3-9 variant led to a significant increase of H3K9me2/me3 levels. While the integrated and therefore low copy Pho4-DBD/dSu8(var)3-9 construct dimethylated 1.2%, and trimethlyated 0.2% of histones, the high copy plasmid lexA-DBD fusion construct led to dimethylation of 10% and trimethylation of 2.5% of the histones. This effect is most likely explained by the different expression levels. However, the two different DBDs may also have different degrees of unspecific DNA binding affinities, which could explain, at least partially, the 10-fold increase of H3K9me2/me3 due to the lexA-DBD construct compared to the Pho4-DBD construct.

dSu(var)3-9 alone, without a DBD, led to only 0.5% monomethylation of H3K9 and no measureable H3K9me2/me3 levels. The poor monomethylation levels due to the non-targeted

dSu(var)3-9 were improved upon coupling to a DBD. Overexpression of a DBD-dSu(var)3-9 facilitated not only the monomethylation levels, but also showed a significant increase of H3K9me/me3. The undetectable levels of H3K9me2/me3 via untargeted dSu(var)3-9 and the very low levels of H3K9me2/3 due to the low copy number Pho4-DBD/dSu(var)3-9 provides further evidence to previous *in vitro* data that suggested dSu(var)3-9 as a non-processive enzyme (Eskeland*, et al* 2004). This means dSu(var)3-9 releases its substrate after monomethylation and has to bind a second or third time to its substrate for generating H3K9me2/me3. For a processive mechanism of dSu(var)3-9, we would have expected equal or more similar amounts of me1, me2 and me3.

HMT activity of dSu(var)3-9 increases in a linear manner dependent on the enzyme concentration, which might explain the observed dosage-dependent effect on PEV (Eskeland*, et al* 2004). The higher methylation levels across all H3K9me states observed with the lexA/dSu(var)3-9 overexpression construct, demonstrates that the extent H3K9me2/me3 is dosage dependent.

The low methylation level of dSu(var)3-9 compared to Pho4-DBD/dSu(var)3-9, which share the same plasmid backbone, implicates that auxiliary factors are needed for the recruitment of dSu(var)3-9 to chromatin. By co-expression of HP1a with dSu(var)3-9 we saw a significant increase not only in monomethylation levels, but also in H3K9me2 and some H3K9me3 (Fig. 11). This confirms, as shown before, that HP1a and dSu(var)3-9 interact with each other and that this interaction leads to a more effective tethering of dSu(var)3-9 to chromatin than just on its own (Schotta*, et al* 2002). Furthermore, we were able to pinpoint this interaction to the chromoshadow domain of HP1a. Expression of the CD / CSD double mutant showed similar low amounts of H3K9me1 as expression of dSu(var)3-9 on its own (Fig. 11), while that of the CD mutant showed the same results as that of the wt HP1a. Our work shows that the CSD is essential for the interaction of HP1a and Su(var)3-9 and is necessary for HP1a to bind chromatin and tether Su(var)3-9 to chromatin.

4.1.2 Testing factors that may counteract H3K9 methylation

In the course of the discovery of histone demethylases, Rph1 was identified as an JmjC-domain containing histone H3K36 demethylase (Klose*, et al* 2007). While characterizing the enzyme's specificity, they described Rph1 not only as an H3K36 demethlylase, but also as an H3K9 demethylase. This made the authors wonder if H3K9 methylation was present in *S. cerevisiae* at some earlier time in evolution. In our case, Rph1 may have counteracted H3K9 methylation by Su(var)3-9. Thus, Rph1 was an ideal candidate to investigate whether we could reach higher methylation levels in *S. cerevisiae* via its deletion. Another candidate was

the kinase Snf1, which targets H3S10 and many other substrates. H3S10 phosphorylation hinders H3K9 methylation by dSu(var)3-9 (Duan, *et al* 2008, Rea, *et al* 2000). Therefore we asked if deletion of *SNF1* increased H3K9 methylation levels.

In neither the *rph1Δ* single nor the *rph1Δ snf1Δ* double mutant did we observe a significant change in global methylation levels, not even for H3K9me2 and me3 (Fig. 9). Although Rph1 was shown to demethlyate H3K9me *in vitro*, our results could simply mean that H3K9me is not a substrate of Rph1 *in vivo*. H3S10 phosphorylation occurs predominantly during mitosis, thus dSu(var)3-9 would only be hindered during the short phase of mitosis and not in the other cell cycle phases. The very high methylation activity of the lexa/dSu(var)3-9 construct might mask the effect seen with the demethylase and kinase deletion strains, as the regularly expressed Rph1 and / or Snf1 concentrations in the cell are simply too low to have a measureable effect on the high methylation levels. To further characterize the influence of Rph1 and / or Snf1, follow up experiments with overexpression of Rph1 and / or Snf1 need to be carried out. Here it would also be important to choose a dSu(var)3-9 construct which is not overexpressed.

4.1.3 Genome-wide influence of dSu(var)3-9 and HP1a on gene expression

With the successful introduction of H3K9 methylation, we performed genome-wide expression studies to analyze the transcriptional effects of not targeted dSu(var)3-9 and HP1a. Genome-wide studies in yeast to identify transcriptional effects of chromatin modifying enzymes have so far mostly been carried out at steady state, i.e., yeast growing in rich medium. However, single locus studies already showed that chromatin regulators play an important role in dynamic processes, for example during gene activation |(Barbaric, *et al* 2001b, Gregory, *et al* 1998, Korber, *et al* 2006). To further uncover the role of chromatin modifying enzymes on a genome-wide level, yeast mutants were exposed to diamide stress, which has been shown to have a rapid effect on the transcriptome, inducing 602 genes more than 2-fold and repressing 593 genes (Gasch, *et al* 2000, Weiner, *et al* 2012). Expression analysis of 83 histone mutants, and 119 gene deletion mutants showed, similar to the single loci studies, a greater change of gene induction / repression upon diamide exposure in the mutants compared to the wt than comparing mutants and wt under steady state condition than yeast growing under steady state conditions (Weiner, *et al* 2012). Thus, the diamide exposure would allow us a better discrimination of expressional changes upon the addition of new chromatin regulators.

Using microarrays to detect transcriptional changes during steady state and diamide induced stress response, we could cluster four different types of expression changes while expressing dSu(var)3-9 and / or HP1a. The majority of genes, representing cluster #1, were induced in

the presence of HP1a or HP1a / dSu(var)3-9 upon diamide exposure. In the second largest group (cluster #3) HP1a or HP1a / dSu(var)3-9 had a repressive effect. One of the genes was *PHO5*, which confirms our results at the *PHO* loci. In the two other small clusters (#2 and #4) either HP1a alone or HP1a / dSu(var)3-9 showed a repressive effect on gene expression. Overall the addition of these heterologous heterochromatin proteins showed an effect in only a small subset of genes (125 genes). This fits with the viability, measured by doubling times, of our yeasts with the various dSu(var)3-9 and HP1a constructs being pretty much unchanged compared to the wt. This could simply imply that untargeted H3K9me and / or HP1a have little effect on the transcriptional machinery in yeast. However, it is not clear if the majority of these effects are due to direct changes in chromatin structure or due to secondary effects, for example, a general repressor could be repressed by H3K9me and / or HP1a leading to an upregulation of target genes.

The interpretation of these data can be further elaborated. We cannot distinguish between direct and indirect effects. We do not have genome-wide H3K9me and HP1a binding profiles in yeast, which would allow for correlation with our gene expression data. This would definitely be very useful to carry out in the future. We also chose the diamide approach in order to compare our data with the Weiner et. al. study. Further bioinformatical analysis could show potential similarities or interaction partners of HP1 and H3K9me with existing chromatin modifiers in yeast.

4.1.4 HP1a / dSu(var)3-9 do not influence the overall expression level in yeast

In view of the HP1a repressive effects seen in the single loci studies, we wondered if HP1a, dSu(var)3-9, or both are general transcriptional repressors. A general repressor would downregulate all transcribed genes to a certain degree when compared to an external reference. Usually, with the internal controls on the expression arrays an overall down- or upregulation of transcription cannot be seen. *S. pombe* RNA spike-in was used as an external reference on our microarrays as developed in the Cramer group (Sun*, et al* 2012). Here too, we didn't see an overall downregulation by HP1, dSu(var)3-9, or both. Although the replicates were not as homogenous as in the previous experiment, especially due to crossover effects of the spiked in *S. pombe* RNA, we can still conclude from this experiment that dSu(var)3-9 and / or HP1a do not influence transcription on a genome-wide level as, for example, has been shown for c-Myc (Lin*, et al* 2012, Nie*, et al* 2012).

4.2 Targeted approach

4.2.1 Methylation is sufficiently targeted via Pho4-DBD to PHO loci with Pho4 binding sites

For the targeted approach we used fusion proteins of a DBD with dSu(var)3-9 to tether dSu(var)3-9 to the loci of interest.

The lexA-DBD/dSu(var)3-9 construct led to a twofold increase of H3K9me2 at the modified *PHO5* locus compared to the *PHO8* locus, although at the telomere control locus, we also observed a significant increase in dimethylation (Fig. 12). Due to the overexpression of lexA-DBD/dSu(var)3-9, we observed very high global H3K9 methylation levels by mass spectrometry, which may obscure any locus specific targeting. The high telomere enrichment might be due to the nearby lexA consensus sequence and due to the lower histone turnover compared to other genomic regions (Dion*, et al* 2005, Svensson*, et al* 2015). In order to make a meaningful conclusion as to whether we have a significant enrichment at the targeted loci compared to other gene regions, we would have needed to test more control loci.

However, since the Pho4-DBD coupled dSu(var)3-9 constructs seemed more promising, we did not follow up on this. For the Pho4-DBD/dSu(var)3-9 construct we had a strong enrichment at the *PHO5* and *PHO84* promoter, but close to no enrichment at *PHO8*. In conjunction with HP1a we observed overall higher H3K9me2 levels (Fig. 13, Fig. S 1, Fig. S 3), although the relative enrichment was similar.

With the successful targeting of our fusion construct to the loci of interest, we were able to directly see methylation-dependent or -independent effects of dSu(var)3-9. Using the well-studied *PHO* promoters, we will discuss changes in gene expression and promoter structure in the following chapters.

4.2.2 Targeted dSu(var)3-9 represses genes independent of histone methylation

Methylation of H3K9 is one of the key features of constitutive heterochromatin. This was shown extensively by correlative studies either with immunofluorescence, damID or genome-wide chromatin immunoprecipitation (Filion*, et al* 2010, Greil*, et al* 2003, Kharchenko*, et al* 2011, Schotta*, et al* 2002). A first attempt to investigate the repressive mechanism of H3K9 methylation was attempted by Snowden and colleagues (Snowden*, et al* 2002). In a mammalian cell culture system, they showed that truncated versions of the methyltransferases G9a and SUV39H1 linked to an engineered zinc-finger transcription factor were able to repress the targeted gene. This was dependent on the methyltransferase activity. With the same system, it was shown that H3K9me2 was sufficient for downregulation of the oncogene HER2/neu. Although here, a control with a SET domain mutant was not carried out, thus providing not fully

conclusive evidence (Falahi*, et al* 2013). Very recently a CRISPR/CAS9 (clustered, regularly interspaced, short palindromic repeat/ CRISPR associated protein)-based targeted approach was carried out to investigate repressive histone marks (O'Geen*, et al* 2017). Again, the mammalian H3K9 methyltransferases G9a and SUV39H1 were linked to a nuclease inactive form of Cas9 and targeted via a sgRNA (single guide RNA) to a specific DNA site. They used the same truncated version of SUV39H1 as previously described. Interestingly, this time, the repression of the HER2/neu gene was independent of H3K9me2/me3 at the target site. ChIP against H3K9me2/me3 showed no enrichment at the site where the SUV39H1 fusion protein was targeted. The G9a construct on the other side was active as a methyltransferase, and also showed a similar HER2/neu repression compared to SUV39H1. For Ezh2, a H3K27 methyltransferase and the catalytic subunit of the polycomb repressive complex 2 (PRC2), repression of the HER2/neu gene was independent of H3K27 methylation, i.e., EZH2 catalytic mutants did repress the HER2/neu to the same degree as wt Ezh2.

In analogy to such studies, our next step was to see potential gene expression changes with the use of our dSu(var)3-9 constructs, especially the targeted ones. Wt dSu(var)3-9 did not show a repressive effect at *PHO5* or *HIS3* (Fig. 14). The lexA-DBD/dSu(var)3-9 construct targeted to the *PHO5* promoter resulted in a small decrease in acid phosphatase activity, indirectly showing successful recruitment. However, this effect was independent of the methyltransferase activity of dSu(var)3-9 (Fig. 16). This result was reproduced in the *rph1Δ* or the *rph1Δ snf1Δ* mutants (Fig. 17). No effect at all on the respective expression levels was observed if the lexA-DBD/dSu(var)3-9 construct was targeted to the *PHO8* or *PHO84 promoters*. Overall, the lexA targeting approach was suboptimal in a couple of ways. At the *PHO5* promoter the lexA insertion site crippled the Pho2 binding site and thereby already strongly affected *PHO5* expression. This could also have been beneficial as it considerably lowered the strong activity of the induced *PHO5* promoter, which might allow better detection of small changes in expression levels. The lack of an effect at the *PHO8* and *PHO84* promoters (Fig. 18, Fig. 19) might be due to their different promoter biology and / or placement of the lexA binding site further away from the transcription start site.

Coupling of the Pho4-DBD domain to dSu(var)3-9 produced more robust results across all three *PHO* genes. At *PHO5* we did see a strong reduction of acid phosphatase activity and mRNA expression with PHO4-DBD/dSu(var)39 compared to wt yeast. Although the Pho4-DBD alone led to a reduction of acid phosphatase activity, the reduction was by far not as strong as with the Pho4-DBD/dSu(var)3-9. A purely competitive effect between Pho4 and

Pho4-DBD/dSu(var)3-9 is thus very unlikely (Fig. 20). A similarly strong effect of downregulated mRNA was observed at *PHO84* (Fig. 21). The effect at *PHO8* was not as strong.
Again, the observed repression was not dependent on the methylation activity of dSu(var)3-9.
An explanation regarding the difference between the methylation-dependent gene repression seen by Snowden et. al / Falahi et. al and O`Geen and our observed methylation-independent gene repression by dSu(var)3-9 could be that the other groups expressed their targeted SUV39H1 and G9a in their "homologous environment", where known and unknown interaction partners can interact with the modified HMTs. For this reason, Snowden et. al used a truncated version of G9a and SUV39H1 because full length SUV39H1 did not repress the targeted gene. Due to the multitude of possible interactions partners of HMTs, interpretation of the data is difficult. O`Geen et. al. even observed that the HER2/neu repression is cell-type dependent. The fusion proteins expressed in a different cell line with a similar epigenetic profile did not repress HER2/neu.
In our heterologous system, the proteins of interest are naturally not existing and introduced via vectors to *S. cerevisiae*. This reduces, albeit not completely, possible interactions with yeast proteins. Thus, the effect of the introduced protein on its own can be investigated in a much cleaner background. Even though there might be some hints of an ancient H3K9me system in *S. cerevisiae* (Klose*, et al* 2007), the possible interactions of dSu(var)3-9 with other proteins should be much lower, especially since *S. cerevisiae* has no orthologues of HP1 at all.
Our data, in line with the O`Geen data, show that the repressive histone mark alone is not sufficient for transcriptional repression.

4.2.3 Repressive effect via Pho4DBD targeted dSu(var)3-9 and Pho4DBD alone requires HDAC Rpd3

Since the methylation activity of dSu(var)3-9 did not seem important for gene repression in our system, we looked for possible interaction partners of dSu(var)3-9. Hypoacetylation is another feature of heterochromatin and *HDAC1* was identified as an interaction partner of dSu(var)3-9 (Czermin*, et al* 2001). Therefore, we created deletion strains of the five existing HDACs in *S. cerevisiae*. To our surprise, Pho5 phosphatase activity was almost restored close to wt levels in the *rpd3Δ* Pho4-DBD/dSu(var)3-9 strain (Fig. 22). This could point to a direct interaction of dSu(var)3-9 and Rpd3 in a heterologous system. Even more astonishing was that *RPD3* is the yeast homologue of *HDAC1*, which already has been identified as an interaction partner in *Drosophila*. Surprising to us was also the Pho4-DBD repressive effect, which we thought to be rather a competition effect between Pho4 and the Pho4-DBD. In the *rpd3Δ*

strain, phosphatase activity levels were also restored close to wt levels with the Pho4-DBD construct. This raises the concern that the competition effect of Pho4 and Pho4-DBD was misinterpreted until now. Instead, we now hypothesize that Rpd3 mediates the repressive effect of Pho4-DBD and Pho4-DBD/dSu(var)3-9. Whether the Pho-4-DBD contains a Rpd3 binding site, or Rpd3 is recruited by the interaction of Pho4-DBD and Pho2 is unknown.
This has to be seen as preliminary data, as direct proof for the interaction of Pho4-DBD or Pho4-DBD/dSu(var)3-9 with Rpd is missing. Co-immunoprecipitation, which has not been carried out yet, could be done to address this point.

4.2.4 HP1a alone represses some genes

The mechanisms of repression by HP1 are still poorly understood. Position effect variegation in *Drosophila* describes the process of random variability regarding the repression of a euchromatic gene placed in the vicinity of heterochromatin. It was one of the first models to study and screen for factors involved in heterochromatin formation. dSu(var)3-9 and HP1a were among the identified proteins that were crucial for heterochromatin formation and maintenance. The defining chromatin structure of repressed clones showed a less accessible chromatin structure measured by restriction enzyme digestion and more regularly spaced nucleosomes (Wallrath and Elgin 1995). Similar results were obtained using HP1a fused to a DBD (Danzer and Wallrath 2004). In combination with associated HDACs HP1 also precludes Pol II access to the heterochromatin domains (Fischer*, et al* 2009). A completely different mechanism was proposed by Keller et. al.. They show that the hinge region of Swi6 (= HP1 in *S. pombe*) captures RNA transcripts, dissociates from the nucleosome and marks RNA for degradation by Cid14, a non-canonical poly(A) polymerase (Keller*, et al* 2012). Recently, a new mechanism of phase separation was described (Larson*, et al* 2017, Strom*, et al* 2017). Local increases of HP1a concentration in the nucleus and subsequent interaction of HP1a proteins lead to the formation of HP1a droplets. HP1a droplets then fuse to larger liquid-like (phase separated) droplets. In this model the surface of the liquid like droplets acts as barrier for molecules. While excluding certain proteins and protein complexes, heterochromatin associated proteins can still access the droplets via charge and / or interaction partners. This would also explain the already observed highly dynamic structure of heterochromatin much better (Cheutin*, et al* 2003, Festenstein*, et al* 2003).
Here we show that HP1a alone already represses *PHO* gene expression, both on the level of mRNA and protein synthesis (Fig. 23). In the phosphatase activity assay measuring PHO84 promoter activity, we observed a kinetic effect of slowed down induction in the presence of HP1a. However, the overnight levels of phosphatase activity were the same as the wt. As al-

ready discussed in the context of genome-wide studies (see 4.1.3), effects on the level of chromatin often mainly affect the kinetics but not necessarily the final level of promoter induction, which has also been seen in the context of *PHO* promoter regulation (Barbaric*, et al* 2007, Barbaric*, et al* 2001b, Musladin*, et al* 2014, Wippo*, et al* 2009).

Similar results were obtained at the *HIS3* locus (Fig. 24). HP1a showed dosage-dependent effects on position effect variegation (Eissenberg*, et al* 1992, Hwang*, et al* 2001), i.e. an upregulated HP-1 protein level led to an enhancement of position effect variegation. A dosage dependency was shown for several other proteins, which led to the hypothesis of a mass action model. They proposed that proteins involved in position effect variegation are structural proteins, which act via multiple interactions in protein complexes. If the concentration of one or more constituents is raised, the chance of assembly of the complexes is also raised (Locke*, et al* 1988). In addition, the phase separation model would explain the observed dosage dependency of heterochromatin proteins. Using an expression library with different expression-levels, allowed us to investigate the concentration dependency of HP1a mediated gene repression. Only the construct with the strongest expression level of HP1a showed some repression of the *HIS3* gene (Fig. 25) and thus points towards dosage dependency.

GAL1 was not repressed by HP1a but instead HP1a led to an increase of gene expression. From the genome-wide studies, we already knew that HP1a just downregulated a few proteins.

However, in this case and especially with the expression library experiments, we wondered why the positive control did not show the same type of repression on the raffinose and galactose carbon source medium as compared to the standard medium. A significant decrease of the *ADH1* promoter activity, which is the promoter we used to drive the expression of HP1a, is described when raffinose and galactose as carbon sources are used (Cell Cycle - Materials and Methods, Pagano 1996, p. 287).

The natural lack of H3K9me in *S. cerevisiae* implies that the observed repressive effect of HP1a is independent of H3K9me. Thus, the chromodomain point mutated HP1a had the same repressive effect on *PHO5*. In line with previous reports, the chromoshadow domain was essential for the repressive effect of HP1a (Cowieson*, et al* 2000, Dawson*, et al* 2009, Lavigne*, et al* 2009, Meehan*, et al* 2003, Richart*, et al* 2012, Zhao*, et al* 2000). The I152F mutated HP1a cannot bind to the PxVxL pentapeptidemotifs of its interaction partners. The mutated CSD rescued the observed phenotype across the *PHO* and *HIS3* genes. As expected, interaction of the CSD and H3 seem to be essential for the repressive effect of HP1a, although, we did not further investigate HP1a interactions with endogenous proteins of *S. cerevisiae*.

Employing both DNase I indirect end-labeling and restriction enzyme accessibility, all *PHO* promoters showed a complete opening upon phosphate starvation in the presence of HP1a (Fig. 32, Fig. 33). The nuclease access is unaffected by the presence of HP1a so the nucleosomes are still remodeled and disassembled upon *PHO5* induction. This argues strongly against the observed less accessible chromatin in *Drosophila* and the CSD mediated inhibition of hSWI/SNF remodeling (Lavigne*, et al* 2009).

The approximate 50% reduction of gene expression, despite full promoter remodeling and histone eviction, argues for effects downstream of chromatin opening. With Trf4/5 *S. cerevisiae* possesses homologues of *S. pombe* Cid14 (Win*, et al* 2006), which could also mark the captured RNA by HP1a for degradation in *S. cerevisiae*, although this is highly speculative, as we do not provide further evidence here. This would definitely be an interesting point to follow up in the future.

With the known high mobility of HP1a (Cheutin*, et al* 2003, Festenstein*, et al* 2003), it could also be hypothesized that HP1a hinders the polymerase from passing through the gene body, while still allowing transcription factors and remodelers access to DNA.

4.2.5 dSu(var)3-9 and HP1a synergistically repress gene expression in *S. cerevisiae*

Finally, we wanted to test how dSu(var)3-9 and HP1a would affect gene expression together, for example, if there was a synergistic repressive effect. This idea was based on the established cooperation of both factors in heterochromatin formation. While dSu(var)3-9 generates the histone mark, HP1a would represent a "reader" that could translate the mark into the repressive effect. Heterochromatin formation in *Drosophila* has been based on two systems so far. In the "classical system", proteins, like D1 or SU(VAR)3-7, binding to satellite repeat units, recruit HP1a and dSU(VAR)3-9 (Aulner*, et al* 2002, Blattes*, et al* 2006, Cleard and Spierer 2001). The other system has been extensively studied in *S. pombe*. Here, an RNAi based system targets the heterochromatin machinery to the different loci and initiates heterochromatin formation (Volpe*, et al* 2002). We circumvented the targeting mechanism in our synthetic biology approach with our chimeric dSu(var)3-9 constructs coupled to DBDs.

4.2.5.1 Two major heterochromatin factors are indeed present at the PHO promoters

In our chromatin immunoprecipitation experiments we saw a strong enrichment of HP1a at the *PHO* promoters, when co-expressed with Pho4-DBD/dSu(var)3-9 construct. Interestingly at the *PHO5* promoter HP1a enrichment was H3K9 methylation-dependent, while at *PHO8* and *PHO84* HP1a was also enriched in the strain containing the SET mutant.

With H3K9me of histones at our targeted loci and concurrent recruitment of HP1, we could target two major heterochromatin factors, which might serve as basic requirement for heterochromatin formation.

Another feature of heterochromatin is the self-sustaining mechanism of spreading, which is thought to be maintained by dSu(var)3-9 and HP1a as described in the Introduction. We did not observe a spreading mechanism neither as a result of H3K9me nor HP1a enrichment up or downstream especially of *PHO5*, where we covered the up- and downstream regions more extensively.

4.2.5.2 Synergy between targeted dSu(var)3-9 and HP1a dependent on chromoshadow domain, but not on H3K9 methylation

Lexa-DBD/dSu(var)3-9 combined with HP1a resulted in an even stronger repression of *PHO5*, as did the HP1a co-expression with Pho4-DBD/dSu(var)3-9 at *PHO5* and *PHO84* and to some degree at *PHO8* (Fig. 28-Fig. 31). Consistent along all studied *PHO* genes was that the downregulation was independent of H3K9me status. The SET mutant of dSu(var)3-9 or the CD mutant of HP1a, both repressed the genes to a similar level as their wt counterparts.

Consistent with the previous chapter, gene repression was highly dependent on the CSD of HP1a, which showed *PHO* gene expression levels similar to the dSu(var)3-9 variants expressed by themselves.

This indirectly provides further evidence for the importance of the chromoshadow domain for heterochromatin formation.

This time, chromatin restriction enzyme accessibility was reduced to about 50% of the wt levels in the HP1a / Su(var)3-9 strain. At the PHO5 promoter, the DNase I pattern was changed, with a wider protected region where usually the -3 nucleosome sits. At *PHO8,* the DNase I pattern was unchanged, and at *PHO84*, binding of Pho4-DBD/dSu(var)3-9 seemed to protect the eHS from DNase I digestion. Unlike HP1a and dSu(var)3-9 alone, which showed a repression of the targeted genes despite unchanged chromatin remodeling, both factors together exerted an effect on chromatin and hindered the effective opening of promoters. This may provide evidence that indeed HP1a and dSu(var)3-9 are basic requirements for heterochromatin formation. Only together they not only repress genes synergistically, but we could also show a structural impact on chromatin opening.

4.3 Summary

Heterochromatin formation and maintenance in eukaryotes, even in *S. pombe*, is a complicated interplay of many macromolecules that affects many levels of chromatin regulation, like

nucleosome stability, histone modifications, processing of RNAs, or hindering chromatin remodelers or RNA polymerases. How heterochromatin is established and maintained is still poorly understood.

In this work, we introduced dSu(var)3-9 and HP1a, two highly conserved heterochromatin proteins from *Drosophila*, into a *S. cerevisiae* thereby generating a heterologous system. In a targeted approach, we were able to show that HP1a and dSu(var)3-9 represent basic requirements necessary for formation of heterochromatin, or at least repressive chromatin, i.e., their combined presence can lead to less accessible chromatin and reduced gene expression of the targeted gene. The HP1a mediated repressive effect was independent of H3K9 methylation. Rather the chromoshadow domain, which among others interacts with H3, was necessary for gene repression.

Our experiments showed that the histone deacetylase Rpd3 might directly interact with Pho4-DBD and Pho4-DBD/dSu(var)3-9 and mediates their repressive effects. This was quite surprising as it implies that the interaction of Rpd3, the yeast HDAC1 homolog, with dSu(var)3-9 is conserved, even though the respective Su(var)3-9 homolog was lost from yeast.

The genome-wide non-targeted approach showed that HP1a and dSu(var)3-9 are not general repressors. Our data rather suggest that for the establishment of heterochromatin a high local concentration of the two proteins is needed, for example, via the direct targeting of dSu(var)3-9 to the *PHO* promoters and by stronger overexpressionof HP1a.

Collectively, our study suggests that the repressive effect of H3K9me could not be reconstituted in the heterologous *S. cerevisae* system, but that both the histone methyl transferase dSu(var)3-9 and HP1a exert repressive effects by themselves, at least in part via recruitment of host cell factors like an HDAC.

5 Supplementary Material

5.1 Supplementary Figures

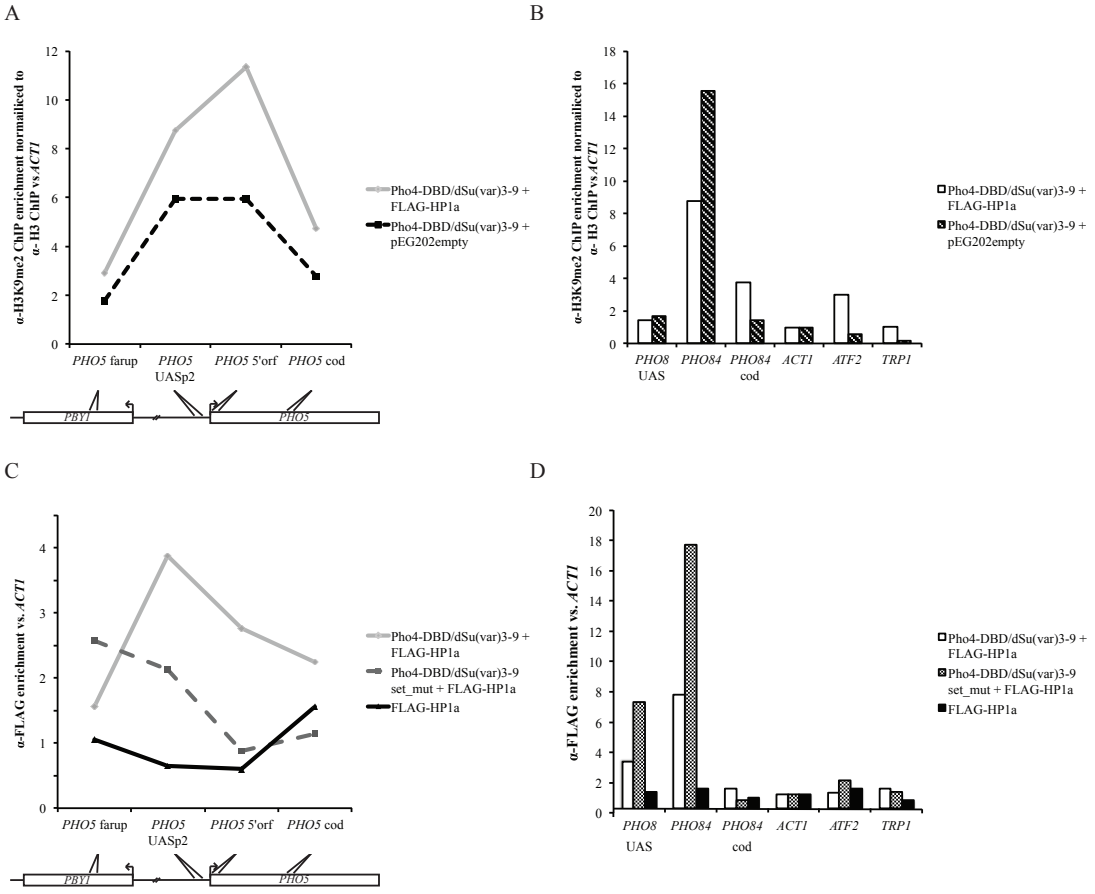

Fig. S 1 H3K9me2 and HP1a enrichment at the targeted loci. Second biological replicate. Description same as Fig. 13.

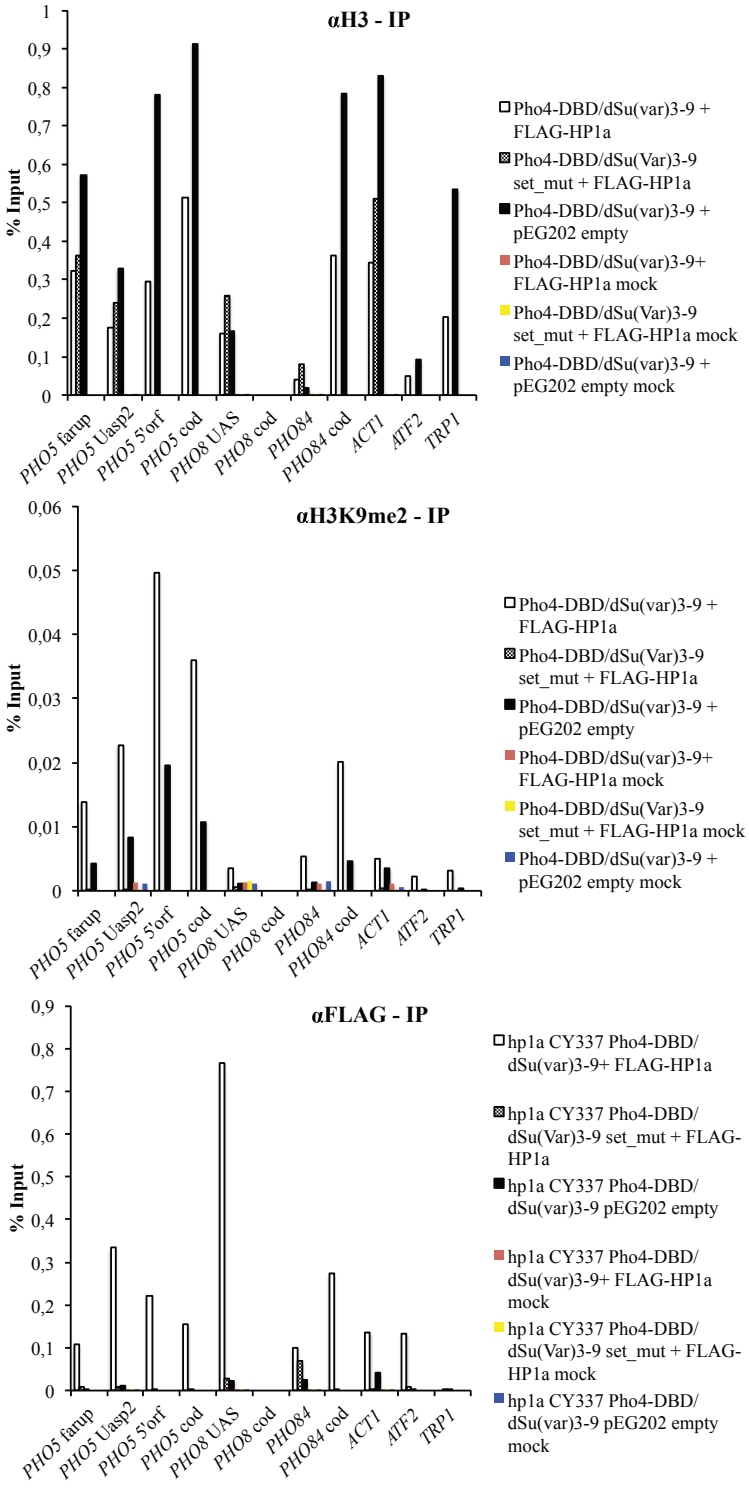

Fig. S 2 ChIP raw data (% Input). Raw data to biological replicate from Fig. 13. X-axis shows the amplicons used. Y axis shows the IP-DNA / Input DNA. Same strains as in Fig. 13.

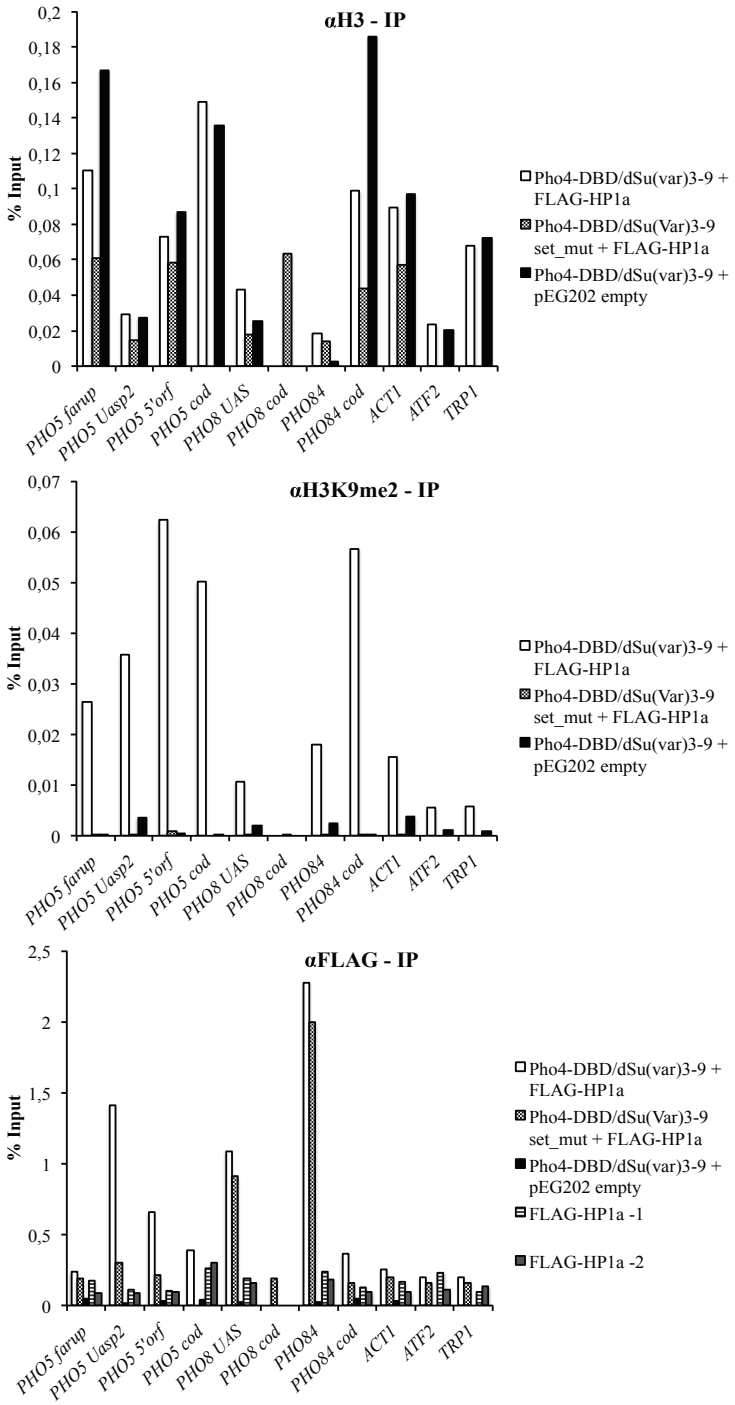

Fig. S 3 ChIP raw data (% Input). Raw data to biological replicate from **Fig. S 1**. X-axis shows the amplicons used. Y axis shows the IP-DNA / Input DNA. Same strains as in Fig. S 1.

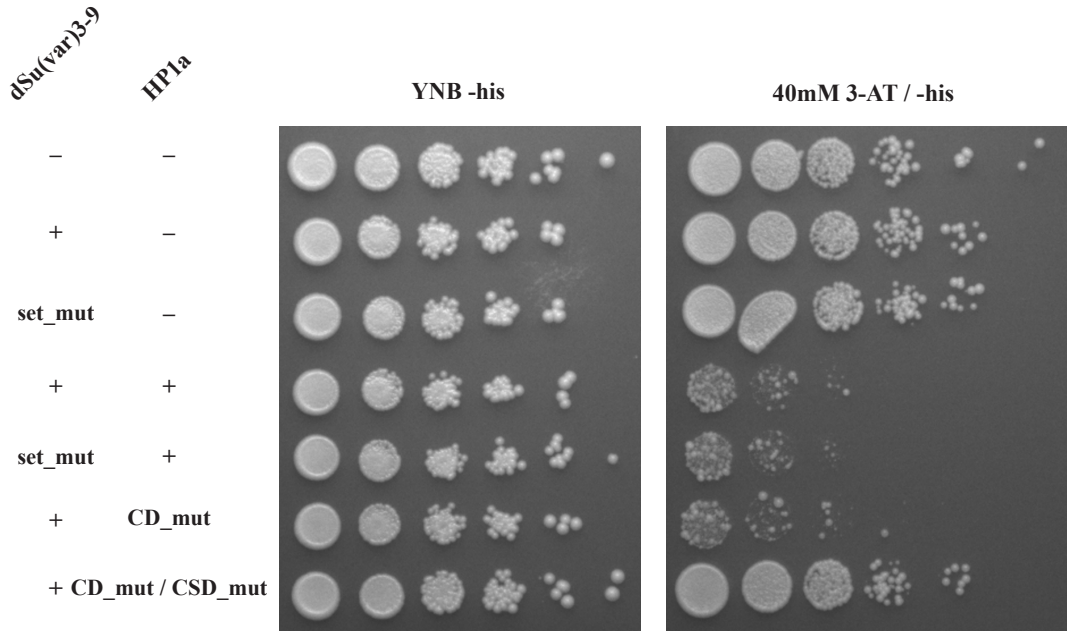

Fig. S 4 The diminished growth with HP1a is not stronger in combination of dSu(var)3-9. Second biological replicates. Fig. description same as in Fig 27

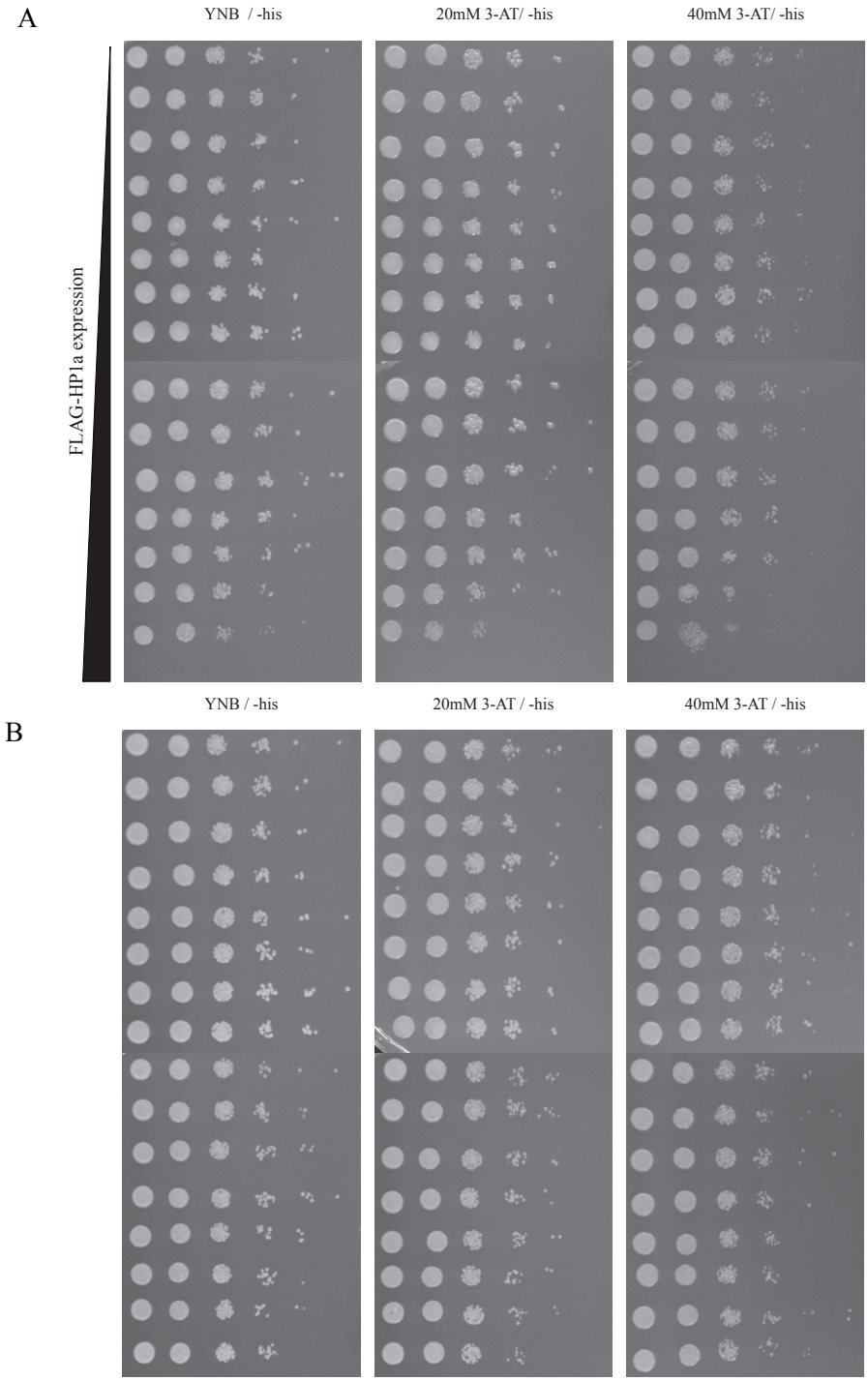

Fig. S 5 Dosage dependent silencing of HP1. HP1a was integrated in a plasmid library with different promoter strength (Blazeck, *et al* 2012). All plasmids were transformed in strain YS18 with the empty pEG202 vector (carrying HIS gene necessary for this assay). (A) HP1a expressed from top to bottom with higher expression (plasmid numbers 284-299). Second biological replicates. Yeast were plated on YNB, YNB + 20 mM 3-AT, YNB + 40 mM 3-AT. (B) Controls with empty plasmid library (from top to bottom 284-299).

5.2 Plasmids

Plasmid	vector-backbone	Primer	REs for Cloning	Comments	Source
bluescript sk-					Korber group
cleu					Korber group
dSu(var)3-9	pEG202	5'-GCT AGC GGG CCT CAG GGG ATG GCC ACG GCT GAA GCC-'3 5'-AAG CTT GGA GTT GAT TGT ATG CTT GGT ATA GCT TG-'3		lexA-DBD was cut out of vector (lexA-DBD/dSu(var)3-9 (pEG202) using the given primers	this study
dSu(var)3-9	pRS406	5'-GCT AGC GGG CCT CAG GGG ATG GCC ACG GCT GAA GCC-'3 5'-AAG CTT GGA GTT GAT TGT ATG CTT GGT ATA GCT TG-'3		lexA-DBD was cut out of vector (lexA-DBD/dSu(var)3-9 (pRS406) using the given primers	this study
FLAG-HP1a	pEG202		NcoI / XhoI	FLAG-HP1a originally in HP1a pPac FLAG	this study
HP1a pPac FLAG	pPac FLAG				Jochen Abel, Imhof group
lexA-DBD/dSu(var)3-9	pEG202				kind gift of Gunter Reuter, Halle
lexA-DBD/Su(var)3-9	pRS406	5'-GGC AGA CCA GAG CTC TGG GAA ATG ATG GTA AAT GAA ATA G-'3 5'-GGC AGA CCA GAG CTC TGG CGA TCC GTG TGG AAG AAC GAT TAC-'3	SacI	ADH promoter LexA-DBD/dSu(var)3-9 and ADH terminator were amplified with given primers (template: lexA-DBD/dSu(var)3-9 pEG202)	this study
p416-GAL1-lacZ					Korber group
pCB84a_l					Korber group
pEG202 empty	pEG202	5'-GAA TTC CCG GGG ATC CGT CGA CCA TGG CGG CCG CTC GA-'3 5'-AAG CTT GGA GTT GAT TGT ATG CTT GGT ATA GCT TG-'3		lexA-DBD/dSu(var)3-9 was cut out of vector using given primers	this study
Pho4-DBD/dSu(var)3-9	pRS406	5'-TCA GTA CGG CCC TCA GGC GTG CTC ACG TTC TGC TGT A-'3 5'-TCA GTA CGG CCC TCA GGC GTG CTC ACG TTC TGC TGT A-'	NHE I / BSU 36 I	PHO4-DBD fragment (template pP4-12 SP4 SP6 mutated) was blunt-end in bluescript sk-, PHO4-DBD was cut out with Nco I / Xho I, then inserted in dSu(var)3-9 (pRS406)	this study

pP4-12neu					Korber group
pP8apain					Korber group
pPZ Ura Var33		5'-CTA GAT AA GCT T C TGA GAG TGC AC CAT ACC AC-'3 5'-CTA GAT AA GCT T T TAG TTT TGC TGG CCG CAT C-'3	Hind III	Leu marker was cut out by Hind III, ura marker was inserted	this study
pPZleuV33					Korber group
pUG6					Kind gift of Ramon Ramos Barrales, Barcelona/ Munich
cleu_neu1	cleu	5'-GTG ACC AAT TCA ACA TCA CCT TGC AGA CTG TCA GTG AAG-3' 5'-CTT CAC TGA CAG TCT GCA AGG TGA TGT TGA ATT GGT CAC-3'		Correction of reading frame, insertion at bp580	this study
cleu_lexA_BS (insertion of lexA_BS)	cleu	5'-AAA CGA AGG TAA AAG GTT CAT AGC GCT TTT TCT TTG TCT GCT ACT GTA TAT ATA TAT TAA ATT AGC ACG TTT TCG CAT AGA ACG CAA CTG-3' 5'-CAG TTG CGT TCT ATG CGA AAA CGT GCT AAT TTA ATA TAT ATA TAC AGT AGC AGA CAA AGA AAA AGC GCT ATG AAC CTT TT A CCT TCG TTT-3' 5'-GTT CTA TGC GAA AAC GTG CTA ATA CTG TAT ATA TAT ACA GTA GCA GAC AAA GAA AAA GCG CTA TGA ACC-3' 5'-GGT TCA TAG CGC TTT TTC TTT GTC TGC TAC TGT ATA TAT ATA CAG TAT TAG CAC GTT TTC GCA TAG AAC-3'		insertion of lexA_BS	this study
pP8apain_lexA_BS	pP8apain	5'-AGA AGA AGG CGT AGC AGA-3' 5'-TAA GAA GTA CTG TAT ATA TA-3'		insertion of lexA_BS	this study

		5‘-T ACA GTA CGG GTA AAG GCA AGG AAG A-3’ 5’-TCT TCC TTG CCT TTA CCC GTA CTG TAT ATA TAT ACA GTA CTT CTT ATC TGC TAC GCC TTC TTC T-3’			
pCB84a_l_lexA_BS		5’-AAG AAA CTA ATT TAT CAG CTA CTG TAT TAT CAA CCG TTA TTA CCA AAT TA-3’ 5’-TAA TTT GGT AAT AAC GGT TGA TAA TAC AGT AGC TGA TAA ATT AGT TTC TT-3’ 5’-CTA ATT TAT CAG CTA CTG TAT ATA TAA CCG TTA TTA CCA A-3’ 5’-TTG GTA ATA ACG GTT ATA TAT ACA GTA GCT GAT AAA TTA G-3’ 5’-TTT ATC AGC TAC TGT ATA TAT ATA CAG TAT TAC CAA ATT A-3’ 5’-TAA TTT GGT AAT ACT GTA TAT ATA TAC AGT AGC TGA TAA A-3’ 5’-GGC AGA CCA GAG CTC TGG GAA ATG ATG GTA AAT GAA ATA G-3’ 5’-GGC AGA CCA GAG CTC TGG CGA TCC GTG TGG AAG AAC GAT TAC-3’ 5’-AGG GAA TTC ACA TGA CGA AAC TAA TCG CTC C-3’ 5’-GGA GCG CCT CGA GTC AGT TTA AAG GTG TAC TCT G-3’ 5’-GGA GCG CCT CGA GAG AAG AGA ACT TTC TTT GGC-3’ 5’-TCA GTA CGG CAC CGG TAT GGG CCG TAC AAC TTC TG-3’		insertion of lexA_BS	This study

		5’-TCA GTA CGG CCC TCA GGC GTG CTC ACG TTC TGC TGT A-3’ 5’-ACC GGT GGG CCT CAG GGG ATG GCC ACG GCT GAA GCC-3’ 5’-TTT ATC AGC TAC TGT ATA TAT ATA CGT TAT TAC CAA ATT A-3’ 5’-TAA TTT GGT AAT AAC GTA TAT ATA TAC AGT AGC TGA TAA A-3’ 5’-TTT ATC AGC TAC TGT ATA TAT ATA CAG TAT TAC CAA ATT A-3’ 5’-TAA TTT GGT AAT ACT GTA TAT ATA TAC AGT AGC TGA TAA A-3’			
lexA-DBD/dSu(var)3-9 set_mut	lexA-DBD/dSu(var)3-9	5’-ACT ATG GCA ACA TCT CGC ACT TTA TCA ATA AGT CTT GCG ATC CTA AT-3’ 5’-ATT AGG ATC GCA AGA CTT ATT GAT AAA GTG CGA GAT GTT GCC ATA GT-3’		SET domain mutant	this study
Pho4-DBD/dSu(var)3-9 set_mut	Pho4-DBD/dSu(var)3-9	5’-ACT ATG GCA ACA TCT CGC ACT TTA TCA ATA AGT CTT GCG ATC CTA AT-3’ 5’-ATT AGG ATC GCA AGA CTT ATT GAT AAA GTG CGA GAT GTT GCC ATA GT-3’		SET domain mutant	this study
dSu(var)3-9 set_mut	dSu(var)3-9	5’-ACT ATG GCA ACA TCT CGC ACT TTA TCA ATA AGT CTT GCG ATC CTA AT-3’ 5’-ATT AGG ATC GCA AGA CTT ATT GAT AAA GTG CGA GAT 5.2.1.1.1.1.1.1 GTT GCC ATA GT-3’		SET domain mutant	this study
FLAG-HP1a V26M	FLAG-HP1a	5’-GGA GGA GGA GTA CGC CAT GGA AAA GAT CAT CGA-3’ 5’-TCG ATG ATC TTT TCC ATG GCG TAC TCC TCC TCC-3’		V26M (CD mutation)	this study

FLAG-HP1a I152F	FLAG-HP1a	5'-TGG AGG CCG AAA AGT TCT TGG GTG CCT CC-3' 5'-GGA GGC ACC CAA GAA CTT TTC GGC CTC CA-3'		I152F (CSD mutation)	this study
PHO4DBD	Pho4-DBD/dSu(var)3-9	5' -TCA GTA CGG CAC CGG TAT GGG CCG TAC AAC TTC TG-3' 5'-TCA GTA CGG CCC TCA GGC GTG CTC ACG TTC TGC TGT A-3'		stop codon after Pho4DBD	this study
pPZ Leu Var33					Korber group
pPZ Ura Var33	pPZ Leu Var33		HIND3	LEU marker swapped with URA marker (pRS406 vector)	this study
Gal4pBS2 Pleum					Kind Gift of (Blazeck, *et al* 2012).
Gal4pBS1 Pleum					
Gal4pBS12 Pleum					
Gal4pBS24 Pleum					
UASgal CU2 Pcyc					
Gal4pBS4 Pleum					
Gal4pBS3 Pleum					
UASgal CU1 Pcyc					
Gal4pBS13 Pleum					
UAS gal Pcyc					
UAS gal A9 Pcyc					
Gal4pBS34 Pleum					
Gal4pBS134 Pleum					
UASgal					
Pgal					
UASgal Pgal					
Gal4pBS2 Pleum +HP1a				See 2.2.4.3.1.2 for gibson cloning primers	this study
Gal4pBS1 Pleum +HP1a					
Gal4pBS12 Pleum					

+HP1a					
Gal4pBS24 Pleum +HP1a					
UASgal CU2 Pcyc +HP1a					
Gal4pBS4 Pleum +HP1a					
Gal4pBS3 Pleum +HP1a					
UASgal CU1 Pcyc +HP1a					
Gal4pBS13 Pleum +HP1a					
UAS gal Pcyc +HP1a					
Gal4pBS34 Pleum +HP1a					
UASgal +HP1a					
Pgal +HP1a					
UASgal Pgal +HP1a					

5.3 Yeast strains

Yeast strain	Transformed plasmids
CY339	cleu_neu1
CY339	cleu_lexA_BS (cleu_mut4_neu1)
CY339	cleu_neu1 lexA-DBD/Su(var)3-9 (pEG202)
CY339	cleu_lexA_BS (cleu_mut4_neu1) lexA-DBD/Su(var)3-9 (pEG202)
CY339	cleu_lexA_BS (cleu_mut4_neu1) lexA-DBD/Su(var)3-9 set_mut (pEG202)
CY339	cleu_lexA_BS (cleu_mut4_neu1) pEG202empty
CY339 Δrph	cleu_neu1
CY339 Δrph	cleu_lexA_BS
CY339 Δrph	cleu_neu1 lexA-DBD/Su(var)3-9 (pEG202)
CY339 Δrph	cleu_lexA_BS lexA-DBD/Su(var)3-9 (pEG202)
CY339 Δrph	cleu_lexA_BS lexA-DBD/Su(var)3-9set_mut (pEG202)
IPY36	cleu_neu1
IPY36	cleu_lexA_BS
LPY7091	cleu_neu1
LPY7091	cleu_lexA_BS
LPY7091	cleu_neu1 lexA-DBD/Su(var)3-9 (pEG202)
LPY7091	cleu_lexA_BS lexA-DBD/Su(var)3-9 (pEG202)
LPY7091	cleu_lexA_BS lexA-DBD/Su(var)3-9set_mut (pEG202)
IPY36 Δrph	cleu_neu1
IPY36 Δrph	cleu_lexA_BS
LPY7091 Δrph	cleu_neu1
LPY7091 Δrph	cleu_lexA_BS
LPY7091 Δrph	cleu_neu1 lexA-DBD/Su(var)3-9 (pEG202)
LPY7091 Δrph	cleu_lexA_BS lexA-DBD/Su(var)3-9 (pEG202)
LPY7091 Δrph	cleu_lexA_BS lexA-DBD/Su(var)3-9set_mut (pEG202)
Y04315 pho8	pP8apain
Y04315 pho8	pP8apain_lexA_BS
Y04315 pho8	pP8apain lexA-DBD/Su(var)3-9 (pEG202)
Y04315 pho8	pP8apain_lexA_BS lexA-DBD/Su(var)3-9 (pEG202)
Y04315 pho8	pP8apain_lexA_BS lexA-DBD/Su(var)3-9set_mut (pEG202)
	lexA-DBD/Su(var)3-9 genome integration (prs406)

CY339	FLAG-HP1a (pEG202)/cleu_neu1
CY339	pEG202 empty/cleu_neu1
CY339	FLAG-HP1a (pEG202)/cleu_lexA_BS
CY339	FLAG-HP1aV26M (pEG202)/cleu_neu1
CY339	pEG202 empty/cleu_lexA_BS
CY339	lexA-DBD/Su(var)3-9 (prs406)
CY339	lexA-DBD/Su(var)3-9 set_mut (prs406)
CY339 pho5::ura	pCB84a_l wt lexA-DBD/Su(var)3-9 (prs406)
CY339 pho5::ura	pCB84a_l_lexA_BS lexA-DBD/Su(var)3-9 (prs406)
CY339 pho5::ura	pCB84a_l_lexA_BS lexA-DBD/Su(var)3-9 set_mut (prs406)
CY339 pho5::ura	pCB84a_l wt lexA-DBD/Su(var)3-9 (prs406) FLAG-HP1a (pEG202)
CY339 pho5::ura	pCB84a_l wt lexA-DBD/Su(var)3-9 (prs406) FLAG-HP1aV26M (pEG202)
CY339 pho5::ura	pCB84a_l_lexA_BS lexA-DBD/Su(var)3-9 (prs406) FLAG-HP1a (pEG202)
CY339 pho5::ura	pCB84a_l_lexA_BS lexA-DBD/Su(var)3-9 (prs406) FLAG-HP1aV26M (pEG202)
CY339 pho5::ura	pCB84a_l_lexA_BS lexA-DBD/Su(var)3-9 set_mut (prs406) FLAG-HP1a (pEG202)
CY339 pho5::ura	pCB84a_l_lexA_BS lexA-DBD/Su(var)3-9 set_mut (prs406) FLAG-HP1aV26M (pEG202)
CY339 pho5::ura	lexA-DBD/Su(var)3-9 (prs406) Rph1Δzf(pEG202)
CY339 pho5::ura	lexA-DBD/Su(var)3-9 set_mut (prs406) Rph1ΔZF (pEG202)
CY339 pho5::ura rph1::KAN	pEG202 empty/cleu_neu1
CY339 pho5::ura rph1::KAN	HP1a/cleu_neu1
CY339 pho5::ura rph1::KAN	lexA-DBD/Su(var)3-9 (prs406)
CY339 pho5::ura rph1::KAN	lexA-DBD/Su(var)3-9 set_mut (prs406)
CY339 pho5::ura rph1::KAN	cleu_neu1_lexA-DBD/Su(var)3-9 (prs406)
CY339 pho5::ura rph1::KAN	cleu_lexA_BS lexA-DBD/Su(var)3-9 (prs406)
CY339 pho5::ura rph1::KAN	cleu_lexA_BS lexA-DBD/Su(var)3-9set_mut (prs406)
CY339 pho5::ura rph1::KAN	HP1a cleu_neu1_lexA-DBD/Su(var)3-9 (prs406)
CY339 pho5::ura rph1::KAN	HP1a cleu_lexA_BS lexA-DBD/Su(var)3-9 (prs406)
CY339 pho5::ura rph1::KAN	HP1a cleu_lexA_BS lexA-DBD/Su(var)3-9set_mut (prs406)
CY339 pho5::ura rph1::KAN	pEG202 empty/cleu_neu1/lexA-DBD/Su(var)3-9 (prs406)
CY339 pho5::ura rph1::KAN	pEG202 empty/cleu_mut4_neu1/lexA-DBD/Su(var)3-9 (prs406)
CY339 pho5::ura rph1::KAN	pCB84a_l wt lexA-DBD/Su(var)3-9 (prs406)
CY339 pho5::ura rph1::KAN	pCB84a_l_lexA_BS lexA-DBD/Su(var)3-9 (prs406)
CY339 pho5::ura rph1::KAN	pCB84a_l_lexA_BS lexA-DBD/Su(var)3-9 set_mut (prs406)
IPY36	lexA-DBD/Su(var)3-9 (prs406)

IPY36	lexA-DBD/Su(var)3-9 set_mut (prs406)
LPY7091	lexA-DBD/Su(var)3-9 (prs406)
LPY7091	lexA-DBD/Su(var)3-9 set_mut (prs406)
LPY7091	cleu_neu1_lexA-DBD/Su(var)3-9 (prs406)
LPY7091	cleu_lexA_BS lexA-DBD/Su(var)3-9 (prs406)
IPY36 Δrph	lexA-DBD/Su(var)3-9 (prs406)
IPY36 Δrph	lexA-DBD/Su(var)3-9 set_mut (prs406)
IPY36 Δrph	cleu_neu1_lexA-DBD/Su(var)3-9 (prs406)
IPY36 Δrph	cleu_lexA_BS lexA-DBD/Su(var)3-9 (prs406)
IPY36 Δrph	cleu_lexA_BS lexA-DBD/Su(var)3-9set_mut (prs406)
LPY7091 Δrph	lexA-DBD/Su(var)3-9 (prs406)
LPY7091 Δrph	lexA-DBD/Su(var)3-9 set_mut (prs406)
LPY7091 pho5::ura rph1::KAN	pCB84a_l wt lexA-DBD/Su(var)3-9 (prs406)
LPY7091 pho5::ura rph1::KAN	pCB84a_l_lexA_BS lexA-DBD/Su(var)3-9 (prs406)
LPY7091 pho5::ura rph1::KAN	pCB84a_l_lexA_BS lexA-DBD/Su(var)3-9 set_mut (prs406)
LPY7091 pho5::ura rph1::KAN	pCB84a_l wt lexA-DBD/Su(var)3-9 (prs406) FLAG-HP1a (pEG202)
LPY7091 pho5::ura rph1::KAN	pCB84a_l wt lexA-DBD/Su(var)3-9 (prs406) FLAG-HP1aV26M (pEG202)
LPY7091 pho5::ura rph1::KAN	pCB84a_l wt lexA-DBD/Su(var)3-9 (prs406) pEG202empty
LPY7091 pho5::ura rph1::KAN	pCB84a_l_lexA_BS lexA-DBD/Su(var)3-9 (prs406) FLAG-HP1a (pEG202)
LPY7091 pho5::ura rph1::KAN	pCB84a_l_lexA_BS lexA-DBD/Su(var)3-9 (prs406) FLAG-HP1aV26M (pEG202)
LPY7091 pho5::ura rph1::KAN	pCB84a_l_lexA_BS lexA-DBD/Su(var)3-9 (prs406) pEG202empty
LPY7091 pho5::ura rph1::KAN	pCB84a_l_lexA_BS lexA-DBD/Su(var)3-9 set_mut (prs406) FLAG-HP1a (pEG202)
LPY7091 pho5::ura rph1::KAN	pCB84a_l_lexA_BS lexA-DBD/Su(var)3-9 set_mut (prs406) FLAG-HP1aV26M (pEG202)
LPY7091 pho5::ura rph1::KAN	pCB84a_l_lexA_BS lexA-DBD/Su(var)3-9 set_mut (prs406) pEG202empty
Y04315 pho8	lexA-DBD/Su(var)3-9 (prs406)
Y04315 pho8	lexA-DBD/Su(var)3-9 set_mut (prs406)
Y04315 pho8	pP8apain lexA-DBD/Su(var)3-9 (prs406)
Y04315 pho8	pP8apain_lexA_BS lexA-DBD/Su(var)3-9 (prs406)
Y04315 pho8	pP8apain_lexA_BS lexA-DBD/Su(var)3-9 set_mut (prs406)
	Pho4-DBD/Su(var)3-9 genome integration (prs406)
CY337	FLAG-HP1a (pEG202)
CY337	FLAG-HP1a V26M (pEG202)

CY337	pEG202 Empty
CY337	FLAG-HP1a I162F (pEG202)
CY337	FLAG-HP1a V26M I162F (pEG202)
YS18	pEG202 Empty
YS18	FLAG-HP1a (pEG202)
YS18	FLAG-HP1a V26M (pEG202)
YS18	FLAG-HP1a I162F (pEG202)
YS18	FLAG-HP1a V26M I162F (pEG202)
CY337	pP4-72
CY337	pP4-72 FLAG-HP1a (pEG202)
CY337	pP4-72 FLAG-HP1aV26M (pEG202)
CY337	pP4-72 pEG202empty
CY337	Pho4-DBD/Su(var)3-9 (pRS406)
CY337	Pho4-DBD/Su(var)3-9 (pRS406) FLAG-HP1a (pEG202)
CY337	Pho4-DBD/Su(var)3-9 (pRS406) FLAG-HP1aV26M (pEG202)
CY337	Pho4-DBD/Su(var)3-9 (pRS406) pEG202empty
CY337	Pho4-DBD/Su(var)3-9 (pRS406) FLAG-HP1aI162F (pEG202)
CY337	Pho4-DBD/Su(var)3-9 (pRS406) FLAG-HP1aIV26M_162F (pEG202)
CY337	Pho4-DBD/Su(var)3-9 set_mut (pRS406)
CY337	Pho4-DBD/Su(var)3-9 set_mut FLAG-HP1a (pEG202)
CY337	Pho4-DBD/Su(var)3-9 set_mut FLAG-HP1aV26M (pEG202)
CY337	Pho4-DBD/Su(var)3-9 set_mut pEG202empty
CY337	Pho4-DBD/Su(var)3-9 set_mut FLAG-HP1aI162F (pEG202)
CY337	Pho4-DBD/Su(var)3-9 set_mut FLAG-HP1aV26M_I162F (pEG202)
CY337	Pho4DBD (pRS406)
CY337	Pho4DBD (pRS406) FLAG-HP1a (pEG202)
CY337	Pho4DBD(pRS406) FLAG-HP1aV26M (pEG202)
CY337	Pho4DBD (pRS406) pEG202empty
CY337	Pho4DBD (pRS406) FLAG-HP1a I162F (pEG202)
CY337	Pho4DBD (pRS406) FLAG-HP1a V26M I162F (pEG202)
CY337	lexA-DBD/Su(var)3-9 (pEG202)
CY337	lexA-DBD/Su(var)3-9 (PEG202) set_mut
CY337	Δ245Su(var)3-9-PHO4DBD set_mut SP4SP6 (pP4-

	12)
CY337	Δ245Su(var)3-9-PHO4DBD set_mut SP4SP6 (pP4-12) FLAG-HP1a (pEG202)
CY337	Δ245Su(var)3-9-PHO4DBD set_mut SP4SP6 (pP4-12) FLAG-HP1aV26M (pEG202)
CY337	Δ245Su(var)3-9-PHO4DBD set_mut SP4SP6 (pP4-12) pEG202empty
	dSu(var)3-9 (pRS406) (Bsu36I, NheI Schnitt-stellen)
CY337	dSu(var)3-9 (pRS406)
CY337	dSu(var)3-9 (pRS406) FLAG-HP1a (pEG202)
CY337	dSu(var)3-9 (pRS406) FLAG-HP1aV26M (pEG202)
CY337	dSu(var)3-9 (pRS406) pEG202empty
CY337	dSu(var)3-9 (pRS406) FLAG-HP1aI162F (pEG202)
CY337	dSu(var)3-9 (pRS406) FLAG-HP1aV26M_I162F (pEG202)
CY337	dSu(var)3-9 set_mut (pRS406)
CY337	dSu(var)3-9 set_mut (pRS406) FLAG-HP1a (pEG202)
CY337	dSu(var)3-9 set_mut (pRS406) FLAG-HP1aV26M (pEG202)
CY337	dSu(var)3-9 set_mut (pRS406) pEG202empty
CY337	dSu(var)3-9 set_mut (pRS406) FLAG-HP1aI162F (pEG202)
CY337	dSu(var)3-9 set_mut (pRS406) FLAG-HP1aV26M_I162F (pEG202)
CY337	dSu(var)3-9 (pRS406) neue TRAFO
CY337	dSu(var)3-9 (pRS406) set_mut neue TRAFO
BY4741	dSu(var)3-9 (pRS406) neue
BY4741	dSu(var)3-9 (pRS406) set_mut
YS18	dSu(var)3-9 (pRS406)
YS18	dSu(var)3-9 set_mut (pRS406)
YS18	dSu(var)3-9 (pRS406) pEG202empty
YS18	dSu(var)3-9 (pRS406) FLAG-HP1a (pEG202)
YS18	dSu(var)3-9 (pRS406) FLAG-HP1aV26M (pEG202)
YS18	dSu(var)3-9 (pRS406) FLAG-HP1aI162F (pEG202)
YS18	dSu(var)3-9 (pRS406) FLAG-HP1aV26M_I162F (pEG202)
YS18	pEG202empty pRS406emty
YS18	FLAG-HP1a (pEG202) pRS406empty
YS18	FLAG-HP1a I162F (pEG202) pRS406empty
YS18	dSu(var)3-9 (pRS406) set_mut pEG202empty

YS18	dSu(var)3-9 (pRS406) set_mut FLAG-HP1a (pEG202)
YS18	dSu(var)3-9 (pRS406) set_mut FLAG-HP1aV26M (pEG202)
YS18	dSu(var)3-9 (pRS406) set_mut FLAG-HP1aI162F (pEG202)
YS18	dSu(var)3-9 (pRS406) set_mut FLAG-HP1aV26M_I162F (pEG202)
	dSu(var)3-9 (pEG202)
YS18	dSu(var)3-9 (pEG202)
YS18	dSu(var)3-9 set_mut (pEG202)
CY337	dSu(var)3-9 (pEG202)
CY337	dSu(var)3-9 set_mut (pEG202)
BY4741	dSu(var)3-9 (pEG202)
BY4741	dSu(var)3-9 set_mut (pEG202)
	Rph1Δzf overexpression
CY339	Rph1ΔZF(pEG202)
	asf1::KAN
CY337 asf1::KAN	FLAG-HP1a (pEG202)
CY337 asf1::KAN	pEG202 empty
	pP416 Gal
CY337	pP416 Gal
CY337	pP416 Gal FLAG-HP1a (pEG202)
CY337	pP416 Gal pEG202 empty
	rph1 Knockouts
CY339 rph1::KAN	pho5::URA rph1::KAN
IPY36 Δrph	pho5::URA rph1::KAN
LPY7091 Δrph	pho5::URA rph1::KAN
CY337 rph1::KAN	rph1::KAN
	URA Knockouts mit FOA-Selektion
CY339	
CY339 rph1::KAN	
IPY36 pho5::ura	
IPY36 pho5::ura rph1::KAN	
LPY7091 pho5::ura	
LPY7091 pho5::ura rph1::KAN	
	HDAC knockouts
CY337	hos1::KanMx
CY337	hos2::KanMx
CY337	hos3::KanMx
CY337	rpd3:KanMx

CY337	hda1::KanMx
	with Pho4-DBD/dSu(var)3-9
CY337	hos1::KanMx Pho4-DBD/dSu(var)3-9 (pRS406)
CY337	hos2::KanMx Pho4-DBD/dSu(var)3-9 (pRS406)
CY337	hos3::KanMx Pho4-DBD/dSu(var)3-9 (pRS406)
CY337	rpd3:KanMx Pho4-DBD/dSu(var)3-9 (pRS406)
CY337	hda1::KanMx Pho4-DBD/dSu(var)3-9 (pRS406)
CY337	rpd3:KanMx Pho4DBD (pRS406)
RANDY MORSE Strains	
BY4742	*MATα his3Δ1 leu2Δ0 lys2Δ0 ura3Δ0*
gal11Δmed3Δ	*MATα pgd1Δ::kanMX4 gal11Δ::kanMX4 his3Δ1 leu2Δ0 lys2Δ0 met15Δ0 ura3Δ0*
RMY521 (SRB4 WT)	*MATa his3Δ1 leu2Δ0 met15Δ0 ura3Δ0 srb4Δ::KanMx SRB5-13MCY::HIS3 (S.K.) RY2844 (CEN LEU2 SRB4)*
RMY522 (srb4 ts)	*MATa his3Δ1 leu2Δ0 met15Δ0 ura3Δ0 srb4Δ::KanMx SRB5-13MCY::HIS3 (S.K.) RY2844 (CEN LEU2 srb4-138)*
Z579 (WT)	*Mat a, his3Δ200, leu2-3,122, ura3-52, srb4Δ2::HIS3 [pCT181/RY2882 (SRB4 LEU2 CEN)]*
Z111 (rpB1ts))	*Mat alpha, ura3-52, his3Δ200, leu2-3,122, rpb1-1, ade2*
BY4742	*MATα his3Δ1 leu2Δ0 lys2Δ0 ura3Δ0* + **pPZ leu V33**
gal11Δmed3Δ	*MATα pgd1Δ::kanMX4 gal11Δ::kanMX4 his3Δ1 leu2Δ0 lys2Δ0 met15Δ0 ura3Δ0* **+ pPZ leu V33**
RMY521 (SRB4 WT)	*MATa his3Δ1 leu2Δ0 met15Δ0 ura3Δ0 srb4Δ::KanMx SRB5-13MCY::HIS3 (S.K.) RY2844 (CEN LEU2 SRB4)* +**pPZ ura V33**
RMY522 (srb4 ts)	*MATa his3Δ1 leu2Δ0 met15Δ0 ura3Δ0 srb4Δ::KanMx SRB5-13MCY::HIS3 (S.K.) RY2844 (CEN LEU2 srb4-138)* ***+pPZ ura V33***
Z579 (WT)	*Mat a, his3Δ200, leu2-3,122, ura3-52, srb4Δ2::HIS3 [pCT181/RY2882 (SRB4 LEU2 CEN)]* +**pPZ ura V33**
Z111 (rpB1ts))	Mat alpha, ura3-52, his3Δ200, leu2-3,122, rpb1-1, ade2 +pPZ ura V33 Mat alpha, ura3-52, his3Δ200, leu2-3,122, rpb1-1, ade2 pPZ ura Var.33
Y06165	BY4741; MAT a; his3Δ1; leu2Δ0;met15Δ0; ura3Δ0; YER169w::kanMX4 (Δrph1)
LPY7091	
IPY36	
L5684	RPD3::Myc (13) *MAT***a** *ura3-52 leu2*Δ
	Promoter library -/+ HP1a (pRS416 vector)
YS18 pEG202empty	Gal4pBS2 Pleum
YS18 pEG202empty	Gal4pBS1 Pleum

YS18 pEG202empty	Gal4pBS12 Pleum
YS18 pEG202empty	Gal4pBS24 Pleum
YS18 pEG202empty	UASgal CU2 Pcyc
YS18 pEG202empty	Gal4pBS4 Pleum
YS18 pEG202empty	Gal4pBS3 Pleum
YS18 pEG202empty	UASgal CU1 Pcyc
YS18 pEG202empty	Gal4pBS13 Pleum
YS18 pEG202empty	UAS gal Pcyc
YS18 pEG202empty	UAS gal A9 Pcyc
YS18 pEG202empty	Gal4pBS34 Pleum
YS18 pEG202empty	Gal4pBS134 Pleum
YS18 pEG202empty	UASgal
YS18 pEG202empty	Pgal
YS18 pEG202empty	UASgal Pgal
YS18 pEG202empty	Gal4pBS2 Pleum +HP1a
YS18 pEG202empty	Gal4pBS1 Pleum +HP1a
YS18 pEG202empty	Gal4pBS12 Pleum +HP1a
YS18 pEG202empty	Gal4pBS24 Pleum +HP1a
YS18 pEG202empty	UASgal CU2 Pcyc +HP1a
YS18 pEG202empty	Gal4pBS4 Pleum +HP1a
YS18 pEG202empty	Gal4pBS3 Pleum +HP1a
YS18 pEG202empty	UASgal CU1 Pcyc +HP1a
YS18 pEG202empty	Gal4pBS13 Pleum +HP1a
YS18 pEG202empty	UAS gal Pcyc +HP1a
YS18 pEG202empty	Gal4pBS34 Pleum +HP1a
YS18 pEG202empty	Gal4pBS134 Pleum +HP1a
YS18 pEG202empty	UASgal +HP1a
YS18 pEG202empty	Pgal +HP1a
YS18 pEG202empty	UASgal Pgal +HP1a

5.4 Spike tides

Index	peptide sequence	ID	sequence synthesized	remark
1	ARTKQTAR	Peptide 1-8	ARTKQTAXZ	k = Kme, m = Kme2, n = Kme3, a = Kac, t = Tpho, s = Spho, X=labelled Arg, Z=JPT-Tag
2	ARTkQTAR		ARTkQTAXZ	k = Kme, m = Kme2, n = Kme3, a = Kac, t = Tpho, s = Spho, X=labelled Arg, Z=JPT-Tag
3	ARTmQTAR		ARTmQTAXZ	k = Kme, m = Kme2, n = Kme3, a = Kac, t = Tpho, s = Spho, X=labelled Arg, Z=JPT-Tag
4	ARTnQTAR		ARTnQTAXZ	k = Kme, m = Kme2, n = Kme3, a = Kac, t = Tpho, s = Spho, X=labelled Arg, Z=JPT-Tag
5	ARTKQtAR		ARTKQtAXZ	k = Kme, m = Kme2, n = Kme3, a = Kac, t = Tpho, s = Spho, X=labelled Arg, Z=JPT-Tag
6	ARTkQtAR		ARTkQtAXZ	k = Kme, m = Kme2, n = Kme3, a = Kac, t = Tpho, s = Spho, X=labelled Arg, Z=JPT-Tag
7	ARtKQTAR		ARtKQTAXZ	k = Kme, m = Kme2, n = Kme3, a = Kac, t = Tpho, s = Spho, X=labelled Arg, Z=JPT-Tag
8	ARKSTGGKAPR	Peptide 7-17	ARKSTGGKAPXZ	k = Kme, m = Kme2, n = Kme3, a = Kac, t = Tpho, s = Spho, X=labelled Arg, Z=JPT-Tag
9	ARkSTGGKAPR		ARkSTGGKAPXZ	k = Kme, m = Kme2, n = Kme3, a = Kac, t = Tpho, s = Spho, X=labelled Arg, Z=JPT-Tag
10	ARmSTGGKAPR		ARmSTGGKAPXZ	k = Kme, m = Kme2, n = Kme3, a = Kac, t = Tpho, s = Spho, X=labelled Arg, Z=JPT-Tag
11	ARnSTGGKAPR		ARnSTGGKAPXZ	k = Kme, m = Kme2, n = Kme3, a = Kac, t = Tpho, s = Spho, X=labelled Arg, Z=JPT-Tag
12	ARKSTGGaAPR		ARKSTGGaAPXZ	k = Kme, m = Kme2, n = Kme3, a = Kac, t = Tpho, s = Spho, X=labelled Arg, Z=JPT-Tag
13	ARKsTGGKAPR		ARKsTGGKAPXZ	k = Kme, m = Kme2, n = Kme3, a = Kac, t = Tpho, s = Spho, X=labelled Arg, Z=JPT-Tag
14	ARKsTGGaAPR		ARKsTGGaAPXZ	k = Kme, m = Kme2, n = Kme3, a = Kac, t = Tpho, s = Spho, X=labelled Arg, Z=JPT-Tag
15	ARaSTGGKAPR		ARaSTGGKAPXZ	k = Kme, m = Kme2, n = Kme3, a = Kac, t = Tpho, s = Spho, X=labelled Arg, Z=JPT-Tag
16	ARaSTGGaAPR		ARaSTGGaAPXZ	k = Kme, m = Kme2, n = Kme3, a = Kac, t = Tpho, s = Spho, X=labelled Arg, Z=JPT-Tag
17	PRKQLATKAAR	Peptide 16-26	PRKQLATKAAXZ	k = Kme, m = Kme2, n = Kme3, a = Kac, t = Tpho, s = Spho, X=labelled Arg, Z=JPT-Tag
18	PRaQLATKAAR		PRaQLATKAAXZ	k = Kme, m = Kme2, n = Kme3, a = Kac, t = Tpho, s = Spho, X=labelled Arg, Z=JPT-Tag
19	PRKQLATaAAR		PRKQLATaAAXZ	k = Kme, m = Kme2, n = Kme3, a = Kac, t = Tpho, s = Spho, X=labelled Arg, Z=JPT-Tag
20	PRaQLATaAAR		PRaQLATaAAXZ	k = Kme, m = Kme2, n = Kme3, a = Kac, t = Tpho, s = Spho, X=labelled Arg, Z=JPT-Tag
21	ARKSAPATGGVKKPHR	Peptide 25-40	ARKSAPATGGVKKPHXZ	k = Kme, m = Kme2, n = Kme3, a = Kac, t = Tpho, s = Spho, X=labelled Arg, Z=JPT-Tag
22	ARkSAPATGGVKKPHR		ARkSAPATGGVKKPHXZ	k = Kme, m = Kme2, n = Kme3, a = Kac, t = Tpho, s = Spho, X=labelled Arg, Z=JPT-Tag
23	ARmSAPATGGVKKPHR		ARmSAPATGGVKKPHXZ	k = Kme, m = Kme2, n = Kme3, a = Kac, t = Tpho, s = Spho, X=labelled Arg, Z=JPT-Tag
24	ARnSAPATGGVKKPHR		ARnSAPATGGVKKPHXZ	k = Kme, m = Kme2, n = Kme3, a = Kac, t = Tpho, s = Spho, X=labelled Arg, Z=JPT-Tag
25	ARKSAPATGGVkKPHR		ARKSAPATGGVkKPHXZ	k = Kme, m = Kme2, n = Kme3, a = Kac, t = Tpho, s = Spho, X=labelled Arg, Z=JPT-Tag
26	ARKSAPATGGVmKPHR		ARKSAPATGGVmKPHXZ	k = Kme, m = Kme2, n = Kme3, a = Kac, t = Tpho, s = Spho, X=labelled Arg, Z=JPT-Tag
27	ARkSAPATGGVkKPHR		ARkSAPATGGVkKPHXZ	k = Kme, m = Kme2, n = Kme3, a = Kac, t = Tpho, s = Spho, X=labelled Arg, Z=JPT-Tag
28	ARkSAPATGGVmKPHR		ARkSAPATGGVmKPHXZ	k = Kme, m = Kme2, n = Kme3, a = Kac, t = Tpho, s = Spho, X=labelled Arg, Z=JPT-Tag

29	ARmSAPATGGVkKPHR		ARmSAPATGGVkKPHXZ	k = Kme, m = Kme2, n = Kme3, a = Kac, t = Tpho, s = Spho, X=labelled Arg, Z=JPT-Tag
30	ARKSAPSTGGVKKPHR	Peptide 25-40 H3.3	ARKSAPSTGGVKKPHXZ	k = Kme, m = Kme2, n = Kme3, a = Kac, t = Tpho, s = Spho, X=labelled Arg, Z=JPT-Tag
31	RYRPGTVALR	Peptide 40-49	RYRPGTVALXZ	k = Kme, m = Kme2, n = Kme3, a = Kac, t = Tpho, s = Spho, X=labelled Arg, Z=JPT-Tag
32	RYQKSTELLIR	Peptide53-63	RYQKSTELLIXZ	k = Kme, m = Kme2, n = Kme3, a = Kac, t = Tpho, s = Spho, X=labelled Arg, Z=JPT-Tag
33	RYQasTELLIR		RYQasTELLIXZ	k = Kme, m = Kme2, n = Kme3, a = Kac, t = Tpho, s = Spho, X=labelled Arg, Z=JPT-Tag
34	RYQaSTELLIR		RYQaSTELLIXZ	k = Kme, m = Kme2, n = Kme3, a = Kac, t = Tpho, s = Spho, X=labelled Arg, Z=JPT-Tag
35	REIAQDFKTDLR	Peptide 72-83	REIAQDFKTDLXZ	k = Kme, m = Kme2, n = Kme3, a = Kac, t = Tpho, s = Spho, X=labelled Arg, Z=JPT-Tag
36	REIAQDFkTDLR		REIAQDFkTDLXZ	k = Kme, m = Kme2, n = Kme3, a = Kac, t = Tpho, s = Spho, X=labelled Arg, Z=JPT-Tag
37	REIAQDFmTDLR		REIAQDFmTDLXZ	k = Kme, m = Kme2, n = Kme3, a = Kac, t = Tpho, s = Spho, X=labelled Arg, Z=JPT-Tag
38	REIAQDFnTDLR		REIAQDFnTDLXZ	k = Kme, m = Kme2, n = Kme3, a = Kac, t = Tpho, s = Spho, X=labelled Arg, Z=JPT-Tag
39	RVTIMPKDIQLAR	Peptide 117-128	RVTIMPKDIQLAXZ	k = Kme, m = Kme2, n = Kme3, a = Kac, t = Tpho, s = Spho, X=labelled Arg, Z=JPT-Tag

6 Abbreviations

3-AT	3-Amino-1,2,4-triazole
5FOA	5-Fluoroorotic acid
AA	amino acids
acetyl-CoA	acetyl coenzyme A
ACN	acetonitrile
ACT1	actin
ATF2	activating transcription factor 1
CD	chromo domain
CD_mut	chromo domain mutant
CFU	colony forming unit
ChIP	chromatin immunoprecipitation
CpG is-lands	cytosine - guanine islands
CSD	chromo shadow domain
CSD_ mut	chromo shadow domain mutant
cryo-EM	cryo-electron microscopy
DBD	DNA binding domain
DEPEC	diethylpyrocarbonate
DNA	deoxyribonucleic acid
eHS	extensive hypersensitive site
E(var)	enhancer of variegation
H	hours
H2 h3 h4	histone H2, histone H3, histone H4
H3K9	histone H3 Lysine 9
HAT	histone acetyltransferase
HDAC	histone deacetylases
HML	hidden MAT Left
HMR	hidden MAT Right
HMT	histone methyltransferase
IAc	isoamylalcohol
KanMX	selection marker for kanamycin
Kpb	Kilobase pair
KDM	histone lysine demethylase
lexA_BS	lexA binding site
Min	minutes
NaAc	sodium acetate
NAOH	sodium hydroxide
NPP	para-Nitrophenylphosphate
o/n	over night
Orc	origin recognition complex
Orf	open reading frame
PEG	polyethylene glycol

PHD domain	plant homeodomain
Pho4-DBD	Pho4 DNA binding domain
P_i	phosphate
PTM	post-translational modification
PVP-40	polyvinylpyrrolidone
RE	restriction enzymes
Rpm	revolutions per minute
RT	room temperature
Sec	seconds
SEM	standard error of the mean
Set_mut	SET domain mutant
sHS	short hypersensitive site
SIR complex	Silent Information Regulator
Su(var)	suppressor of variegation
TCA	trichloroacetic acid
TE	tris EDTA
TEL	telomere
TFA	trifluoroacetic acid
TRP1	tryptophan
TSS	transcription Start Site
UASp	upstream activating sequence
w/o	without
w/v	mass/volume
WCE	whole cell extract
wt	wild type
YNB	yeast nitrogen base
YPDA	yeast extract-peptone-dextrose-adenine

7 References

In-Fusion® Molar Ratio Calculator. http://bioinfo.clontech.com/infusion/molarRatio.do. Access date 08.08.2018.

Akey, C.W. & Luger, K. (2003) Histone chaperones and nucleosome assembly. *Current Opinion in Structural Biology,* **13,** 6-14.

Al-Sady, B., Madhani, H.D. & Narlikar, G.J. (2013) Division of labor between the chromodomains of HP1 and Suv39 methylase enables coordination of heterochromatin spread. *Mol Cell,* **51,** 80-91.

Alabert, C., Barth, T.K., Reveron-Gomez, N., Sidoli, S., Schmidt, A., Jensen, O.N., Imhof, A. & Groth, A. (2015) Two distinct modes for propagation of histone PTMs across the cell cycle. *Genes Dev,* **29,** 585-590.

Alberts, B., Johnson, A., Lewis, J., Raff, M., Roberts, K. & Walter, P. (2007) *Molecular Biology of the Cell.* Garland Science.

Allan, J., Hartman, P.G., Crane-Robinson, C. & Aviles, F.X. (1980) The structure of histone H1 and its location in chromatin. *Nature,* **288,** 675-679.

Allfrey, V.G., Faulkner, R. & Mirsky, A.E. (1964) ACETYLATION AND METHYLATION OF HISTONES AND THEIR POSSIBLE ROLE IN THE REGULATION OF RNA SYNTHESIS. *Proc Natl Acad Sci U S A,* **51,** 786-794.

Allshire, R.C. & Madhani, H.D. (2018) Ten principles of heterochromatin formation and function. *Nat Rev Mol Cell Biol,* **19,** 229-244.

Almer, A. & Horz, W. (1986) Nuclease hypersensitive regions with adjacent positioned nucleosomes mark the gene boundaries of the PHO5/PHO3 locus in yeast. *Embo j,* **5,** 2681-2687.

Almer, A. & Hörz, W. (1986) Nuclease hypersensitive regions with adjacent positioned nucleosomesmarkthegene boundariesofthePH05/PH03locus in yeast. *Embo J.,* **5,** 2681 – 2687.

Almer, A., Rudolph, H., Hinnen, A. & Horz, W. (1986) Removal of positioned nucleosomes from the yeast PHO5 promoter upon PHO5 induction releases additional upstream activating DNA elements. *Embo j,* **5,** 2689-2696.

Ansari, S.A. & Morse, R.H. (2013) Mechanisms of Mediator complex action in transcriptional activation. *Cell Mol Life Sci,* **70,** 2743-2756.

Ansari, S.A., Paul, E., Sommer, S., Lieleg, C., He, Q., Daly, A.Z., Rode, K.A., Barber, W.T., Ellis, L.C., LaPorta, E., Orzechowski, A.M., Taylor, E., Reeb, T., Wong, J., Korber, P. & Morse, R.H. (2014) Mediator, TATA-binding protein, and RNA polymerase II contribute to low histone occupancy at active gene promoters in yeast. *J Biol Chem,* **289,** 14981-14995.

Aparicio, O., Geisberg, J.V., Sekinger, E., Yang, A., Moqtaderi, Z. & Struhl, K. (2005) Chromatin immunoprecipitation for determining the association of proteins with specific genomic sequences in vivo. *Curr Protoc Mol Biol,* **Chapter 21,** Unit 21.23.

Arnaudo, A.M. & Garcia, B.A. (2013) Proteomic characterization of novel histone post-translational modifications. *Epigenetics Chromatin,* **6,** 24.

Aulner, N., Monod, C., Mandicourt, G., Jullien, D., Cuvier, O., Sall, A., Janssen, S., Laemmli, U.K. & Kas, E. (2002) The AT-hook protein D1 is essential for Drosophila melanogaster development and is implicated in position-effect variegation. *Mol Cell Biol,* **22,** 1218-1232.

Aygun, O., Mehta, S. & Grewal, S.I. (2013) HDAC-mediated suppression of histone turnover promotes epigenetic stability of heterochromatin. *Nat Struct Mol Biol,* **20,** 547-554.

Ayoub, N., Jeyasekharan, A.D., Bernal, J.A. & Venkitaraman, A.R. (2008) HP1-beta mobilization promotes chromatin changes that initiate the DNA damage response. *Nature,* **453,** 682-686.

Azzaz, A.M., Vitalini, M.W., Thomas, A.S., Price, J.P., Blacketer, M.J., Cryderman, D.E., Zirbel, L.N., Woodcock, C.L., Elcock, A.H., Wallrath, L.L. & Shogren-Knaak, M.A. (2014) Human heterochromatin protein 1alpha promotes nucleosome associations that drive chromatin condensation. *J Biol Chem,* **289,** 6850-6861.

Ball, A.R., Jr. & Yokomori, K. (2009) Revisiting the role of heterochromatin protein 1 in DNA repair. *J Cell Biol,* **185,** 573-575.

Bannister, A.J. & Kouzarides, T. (2011) Regulation of chromatin by histone modifications. *Cell Res,* **21,** 381-395.

Bannister, A.J., Zegerman, P., Partridge, J.F., Miska, E.A., Thomas, J.O., Allshire, R.C. & Kouzarides, T. (2001) Selective recognition of methylated lysine 9 on histone H3 by the HP1 chromo domain. *Nature,* **410,** 120-124.

Barbarić, S., Fascher, K.D. & Hörz, W. (1992) Activation of the weakly regulated PHO8 promoter in S. cerevisiae: chromatin transition and binding sites for the positive regulatory protein PHO4. *Nucleic Acids Res,* **20,** 1031-1038.

Barbaric, S., Luckenbach, T., Schmid, A., Blaschke, D., Horz, W. & Korber, P. (2007) Redundancy of chromatin remodeling pathways for the induction of the yeast PHO5 promoter in vivo. *J Biol Chem,* **282,** 27610-27621.

Barbaric, S., Walker, J., Schmid, A., Svejstrup, J.Q. & Horz, W. (2001a) Increasing the rate of chromatin remodeling and gene activation--a novel role for the histone acetyltransferase Gcn5. *Embo j,* **20,** 4944-4951.

Barbaric, S., Walker, J., Schmid, A., Svejstrup, J.Q. & Hörz, W. (2001b) *Increasing the rate of chromatin remodeling and gene activation—a novel role for the histone acetyltransferase Gcn5.*

Barrales, R.R., Korber, P., Jimenez, J. & Ibeas, J.I. (2012) Chromatin Modulation at the FLO11 Promoter of Saccharomyces cerevisiae by HDAC and Swi/Snf Complexes. *Genetics,* **191,** 791-803.

Bird, A. (2002) DNA methylation patterns and epigenetic memory. *Genes Dev,* **16,** 6-21.

Bird, A.P. & Wolffe, A.P. (1999) Methylation-induced repression--belts, braces, and chromatin. *Cell,* **99,** 451-454.

Black, J.C., Van Rechem, C. & Whetstine, J.R. (2012) Histone lysine methylation dynamics: establishment, regulation, and biological impact. *Mol Cell,* **48,** 491-507.

Blattes, R., Monod, C., Susbielle, G., Cuvier, O., Wu, J.H., Hsieh, T.S., Laemmli, U.K. & Kas, E. (2006) Displacement of D1, HP1 and topoisomerase II from satellite heterochromatin by a specific polyamide. *Embo j,* **25,** 2397-2408.

Blazeck, J., Garg, R., Reed, B. & Alper, H.S. (2012) Controlling promoter strength and regulation in Saccharomyces cerevisiae using synthetic hybrid promoters. *Biotechnol Bioeng,* **109,** 2884-2895.

Boeger, H., Griesenbeck, J., Strattan, J.S. & Kornberg, R.D. (2003) Nucleosomes unfold completely at a transcriptionally active promoter. *Mol Cell,* **11,** 1587-1598.

Boeger, H., Griesenbeck, J., Strattan, J.S. & Kornberg, R.D. (2004) Removal of promoter nucleosomes by disassembly rather than sliding in vivo. *Mol Cell,* **14,** 667-673.

Brachmann, C.B., Davies, A., Cost, G.J., Caputo, E., Li, J., Hieter, P. & Boeke, J.D. (1998) Designer deletion strains derived from Saccharomyces cerevisiae S288C: a useful set of strains and plasmids for PCR-mediated gene disruption and other applications. *Yeast,* **14,** 115-132.

Brasher, S.V., Smith, B.O., Fogh, R.H., Nietlispach, D., Thiru, A., Nielsen, P.R., Broadhurst, R.W., Ball, L.J., Murzina, N.V. & Laue, E.D. (2000) The structure of mouse HP1

suggests a unique mode of single peptide recognition by the shadow chromo domain dimer. *Embo j,* **19,** 1587-1597.

Bulut-Karslioglu, A., Perrera, V., Scaranaro, M., de la Rosa-Velazquez, I.A., van de Nobelen, S., Shukeir, N., Popow, J., Gerle, B., Opravil, S., Pagani, M., Meidhof, S., Brabletz, T., Manke, T., Lachner, M. & Jenuwein, T. (2012) A transcription factor-based mechanism for mouse heterochromatin formation. *Nat Struct Mol Biol,* **19,** 1023-1030.

Buschbeck, M. & Hake, S.B. (2017) Variants of core histones and their roles in cell fate decisions, development and cancer. *Nat Rev Mol Cell Biol,* **18,** 299-314.

Canzio, D., Chang, E.Y., Shankar, S., Kuchenbecker, K.M., Simon, M.D., Madhani, H.D., Narlikar, G.J. & Al-Sady, B. (2011) Chromodomain-mediated oligomerization of HP1 suggests a nucleosome-bridging mechanism for heterochromatin assembly. *Mol Cell,* **41,** 67-81.

Canzio, D., Larson, A. & Narlikar, G.J. (2014) Mechanisms of functional promiscuity by HP1 proteins. *Trends Cell Biol,* **24,** 377-386.

Capuano, F., Mülleder, M., Kok, R., Blom, H.J. & Ralser, M. (2014) Cytosine DNA Methylation Is Found in Drosophila melanogaster but Absent in Saccharomyces cerevisiae, Schizosaccharomyces pombe, and Other Yeast Species. *Analytical Chemistry,* **86,** 3697-3702.

Carrozza, M.J., Li, B., Florens, L., Suganuma, T., Swanson, S.K., Lee, K.K., Shia, W.J., Anderson, S., Yates, J., Washburn, M.P. & Workman, J.L. (2005) Histone H3 methylation by Set2 directs deacetylation of coding regions by Rpd3S to suppress spurious intragenic transcription. *Cell,* **123,** 581-592.

Carvin, C.D. & Kladde, M.P. (2004) Effectors of lysine 4 methylation of histone H3 in Saccharomyces cerevisiae are negative regulators of PHO5 and GAL1-10. *J Biol Chem,* **279,** 33057-33062.

Cheng, J., Blum, R., Bowman, C., Hu, D., Shilatifard, A., Shen, S. & Dynlacht, Brian D. (2014) A Role for H3K4 Monomethylation in Gene Repression and Partitioning of Chromatin Readers. *Mol Cell,* **53,** 979-992.

Cheutin, T., McNairn, A.J., Jenuwein, T., Gilbert, D.M., Singh, P.B. & Misteli, T. (2003) Maintenance of stable heterochromatin domains by dynamic HP1 binding. *Science,* **299,** 721-725.

Clapier, C.R. & Cairns, B.R. (2009) The biology of chromatin remodeling complexes. *Annu Rev Biochem,* **78,** 273-304.

Cleard, F. & Spierer, P. (2001) Position-effect variegation in Drosophila: the modifier Su(var)3-7 is a modular DNA-binding protein. *EMBO Rep,* **2,** 1095-1100.

Clements, A., Poux, A.N., Lo, W.S., Pillus, L., Berger, S.L. & Marmorstein, R. (2003) Structural basis for histone and phosphohistone binding by the GCN5 histone acetyltransferase. *Mol Cell,* **12,** 461-473.

Cowieson, N.P., Partridge, J.F., Allshire, R.C. & McLaughlin, P.J. (2000) Dimerisation of a chromo shadow domain and distinctions from the chromodomain as revealed by structural analysis. *Curr. Biol.,* **10,** 517-525.

Cryderman, D.E., Tang, H., Bell, C., Gilmour, D.S. & Wallrath, L.L. (1999) Heterochromatic silencing of Drosophila heat shock genes acts at the level of promoter potentiation. *Nucleic Acids Res,* **27,** 3364-3370.

Czermin, B., Schotta, G., Hulsmann, B.B., Brehm, A., Becker, P.B., Reuter, G. & Imhof, A. (2001) Physical and functional association of SU(VAR)3-9 and HDAC1 in Drosophila. *EMBO Rep,* **2,** 915-919.

Danzer, J.R. & Wallrath, L.L. (2004) Mechanisms of HP1-mediated gene silencing in Drosophila. *Development,* **131,** 3571-3580.

Davie, J.R., Saunders, C.A., Walsh, J.M. & Weber, S.C. (1981) Histone modifications in the yeast S. Cerevisiae. *Nucleic Acids Res,* **9,** 3205-3216.

Dawson, M.A., Bannister, A.J., Göttgens, B., Foster, S.D., Bartke, T., Green, A.R. & Kouzarides, T. (2009) JAK2 phosphorylates histone H3Y41 and excludes HP1α from chromatin. *Nature,* **461,** 819-822.

de Wit, E., Greil, F. & van Steensel, B. (2007) High-resolution mapping reveals links of HP1 with active and inactive chromatin components. *PLoS Genet,* **3,** e38.

Di Lorenzo, A. & Bedford, M.T. (2011) Histone arginine methylation. *FEBS Letters,* **585,** 2024-2031.

Dinant, C. & Luijsterburg, M.S. (2009) The emerging role of HP1 in the DNA damage response. *Mol Cell Biol,* **29,** 6335-6340.

Dion, M.F., Altschuler, S.J., Wu, L.F. & Rando, O.J. (2005) Genomic characterization reveals a simple histone H4 acetylation code. *Proc Natl Acad Sci U S A,* **102,** 5501-5506.

Duan, Q., Chen, H., Costa, M. & Dai, W. (2008) Phosphorylation of H3S10 Blocks the Access of H3K9 by Specific Antibodies and Histone Methyltransferase: IMPLICATION IN REGULATING CHROMATIN DYNAMICS AND EPIGENETIC INHERITANCE DURING MITOSIS. *J Biol Chem,* **283,** 33585-33590.

Eden, A., Gaudet, F., Waghmare, A. & Jaenisch, R. (2003) Chromosomal instability and tumors promoted by DNA hypomethylation. *Science,* **300,** 455.

Edmondson, D.G., Smith, M.M. & Roth, S.Y. (1996) Repression domain of the yeast global repressor Tup1 interacts directly with histones H3 and H4. *Genes Dev,* **10,** 1247-1259.

Eickbush, T.H. & Moudrianakis, E.N. (1978) The histone core complex: an octamer assembled by two sets of protein-protein interactions. *Biochemistry,* **17,** 4955-4964.

Eissenberg, J.C. & Elgin, S.C. (2014) HP1a: a structural chromosomal protein regulating transcription. *Trends Genet,* **30,** 103-110.

Eissenberg, J.C., James, T.C., Foster-Hartnett, D.M., Hartnett, T., Ngan, V. & Elgin, S.C. (1990) Mutation in a heterochromatin-specific chromosomal protein is associated with suppression of position-effect variegation in Drosophila melanogaster. *Proc Natl Acad Sci U S A,* **87,** 9923-9927.

Eissenberg, J.C., Morris, G.D., Reuter, G. & Hartnett, T. (1992) The heterochromatin-associated protein HP-1 is an essential protein in Drosophila with dosage-dependent effects on position-effect variegation. *Genetics,* **131,** 345-352.

Elgin, S.C. & Reuter, G. (2013) Position-effect variegation, heterochromatin formation, and gene silencing in Drosophila. *Cold Spring Harb Perspect Biol,* **5,** a017780.

Elgin, S.C.R. & Grewal, S.I.S. (2003) Heterochromatin: silence is golden. *Current Biology,* **13,** R895-R898.

Ernst, J., Kheradpour, P., Mikkelsen, T.S., Shoresh, N., Ward, L.D., Epstein, C.B., Zhang, X., Wang, L., Issner, R., Coyne, M., Ku, M., Durham, T., Kellis, M. & Bernstein, B.E. (2011) Mapping and analysis of chromatin state dynamics in nine human cell types. *Nature,* **473,** 43-49.

Eskeland, R., Czermin, B., Boeke, J., Bonaldi, T., Regula, J.T. & Imhof, A. (2004) The N-terminus of Drosophila SU(VAR)3-9 mediates dimerization and regulates its methyltransferase activity. *Biochemistry,* **43,** 3740-3749.

Eskeland, R., Eberharter, A. & Imhof, A. (2007) HP1 binding to chromatin methylated at H3K9 is enhanced by auxiliary factors. *Mol Cell Biol,* **27,** 453-465.

Falahi, F., Huisman, C., Kazemier, H.G., van der Vlies, P., Kok, K., Hospers, G.A. & Rots, M.G. (2013) Towards sustained silencing of HER2/neu in cancer by epigenetic editing. *Mol Cancer Res,* **11,** 1029-1039.

Fan, X., Lamarre-Vincent, N., Wang, Q. & Struhl, K. (2008) Extensive chromatin fragmentation improves enrichment of protein binding sites in chromatin immunoprecipitation experiments. *Nucleic Acids Res,* **36,** e125.

Fan, Y., Nikitina, T., Morin-Kensicki, E.M., Zhao, J., Magnuson, T.R., Woodcock, C.L. & Skoultchi, A.I. (2003) H1 linker histones are essential for mouse development and affect nucleosome spacing in vivo. *Mol Cell Biol,* **23,** 4559-4572.

Fan, Y., Sirotkin, A., Russell, R.G., Ayala, J. & Skoultchi, A.I. (2001) Individual somatic H1 subtypes are dispensable for mouse development even in mice lacking the H1(0) replacement subtype. *Mol Cell Biol,* **21,** 7933-7943.

Fanti, L., Giovinazzo, G., Berloco, M. & Pimpinelli, S. (1998) The heterochromatin protein 1 prevents telomere fusions in Drosophila. *Mol Cell,* **2,** 527-538.

Fatica, A. & Bozzoni, I. (2014) Long non-coding RNAs: new players in cell differentiation and development. *Nat Rev Genet,* **15,** 7-21.

Festenstein, R., Pagakis, S.N., Hiragami, K., Lyon, D., Verreault, A., Sekkali, B. & Kioussis, D. (2003) Modulation of heterochromatin protein 1 dynamics in primary Mammalian cells. *Science,* **299,** 719-721.

Filion, G.J., van Bemmel, J.G., Braunschweig, U., Talhout, W., Kind, J., Ward, L.D., Brugman, W., de Castro, I.J., Kerkhoven, R.M., Bussemaker, H.J. & van Steensel, B. (2010) Systematic Protein Location Mapping Reveals Five Principal Chromatin Types in Drosophila Cells. *Cell,* **143,** 212-224.

Finch, J.T. & Klug, A. (1976) Solenoidal model for superstructure in chromatin. *Proc Natl Acad Sci U S A,* **73,** 1897-1901.

Fischer, T., Cui, B., Dhakshnamoorthy, J., Zhou, M., Rubin, C., Zofall, M., Veenstra, T.D. & Grewal, S.I. (2009) Diverse roles of HP1 proteins in heterochromatin assembly and functions in fission yeast. *Proc Natl Acad Sci U S A,* **106,** 8998-9003.

Fischle, W., Tseng, B.S., Dormann, H.L., Ueberheide, B.M., Garcia, B.A., Shabanowitz, J., Hunt, D.F., Funabiki, H. & Allis, C.D. (2005) Regulation of HP1-chromatin binding by histone H3 methylation and phosphorylation. *Nature,* **438,** 1116-1122.

Frederiks, F., Tzouros, M., Oudgenoeg, G., van Welsem, T., Fornerod, M., Krijgsveld, J. & van Leeuwen, F. (2008) Nonprocessive methylation by Dot1 leads to functional redundancy of histone H3K79 methylation states. *Nat Struct Mol Biol,* **15,** 550-557.

Fussner, E., Ching, R.W. & Bazett-Jones, D.P. (2011) Living without 30nm chromatin fibers. *Trends Biochem Sci,* **36,** 1-6.

Gasch, A.P., Spellman, P.T., Kao, C.M., Carmel-Harel, O., Eisen, M.B., Storz, G., Botstein, D. & Brown, P.O. (2000) Genomic expression programs in the response of yeast cells to environmental changes. *Mol Biol Cell,* **11,** 4241-4257.

Gaudet, F., Hodgson, J.G., Eden, A., Jackson-Grusby, L., Dausman, J., Gray, J.W., Leonhardt, H. & Jaenisch, R. (2003) Induction of tumors in mice by genomic hypomethylation. *Science,* **300,** 489-492.

Gibson, D.G., Smith, H.O., Hutchison, C.A., Venter, J.C. & Merryman, C. (2010) Chemical synthesis of the mouse mitochondrial genome. *Nat Meth,* **7,** 901-903.

Gibson, D.G., Young, L., Chuang, R.-Y., Venter, J.C., Hutchison, C.A. & Smith, H.O. (2009) Enzymatic assembly of DNA molecules up to several hundred kilobases. *Nat Meth,* **6,** 343-345.

Gregory, P., Barbaric, S. & Hörz, W. (1999a) Restriction Nucleases as Probes for Chromatin Structure. In: *Chromatin Protocols* (ed. by Becker, P.), Vol. 119, pp. 417-425. Humana Press.

Gregory, P.D. & Hörz, W. (1999) Mapping chromatin structure in yeast. In: *Methods in Enzymology* (ed. by Paul M. Wassarman, A.P.W.), Vol. Volume 304, pp. 365-376. Academic Press.

Gregory, P.D., Schmid, A., Zavari, M., Lui, L., Berger, S.L. & Hörz, W. (1998) Absence of Gcn5 HAT Activity Defines a Novel State in the Opening of Chromatin at the PHO5 Promoter in Yeast. *Mol Cell,* **1,** 495-505.

Gregory, P.D., Schmid, A., Zavari, M., Münsterkötter, M. & Hörz, W. (1999b) Chromatin remodelling at the PHO8 promoter requires SWI–SNF and SAGA at a step subsequent to activator binding. *The EMBO Journal,* **18,** 6407-6414.

Greil, F., van der Kraan, I., Delrow, J., Smothers, J.F., de Wit, E., Bussemaker, H.J., van Driel, R., Henikoff, S. & van Steensel, B. (2003) Distinct HP1 and Su(var)3-9 complexes bind to sets of developmentally coexpressed genes depending on chromosomal location. *Genes Dev,* **17,** 2825-2838.

Grunstein, M. & Gasser, S.M. (2013) Epigenetics in Saccharomyces cerevisiae. *Cold Spring Harb Perspect Biol,* **5**.

Guarente, L. (1983) Yeast promoters and lacZ fusions designed to study expression of cloned genes in yeast. *Methods Enzymol,* **101,** 181-191.

Guy, J., Cheval, H., Selfridge, J. & Bird, A. (2011) The role of MeCP2 in the brain. *Annu Rev Cell Dev Biol,* **27,** 631-652.

Haguenauer-Tsapis, R., Nagy, M. & Ryter, A. (1986) A deletion that includes the segment coding for the signal peptidase cleavage site delays release of Saccharomyces cerevisiae acid phosphatase from the endoplasmic reticulum. *Mol Cell Biol,* **6,** 723-729.

Hall, I.M., Shankaranarayana, G.D., Noma, K., Ayoub, N., Cohen, A. & Grewal, S.I. (2002) Establishment and maintenance of a heterochromatin domain. *Science,* **297,** 2232-2237.

Han, M. & Grunstein, M. (1988) Nucleosome loss activates yeast downstream promoters in vivo. *Cell,* **55,** 1137-1145.

Han, M., Kim, U.J., Kayne, P. & Grunstein, M. (1988) Depletion of histone H4 and nucleosomes activates the PHO5 gene in Saccharomyces cerevisiae. *Embo j,* **7,** 2221-2228.

Hansen, J.C. (2012) Human mitotic chromosome structure: what happened to the 30-nm fibre? *Embo j,* **31,** 1621-1623.

Harshman, S.W., Young, N.L., Parthun, M.R. & Freitas, M.A. (2013) H1 histones: current perspectives and challenges. *Nucleic Acids Res,* **41,** 9593-9609.

Hassan, A.H., Prochasson, P., Neely, K.E., Galasinski, S.C., Chandy, M., Carrozza, M.J. & Workman, J.L. (2002) Function and Selectivity of Bromodomains in Anchoring Chromatin-Modifying Complexes to Promoter Nucleosomes. *Cell,* **111,** 369-379.

Haynes, K.A., Caudy, A.A., Collins, L. & Elgin, S.C. (2006) Element 1360 and RNAi components contribute to HP1-dependent silencing of a pericentric reporter. *Curr Biol,* **16,** 2222-2227.

Heitz, E. (1928) Das heterochromatin der moose. I Jahrb wiss Bot 69: 762–818. *Find this article online*.

Hendzel, M.J., Wei, Y., Mancini, M.A., Van Hooser, A., Ranalli, T., Brinkley, B.R., Bazett-Jones, D.P. & Allis, C.D. (1997) Mitosis-specific phosphorylation of histone H3 initiates primarily within pericentromeric heterochromatin during G2 and spreads in an ordered fashion coincident with mitotic chromosome condensation. *Chromosoma,* **106,** 348-360.

Hilton, J.L., Kearney, P.C. & Ames, B.N. (1965) Mode of action of the herbicide, 3-amino-1,2,4-triazole(amitrole): Inhibition of an enzyme of histidine biosynthesis. *Archives of Biochemistry and Biophysics,* **112,** 544-547.

Hiragami-Hamada, K., Shinmyozu, K., Hamada, D., Tatsu, Y., Uegaki, K., Fujiwara, S. & Nakayama, J. (2011) N-terminal phosphorylation of HP1{alpha} promotes its chromatin binding. *Mol Cell Biol,* **31,** 1186-1200.

Holoch, D. & Moazed, D. (2015) RNA-mediated epigenetic regulation of gene expression. *Nat Rev Genet,* **16,** 71-84.

Horn, P.J. & Peterson, C.L. (2002) Molecular biology. Chromatin higher order folding--wrapping up transcription. *Science,* **297,** 1824-1827.
Huang, X.A., Yin, H., Sweeney, S., Raha, D., Snyder, M. & Lin, H. (2013) A major epigenetic programming mechanism guided by piRNAs. *Dev Cell,* **24,** 502-516.
Hwang, K.K., Eissenberg, J.C. & Worman, H.J. (2001) Transcriptional repression of euchromatic genes by Drosophila heterochromatin protein 1 and histone modifiers. *Proc Natl Acad Sci U S A,* **98,** 11423-11427.
Hyland, E.M., Cosgrove, M.S., Molina, H., Wang, D., Pandey, A., Cottee, R.J. & Boeke, J.D. (2005) Insights into the role of histone H3 and histone H4 core modifiable residues in Saccharomyces cerevisiae. *Mol Cell Biol,* **25,** 10060-10070.
Jack, A.M. & Hake, S. (2014) Getting down to the core of histone modifications. *Chromosoma,* **123,** 355-371.
Jacobs, S.A., Harp, J.M., Devarakonda, S., Kim, Y., Rastinejad, F. & Khorasanizadeh, S. (2002) The active site of the SET domain is constructed on a knot. *Nat Struct Biol,* **9,** 833-838.
Jacobs, S.A., Taverna, S.D., Zhang, Y., Briggs, S.D., Li, J., Eissenberg, J.C., Allis, C.D. & Khorasanizadeh, S. (2001) Specificity of the HP1 chromo domain for the methylated N‐terminus of histone H3. *The EMBO Journal,* **20,** 5232-5241.
Jacobson, R.H., Ladurner, A.G., King, D.S. & Tjian, R. (2000) Structure and Function of a Human TAFII250 Double Bromodomain Module. *Science,* **288,** 1422-1425.
James, T.C. & Elgin, S.C. (1986) Identification of a nonhistone chromosomal protein associated with heterochromatin in Drosophila melanogaster and its gene. *Mol Cell Biol,* **6,** 3862-3872.
Jenuwein, T. & Allis, C.D. (2001) Translating the histone code. *Science,* **293,** 1074-1080.
Jiang, C. & Pugh, B.F. (2009) Nucleosome positioning and gene regulation: advances through genomics. *Nat Rev Genet,* **10,** 161-172.
Jones, P.A. (2012) Functions of DNA methylation: islands, start sites, gene bodies and beyond. *Nat Rev Genet,* **13,** 484-492.
Jones, P.A. & Baylin, S.B. (2002) The fundamental role of epigenetic events in cancer. *Nat Rev Genet,* **3,** 415-428.
Joshi, A.A. & Struhl, K. (2005) Eaf3 Chromodomain Interaction with Methylated H3-K36 Links Histone Deacetylation to Pol II Elongation. *Mol Cell,* **20,** 971-978.
Keller, C., Adaixo, R., Stunnenberg, R., Woolcock, K.J., Hiller, S. & Buhler, M. (2012) HP1(Swi6) mediates the recognition and destruction of heterochromatic RNA transcripts. *Mol Cell,* **47,** 215-227.
Kharchenko, P.V., Alekseyenko, A.A., Schwartz, Y.B., Minoda, A., Riddle, N.C., Ernst, J., Sabo, P.J., Larschan, E., Gorchakov, A.A., Gu, T., Linder-Basso, D., Plachetka, A., Shanower, G., Tolstorukov, M.Y., Luquette, L.J., Xi, R., Jung, Y.L., Park, R.W., Bishop, E.P., Canfield, T.K., Sandstrom, R., Thurman, R.E., MacAlpine, D.M., Stamatoyannopoulos, J.A., Kellis, M., Elgin, S.C.R., Kuroda, M.I., Pirrotta, V., Karpen, G.H. & Park, P.J. (2011) Comprehensive analysis of the chromatin landscape in Drosophila melanogaster. *Nature,* **471,** 480-485.
Klose, R.J., Gardner, K.E., Liang, G., Erdjument-Bromage, H., Tempst, P. & Zhang, Y. (2007) Demethylation of histone H3K36 and H3K9 by Rph1: a vestige of an H3K9 methylation system in Saccharomyces cerevisiae? *Mol Cell Biol,* **27,** 3951-3961.
Knezetic, J.A. & Luse, D.S. (1986) The presence of nucleosomes on a DNA template prevents initiation by RNA polymerase II in vitro. *Cell,* **45,** 95-104.
Komeili, A. (1999) Roles of Phosphorylation Sites in Regulating Activity of the Transcription Factor Pho4. *Science,* **284,** 977-980.

Korber, P. & Barbaric, S. (2014) The yeast PHO5 promoter: from single locus to systems biology of a paradigm for gene regulation through chromatin. *Nucleic Acids Res,* **42,** 10888-10902.

Korber, P., Barbaric, S., Luckenbach, T., Schmid, A., Schermer, U.J., Blaschke, D. & Horz, W. (2006) The histone chaperone Asf1 increases the rate of histone eviction at the yeast PHO5 and PHO8 promoters. *J Biol Chem,* **281,** 5539-5545.

Korber, P., Luckenbach, T., Blaschke, D. & Horz, W. (2004) Evidence for histone eviction in trans upon induction of the yeast PHO5 promoter. *Mol Cell Biol,* **24,** 10965-10974.

Kornberg, R.D. (1974) Chromatin Structure: A Repeating Unit of Histones and DNA. *Science,* **184,** 868-871.

Kornberg, R.D. & Klug, A. (1981) The nucleosome. *Sci Am,* **244,** 52-64.

Kornberg, R.D. & Lorch, Y. (1999) Twenty-five years of the nucleosome, fundamental particle of the eukaryote chromosome. *Cell,* **98,** 285-294.

Kouzarides, T. (2007) Chromatin modifications and their function. *Cell,* **128,** 693-705.

Krogan, N.J., Dover, J., Wood, A., Schneider, J., Heidt, J., Boateng, M.A., Dean, K., Ryan, O.W., Golshani, A., Johnston, M., Greenblatt, J.F. & Shilatifard, A. (2003) The Paf1 Complex Is Required for Histone H3 Methylation by COMPASS and Dot1p: Linking Transcriptional Elongation to Histone Methylation. *Mol Cell,* **11,** 721-729.

Kurdistani, S.K. & Grunstein, M. (2003) Histone acetylation and deacetylation in yeast. *Nat Rev Mol Cell Biol,* **4,** 276-284.

Kushnirov, V.V. (2000) Rapid and reliable protein extraction from yeast. *Yeast,* **16,** 857-860.

Kwon, D.W. & Ahn, S.H. (2011) Role of yeast JmjC-domain containing histone demethylases in actively transcribed regions. *Biochem Biophys Res Commun,* **410,** 614-619.

Kwon, S.H. & Workman, J.L. (2011) The changing faces of HP1: From heterochromatin formation and gene silencing to euchromatic gene expression: HP1 acts as a positive regulator of transcription. *Bioessays,* **33,** 280-289.

Lachner, M., O'Carroll, D., Rea, S., Mechtler, K. & Jenuwein, T. (2001) Methylation of histone H3 lysine 9 creates a binding site for HP1 proteins. *Nature,* **410,** 116-120.

Lanctot, C., Cheutin, T., Cremer, M., Cavalli, G. & Cremer, T. (2007) Dynamic genome architecture in the nuclear space: regulation of gene expression in three dimensions. *Nat Rev Genet,* **8,** 104-115.

Lantermann, A.B., Straub, T., Stralfors, A., Yuan, G.C., Ekwall, K. & Korber, P. (2010) Schizosaccharomyces pombe genome-wide nucleosome mapping reveals positioning mechanisms distinct from those of Saccharomyces cerevisiae. *Nat Struct Mol Biol,* **17,** 251-257.

Larson, A.G., Elnatan, D., Keenen, M.M., Trnka, M.J., Johnston, J.B., Burlingame, A.L., Agard, D.A., Redding, S. & Narlikar, G.J. (2017) Liquid droplet formation by HP1alpha suggests a role for phase separation in heterochromatin. *Nature,* **547,** 236-240.

Lavigne, M., Eskeland, R., Azebi, S., Saint-Andre, V., Jang, S.M., Batsche, E., Fan, H.Y., Kingston, R.E., Imhof, A. & Muchardt, C. (2009) Interaction of HP1 and Brg1/Brm with the globular domain of histone H3 is required for HP1-mediated repression. *PLoS Genet,* **5,** e1000769.

Le Thomas, A., Rogers, A.K., Webster, A., Marinov, G.K., Liao, S.E., Perkins, E.M., Hur, J.K., Aravin, A.A. & Toth, K.F. (2013) Piwi induces piRNA-guided transcriptional silencing and establishment of a repressive chromatin state. *Genes Dev,* **27,** 390-399.

LeRoy, G., Weston, J.T., Zee, B.M., Young, N.L., Plazas-Mayorca, M.D. & Garcia, B.A. (2009) Heterochromatin protein 1 is extensively decorated with histone code-like post-translational modifications. *Mol Cell Proteomics,* **8,** 2432-2442.

Lewis, L.K., Harlow, G.R., Gregg-Jolly, L.A. & Mount, D.W. (1994) Identification of High Affinity Binding Sites for LexA which Define New DNA Damage-inducible Genes in Escherichia coli. *Journal of Molecular Biology,* **241,** 507-523.

Li, B., Howe, L., Anderson, S., Yates, J.R., 3rd & Workman, J.L. (2003) The Set2 histone methyltransferase functions through the phosphorylated carboxyl-terminal domain of RNA polymerase II. *J Biol Chem,* **278,** 8897-8903.

Lin, C.Y., Loven, J., Rahl, P.B., Paranal, R.M., Burge, C.B., Bradner, J.E., Lee, T.I. & Young, R.A. (2012) Transcriptional amplification in tumor cells with elevated c-Myc. *Cell,* **151,** 56-67.

Ling, M., Merante, F. & Robinson, B.H. (1995) A rapid and reliable DNA preparation method for screening a large number of yeast clones by polymerase chain reaction. *Nucleic Acids Res,* **23,** 4924-4925.

Lo, W.-S., Gamache, E.R., Henry, K.W., Yang, D., Pillus, L. & Berger, S.L. (2005) Histone H3 phosphorylation can promote TBP recruitment through distinct promoter-specific mechanisms. *The EMBO Journal,* **24,** 997-1008.

Lo, W.S., Duggan, L., Emre, N.C., Belotserkovskya, R., Lane, W.S., Shiekhattar, R. & Berger, S.L. (2001) Snf1--a histone kinase that works in concert with the histone acetyltransferase Gcn5 to regulate transcription. *Science,* **293,** 1142-1146.

Locke, J., Kotarski, M.A. & Tartof, K.D. (1988) Dosage-dependent modifiers of position effect variegation in Drosophila and a mass action model that explains their effect. *Genetics,* **120,** 181-198.

Lomberk, G., Bensi, D., Fernandez-Zapico, M.E. & Urrutia, R. (2006a) Evidence for the existence of an HP1-mediated subcode within the histone code. *Nat Cell Biol,* **8,** 407-415.

Lomberk, G., Wallrath, L. & Urrutia, R. (2006b) The Heterochromatin Protein 1 family. *Genome Biol,* **7,** 228.

Lorch, Y., LaPointe, J.W. & Kornberg, R.D. (1987) Nucleosomes inhibit the initiation of transcription but allow chain elongation with the displacement of histones. *Cell,* **49,** 203-210.

Lorenz, M.C., Muir, R.S., Lim, E., McElver, J., Weber, S.C. & Heitman, J. (1995) Gene disruption with PCR products in Saccharomyces cerevisiae. *Gene,* **158,** 113-117.

Lu, B.Y., Bishop, C.P. & Eissenberg, J.C. (1996) Developmental timing and tissue specificity of heterochromatin-mediated silencing. *Embo j,* **15,** 1323-1332.

Luger, K., Mader, A.W., Richmond, R.K., Sargent, D.F. & Richmond, T.J. (1997) Crystal structure of the nucleosome core particle at 2.8 A resolution. *Nature,* **389,** 251-260.

Luger, K. & Richmond, T.J. (1998a) DNA binding within the nucleosome core. *Curr Opin Struct Biol,* **8,** 33-40.

Luger, K. & Richmond, T.J. (1998b) The histone tails of the nucleosome. *Curr Opin Genet Dev,* **8,** 140-146.

Luijsterburg, M.S., Dinant, C., Lans, H., Stap, J., Wiernasz, E., Lagerwerf, S., Warmerdam, D.O., Lindh, M., Brink, M.C., Dobrucki, J.W., Aten, J.A., Fousteri, M.I., Jansen, G., Dantuma, N.P., Vermeulen, W., Mullenders, L.H., Houtsmuller, A.B., Verschure, P.J. & van Driel, R. (2009) Heterochromatin protein 1 is recruited to various types of DNA damage. *J Cell Biol,* **185,** 577-586.

MacAlpine, D.M. & Almouzni, G. (2013) Chromatin and DNA replication. *Cold Spring Harb Perspect Biol,* **5,** a010207.

Maeshima, K., Hihara, S. & Eltsov, M. (2010) Chromatin structure: does the 30-nm fibre exist in vivo? *Curr Opin Cell Biol,* **22,** 291-297.

Maeshima, K., Imai, R., Tamura, S. & Nozaki, T. (2014) Chromatin as dynamic 10-nm fibers. *Chromosoma,* **123,** 225-237.

Maison, C. & Almouzni, G. (2004) HP1 and the dynamics of heterochromatin maintenance. *Nat Rev Mol Cell Biol,* **5,** 296-305.

Maison, C., Bailly, D., Peters, A.H., Quivy, J.P., Roche, D., Taddei, A., Lachner, M., Jenuwein, T. & Almouzni, G. (2002) Higher-order structure in pericentric heterochromatin involves a distinct pattern of histone modification and an RNA component. *Nat Genet,* **30,** 329-334.

Maison, C., Bailly, D., Roche, D., Montes de Oca, R., Probst, A.V., Vassias, I., Dingli, F., Lombard, B., Loew, D., Quivy, J.P. & Almouzni, G. (2011) SUMOylation promotes de novo targeting of HP1alpha to pericentric heterochromatin. *Nat Genet,* **43,** 220-227.

Martin, A.M., Pouchnik, D.J., Walker, J.L. & Wyrick, J.J. (2004) Redundant roles for histone H3 N-terminal lysine residues in subtelomeric gene repression in Saccharomyces cerevisiae. *Genetics,* **167,** 1123-1132.

Mavrich, T.N., Jiang, C., Ioshikhes, I.P., Li, X., Venters, B.J., Zanton, S.J., Tomsho, L.P., Qi, J., Glaser, R.L., Schuster, S.C., Gilmour, D.S., Albert, I. & Pugh, B.F. (2008) Nucleosome organization in the Drosophila genome. *Nature,* **453,** 358-362.

Mayer, A., Lidschreiber, M., Siebert, M., Leike, K., Soding, J. & Cramer, P. (2010) Uniform transitions of the general RNA polymerase II transcription complex. *Nat Struct Mol Biol,* **17,** 1272-1278.

Maze, I., Noh, K.-M., Soshnev, A.A. & Allis, C.D. (2014) Every amino acid matters: essential contributions of histone variants to mammalian development and disease. *Nat Rev Genet,* **15,** 259-271.

McBryant, S., Adams, V. & Hansen, J. (2006) Chromatin architectural proteins. *Chromosome Research,* **14,** 39-51.

Meehan, R.R., Kao, C.F. & Pennings, S. (2003) HP1 binding to native chromatin in vitro is determined by the hinge region and not by the chromodomain. *Embo j,* **22,** 3164-3174.

Megee, P.C., Morgan, B.A., Mittman, B.A. & Smith, M.M. (1990) Genetic analysis of histone H4: essential role of lysines subject to reversible acetylation. *Science,* **247,** 841-845.

Mercer, T.R., Dinger, M.E. & Mattick, J.S. (2009) Long non-coding RNAs: insights into functions. *Nat Rev Genet,* **10,** 155-159.

Millar, C.B. & Grunstein, M. (2006) Genome-wide patterns of histone modifications in yeast. *Nat Rev Mol Cell Biol,* **7,** 657-666.

Min, J., Feng, Q., Li, Z., Zhang, Y. & Xu, R.M. (2003) Structure of the catalytic domain of human DOT1L, a non-SET domain nucleosomal histone methyltransferase. *Cell,* **112,** 711-723.

Min, J., Zhang, X., Cheng, X., Grewal, S.I. & Xu, R.M. (2002) Structure of the SET domain histone lysine methyltransferase Clr4. *Nat Struct Biol,* **9,** 828-832.

Muchardt, C., Guilleme, M., Seeler, J.S., Trouche, D., Dejean, A. & Yaniv, M. (2002) Coordinated methyl and RNA binding is required for heterochromatin localization of mammalian HP1alpha. *EMBO Rep,* **3,** 975-981.

Muller, H.J. (1930) Types of visible variations induced by X-rays inDrosophila. *Journal of Genetics,* **22,** 299-334.

Munari, F., Soeroes, S., Zenn, H.M., Schomburg, A., Kost, N., Schroder, S., Klingberg, R., Rezaei-Ghaleh, N., Stutzer, A., Gelato, K.A., Walla, P.J., Becker, S., Schwarzer, D., Zimmermann, B., Fischle, W. & Zweckstetter, M. (2012) Methylation of lysine 9 in histone H3 directs alternative modes of highly dynamic interaction of heterochromatin protein hHP1beta with the nucleosome. *J Biol Chem,* **287,** 33756-33765.

Münsterkötter, M., Barbaric, S. & Hörz, W. (2000) Transcriptional Regulation of the Yeast PHO8 Promoter in Comparison to the Coregulated PHO5 Promoter. *Journal of Biological Chemistry,* **275,** 22678-22685.

Musladin, S., Krietenstein, N., Korber, P. & Barbaric, S. (2014) The RSC chromatin remodeling complex has a crucial role in the complete remodeler set for yeast PHO5 promoter opening. *Nucleic Acids Res,* **42,** 4270-4282.

Nakayama, J.-i., Rice, J.C., Strahl, B.D., Allis, C.D. & Grewal, S.I.S. (2001) Role of Histone H3 Lysine 9 Methylation in Epigenetic Control of Heterochromatin Assembly. *Science,* **292,** 110-113.

Narlikar, Geeta J., Sundaramoorthy, R. & Owen-Hughes, T. (2013) Mechanisms and Functions of ATP-Dependent Chromatin-Remodeling Enzymes. *Cell,* **154,** 490-503.

Neumann, H., Hancock, S.M., Buning, R., Routh, A., Chapman, L., Somers, J., Owen-Hughes, T., van Noort, J., Rhodes, D. & Chin, J.W. (2009) A Method for Genetically Installing Site-Specific Acetylation in Recombinant Histones Defines the Effects of H3 K56 Acetylation. *Mol Cell,* **36,** 153-163.

Nguyen, A.T. & Zhang, Y. (2011) The diverse functions of Dot1 and H3K79 methylation. *Genes Dev,* **25,** 1345-1358.

Nie, Z., Hu, G., Wei, G., Cui, K., Yamane, A., Resch, W., Wang, R., Green, D.R., Tessarollo, L., Casellas, R., Zhao, K. & Levens, D. (2012) c-Myc is a universal amplifier of expressed genes in lymphocytes and embryonic stem cells. *Cell,* **151,** 68-79.

Nielsen, P.R., Nietlispach, D., Mott, H.R., Callaghan, J., Bannister, A., Kouzarides, T., Murzin, A.G., Murzina, N.V. & Laue, E.D. (2002) Structure of the HP1 chromodomain bound to histone H3 methylated at lysine 9. *Nature,* **416,** 103-107.

Nightingale, K.P., O'Neill, L.P. & Turner, B.M. (2006) Histone modifications: signalling receptors and potential elements of a heritable epigenetic code. *Curr Opin Genet Dev,* **16,** 125-136.

Nishibuchi, G. & Nakayama, J. (2014) Biochemical and structural properties of heterochromatin protein 1: understanding its role in chromatin assembly. *J Biochem,* **156,** 11-20.

Noll, M. & Kornberg, R.D. (1977) Action of micrococcal nuclease on chromatin and the location of histone H1. *J Mol Biol,* **109,** 393-404.

North, J.A., Javaid, S., Ferdinand, M.B., Chatterjee, N., Picking, J.W., Shoffner, M., Nakkula, R.J., Bartholomew, B., Ottesen, J.J., Fishel, R. & Poirier, M.G. (2011) Phosphorylation of histone H3(T118) alters nucleosome dynamics and remodeling. *Nucleic Acids Res,* **39,** 6465-6474.

O'Geen, H., Ren, C., Nicolet, C.M., Perez, A.A., Halmai, J., Le, V.M., Mackay, J.P., Farnham, P.J. & Segal, D.J. (2017) dCas9-based epigenome editing suggests acquisition of histone methylation is not sufficient for target gene repression. *Nucleic Acids Res,* **45,** 9901-9916.

Olins, D.E. & Olins, A.L. (2003) Chromatin history: our view from the bridge. *Nat Rev Mol Cell Biol,* **4,** 809-814.

Ou, H.D., Phan, S., Deerinck, T.J., Thor, A., Ellisman, M.H. & O'Shea, C.C. (2017) ChromEMT: Visualizing 3D chromatin structure and compaction in interphase and mitotic cells. *Science,* **357**.

Pagano, M. (1996) *Cell Cycle - Materials and Methods.* Springer-Verlag Berlin Heidelberg.

Pal-Bhadra, M., Leibovitch, B.A., Gandhi, S.G., Chikka, M.R., Bhadra, U., Birchler, J.A. & Elgin, S.C. (2004) Heterochromatic silencing and HP1 localization in Drosophila are dependent on the RNAi machinery. *Science,* **303,** 669-672.

Patterton, H.G., Landel, C.C., Landsman, D., Peterson, C.L. & Simpson, R.T. (1998) The Biochemical and Phenotypic Characterization of Hho1p, the Putative Linker Histone H1 of Saccharomyces cerevisiae. *Journal of Biological Chemistry,* **273,** 7268-7276.

Perrini, B., Piacentini, L., Fanti, L., Altieri, F., Chichiarelli, S., Berloco, M., Turano, C., Ferraro, A. & Pimpinelli, S. (2004) HP1 controls telomere capping, telomere

elongation, and telomere silencing by two different mechanisms in Drosophila. *Mol Cell,* **15,** 467-476.

Piacentini, L., Fanti, L., Berloco, M., Perrini, B. & Pimpinelli, S. (2003) Heterochromatin protein 1 (HP1) is associated with induced gene expression in Drosophila euchromatin. *J Cell Biol,* **161,** 707-714.

Piacentini, L., Fanti, L., Negri, R., Del Vescovo, V., Fatica, A., Altieri, F. & Pimpinelli, S. (2009) Heterochromatin Protein 1 (HP1a) Positively Regulates Euchromatic Gene Expression through RNA Transcript Association and Interaction with hnRNPs in Drosophila. *PLoS Genet,* **5,** e1000670.

Pinskaya, M., Gourvennec, S. & Morillon, A. (2009) H3 lysine 4 di- and tri-methylation deposited by cryptic transcription attenuates promoter activation. *Embo j,* **28,** 1697-1707.

Platero, J.S., Hartnett, T. & Eissenberg, J.C. (1995) Functional analysis of the chromo domain of HP1. *Embo j,* **14,** 3977-3986.

Polo, S.E. & Almouzni, G. (2006) Chromatin assembly: a basic recipe with various flavours. *Curr Opin Genet Dev,* **16,** 104-111.

Qian, C. & Zhou, M.M. (2006) SET domain protein lysine methyltransferases: Structure, specificity and catalysis. *Cell Mol Life Sci,* **63,** 2755-2763.

Rando, O.J. & Winston, F. (2012) Chromatin and Transcription in Yeast. *Genetics,* **190,** 351-387.

Rea, S., Eisenhaber, F., O'Carroll, D., Strahl, B.D., Sun, Z.-W., Schmid, M., Opravil, S., Mechtler, K., Ponting, C.P., Allis, C.D. & Jenuwein, T. (2000) Regulation of chromatin structure by site-specific histone H3 methyltransferases. *Nature,* **406,** 593-599.

Reinke, H. & Horz, W. (2004) Anatomy of a hypersensitive site. *Biochim Biophys Acta,* **1677,** 24-29.

Reinke, H. & Hörz, W. (2003) Histones Are First Hyperacetylated and Then Lose Contact with the Activated PHO5 Promoter. *Mol Cell,* **11,** 1599-1607.

Reynolds, N., O'Shaughnessy, A. & Hendrich, B. (2013) Transcriptional repressors: multifaceted regulators of gene expression. *Development,* **140,** 505-512.

Richart, A.N., Brunner, C.I., Stott, K., Murzina, N.V. & Thomas, J.O. (2012) Characterization of chromoshadow domain-mediated binding of heterochromatin protein 1alpha (HP1alpha) to histone H3. *J Biol Chem,* **287,** 18730-18737.

Robinson, P.J. & Rhodes, D. (2006) Structure of the '30 nm' chromatin fibre: a key role for the linker histone. *Curr Opin Struct Biol,* **16,** 336-343.

Robinson, P.J.J., An, W., Routh, A., Martino, F., Chapman, L., Roeder, R.G. & Rhodes, D. (2008) `30nm' chromatin fibre decompaction requires both H4-K16 acetylation and linker histone eviction. *Journal of Molecular Biology,* **381,** 10.1016/j.jmb.2008.1004.1050.

Robyr, D., Suka, Y., Xenarios, I., Kurdistani, S.K., Wang, A., Suka, N. & Grunstein, M. (2002) Microarray deacetylation maps determine genome-wide functions for yeast histone deacetylases. *Cell,* **109,** 437-446.

Rossetto, D., Avvakumov, N. & Cote, J. (2012) Histone phosphorylation: a chromatin modification involved in diverse nuclear events. *Epigenetics,* **7,** 1098-1108.

Sambrook, J., Fritsch, E.F. & Maniatis, T. (1989) *Molecular cloning.* Cold spring harbor laboratory press New York.

Sawada, K., Yang, Z., Horton, J.R., Collins, R.E., Zhang, X. & Cheng, X. (2004) Structure of the Conserved Core of the Yeast Dot1p, a Nucleosomal Histone H3 Lysine 79 Methyltransferase. *Journal of Biological Chemistry,* **279,** 43296-43306.

Schaft, D., Roguev, A., Kotovic, K.M., Shevchenko, A., Sarov, M., Shevchenko, A., Neugebauer, K.M. & Stewart, A.F. (2003) The histone 3 lysine 36 methyltransferase, SET2, is involved in transcriptional elongation. *Nucleic Acids Res,* **31,** 2475-2482.

Schalch, T., Job, G., Noffsinger, V.J., Shanker, S., Kuscu, C., Joshua-Tor, L. & Partridge, J.F. (2009) High-affinity binding of Chp1 chromodomain to K9 methylated histone H3 is required to establish centromeric heterochromatin. *Mol Cell,* **34,** 36-46.

Schotta, G., Ebert, A., Krauss, V., Fischer, A., Hoffmann, J., Rea, S., Jenuwein, T., Dorn, R. & Reuter, G. (2002) Central role of Drosophila SU(VAR)3-9 in histone H3-K9 methylation and heterochromatic gene silencing. *Embo j,* **21,** 1121-1131.

Sengstag, C. & Hinnen, A. (1987) The sequence of the Saccharomyces cerevisiae gene PHO2 codes for a regulatory protein with unusual aminoacid composition. *Nucleic Acids Res,* **15,** 233-246.

Shi, Y., Lan, F., Matson, C., Mulligan, P., Whetstine, J.R., Cole, P.A., Casero, R.A. & Shi, Y. (2004) Histone demethylation mediated by the nuclear amine oxidase homolog LSD1. *Cell,* **119,** 941-953.

Shi, Y., Sawada, J., Sui, G., Affar el, B., Whetstine, J.R., Lan, F., Ogawa, H., Luke, M.P., Nakatani, Y. & Shi, Y. (2003) Coordinated histone modifications mediated by a CtBP co-repressor complex. *Nature,* **422,** 735-738.

Shilatifard, A. (2012) The COMPASS family of histone H3K4 methylases: mechanisms of regulation in development and disease pathogenesis. *Annu Rev Biochem,* **81,** 65-95.

Shogren-Knaak, M., Ishii, H., Sun, J.M., Pazin, M.J., Davie, J.R. & Peterson, C.L. (2006) Histone H4-K16 acetylation controls chromatin structure and protein interactions. *Science,* **311,** 844-847.

Sienski, G., Donertas, D. & Brennecke, J. (2012) Transcriptional silencing of transposons by Piwi and maelstrom and its impact on chromatin state and gene expression. *Cell,* **151,** 964-980.

Simon, J.A. & Kingston, R.E. (2009) Mechanisms of polycomb gene silencing: knowns and unknowns. *Nat Rev Mol Cell Biol,* **10,** 697-708.

Smith, Z.D. & Meissner, A. (2013) DNA methylation: roles in mammalian development. *Nat Rev Genet,* **14,** 204-220.

Smothers, J.F. & Henikoff, S. (2001) The hinge and chromo shadow domain impart distinct targeting of HP1-like proteins. *Mol Cell Biol,* **21,** 2555-2569.

Snowden, A.W., Gregory, P.D., Case, C.C. & Pabo, C.O. (2002) Gene-specific targeting of H3K9 methylation is sufficient for initiating repression in vivo. *Curr Biol,* **12,** 2159-2166.

Song, F., Chen, P., Sun, D., Wang, M., Dong, L., Liang, D., Xu, R.-M., Zhu, P. & Li, G. (2014) Cryo-EM Study of the Chromatin Fiber Reveals a Double Helix Twisted by Tetranucleosomal Units. *Science,* **344,** 376-380.

Southern, E.M. (1975) Detection of specific sequences among DNA fragments separated by gel electrophoresis. *Journal of Molecular Biology,* **98,** 503-517.

Steger, D.J., Lefterova, M.I., Ying, L., Stonestrom, A.J., Schupp, M., Zhuo, D., Vakoc, A.L., Kim, J.E., Chen, J., Lazar, M.A., Blobel, G.A. & Vakoc, C.R. (2008) DOT1L/KMT4 recruitment and H3K79 methylation are ubiquitously coupled with gene transcription in mammalian cells. *Mol Cell Biol,* **28,** 2825-2839.

Strahl, B.D. & Allis, C.D. (2000) The language of covalent histone modifcations. *Nature,* **403,** 41-45.

Strahl, B.D., Grant, P.A., Briggs, S.D., Sun, Z.W., Bone, J.R., Caldwell, J.A., Mollah, S., Cook, R.G., Shabanowitz, J., Hunt, D.F. & Allis, C.D. (2002) Set2 is a nucleosomal histone H3-selective methyltransferase that mediates transcriptional repression. *Mol Cell Biol,* **22,** 1298-1306.

Straka, C. & Horz, W. (1991) A functional role for nucleosomes in the repression of a yeast promoter. *Embo j,* **10,** 361-368.

Strom, A.R., Emelyanov, A.V., Mir, M., Fyodorov, D.V., Darzacq, X. & Karpen, G.H. (2017) Phase separation drives heterochromatin domain formation. *Nature,* **547,** 241-245.

Struhl, K. & Davis, R.W. (1977) Production of a functional eukaryotic enzyme in Escherichia coli: cloning and expression of the yeast structural gene for imidazole-glycerolphosphate dehydratase (his3). *Proc Natl Acad Sci U S A,* **74,** 5255-5259.

Sun, F.L., Cuaycong, M.H. & Elgin, S.C. (2001) Long-range nucleosome ordering is associated with gene silencing in Drosophila melanogaster pericentric heterochromatin. *Mol Cell Biol,* **21,** 2867-2879.

Sun, M., Schwalb, B., Schulz, D., Pirkl, N., Etzold, S., Lariviere, L., Maier, K.C., Seizl, M., Tresch, A. & Cramer, P. (2012) Comparative dynamic transcriptome analysis (cDTA) reveals mutual feedback between mRNA synthesis and degradation. *Genome Res,* **22,** 1350-1359.

Svaren, J., Schmitz, J. & Hörz, W. (1994) The transactivation domain of Pho4 is required for nucleosome disruption at the PHO5 promoter. *The EMBO Journal,* **13,** 4856-4862.

Svensson, J.P., Shukla, M., Menendez-Benito, V., Norman-Axelsson, U., Audergon, P., Sinha, I., Tanny, J.C., Allshire, R.C. & Ekwall, K. (2015) A nucleosome turnover map reveals that the stability of histone H4 Lys20 methylation depends on histone recycling in transcribed chromatin. *Genome Res,* **25,** 872-883.

Syed, S.H., Goutte-Gattat, D., Becker, N., Meyer, S., Shukla, M.S., Hayes, J.J., Everaers, R., Angelov, D., Bednar, J. & Dimitrov, S. (2010) Single-base resolution mapping of H1–nucleosome interactions and 3D organization of the nucleosome. *Proc Natl Acad Sci U S A,* **107,** 9620-9625.

Szerlong, H.J. & Hansen, J.C. (2011) Nucleosome distribution and linker DNA: connecting nuclear function to dynamic chromatin structure. *Biochemistry and cell biology = Biochimie et biologie cellulaire,* **89,** 24-34.

Talbert, P.B. & Henikoff, S. (2010) Histone variants--ancient wrap artists of the epigenome. *Nat Rev Mol Cell Biol,* **11,** 264-275.

Tan, M., Luo, H., Lee, S., Jin, F., Yang, J.S., Montellier, E., Buchou, T., Cheng, Z., Rousseaux, S., Rajagopal, N., Lu, Z., Ye, Z., Zhu, Q., Wysocka, J., Ye, Y., Khochbin, S., Ren, B. & Zhao, Y. (2011) Identification of 67 histone marks and histone lysine crotonylation as a new type of histone modification. *Cell,* **146,** 1016-1028.

Tartof, K.D., Hobbs, C. & Jones, M. (1984) A structural basis for variegating position effects. *Cell,* **37,** 869-878.

Thoma, F. & Koller, T. (1977) Influence of histone H1 on chromatin structure. *Cell,* **12,** 101-107.

Tremethick, D.J. (2007) Higher-Order Structures of Chromatin: The Elusive 30 nm Fiber. *Cell,* **128,** 651-654.

Trievel, R.C., Beach, B.M., Dirk, L.M., Houtz, R.L. & Hurley, J.H. (2002) Structure and catalytic mechanism of a SET domain protein methyltransferase. *Cell,* **111,** 91-103.

Tropberger, P. & Schneider, R. (2013) Scratching the (lateral) surface of chromatin regulation by histone modifications. *Nat Struct Mol Biol,* **20,** 657-661.

Tsukada, Y., Fang, J., Erdjument-Bromage, H., Warren, M.E., Borchers, C.H., Tempst, P. & Zhang, Y. (2006) Histone demethylation by a family of JmjC domain-containing proteins. *Nature,* **439,** 811-816.

Turner, B.M. (2014) Nucleosome signalling; an evolving concept. *Biochim Biophys Acta,* **1839,** 623-626.

van Leeuwen, F., Gafken, P.R. & Gottschling, D.E. (2002) Dot1p modulates silencing in yeast by methylation of the nucleosome core. *Cell,* **109,** 745-756.

Verdel, A., Jia, S., Gerber, S., Sugiyama, T., Gygi, S., Grewal, S.I. & Moazed, D. (2004) RNAi-mediated targeting of heterochromatin by the RITS complex. *Science,* **303,** 672-676.

Vogelauer, M., Wu, J., Suka, N. & Grunstein, M. (2000) Global histone acetylation and deacetylation in yeast. *Nature,* **408,** 495-498.

Volpe, T. & Martienssen, R.A. (2011) RNA interference and heterochromatin assembly. *Cold Spring Harb Perspect Biol,* **3,** a003731.

Volpe, T.A., Kidner, C., Hall, I.M., Teng, G., Grewal, S.I. & Martienssen, R.A. (2002) Regulation of heterochromatic silencing and histone H3 lysine-9 methylation by RNAi. *Science,* **297,** 1833-1837.

Wakimoto, B.T. & Hearn, M.G. (1990) The effects of chromosome rearrangements on the expression of heterochromatic genes in chromosome 2L of Drosophila melanogaster. *Genetics,* **125,** 141-154.

Wallrath, L.L. & Elgin, S.C. (1995) Position effect variegation in Drosophila is associated with an altered chromatin structure. *Genes Dev,* **9,** 1263-1277.

Wang, A., Kurdistani, S.K. & Grunstein, M. (2002) Requirement of Hos2 histone deacetylase for gene activity in yeast. *Science,* **298,** 1412-1414.

Wang, S.S., Zhou, B.O. & Zhou, J.Q. (2011) Histone H3 lysine 4 hypermethylation prevents aberrant nucleosome remodeling at the PHO5 promoter. *Mol Cell Biol,* **31,** 3171-3181.

Weiner, A., Chen, H.V., Liu, C.L., Rahat, A., Klien, A., Soares, L., Gudipati, M., Pfeffner, J., Regev, A., Buratowski, S., Pleiss, J.A., Friedman, N. & Rando, O.J. (2012) Systematic dissection of roles for chromatin regulators in a yeast stress response. *PLoS Biol,* **10,** e1001369.

Wilson, J.R., Jing, C., Walker, P.A., Martin, S.R., Howell, S.A., Blackburn, G.M., Gamblin, S.J. & Xiao, B. (2002) Crystal structure and functional analysis of the histone methyltransferase SET7/9. *Cell,* **111,** 105-115.

Win, T.Z., Draper, S., Read, R.L., Pearce, J., Norbury, C.J. & Wang, S.W. (2006) Requirement of fission yeast Cid14 in polyadenylation of rRNAs. *Mol Cell Biol,* **26,** 1710-1721.

Wippo, C.J., Krstulovic, B.S., Ertel, F., Musladin, S., Blaschke, D., Sturzl, S., Yuan, G.C., Horz, W., Korber, P. & Barbaric, S. (2009) Differential cofactor requirements for histone eviction from two nucleosomes at the yeast PHO84 promoter are determined by intrinsic nucleosome stability. *Mol Cell Biol,* **29,** 2960-2981.

Wood, A., Shukla, A., Schneider, J., Lee, J.S., Stanton, J.D., Dzuiba, T., Swanson, S.K., Florens, L., Washburn, M.P., Wyrick, J., Bhaumik, S.R. & Shilatifard, A. (2007) Ctk complex-mediated regulation of histone methylation by COMPASS. *Mol Cell Biol,* **27,** 709-720.

Woodcock, C.L., Frado, L.L. & Rattner, J.B. (1984) The higher-order structure of chromatin: evidence for a helical ribbon arrangement. *The Journal of Cell Biology,* **99,** 42-52.

Xhemalce, B. & Kouzarides, T. (2010) A chromodomain switch mediated by histone H3 Lys 4 acetylation regulates heterochromatin assembly. *Genes Dev,* **24,** 647-652.

Zhang, K., Mosch, K., Fischle, W. & Grewal, S.I. (2008) Roles of the Clr4 methyltransferase complex in nucleation, spreading and maintenance of heterochromatin. *Nat Struct Mol Biol,* **15,** 381-388.

Zhang, W., Bone, J.R., Edmondson, D.G., Turner, B.M. & Roth, S.Y. (1998) Essential and redundant functions of histone acetylation revealed by mutation of target lysines and loss of the Gcn5p acetyltransferase. *The EMBO Journal,* **17,** 3155-3167.

Zhang, X., Tamaru, H., Khan, S.I., Horton, J.R., Keefe, L.J., Selker, E.U. & Cheng, X. (2002) Structure of the Neurospora SET domain protein DIM-5, a histone H3 lysine methyltransferase. *Cell,* **111,** 117-127.

Zhao, T. & Eissenberg, J.C. (1999) Phosphorylation of heterochromatin protein 1 by casein kinase II is required for efficient heterochromatin binding in Drosophila. *J Biol Chem,* **274,** 15095-15100.

Zhao, T., Heyduk, T., Allis, C.D. & Eissenberg, J.C. (2000) Heterochromatin protein 1 binds to nucleosomes and DNA in vitro. *J Biol Chem,* **275,** 28332-28338.

Zhao, T., Heyduk, T. & Eissenberg, J.C. (2001) Phosphorylation site mutations in heterochromatin protein 1 (HP1) reduce or eliminate silencing activity. *J Biol Chem,* **276,** 9512-9518.

Zhou, Y.B., Gerchman, S.E., Ramakrishnan, V., Travers, A. & Muyldermans, S. (1998) Position and orientation of the globular domain of linker histone H5 on the nucleosome. *Nature,* **395,** 402-405.

Zink, L.M. & Hake, S.B. (2016) Histone variants: nuclear function and disease. *Curr Opin Genet Dev,* **37,** 82-89.

8 Acknowledgements

Zuerst möchte ich Prof. Axel Imhof und Dr. Philipp Korber dafür danken mir die Möglichkeit gegeben zu haben an diesem interessanten Thema zu arbeiten.

Danke Axel, dass du mir zu Beginn der Dissertation den Einstieg in das Laborleben mit Hilfestellungen, interessanten, und manchmal auch lustigen Labmeetings vereinfacht hast. Und stets mit wertvollen Ratschlägen das Projekt vorangetrieben hast.

Ein besonderer Dank gilt dir, Philipp. Ich hätte mir keinen besseren Doktorvater vorstellen können. Mit unermüdlicher Ruhe hast du einem Mediziner die Grundlagen für wissenschaftliches Arbeiten beigebracht. Hattest immer Zeit für Fragen und Diskussionen, konntest einen immer wieder erneut motivieren und hast durch deine Ideen das Projekt immer wieder bereichert.

Prof. Peter Becker möchte ich für die herausragende Atmosphäre an seinem Lehrstuhl danken, die eine rege wissenschaftliche Diskussion über die einzelnen Arbeitsgruppen hinweg ermöglicht hat. Und aber auch abseits der Wissenschaft zu anhaltenden Freundschaften geführt hat.

In diesem Zuge ist natürlich ganz herzlich dem „North Lab“ zu danken, insbesondere Alexandra, Franzi, Dorle, Andrea, Wippo, Nils, Corinna, Julia, Sandra, Lisa, Sebastian, Clemens, und Antonia. Vielen Dank für eine nicht zu vergessene wunderschöne Laborzeit, die Geduld einem Mediziner das pipettieren, klonieren etc. beizubringen, und für die stets volle Süßigkeiten-Schublade, auch wenn diese immer durch Clemens bedroht war.

Für die Hilfe bei den massenspektrometrischen Untersuchungen möchte ich mich bei Marc, Teresa, und Ignasi ganz herzlich bedanken.

Am Genzentrum möchte ich Prof. Patrick Cramer und insbesondere Kerstin Maier danken, dass wir unsere Expressionsarrays bei Ihnen durchführen konnten.

Für die Auswertung der Expressionsarrays gilt der Dank Tobias Straub.

Edith Müller und Caroline Brieger danke ich für die Unterstützung bei den bürokratischen Dingen des Lebens und die hervorragende Organisation, die alles im Labor am Laufen gehalten hat.

Ich danke allen Mitarbeitern des Lehrstuhls für ein sehr schöne, lehrreiche, aber auch spaßige Zeit! Hier hervorzuheben sind neben dem „North Lab“ insbesondere Simone, Edith, Irene, Gabi, Tobias, Raffi, Felix, Jochen, Henrike, Manolo.

Ich bin dankbar für die Aufnahme in das “Promotionsstudium des Förderprogramms für Forschung und Lehre” (FöFoLe) der LMU, durch welche dieses Projekt erst möglich wurde.

Meinen Freunden von daheim und aus Studium danke ich für die abwechslungsreiche Stunden außerhalb des Labors. Insbesondere gilt hier der Dank der GDFL.
Zum Schluss gilt der größte Dank meiner Familie Christoph, Regina, Ruth und Fritz. Insbesondere meinen Eltern möchte ich für deren stete Unterstützung und das uneingeschränkte Vertrauen danken, ohne diese wäre vieles nicht möglich gewesen.

9 Curriculum Vitae

Removed in this public version.